Luis Gustavo Morello

Caracterização Funcional das Proteínas NIP7 e FTSJ3 no Processamento do RNA Ribossomal em Células Humanas

Campinas, 2012

UNIVERSIDADE ESTADUAL DE CAMPINAS
INSTITUTO DE BIOLOGIA

Luis Gustavo Morello

Caracterização Funcional das Proteínas NIP7 e FTSJ3 no Processamento do RNA Ribossomal em Células Humanas

Tese apresentada ao Instituto de Biologia para obtenção do Título de Doutor em Genética e Biologia Molecular, na área de Genética Animal e Evolução.

Orientador: Prof. Dr. Nilson Ivo Tonin Zanchin

Campinas, 2012

FICHA CATALOGRÁFICA ELABORADA POR
ROBERTA CRISTINA DAL' EVEDOVE TARTAROTTI – CRB8/7430
BIBLIOTECA DO INSTITUTO DE BIOLOGIA - UNICAMP

M815c

Morello, Luis Gustavo, 1982-
Caracterização funcional das proteínas NIP7 e FTSJ3 no processamento do RNA ribossomal em células humanas / Luis Gustavo Morello. – Campinas, SP: [s.n.], 2012.

Orientador: Nilson Ivo Tonin Zanchin.
Tese (doutorado) – Universidade Estadual de Campinas, Instituto de Biologia.

1. Ribossomos – Biossíntese. 2. RNA ribossômico. 3. Proteína NIP7. 4. Proteína FTSJ3. I. Zanchin, Nilson Ivo Tonin. II. Universidade Estadual de Campinas. Instituto de Biologia. III. Título.

Informações para Biblioteca Digital

Título em Inglês: Functional characterization of proteins NIP7 and FTSJ3 in ribosomal RNA processing in human cells
Palavras-chave em Inglês:
Ribosomes – Biosynthesis
Ribosomal RNA
NIP7 protein
FTSJ3 protein
Área de concentração: Genética Animal e Evolução
Titulação: Doutor em Genética e Biologia Molecular
Banca examinadora:
Nilson Ivo Tonin Zanchin [Orientador]
Marcelo Damario Gomes
Ana Paula Ulian de Araújo
José Andrés Yunes
Celso Eduardo Benedetti
Data da defesa: 29-06-2012
Programa de Pós Graduação: Genética e Biologia Molecular

Campinas, 29 de junho de 2012.

BANCA EXAMINADORA

Prof. Dr. Nilson Ivo Tonin Zanchin (Orientador)

Assinatura

Prof. Dr. Marcelo Damario Gomes

Assinatura

Profa. Dra. Ana Paula Ulian de Araújo

Assinatura

Prof. Dr. José Andrés Yunes

Assinatura

Prof. Dr. Celso Eduardo Benedetti

Assinatura

Prof. Dr. Paulo Sérgio Rodrigues Coelho

Assinatura

Profa. Dra. Ângela Kaysel Cruz

Assinatura

Prof. Dr. Carlos Frederico Martins Menck

Assinatura

"Nos campos da observação, o acaso

favorece apenas as mentes preparadas".

Louis Pasteur

Dedico este trabalho...

Aos meus amados pais, ***Walter & Elizabete****, pelo incentivo, confiança, amor e apoio em todos os momentos da minha vida.*

Ao meu amado irmão, ***Lucas****, por estar sempre presente, dando-me força e apoio.*

À minha querida e amada companheira ***Aline****, pelo amor, carinho e paciência.*

AGRADECIMENTOS

Quero, por meio deste, expressar meus sinceros agradecimentos a todos que contribuíram para o desenvolvimento do presente trabalho, pois, por mais forte, duro e independente que possas ser, sempre haverá momentos em que precisarás de ajuda.

À minha amada família, meu pai Walter, minha mãe Elizabete e meu irmão Lucas, por terem confiado em mim e apoiado meus sonhos, sem os quais eu não teria chegado até aqui.

À minha namorada Aline que, com amor, compreensão e paciência, me apoia e me dá forças para seguir em frente.

Ao Dr. Nilson Ivo Tonin Zanchin pela oportunidade de integrar seu grupo de pesquisa e pela orientação ao longo do desenvolvimento deste trabalho.

À Dr^{a}. Melissa Moore, pela oportunidade de desenvolver parte do meu projeto em seu laboratório na *University of Massachusetts Medical School* e pelas imensuráveis contribuições científicas.

À Dr^{a}. Adriana Franco Paes Leme por estar sempre disposta a ajudar.

À professora Dr^{a}. Carla Columbano de Oliveira pelas sugestões pertinentes ao desenvolvimento do projeto.

Aos pesquisadores do LNBio, Dr. Jörg Kobarg e Dr. Celso Eduardo Benedetti, pelas discussões científicas inestimáveis.

Aos caros amigos, Carlos Paier, Dr. Gustavo Bressan, Dr. Daniel Lanza e José Jadsom, com quem aprendi muito, tanto profissional quanto pessoalmente.

Aos amigos Marcos dos Santos, André Pereira e Tiago Antônio, pela convivência agradável dentro e fora do laboratório.

Às técnicas do LNBio, Tereza Lima, Adriana Alves, Elaine Teixeira, Givanil Garrido, Caroline Bondarik e Marina Dias pelo suporte.

A todos os colegas do LNBio que sempre proporcionaram um ótimo ambiente de trabalho.

Ao prezado amigo Dr. Alexandre Quaresma pela ótima convivência e pela colaboração científica na *University of Massachusetts Medical School*.

Aos colegas do Moore Lab, em especial: Emiliano, Alper, Can, Guramrit, Daniela, Erin, Laureen, Rina, Ami, Akiko e Chris Merrikh.

Aos membros da banca por terem aceitado participar da avaliação desse trabalho.

À Fundação de Amparo à Pesquisa do Estado de São Paulo (FAPESP) e ao Conselho Nacional de Desenvolvimento Científico e Tecnológico (CNPq) pelo auxílio financeiro.

Ao Laboratório Nacional de Biociências (LNBio) pela excelente infraestrutura oferecida à pesquisa.

Ao Programa de Pós-Graduação em Genética e Biologia Molecular da UNICAMP.

ÍNDICE

LISTA DE FIGURAS

LISTA DE ABREVIAÇÕES

3'ETS Sequência espaçadora externa 3' (*External Transcribed Spacer 3'*)

5'ETS Sequência espaçadora externa 5' (*External Transcribed Spacer 5'*)

5'-TOP Trato rico em oligopirimidinas na extremidade 5' (*5' Tract rich in OligoPyrimidines*)

FRAP Recuperação de fluorescência após fotodegradação (*Fluorescence Recovery After Photobleaching*)

FTSJ3 Proteína hipotética com domínio FtsJ de RNA-metil-transferase, provável ortólogo 3 de *E. coli*. (*FtsJ homolog 3* (*E. coli*))

GFP Proteína fluorescente verde (*Green Fluorescent Protein*)

GST Glutationa S-transferase (*Glutathionine S-Transferase*)

ITS1 Sequência espaçadora interna 1 (*Internal Transcribed Spacer 1*)

ITS2 Sequência espaçadora interna 2 (*Internal Transcribed Spacer 2*)

LUCA Último Ancestral Universal Comum (*Last Universal Common Ancestor*)

Nip7p Proteína de importação nuclear 7 de *Saccharomyces cerevisiae* (*Nuclear import protein 7*)

NIP7 Provável proteína de importação nuclear 7 de humanos (*Nuclear Import Protein 7*)

PTC Centro de peptidil transferase (*Peptidyl Transferase Center*)

PUA Domínio encontrado em pseudo-uridina sintases e archaeosina transglicosilases (*PseudoUridine synthases and Archaeosine tranglycosilases*)

mRFP Proteína de fluorescência vermelha monomérica (*monomeric Red Fluorescent Protein*)

RNA Pol RNA Polimerase

RNA Pol I RNA Polimerase I

RNA Pol II RNA Polimerase II

RNA Pol III RNA Polimerase III

RNA Ácido ribonucleico (*RiboNucleic Acid*)

mRNA	RNA mensageiro (*messenger RNA*)
rRNA	RNA ribossomal (*ribosomal RNA*)
tRNA	RNA transportador (*transfer RNA*)
r-proteínas	proteínas ribossomais (*ribossomal proteins*)
RP	proteína ribossomal (*Ribosomal Protein*)
snoRNA	pequeno RNA nucleolar (*small nulceolar RNA*)
hnRNP	Ribonucleoproteína nuclear heterogênea (*heterogeneous nuclear RiboNucleoProtein*)
snoRNP	pequena partícula ribonucleoprotéica nucleolar (*small nucleolar RiboNucleoProtein*)
SBDS	Proteína associada a síndrome de *Shwachman-Bodian-Diamond* (*Shwachman-Bodian-Diamond Syndrome*)
SSU	Subunidade menor (*Small SUbunit*)

RESUMO

Estudos prévios realizados em nosso laboratório demonstraram a interação entre as proteínas humanas SBDS e NIP7. SBDS participa da biogênese de ribossomos e sua deficiência está associada à síndrome de *Shwachman–Bodian–Diamond*. NIP7 é uma proteína conservada e já foi caracterizada em levedura, onde participa da formação da subunidade ribossomal 60S. Neste trabalho, nós investigamos o papel de NIP7 na síntese de ribossomos em células humanas. A depleção de NIP7 revelou defeitos no processamento do pré-rRNA associado à produção do rRNA 18S, causando déficit na formação da subunidade ribossomal 40S. Essa divergência de resultados entre a função de NIP7 em levedura e células humanas é consistente com o fato de que NIP7 humana não complementa levedura deficiente em Nip7p. Ainda, um rastreamento em sistema de duplo-híbrido tendo NIP7 humana como isca revelou parceiros de interação diferentes daqueles reportados para Nip7p em levedura. FTSJ3 foi a parceira isolada com maior frequência. FTSJ3 é a provável ortóloga de Spb1p em levedura, a qual está envolvida na formação da subunidade ribossomal 60S. A associação entre FTSJ3 e NIP7 foi demonstrada por ensaios de *pull-down* e imunoprecipitação, como sendo dependente de RNA. A co-localização nucleolar e co-sedimentação dessas proteínas em fracionamento em gradiente de sacarose corroboram a associação. Além disso, células humanas deficientes em FTSJ3 revelaram defeitos na via de maturação do rRNA 18S, mesma via afetada pela depleção de NIP7. Em adição, a caracterização proteômica de complexos contendo FTSJ3 e NIP7 revelaram que essas proteínas co-purificam complexos pré-ribossomais. Uma comparação entre o conjunto de proteínas que interagem com Spb1p e as proteínas identificadas nos ensaios de pull-down com FLAG-FTSJ3 revelou que elas apresentam apenas um ortólogo em comum, o qual, incrivelmente, é Nip7/NIP7. Essas observações revelaram diferenças significativas na função desses fatores durante a síntese de ribossomos em levedura e células humanas, adicionando NIP7 e FTSJ3 na lista crescente de fatores com funções divergentes nas vias de processamento do rRNA em levedura e humanos.

ABSTRACT

Previous studies from our laboratory have demonstrated the interaction between the SBDS and NIP7 human proteins. SBDS play a role in ribosome biogenesis and its deficiency is associated to the Shwachman-Bodian-Diamond syndrome. NIP7 is a conserved protein and has already been characterized in yeast, where it participates in the 60S ribosomal subunit formation. In this work, we investigated the role of NIP7 in ribosome biogenesis in human cells. NIP7 knockdown caused pre-rRNA processing defects associated to the 18S rRNA maturation, leading to deficiency in 40S ribosomal subunit synthesis. The divergence between NIP7 function in yeast and human cells is further supported by the fact that human NIP7 does not complement yeast deficient in Nip7p. In addition, a two-hybrid screen using human NIP7 as bait revealed interaction partners different from those reported for yeast Nip7p. FTSJ3 was isolated as one of the most frequent human NIP7-interacting candidates. FTSJ3 is a putative ortholog of yeast Spb1p, which has been implicated in 60S ribosomal subunit synthesis. The association between FTSJ3 and NIP7 was showed by pull-down and immunoprecipitation assays as an RNA-dependent interaction. Nucleolar co-localization and co-sedimentation on a sucrose gradiente fractionation corroborate this association. Furthermore, RNAi-mediated knockdown revealed that depletion of FTSJ3 causes pre-rRNA processing defects in the pathway leading to 18S rRNA maturation, the same pathway affected by NIP7 downregulation. In additon, proteomic characterization of FTSJ3- and NIP7-containing complexes showed that these proteins copurify pre-ribosomal complexes. A comparison of the set of Spb1p-interacting proteins with the proteins identified in the pulldown with FLAG-FTSJ3 showed that they share only one ortholog which, incredibly, is Nip7/NIP7. These observations revealed significant differences in the function of these factors during the synthesis of ribosomes in yeast and human cells, adding NIP7 and FTSJ3 to the growing list of factors with different functions in yeast and human rRNA processing pathways.

1. INTRODUÇÃO

1.1. O ribossomo

O ribossomo é responsável pela síntese de proteínas, um processo fundamental em todas as células. A síntese de proteínas acontece no citoplasma através de um mecanismo conhecido como tradução. Na tradução, a informação genética contida na sequência de nucleotídeos do RNA mensageiro (mRNA) é decodificada, ou seja, traduzida em uma sequência de aminoácidos, dando origem às proteínas. Em nível molecular, isso significa o estabelecimento da correlação entre genótipo e fenótipo, o chamado dogma central da biologia molecular (Crick, 1970). De acordo com (Woese, 2001) “a tradução não é apenas um outro mecanismo molecular a ser resolvido. Ela representa a transição evolutiva de algum tipo de mundo baseado em ácidos nucleicos para o mundo baseado em proteínas, das células modernas”.

O ribossomo é considerado uma das mais antigas maquinarias moleculares da vida por ter praticamente a mesma estrutura e função nos três domínios dos seres vivos. Acredita-se que o ribossomo primordial surgiu em um mundo à base de RNA, onde aminoácidos ou moléculas semelhantes associadas a pequenos oligômeros de RNAs seriam unidas através de ligações semelhantes a ligações peptídicas na presença de um RNA catalizador, ancestral ao RNA presente no centro de peptidil transferase (PTC) do ribossomo. Com a elucidação da estrutura do ribossomo e estudos posteriores, constatou-se que as proteínas ribossomais (r-proteínas) são efetivamente ausentes na região do PTC, suportando, de forma indireta, a ideia de que o ribossomo é uma máquina fundamentada em RNA, isto é, uma ribozima (Ban *et al.,* 2000; Hsiao *et al.,* 2009). Dessa maneira, considera-se que o ribossomo, em seu modelo atual (Figura 1.1), foi estabelecido antes do último ancestral universal comum (LUCA) da vida, ou seja, antes da raiz da árvore filogenética.

O ribossomo é uma macromolécula ribonucleoprotéica, constituído por aproximadamente 2/3 de RNAs e 1/3 de proteínas. O ribossomo procariótico

sedimenta com coeficiente de sedimentação igual a 70S e é formado por 2 subunidades distintas, a subunidade 30S e a subunidade 50S. Em *Escherichia coli*, o ribossomo 70S é uma partícula de 210 Å (Schuwirth *et al.,* 2005). A subunidade menor, ou 30S, é composta pelo rRNA 16S (1.542 nucleotídeos) e 21 proteínas ribossomais (r-proteínas), enquanto a subunidade maior, ou 50S, é formada por dois rRNAs, o 23S (2.904 nucleotídeos) e o 5S (120 nucleotídeos) e 33 r-proteínas (Schuwirth *et al.,* 2005). Em eucariotos, o ribossomo completo sedimenta com coeficiente de 80S e é aproximadamente 40% maior que o ribossomo bacteriano. A subunidade menor, ou 40S, contém aproximadamente 33 r-proteínas associadas ao rRNA 18S, enquanto a subunidade maior, ou 60S, é composta por aproximadamente 46 r-proteínas e três rRNAs (25S/28S; 5,8S e 5S) (Ben-Shem *et al.,* 2010).

As subunidades ribossomais têm diferentes funções no processo de tradução, quando associam-se através de uma rede de interações intermoleculares ao longo de suas interfaces (Hennelly *et al.,* 2005) (Figura 1.1 C). A subunidade menor está diretamente associada à interação com o mRNA durante a iniciação da tradução e à decodificação da informação genética contida na sequência de nucleotídeos do mRNA. Já a subunidade maior contém o sítio catalítico do ribossomo, onde ocorre a formação da ligação peptídica. Existem 3 sítios de ligação para RNAs transportadores (tRNAs) na subunidade maior: o sítio A que recebe o tRNA aminoacilado contendo o aminoácido a ser incorporado na cadeia polipeptídica; o sítio P que abriga o tRNA ligado à cadeia polipeptídica em crescimento e o sítio E, ou sítio de saída, para onde o tRNA desacetilado é movido após a formação da ligação peptídica, antes de ser ejetado do ribossomo.

1.2. Biogênese de ribossomos

A biogênese de ribossomos, isto é, a síntese de ribossomos, é um dos processos de maior consumo energético nas células. O processo como um todo

é altamente coordenado, tanto no tempo quanto no espaço, assegurando a montagem e maturação das subunidades ribossomais de forma correta. Os principais passos envolvidos na síntese de ribossomos são: a) transcrição, processamento e modificação dos rRNAs; b) tradução e modificação de proteínas ribossomais; c) enovelamento dos rRNAs e ligação de proteínas ribossomais; e d) participação ordenada de fatores não-ribossomais.

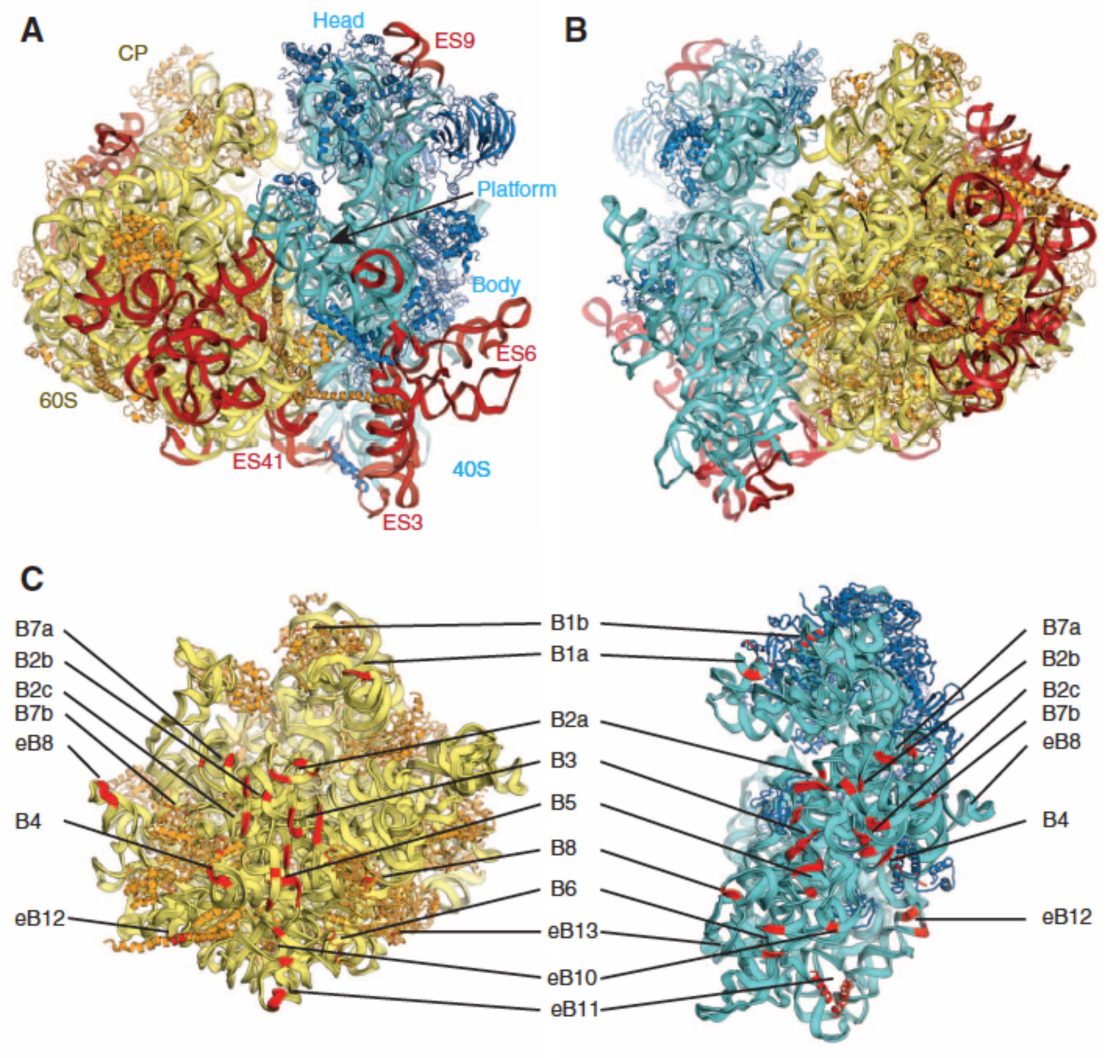

Figura 1.1: Visão geral da estrutura cristalográfica do ribossomo eucarioto (*S. cerevisiae*). **A)** Visão do síto E. rRNA e proteínas da subunidade 40S estão coloridos em azul claro e azul escuro, respectivamente. rRNAs e proteínas da subunidade 60S estão coloridos em amarelo claro e amarelo escuro, respectivamente. Segmentos de expansão estão indicados em vermelho. **B)** Visão do síto A. **C)** Visão das interfaces das subunidades 60S e 40S. As interações estão numeradas e coloridas em vermelho. São 38 interações no total, sendo 4 proteína-proteína (~11%); 21 RNA-RNA (~55%); e 13 proteína-RNA (~34%). Figura extraída de (Ben-Shem *et al.,* 2010).

A síntese de ribossomos inicia-se com a transcrição policistrônica dos rRNAs, os quais são sintetizados como partes de um transcrito único, chamado transcrito primário. Tanto em procariotos quanto em eucariotos, os rRNAs maduros são processados a partir do transcrito primário através de sucessivas clivagens endo e exonucleolíticas.

Em procariotos, a síntese de ribossomos é feita no citoplasma. A maturação dos rRNAs 16S, 23S e 5S, a partir do transcrito primário (Figura 1.2) ocorre antes mesmo do término da transcrição, logo após o surgimento de estruturas secundárias locais que permitem a ligação de proteínas ribossomais. Simultaneamente, o rRNA é modificado quimicamente em diversas posições e processado por diversas RNases até que os rRNAs maduros sejam gerados (Williamson, 2003). A primeira endorribonuclease a clivar o transcrito primário é a RNase III, separando os precursores para os rRNAs 16S (17S), 23S e 5S (9S), e dependendo do operon, ainda pode gerar alguns tRNAs presentes no transcrito primário (Figura 1.2). Após a clivagem do transcrito primário pela

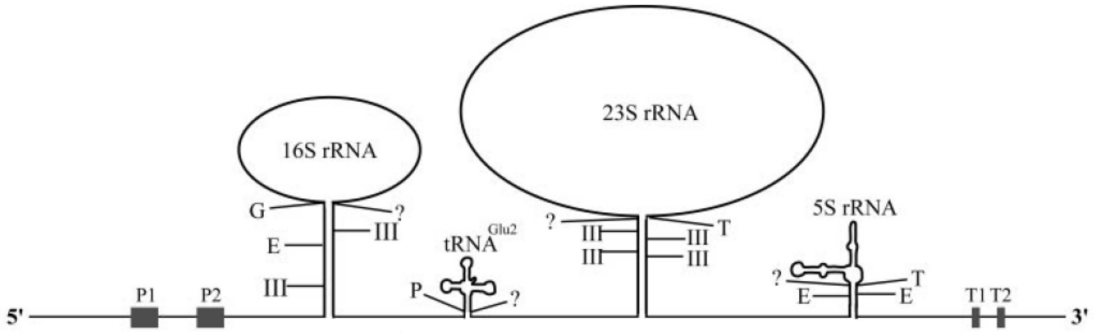

Figura 1.2: Organização esquemática do rRNA transcrito primário em bactérias (operon *rrnB*). Os rRNAs 16S e 23S, tRNAs, promotores P1 e P2 e terminadores T1 e T2, bem como os sítios de processamento para RNase III (III), RNase G (G), RNase E (E), RNase P (P), RNase T (T) e RNases desconhecidas (?) estão indicados. Figura extraída de (Kaczanowska & Rydén-Aulin, 2007).

RNase III, o precursor 17S é clivado na extremidade 5' pelas RNases E e G (Li *et al.,* 1999b), e também clivado na extremidade 3' por uma RNase ainda

desconhecida (Hayes & Vasseur, 1976), gerando, dessa forma, o rRNA 16S maduro. O precursor do 23S, contendo apenas alguns nucleotídeos flanqueando o rRNA maduro é processado na extremidade 5' por uma enzima desconhecida ao passo que a maturação da extremidade 3' requer a atividade da exorribonuclease RNase T (Li *et al.,* 1999a). O rRNA 5S é gerado a partir do precursor 9S, o qual é processado rapidamente pela RNase E em ambas as extremidades (Roy *et al.,* 1983). A maturação final do rRNA 5S é feita pela exorribonuclease RNase T na extremidade 3' (Li & Deutscher, 1995) enquanto a RNase envolvida na maturação da extremidade 5' ainda não foi identificada.

Em eucariotos, a biogênese de ribossomos acontece principalmente no nucléolo, um compartimento especializado dentro do núcleo da célula. O processo envolve a atividade das três RNA polimerases (RNA Pol), a síntese e associação de 4 rRNAs e pelo menos 79 proteínas ribossomais e a atuação de mais de 200 fatores transientes (Ben-Shem *et al.,* 2010; Kressler *et al.,* 2010). A RNA polimerase II (RNA Pol II) sintetiza o pré-mRNA para as proteínas ribossomais e para os fatores transientes envolvidos na biogênese de ribossomos. A RNA polimerase III (RNA Pol III) transcreve o precursor para o rRNA 5S ao passo que a RNA polimerase I (RNA Pol I) produz um RNA ribossomal longo e policistrônico, o pré-rRNA 35S em levedura ou o pré-rRNA 47S em mamíferos, conhecido também como transcrito primário. O transcrito primário contém os rRNAs 18S, 5,8S e 25S (levedura) ou 28S (mamíferos) flanqueados por sequências espaçadoras externas, nas extremidades 5' e 3' (5'ETS e 3'ETS), e separados por sequências espaçadoras internas (ITS1 e ITS2) (Figura 1.3). Os rRNAs maduros 18S, 5,8S e 25S/28S são produzidos por meio de diversas clivagens endo e exonucleolíticas e modificações covalentes de nucleotídeos. Concomitantemente com o processamento do pré-rRNA, ocorre a associação de proteínas ribossomais e não-ribossomais, formando-se o que é conhecido como partículas pré-ribossomais. A associação inicial de proteínas ribossomais e fatores transientes ao pré-rRNA 35S/47S no nucléolo dá origem ao complexo pré-ribossomal 90S. Este, por sua vez, é separado em duas partículas pré-ribossomais, a pré-40S e a pré-60S. Então essas partículas pré-

ribossomais são exportadas do nucleoplasma para o citoplasma, onde os passos de maturação e montagem finais acontecem, produzindo as subunidades ribossomais maduras e o ribossomo funcional.

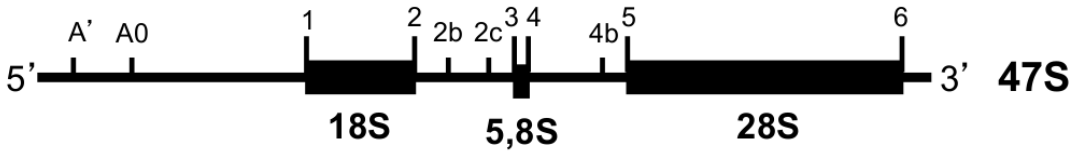

Figura 1.3: Representação esquemática do pré-rRNA 47S de mamíferos. Os rRNAs, as sequências espaçadoras internas e externas e os principais sítios de clivagens estão indicados. Figura com base em (Hadjiolova *et al.,* 1993, Rouquette *et al.,* 2005, Kent *et al.,* 2009).

1.3. Processamento do pré-rRNA em eucariotos

A biogênese de ribossomos inicia-se com a síntese do pré-rRNA pela atividade da RNA Pol I e foi melhor caracterizada em *Saccharomyces cerevisiae*. Neste modelo biológico, o primeiro precursor detectado é o pré-rRNA 35S, o qual contém sequências espaçadoras externas nas extremidades 5' e 3' (5'ETS e 3'ETS) bem como os rRNAs maduros 18S, 5,8S e 25S separados por sequências espaçadoras internas (ITS1 e ITS2) (Figura 1.4). O rRNA 18S é componente da subunidade ribossomal 40S ao passo que os rRNAs 5,8S e 25S, juntamente com o rRNA 5S, transcrito de forma independente pela RNA Pol III, compõem a subunidade ribossomal 60S.

O pré-rRNA 35S é primeiramente clivado na região 5'ETS no sítio A_0, gerando o pré-rRNA 33S, seguido de clivagem no sítio A_1, na extremidade 5' do rRNA 18S, gerando o pré-rRNA 32S que por sua vez é clivado no sítio A_2 na região ITS1, gerando os intermediários 20S e $27SA_2$ (figura 1.4). O pré-rRNA 20S, precursor do rRNA 18S, é então clivado no sítio D gerando o rRNA 18S maduro, já no citoplasma, enquanto o pré-rRNA $27SA_2$, precursor dos rRNAs 5,8S e 25S, continua sendo processado no núcleo. O pré-rRNA $27SA_2$ é processado nas versões maduras dos rRNAs 5,8S e 25S por duas vias

alternativas. Aproximadamente 85% da quantidade de pré-rRNA $27SA_2$ é clivada no sítio A_3, na região ITS1 pela RNase MRP, seguido da digestão exonucleolítica de Rat1 até o sítio B_{1S}. Os 15% restantes de $27SA_2$ é clivado diretamente no sítio B_{1L}. A clivagem do sítio B_2, na extremidade 3' do rRNA 25S ocorre simultaneamente à clivagem no sítio B_1. Então, as duas formas do 27SB geradas, $27SB_S$ e $27SB_L$, são processadas por vias idênticas, com clivagens no sítio C2 e C1, na região ITS2, gerando o rRNA 25S e os precursores $7S_S$ e $7S_L$. A extremidade 3' dos precursores $7S_S$ e $7S_L$ é processada pelo exossomo, gerando os rRNAs 5,8S, sendo um mais curto ($5,8S_S$) e outro mais longo ($5,8S_L$), respectivamente (Figura 1.4).

Em levedura, o processamento do pré-rRNA segue uma ordenação hierárquica nas clivagens endonucleolíticas no sentido 5' → 3', onde as primeiras clivagens ocorrem na região 5'ETS, seguida de clivagens na região ITS1 e só então os sítios na região ITS2 são processados (Grandi & Rybin, 2002; Nissan *et al.,* 2002; Kopp *et al.,* 2007; Henras *et al.,* 2008). Por outro lado, essa regra não é aplicada em mamíferos. Em mamíferos, o pré-rRNA 47S é primeiramente convertido em pré-rRNA 45S por uma clivagem no sítio A' na região 5'ETS (Kass & Craig, 1987). Em seguida, o pré-45S pode ser processado por 3 vias alternativas, dependendo de onde acontece a primeira clivagem. Na via A, a primeira clivagem ocorre no sítio 1, removendo a região 5'ETS completamente. Já na via B, o primeiro sítio a ser processado é o 2c na região ITS1, ao passo que na via C, o primeiro sítio clivado é o 4b, na região ITS2 (Figura 1.5) (Bowman *et al.,* 1981; Hadjiolova *et al.,* 1993).

Via de processamento A: na via de processamento A, a primeira clivagem no pré-rRNA 45S ocorre nos sítios A0 e 1 (5'ETS), gerando o pré-rRNA 41S contendo a extremidade 5' correspondente à extremidade 5' do rRNA 18S. O pré-rRNA 41S é então processado no sítio 2c (ITS1), separando o pré-rRNA 21S do pré-rRNA 32S. A extremidade 3' do pré-rRNA 21S é processada para gerar o rRNA 18S. O pré-rRNA 32S é clivado no sítio 4b (ITS2), gerando o pré-rRNA 12S e o rRNA 28S. Finalmente, a extremidade 3' do pré-rRNA 12S é processada, gerando o rRNA 5,8S (Figura 1.5 A e B).

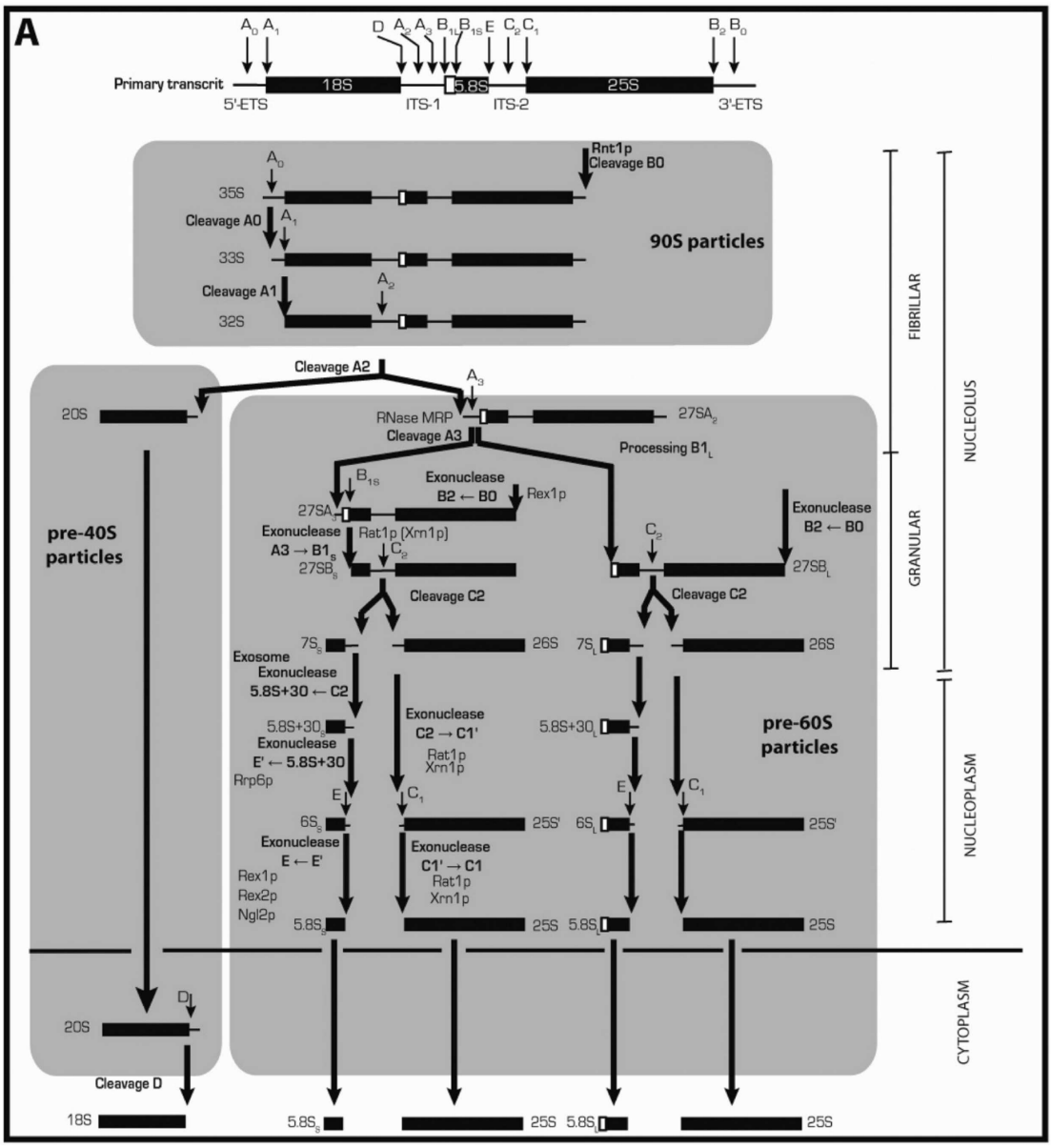

Figura 1.4: Esquema do processamento do pré-rRNA 35S em *Saccharomyces cerevisiae.* Figura extraída de (Henras *et al.,* 2008).

Via de processamento B: na via de processamento B, a primeira clivagem no pré-rRNA 45S se dá no sítio 2c (ITS1), gerando o pré-rRNA 34S e o pré-rRNA 32S. O pré-rRNA 34S é processado no sítio 1 (5'ETS), gerando o pré-rRNA 21S. Então, a extremidade 3' do pré-rRNA 21S é processada, dando

origem ao rRNA 18S. O pré-rRNA 32S é processado como na via A, sendo clivado no sítio 4b (ITS2), gerando o pré-rRNA 12S e o rRNA 28S. Então, a extremidade 3' do pré-rRNA 12S é processada gerando o rRNA 5,8S (Figura 1.5 A e B).

Via de processamento C: na via de processamento C, a primeira clivagem no pré-rRNA 45S acontece no sítio 4b (ITS2), gerando o pré-rRNA 37S e o rRNA 28S. Então o pré-rRNA 37S é processado no sítio 1 (5'ETS), gerando o pré-rRNA 26S, o qual é clivado no sítio 2 (ITS1), dando origem ao rRNA 18S e ao pré-rRNA 17S. Em seguida, o pré-rRNA 17S é processado no sítio 3 (ITS1), gerando o pré-rRNA 12S, que por sua vez, é processado na extremidade 3', originando o rRNA 5,8S (Figura 1.5 A).

A presença de diferentes precursores intermediários aos rRNAs 18S, 5,8S e 28S fornecem evidências de que, em células humanas, as vias alternativas de processamento do pré-rRNA ocorrem simultaneamente, como resultado de uma alteração temporal na ordem das clivagens nos sítios das regiões 5'ETS, ITS1 e ITS2 (Bowman *et al.,* 1981; Hadjiolova *et al.,* 1993).

O estudo sistemático do processamento do pré-rRNA 47S ainda é precário em mamíferos. As vias alternativas de processamento são revistas continuamente e novos precursores e sítios de clivagens tem sido descritos. A presença do precursor 46S sugere que o sítio A' é o primeiro sítio a ser clivado (Kass & Craig, 1987), antes da clivagem no sítio 6 na extremidade 3' do rRNA 28S. Por outro lado, a presença do precursor 45.5S sugere que a clivagem no sítio 6 acontece antes da clivagem no sítio A'. Além disso, o intermediário 45.5S pode ser clivado na região ITS1, originando o pré-rRNA 34.5S (Wang & Pestov, 2011).

A presença do precursor 29S indica que o pré-rRNA 34S é clivado no sítio A0 antes de ser clivado no sítio 1, correspondente à extremidade 5' do rRNA 18S. O intermediário 21S-C, precursor do rRNA 18S, sugere um novo sitio de processamento na região ITS1, entre os nucleotídeos 620 e 655 (Carron *et al.,* 2011). Um outro precursor, denominado 18S-E, contém cerca de 20 a 30 nucleo-

A

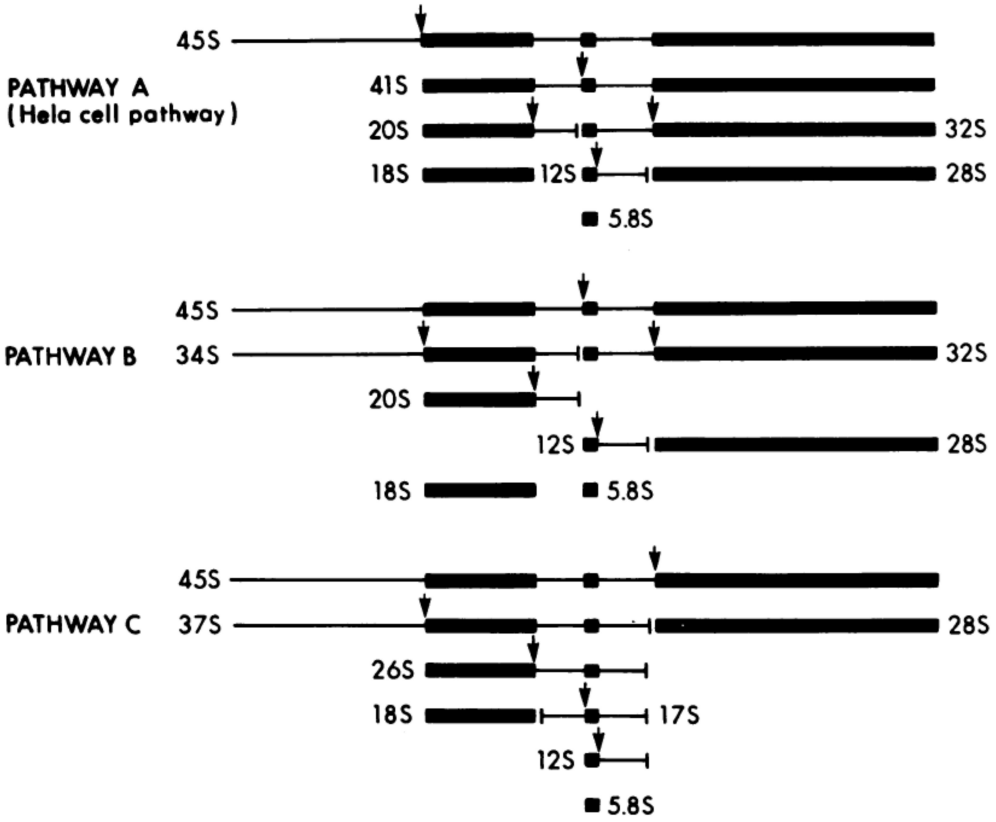

B

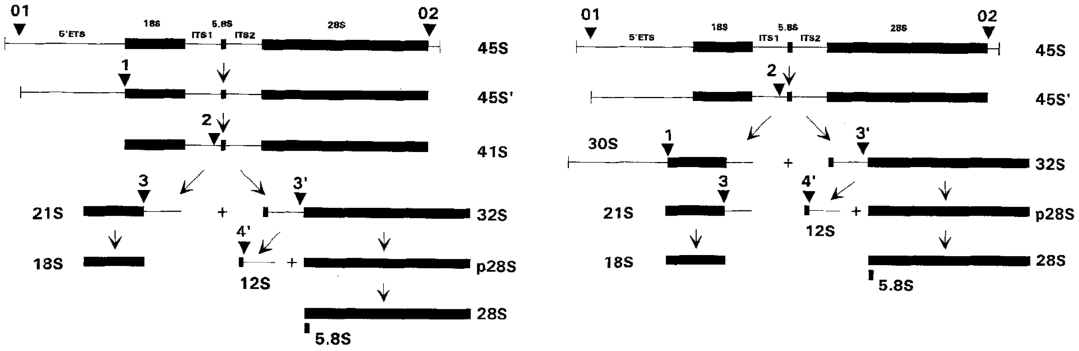

Figura 1.5: Representação esquemática das vias alternativas de processamento do pré-rRNA em células humanas. A distinção está na primeira clivagem que pode ocorrer na região 5'ETS, ITS1 ou ITS2. Figura A extraída de (Bowman *et al.,* 1981). Figura B modificada de (Hadjiolova *et al.,* 1993).

tídeos da região ITS1 em sua extremidade 3' e já foi detectado em ribossomos funcionais no citoplasma (Rouquette *et al.,* 2005). Por fim, alguns produtos das regiões ETSs e ITSs, gerados a partir das clivagens endonucleolíticas, são estáveis o bastante para serem detectados, acrescentando novos intermediários às vias de processamento do pré-rRNA 47S (Kent *et al.,* 2009; Wang & Pestov, 2011).

Muitos dos avanços recentes feitos para a identificação de fatores envolvidos no processamento do pré-rRNA em eucariotos são provenientes de estudos bioquímicos e genéticos em leveduras. Dentre esses fatores, estão endorribonucleases (Rnt1p e RNase MRP) (Elela *et al.,* 1996; Lygerou *et al.,* 1996), exorribonucleases com atividade no sentido 5' → 3' (Xrn1p e Rat1p) (Henry *et al.,* 1994; Johnson, 1997), mais de 10 exorribonucleases com atividade no sentido 3' → 5' que compõem o exossomo (Mitchell *et al.,* 1997; Allmang *et al.,* 1999b), RNA helicases (Drs1p, Sbp4p, Rrp3p e Rok1p) (O'Day *et al.,* 1996; Venema *et al.,* 1997; la Cruz *et al.,* 1998) e diversos fatores não catalíticos necessários para o processamento correto dos rRNAs, como Nop1p, Nop2p, Nop3p, Nop8p, Nip7p, entre outros) (Henríquez *et al.,* 1990; Russell & Tollervey, 1992; Hong *et al.,* 1997; Zanchin *et al.,* 1997; Zanchin & Goldfarb, 1999a).

Em mamíferos, diferentemente de leveduras, relativamente poucos fatores envolvidos no processamento dos rRNAs foram caracterizados. Dentre os fatores já descritos, temos aqueles que associam-se com o complexo snoRNP contendo o snoRNA U3, o qual participa das clivagens iniciais na região 5'ETS do pré-rRNA. Este complexo ribonucleoprotéico, conhecido como "processomo SSU" (*Small Subunit Processome*), atua diretamente na maturação do rRNA 18S (Fromont-Racine *et al.,* 2003). Neste grupo estão a nucleolina (Ginisty *et al.,* 1998), fibrilarina (Kass *et al.,* 1990), WDR3 (McMahon *et al.,* 2010), MPP10 (Westendorf *et al.,* 1998), Imp3 e Imp4 (Granneman *et al.,* 2003) e as UTPs – hUtp14a (Hu *et al.,* 2011), UTP4, UTP5, UTP10, UTP15, UTP17 (Prieto & McStay, 2007). Outros fatores também associados à maturação do rRNA 18S são: hRio2 (Rouquette *et al.,* 2005), NOP132 (Sekiguchi *et al.,* 2006), bysl (Adachi *et al.,* 2007), RPS19 (Idol *et al.,* 2007) e hTrs1 e bystin (Carron *et al.,*

2011). Com relação aos fatores envolvidos na maturação dos rRNAs 5,8S e 28S, tem-se o complexo PeBoW, formado pelas proteínas Pes1, Bop1 e WDR12 (Strezoska *et al.,* 2000; Lapik *et al.,* 2004; Hölzel *et al.,* 2005; Grimm *et al.,* 2006); as proteínas p120 (Gustafson *et al.,* 1998), B23/nucleofosmina (Savkur & Olson, 1998), RNase III (Wu *et al.,* 2000), p68 e p72/p82 (Jalal *et al.,* 2007), ISG20L2 (Couté *et al.,* 2008), ERI-1 (Ansel *et al.,* 2008), SENP3 (Haindl *et al.,* 2008), nucleostemina (Romanova *et al.,* 2009), Nol9 (Heindl & Martinez, 2010), Las1L (Castle *et al.,* 2010), Xrn2 (Wang & Pestov, 2011) e o exossomo. Um caso em particular é a proteína Par-14, a qual mostrou-se envolvida na via de maturação do rRNA 18S bem como na via de maturação dos rRNAs 5,8S e 28S (Fujiyama-Nakamura *et al.,* 2009).

O exossomo humano é um complexo protéico com atividade exorribonuclease no sentido 3' → 5'. É formado por 9 componentes principais e pela proteína associada PM/Scl-100. Em levedura, o exossomo está associado principalmente à maturação da extremidade 3' do rRNA 5,8S, além de ter sido associado a clivagens do pré-rRNA nos sítios A_0, A_1, A_2 e A_3 (Mitchell *et al.,* 1996; Briggs *et al.,* 1998; Zanchin & Goldfarb, 1999b; Allmang *et al.,* 1999a; 2000; Schneider *et al.,* 2008; Lebreton *et al.,* 2008b). A função na maturação da extremidade 3' do rRNA 5,8S é conservada no exossomo humano na presença das proteínas associadas PM/Scl-100, MPP6, C1D e hMtr4a (Schilders *et al.,* 2005; Schilders *et al.,* 2007).

Embora os fatores acima descritos sejam necessários para o processamento correto dos rRNAs em mamíferos, as endorribonucleases responsáveis pelas clivagens endonucleolíticas ainda não foram identificadas. A atividade de endonuclease do exossomo já foi demonstrada em levedura (Schneider *et al.,* 2008; Lebreton *et al.,* 2008b), sugerindo que o mesmo possa desempenhar tal função em mamíferos. B23/nucleofosmina já foi associada a clivagens endonucleolíticas preferenciais na região ITS2, porém apenas *in vitro* (Savkur & Olson, 1998). Em células humanas, foi demonstrado que a depleção da RNase III leva ao aumento dos níveis dos precursores 32S e 12S, sugerindo o envolvimento dessa ribonuclease nas clivagens na região ITS2 (Wu *et al.,*

2000). No entanto, em levedura, os sítios de clivagens da RNase III (RNT1) foram mapeados nas regiões 5'ETS e 3'ETS (Elela *et al.,* 1996). Assim, a RNase III humana parece estar envolvida em clivagens do pré-rRNA distintas daquelas observadas em levedura.

Levando-se em consideração o número de fatores envolvidos no processamento do pré-rRNA em levedura, é possível inferir que a maioria dos fatores envolvidos no processamento do pré-rRNA em mamíferos ainda não foi caracterizada. A caracterização desses fatores será necessária para o entendimento completo do mecanismo de processamento do pré-rRNA e montagem dos ribossomos em células humanas.

1.4. Modificações covalentes nos rRNAs

Durante a transcrição e processamento do pré-RNA, os RNAs ribossomais são modificados de forma covalente em nucleotídeos específicos. Pseudo-uridinilação e metilação são os dois principais tipos de modificações. No processo de pseudo-uridinilação, uridinas são isomerizadas em pseudo-uridinas (ψ) por meio de rotação de base (Figura 1.6). Na metilação, o grupo metil é adicionado principalmente na posição 2'-OH da ribose (Nm) (Figura 1.6) e, em alguns casos, o grupo metil pode ser adicionado nas bases (mN). O número de modificações e a complexidade dos mecanismos envolvidos variam entre e dentro dos domínios filogenéticos. Em *E. coli*, os rRNAs apresentam 10 ψ, 4 Nm e 19 mN, sendo estas modificações, realizadas diretamente por enzimas sítio-específicas. *S. cerevisiae* apresenta 44 ψ, 54 Nm e 10 mN, ao passo que em *H. sapiens*, os números representam ~91 ψ, 105 Nm e 10 mN (Maden, 1990; Ofengand & Bakin, 1997; Ofengand & Fournier, 1998).

Em contraste ao sistema bacteriano, onde a metilação e a pseudo-uridinilação são mediadas por enzimas sítio-específicas, em eucariotos, as modificações equivalentes nos rRNAs são direcionadas por pequenos RNAs nucleolares (*small nucleolar RNAs,* snoRNAs) associados a proteínas em

complexos ribonucleoprotéicos (*small nucleolar RiboNucleoProtein*, snoRNP). Neste caso, o mecanismo de modificação depende da complementariedade e pareamento de bases entre o snoRNA e o rRNA na região do nucleotídeo a ser modificado (Balakin *et al.,* 1996; Kiss-László *et al.,* 1996). Dessa forma, esses pequenos RNAs nucleolares são conhecidos como “guias”, pois direcionam a maquinaria de modificação, os snoRNPs, aos alvos a serem modificados. Exceção à regra, em levedura, duas proteínas, Dim1p e Spb1p, já foram associadas à metilação sítio-específica de bases e riboses no rRNA, respectivamente (Lafontaine *et al.,* 1994; 1995; Lapeyre & Purushothaman, 2004).

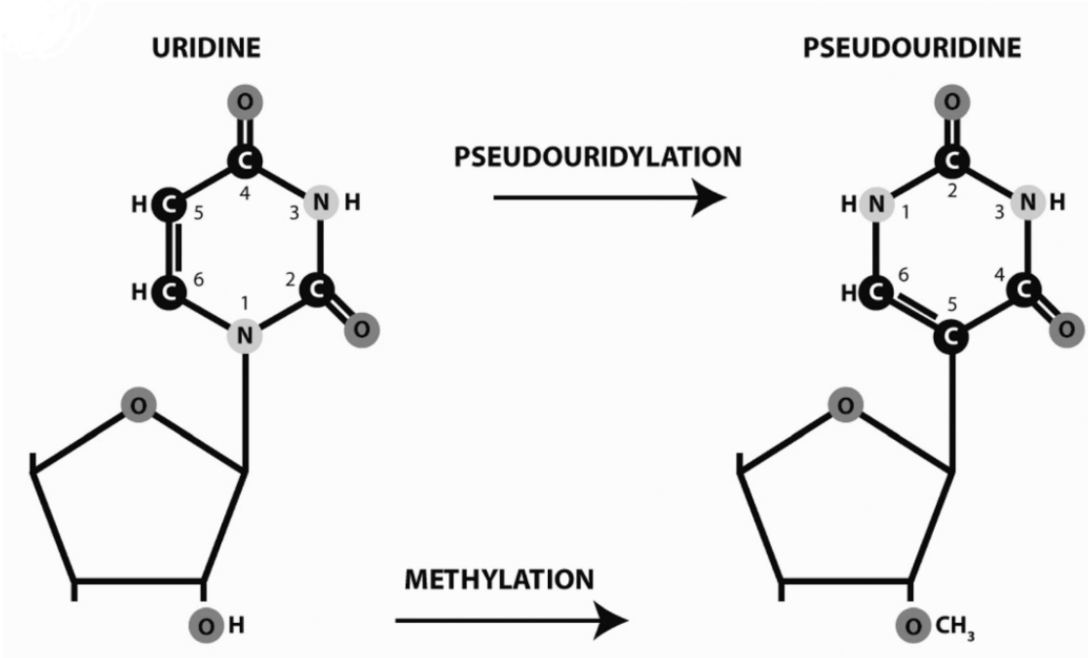

Figura 1.6: Principais tipos de modificações encontradas em rRNAs. Pseudo-uridinilação (conversão de uridina em pseudo-uridina) e metilação na posição 2’-OH da ribose. Figura modificada de (Henras *et al.,* 2008).

Existem 2 grupos de snoRNPs: o snoRNP *C/D box*, associado ao processo de metilação (Tycowski *et al.,* 1996) e o snoRNP *H/ACA box*, responsável pela pseudo-uridinilação (Ganot *et al.,* 1997; Ni *et al.,* 1997). A terminologia *C/D box* e *H/ACA box* é derivada de elementos de sequência conservada presentes nos

pequenos RNAs nucleolares componentes dos snoRNPs. No *C/D box*, o snoRNA contém as sequências UGAUGA (*box C*) e CUGA (*box D*) perto das extremidades 5' e 3', respectivamente (Figura 1.7). Alguns desses snoRNAs apresentam sequências adicionais conservadas no centro, chamadas *C'* e *D'* (Figura 1.7). A complementariedade de bases entre o snoRNA (10 a 20 nucleotídeos), próximo do *box D*, e o rRNA alvo, direciona a metilação do 5º nucleotídeo antes do elemento *D*/*D'* (Figura 1.7) (Kiss-László *et al.,* 1996). O snoRNA *H/ACA box* é caracterizado por um tipo de snoRNA com estrutura secundária definida como "*hairpin-hinge-hairpin-tail*" contendo duas sequências curtas conservadas, chamadas *box H* e *box ACA* (Figura 1.7). Os *hairpins* formam *loops* com sequências complementares ao rRNA alvo em ambos os lados internos do *loop*, imediatamente antes e depois da uridina a ser modificada, de forma que esta uridina, não pareada, fique exposta no bolso de pseudo-uridinilação, localizada a 14-16 nucleotídeos dos elementos *H* ou *ACA* (Ganot *et al.,* 1997) (Figura 1.7).

Os snoRNAs são encontrados em associação com proteínas específicas para cada um dos dois grupos de snoRNPs: fibrilarina/Nop1, Nop56, Nop58/Nop5 e Snu13 constituem os snoRNPs *C/D box*, ao passo que disquerina/Cbf5, Gar1, Nhp2 e Nop10p formam os snoRNPs *H/ACA box* (Kiss, 2001) (Figura 1.7). Aparentemente, uma única enzima é responsável por cada tipo de modificação em seu respectivo complexo, sendo a fibrilarina/Nop1 associada à metilação (Tollervey *et al.,* 1993) e a disquerina/Cbf5 associada à pseudo-uridinilação (Lafontaine *et al.,* 1998).

Ortólogos de snoRNAs *C/D box* foram caracterizados em Archaea (Dennis *et al.,* 2001). Estas moléculas têm um repertório simples de proteínas associadas e apresentam habilidade de formarem complexos proteína-RNA funcionais no núcleo de *Xenopus laevis* (Speckmann *et al.,* 2002), evidenciando sua relação evolutiva. O conceito de RNAs que direcionam a formação de Ψ (*H/ACA box*) também está presente em Archaea, pois estudos identificaram proteínas ortólogas às encontradas nos snoRNPs *H/ACA box* de eucariotos (Watanabe & Gray, 2000).

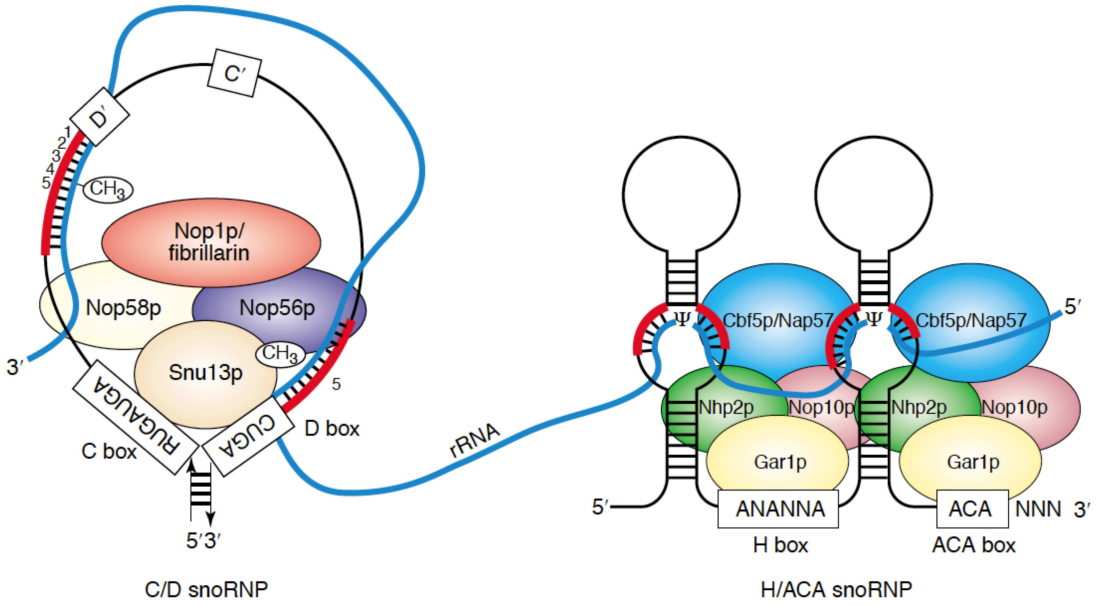

Figura 1.7: Esquema das interações estabelecidas entre o pré-rRNA e os snoRNAs *C/D box* (esquerda) e *H/ACA box* (direita) e proteínas associadas. Figura extraída de (Brown *et al.,* 2003).

Notavelmente, as modificações são quase ausentes em regiões dos rRNAs associadas a proteínas ribossomais (Yusupov *et al.,* 2001). A ausência de nucleotídeos modificados nestas regiões indicam que a maioria das interações proteína-rRNA no ribossomo não são afetadas diretamente por essas modificações. Consequentemente, essas modificações acumulam-se em regiões funcionais do ribossomo, sugerindo que as mesmas são essenciais para a estrutura e estabilidade dos rRNAs, bem como para o processo de tradução (Decatur & Fournier, 2002). No entanto, o papel das bases e riboses modificadas nos rRNAs não está claro, uma vez que a eliminação isolada de muitas delas tem pouco efeito no crescimento celular e biogênese e função dos ribossomos (Parker *et al.,* 1988; King *et al.,* 2003).

Enquanto a atividade dos snoRNAs parece não ser regulada, sua biossíntese é coordenada com os componentes da maquinaria de tradução. Surpreendentemente, a maioria desses snoRNAs em vertebrados e levedura

estão albergados em regiões intrônicas de genes que codificam proteínas envolvidas na biogênese de ribossomos (Bachellerie *et al.,* 2002; Brown *et al.,* 2003). Estes snoRNAs ainda podem ser transcritos de forma independente, mono- ou policistronicamente, porém as regiões promotoras desses genes apresentam sítio de ligação para Rat1p, proteína relacionada ao controle da atividade transcricional de proteínas ribossomais (Qu *et al.,* 1999).

1.5. Complexos pré-ribossomais em eucariotos

A síntese de ribossomos começa no nucléolo das células eucarióticas, com a produção do transcrito primário, contendo os rRNAs 18S, 5,8S e 25/28S. Concomitantemente à transcrição do pré-rRNA, diversos fatores envolvidos na biogênese de ribossomos, bem como componentes integrais das partículas ribossomais se juntam formando o complexo inicial, chamado partícula pré-ribossomal 90S, ou simplesmente pré-rRNP 90S (Figura 1.8) (Grandi & Rybin, 2002). A composição do pré-rRNP 90S já foi investigada em levedura, demonstrando a presença do pré-rRNA 35S e do snoRNA U3 (Grandi & Rybin, 2002). Uma característica notável do pré-rRNP 90S, em termos de composição protéica, é a presença predominante de fatores envolvidos na formação da subunidade ribossomal 40S (Grandi & Rybin, 2002). Dentre as 40 proteínas não-ribossomais identificadas no pré-rRNP 90S, 14 estão envolvidas no processamento e maturação do rRNA 18S (Gar1p, Rrp12p, Krr1p, Kre31p, Kre33p, Utp20p, Utp22p, Noc4p, Nop14p, Emg1p/Nep1p, Enp1p, Enp2p, Bfr2p e YKR060wp) e 22 são proteínas associadas com o snoRNA U3 (Bms1p, Nop1p, Nop5/58p, Nop56p/Sik1p, Sof1p, Rrp5p, Rrp9p, Dhr1p, Imp3p, Imp4p, Mpp10p, Utp1p, Utp2p, Utp4p, Utp6p, Utp8p, Utp9p, Utp10p, Utp12p, Utp13p, Utp15p e Utp17p), sendo 21 destas, proteínas componentes do processomo SSU (Dragon *et al.,* 2002; Grandi & Rybin, 2002). A presença dessas proteínas do processomo SSU indicam que o pré-rRNP 90S é uma partícula pré-ribossomal associada ao processomo SSU. No entanto, sete componentes do processomo

SSU (Snu13p, Utp3p, Utp5p, Utp7p, Utp11p, Utp14p e Utp16p) não foram identificados em nenhum complexo pré-rRNP 90S (Takahashi *et al.,* 2003). Ainda, a proteína Bms1p, associada ao snoRNA U3 e à formação da subunidade ribossomal 40S, porém não associada ao processomo SSU, foi detectada nos complexos pré-RNP 90S (Takahashi *et al.,* 2003). A hipótese é de que a substituição de Snu13p por Bms1p leva ao desligamento sucessivo dos componentes do processomo SSU do pré-rRNP 90S, porém isso ainda não foi demonstrado.

A ausência de fatores envolvidos na síntese da subunidade ribossomal 60S no pré-rRNP 90S é uma característica intrigante. Isso leva à crer que a síntese de ribossomos inicia-se com a formação da subunidade ribossomal 40S, uma vez que a maioria dos componentes do pré-rRNP 90S estão associados com a formação da partícula ribossomal 40S e a clivagens iniciais no pré-rRNA 35S. Sendo assim, Takahashi e colaboradores (2003) nomearam o pré-rRNP 90S como VEN pré-90S, do termo em inglês, *Very Early Nucleolar* pré-90S. A caracterização proteômica do pré-rRNP 90S suporta a dicotomia na formação das subunidades ribossomais, sendo a subunidade 40S formada incialmente, seguida da ligação de fatores envolvidos na síntese da subunidade 60S (Figura 1.8) (Grandi & Rybin, 2002).

A partícula pré-ribossomal 40S é liberada do complexo pré-rRNP 90S após a clivagem do pré-rRNA 32S no sítio A_2 na região ITS1. A partícula pré-40S apresenta poucos componentes não ribossomais. Alguns deles provenientes do pré-RNP 90S (Dim1p, Dim2p, Enp1p, Hrr25p, Nob1p, Prp43p, Rrp12p e Tsr1p) (Chen *et al.,* 2003; Fatica *et al.,* 2003; Schäfer *et al.,* 2003; Oeffinger *et al.,* 2004; Vanrobays *et al.,* 2004; Lebaron *et al.,* 2005) e outros que associam-se à partícula pré-40S já individualizada (Ltv1p, Pfa1p/Sqs1p, Rio1p e Rio2p) (Vanrobays *et al.,* 2001; Schäfer *et al.,* 2003; Vanrobays *et al.,* 2003; Loar *et al.,* 2004; Lebaron *et al.,* 2005).

Por outro lado, a partícula pré-60S apresenta diversos fatores não-ribossomais que se dissociam ao passo que a maturação do pré-rRNA procede e a partícula pré-60S move-se do nucléolo para o nucleoplasma até ser

transportada para o citoplasma (Nissan *et al.,* 2002). Baseado na composição protéica, Nissan e colaboradores (2002) propuseram 5 classes de partículas pré-60S, representando 5 estágios distintos para a maturação da subunidade ribossomal 60S: 1 – partícula pré-60S nucleolar altamente complexa (HCN pré-60S); 2 – partícula pré-60S nuclear/nucleolar complexa (CNN pré-60S); 3 – partícula pré-60S nucleoplásmica intermediária complexa (ICN pré-60S); 4 – pré-ribossomo 60S nuclear-citoplasmático intermediário complexo (ICNC pré-60S) e 5 – pré-ribossomo 60S citoplasmático simples (SC 60S).

Como exemplo do complexo HCN, Nissan e colaboradores (2002) purificaram partículas contendo a proteína Nsa3p. Eles encontraram 21 proteínas envolvidas na biogênese da subunidade ribossomal 60S (Brx1p, Drs1p, Ebp2p, Nip7p, Noc1p, Noc2p, Nop2p, Nop4p, Nop7p, Nop12p, Nop16p, Rlp7p, Rlp24p, Rpf1p, Rpf2p, Rrp1p, Rrp6p, Sda1p, Sqt1p, Tif6p e Ytm1p) e 10 proteínas envolvidas na síntese da subunidade 40S, muitas delas envolvidas no processamento do pré-rRNA na região ITS1 (Rrp5p, Rrp8p, Rrp9p, Ssf1p e Ssf2p). Os autores concluíram que Nsa3p liga-se à pré-partícula 60S inicial e possivelmente ao pré-rRNP 90S. Num outro exemplo, o complexo HCN foi purificado a partir de partículas contendo a proteína Nop7p. Neste caso Nissan e colaboradores (2002) encontraram apenas fatores envolvidos na síntese da subunidade 60S (Nop7p, Tif6p, Nip7p, Brix1p, Nog1p, Mak16p, Has1p, Drs1p, Erb1p, Rpf1p, Ebp2p, Rlp7p, Rrp1p, Spb1p, Ytm1p, Nsa3p, Nsa1p, Nsa2p, Rlp24p, Nop15p, Lcp1p, Mrt4p e Nop16p). Embora Nissan e colaboradores (2002) classificaram os pré-RNPs 60S contendo Nsa3p e Nop7p na mesma categoria, HCN, Takahashi e colaboradores (2003) propuseram alocar o complexo pré-RNP 60S contendo Nsa3p em uma nova classe, HCNT, partícula pré-40-60S nucleolar altamente complexa transitória, devido à presença de fatores envolvidos na síntese da subunidade 40S.

As partículas pré-60S nuclear/nucleolar complexa (CNN pré-60S) foram purificadas a partir de complexos contendo a proteína Nug1p. Estes complexos apresentaram os seguintes componentes: Arx1p, Dbp2p, Dbp10p, Nop2p, Sqt1p, Sda1p, Nug1p, Nug2p, Rea1p, YCR072cp, YPL146cp, Mdn1p,

YHR197wp, Kre32p, Nog2p, Rix1p e Noc3p. Alguns desses componentes, envolvidos com o transporte das partículas pré-60S, já haviam sido identificados em complexos contendo Nug1p (Nug1p, Nug2p, Kre32p, YPL146cp, Rix1p e Noc3p) (Rout *et al.,* 2000; Milkereit *et al.,* 2001; Takahashi *et al.,* 2003).

A composição protéica das partículas pré-ribossomais tornam-se menos complexas ao passo que estas vão sendo formadas, devido à dissociação dos fatores não-ribossomais ao longo do processo de maturação. Por exemplo, os complexos pré-RNPs 60S contendo as proteínas Rix1p e Sda1p, classificados como ICN pré-60S (partícula pré-60S nucleoplásmica intermediária complexa) apresentam diversos fatores envolvidos na formação e transporte da subunidade ribossomal 60S. Ambos apresentam basicamente a mesma composição protéica (Arx1p, Nap1p, Nog1p, Nop7p, Nug1p, Nug2p, Rea1p, Rix1p, Sqt1p, Tif6p, YCR072cp, YNL182cp e YPL146cp). Já os complexos pré-RNPs 60S contendo a proteína Arx1p, são classificados como pré-ribossomo 60S nuclear-citoplasmático intermediário complexo (ICNC pré-60S). Embora o complexo ICNC pré-60S apresente 22 fatores não-ribossomais, apenas 4 fatores estão envolvidos com a formação da subunidade 60S (Nop7p, Sda1p, Sqt1p e Tif6p). Após o transporte da partícula pré-60S do núcleo para o citoplasma, muitos dos fatores são dissociados e a partícula torna-se muito mais simples, representada por complexos contendo a proteína Kre35p (Arx1p, Kre35p, Nmd3p, Sqt1p, YBR267wp, YCR072cp e Yvh1p). Dessa forma, o complexo localizado no citoplasma é classificado como pré-ribossomo 60S citoplasmático simples (SC 60S).

Em geral, as características básicas de processamento do pré-rRNA e montagem e transporte das subunidades ribossomais são conservadas evolutivamente dentro dos eucariotos. Dessa forma, os estudos genéticos e a caracterização proteômica de complexos pré-ribossomais feitos em levedura podem ser úteis no entendimento do sistema em eucariotos superiores, como por exemplo, em mamíferos.

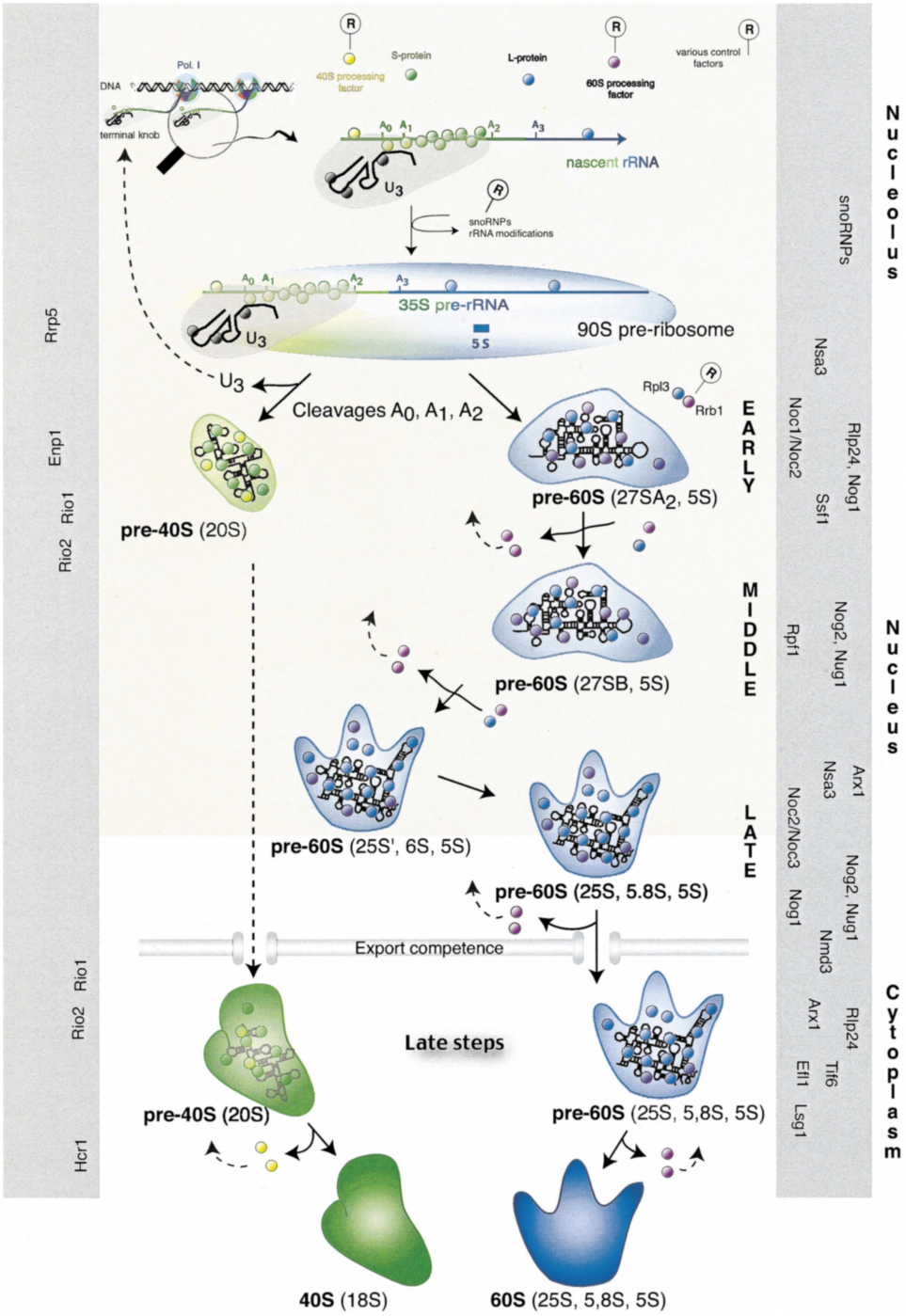

Figura 1.8: Representação geral simplificada da síntese de ribossomos em eucariotos. A figura mostra a dicotomia na maquinaria de síntese das subunidades ribossomais. A montagem da subunidade ribossomal 40S inicia-se enquanto o pré-rRNA 35S ainda é transcrito. Destaque para alta quantidade de proteínas ribossomais componentes da subunidade 40S no complexo pré-RNP 90S e para a montagem e maturação da subunidade 60S que compreendem os passos inicial, médio e tardio, ao longo do nucléolo e nucleoplasma. A maturação final de ambas as subunidades se dá no citoplasma (*Late steps*). Alguns fatores envolvidos na biogênese de ribossomos estão descritos ao lado. Figura extraída de (Fromont-Racine *et al.,* 2003).

Em mamíferos, alguns complexos contendo proteínas envolvidas na biogênese de ribossomos, bem como proteínas ribossomais, já foram caracterizados de acordo com sua composição protéica. Este é o caso para a nucleolina (NCL), parvulina (Par14), NOP56, nucleofosmina (NPM), SBDS, ISG20L2 e RPS19. O complexo contendo a NCL, proteína envolvida na biogênese de ribossomos em células humanas (Ginisty *et al.,* 1998; Ginisty *et al.,* 2000), revelou a presença de 92 proteínas, sendo 64 proteínas ribossomais e 28 fatores não-ribossomais (Yanagida *et al.,* 2001; Natsume *et al.,* 2002). Baseado na composição protéica, esse complexo foi proposto como pertencente à partícula pré-60S nucleolar altamente complexa (HCN pré-60S), embora foram identificados 4 fatores associados à biogênese da subunidade ribossomal 40S (Takahashi *et al.,* 2003). No complexo contendo a Par14, proteína envolvida no processamento do pré-rRNA em células humanas (Fujiyama-Nakamura *et al.,* 2009), foram identificadas 102 proteínas, sendo 45 proteínas ribossomais e 57 fatores não-ribossomais (Fujiyama *et al.,* 2002; Takahashi *et al.,* 2003). Desses 57 fatores não-ribossomais, 35 estão envolvidos na biogênese de ribossomos, fazendo-se analogia com seus prováveis ortólogos em leveduras. Dentre eles, encontram-se NIP7 e FTSJ3. Este complexo apresenta proteínas ribossomais e fatores envolvidos na síntese de ambas as subunidades ribossomais. A presença dos prováveis ortólogos de levedura Noc1 e Noc2 sugere que o complexo contendo Par14 seja formado em estágios iniciais da biogênese de ribossomos no nucléolo em células humanas. Devido à ausência de uma provável ortóloga em levedura, o papel da Par14 na biogênese de ribossomos em células humanas deve ser único.

Hayano e colaboradores (2003) caracterizaram o proteoma de complexos contento a proteína NOP56 em células humanas. A NOP56 é um componente do *box C/D*, associado à metilação de rRNAs (Gautier *et al.,* 1997; Newman *et al.,* 2000). Neste complexo foram identificadas um total de 107 proteínas. Destas, 62 proteínas ribossomais e 45 fatores não-ribossomais. Devido à presença do pré-rRNA 47S no complexo pré-rRNP contendo a NOP56, os autores inferiram que este complexo contém partículas pré-ribossomais em

estágios iniciais na biogênese de ribossomos. No entanto, curiosamente, não foram identificados fatores associados ao processomo SSU ou fatores envolvidos na biogênese da subunidade ribossomal 40S neste complexo. Dessa forma, o complexo pré-rRNP contendo NOP56 difere substancialmente do pré-rRNP 90S de levedura, o qual contém os componentes do processomo SSU.

Complexos de massa molecular acima de 370 kDa contendo a proteína nucleofosmina foram isolados e caracterizados a partir de extratos de células HeLa (Maggi *et al.,* 2008). Neste complexo, os autores identificaram um total de 23 proteínas, sendo 10 proteínas ribossomais constituintes das subunidades 40S e 60S. Além disso, foram identificadas proteínas associadas à biogênese e transporte das partículas pré-ribossomais (Bop1, Ebp1, Nup50 , Nup62 e Crm1).

A caracterização de complexos contendo a proteína SBDS foi feita através de imunoprecipitação e identificação dos componentes associados aos complexos contendo a proteína recombinante SBDS-FLAG em células HEK293 (Ball *et al.,* 2009). Consistente com a função da SBDS na biogênese da subunidade ribossomal 60S, neste trabalho foram identificadas 27 proteínas, sendo muitas delas, proteínas ribossomais com significativo enriquecimento em componentes da subunidade ribossomal 60S (RPL3, RPL4, RPL5, RPL6, RPL7, RPL7a, RPL8, RPL12, RPL13, RPL14, RPL18, RPLP0) contra apenas uma proteína da subunidade 40S (RPS3). A presença da nucleolina e nucleofosmina suportam ainda mais a hipótese de que o complexo contento SBDS participa da biogênese de ribossomos.

A proteína ISG20L2 também foi caracterizada como fator envolvido na biogênese de ribossomos em células humanas (Couté *et al.,* 2008). Complexos contendo ISG20L2 revelaram 18 proteínas, dentre as quais, 3 proteínas envolvidas na biogênese de ribossomos (nucleolina, B23/nucleofosmina e RNA helicase II), 11 proteínas ribossomais da subunidade 60S (RPL4, RPL6, RPL7, RPL7a, RPL8, RPL10a, RPL18, RPL18a, RPL21, RPL27 e RPL31) e 4 proteínas ribossomais da subunidade 40S (RPS6, RPS9, RPS23 e RPS26).

Componentes integrais do ribossomo também já foram utilizados na caracterização proteômica de complexos pré-ribossomais em células humanas.

Como exemplo, tem-se o complexo contendo a proteína ribossomal S19, componente da subunidade 40S (RPS19) (Orrù *et al.,* 2007). Neste trabalho, os autores identificaram 159 proteínas, sendo 101 proteínas nucleolares e muitas delas componentes do pré-rRNP 90S, fazendo-se analogia ao pré-rRNP 90S de levedura. Dentre as diversas classes de proteínas identificadas no complexo contendo RPS19, destacam-se proteínas ribossomais da subunidade 60S (RPL3, RPL4, RPL6, RPL7, RPL7a, RPL8, RPL9, RPL10a, RPL14, RPL24, RPL27a, RPLP0, RPLP1, RPLP2), da subunidade 40S (RPS2, RPS3, RPS4x, RPS5, RPS6, RPS7, RPS8, RPS10, RPS14, RPS16, RPS23, RPS24, RPS26, RPSA) e fatores envolvidos na biogênese de ribossomos (NIP7, FTSJ3, nucleolina, fibrilarina, XRN2, DKC1, XPO5, XPO1, IMP3, NOP56, PES1, entre outros).

Uma revisão da literatura sugere a existência de três tipos principais de complexos pré-ribossomais com base no conteúdo de proteínas ribossomais. Um tipo de complexo contém proteínas ribossomais de ambas as subunidades, 40S e 60S, com maior quantidade de proteínas componentes da subunidade 40S, como os complexos isolados através de purificação por afinidade à RPS19 (Orrù *et al.,* 2007). Um segundo tipo de complexo contém proteínas ribossomais das subunidades 40S e 60S, porém com maior quantidade de proteínas integrais da subunidade 60S, como por exemplo, os complexos descritos para nucleolina (Yanagida *et al.,* 2001) e nucleofosmina (Lindström & Zhang, 2008; Maggi *et al.,* 2008). Nesta categoria pode-se também incluir complexos contendo Par14 (Fujiyama-Nakamura *et al.,* 2009) e NOP56 (Hayano *et al.,* 2003). Estes complexos provavelmente contém pré-rRNAs não clivados na região ITS1. Alternativamente, estes fatores associados à síntese de ribossomos podem atuar na formação de ambas as subunidades ribossomais. O terceiro tipo de complexo é altamente enriquecido em componentes integrais da subunidade ribossomal 60S, incluindo os complexos contendo as proteínas SBDS (Ball *et al.,* 2009) e ISG20L2 (Couté *et al.,* 2008). A presença desses complexos sugere que estes fatores sejam específicos para a síntese da subunidade ribossomal 60S.

1.6. Síntese de ribossomos e a regulação de p53

As células crescem, as células dividem-se. Algumas células crescem sem se dividir (exemplo: neurônios e oócitos), outras células dividem-se sem crescer (exemplo: zigoto em desenvolvimento). Para a maioria das células, entretanto, o crescimento em tamanho e a divisão celular são acoplados. Considerando-se o crescimento celular, em tamanho e número, um aspecto é extremamente importante: o crescimento celular exige a síntese de proteínas, e a síntese de proteínas exige ribossomos. Consequentemente, o crescimento celular envolve o controle da síntese de ribossomos.

A síntese de ribossomos é um processo altamente coordenado no tempo e no espaço, com início no nucléolo e término no citoplasma. Requer a atividade coordenada das três RNA Polimerases, quantidades equimolares dos rRNAs e proteínas ribossomais e a ordenação do processamento dos rRNAs e montagem das partículas ribossomais mediadas pela atividade de mais de 200 fatores que associam-se de maneira transiente ao processo. Considerando-se o consumo energético, a transcrição dos rRNAs representa cerca de 60% da transcrição celular total em levedura e os mRNAs para proteínas ribossomais representam cerca de 50% dos transcritos totais sintetizados pela RNA polimerase II (Warner, 1999). Interessantemente, a integridade do processo de síntese de ribossomos em mamíferos é monitorada pela via de HDM2-p53 (Pestov *et al.,* 2001).

O gene *TP53*, o qual codifica para a proteína p53, é um dos mais importantes supressores tumorais na célula. Este gene apresenta mutações em mais de 50% dos cânceres humanos, e ainda, os demais cânceres são frequentemente associados a fatores que modulam a estabilidade e atividade de p53 (Hollstein *et al.,* 1994; Lohrum & Vousden, 2000). Em condições normais, p53 é uma proteína pouco abundante nas células e com meia-vida curta. Porém, em resposta ao estresse celular, p53 é estabilizada e ativada para induzir parada do ciclo celular, apoptose ou senescência (Oren, 2003).

Existem diversos fatores associados à regulação de p53. Dentre os mais estudados, estão: p21, controlando o ciclo celular nas fases G1/S; 14-3-3σ,

controlando o ciclo celular nas fases G2/M; Gadd45, importante no reparo de DNA; bax, ativador da apoptose e HDM2, associada ao controle da atividade, estabilidade e localização celular de p53 (el-Deiry, 1998). HDM2, através de sua atividade de ubiquitina ligase E3, regula os níveis de p53 nas células, direcionando-a ao proteassomo para que a mesma seja degradada. Por sua vez, p53 tem HDM2 como alvo de regulação em nível transcricional. Dessa forma, HDM2 estabelece um mecanismo de regulação cíclica negativa com p53 (Haupt *et al.,* 1997; Kubbutat *et al.,* 1997).

Nos últimos anos, foi demonstrado que p53 é ativada por estresse nucleolar, via inibição de HDM2. O estresse nucleolar, por sua vez, é induzido por deficiências no processo de biogênese de ribossomos, incluindo a síntese e o processamento dos rRNAs e montagem das partículas ribossomais no nucléolo, bem como a exportação das subunidades ribossomais para o citoplasma (Rudra & Warner, 2004). O acúmulo de evidências apontam para uma função fundamental de p53 como sensor de estresse ribossomal. A primeira evidência de interação entre proteínas ribossomais e HDM2 foi demonstrada para RPL5 ligando-se em HDM2 na presença do rRNA 5S, formando um complexo ribonucleoprotéico (rRNA)-RPL5-HDM2-p53. Porém, naquele momento, o significado dessa interação não era claro (Marechal *et al.,* 1994).

Uma década mais tarde, esforços direcionados à busca de novas proteínas moduladoras de HDM2 revelaram que as proteínas integrais da subunidade ribossomal 60S, RPL5, RPL11 e RPL23, ligavam-se à HDM2 (Lohrum *et al.,* 2003; Zhang *et al.,* 2003; Bhat *et al.,* 2004; Dai & Lu, 2004; Dai *et al.,* 2004; Jin *et al.,* 2004). Estudos posteriores revelaram a interação de HDM2 com outras proteínas ribossomais da subunidade 60S (RPL26) (Ofir-Rosenfeld *et al.,* 2008), bem como proteínas ribossomais da subunidade 40S (RPS7 e RPS3) (Chen *et al.,* 2007; Yadavilli *et al.,* 2009). Esses estudos serviram de base para o estabelecimento da via de resposta ao estresse ribossomal RP-HDM2-p53, na qual proteínas ribossomais ligam-se à HDM2, inibindo sua atividade de ubiquitina ligase E3, promovendo, dessa forma, o acúmulo de p53 (Figura 1.9). A

hipótese é de que com a perturbação da síntese de ribossomos por estresse no nucléolo, haveria um desequilíbrio na estequeometria dos componentes das subunidades ribossomais, de forma que as proteínas ribossomais livres possam então interagir com HDM2, inibindo sua atividade, o que resultaria na estabilização de p53.

Estudos sobre a interação RP-HDM2 tem sugerido que o estresse nucleolar é o evento responsável pela indução da via de resposta RP-HDM2-p53. Neste contexto, estresse nucleolar significa, especificamente, perturbações no processo de síntese de ribossomos, resultando na ativação de p53. Em parte, essas observações levaram à hipótese de que o nucléolo é o regulador central da resposta ao estresse ribossomal com consequente ativação de p53 (Rubbi & Milner, 2003). Sendo assim, perturbações na síntese e processamento de rRNAs bem como em proteínas ribossomais e fatores associados à maquinaria de síntese de ribossomos podem ativar p53 (Figura 1.9).

A inibição da síntese do pré-rRNA por compostos químicos, como Actinomicina D (Ashcroft *et al.,* 2000), 5-fluorouracil (Gilkes *et al.,* 2006; Sun *et al.,* 2007) e ácido micofenólico (Sun *et al.,* 2008), bem como inativação genética de componentes associados à RNA Pol I (Yuan *et al.,* 2005; Donati *et al.,* 2011), demonstraram a ativação de p53 via RP-HDM2-p53, causando parada do ciclo celular em fase G1. Essa via também é ativada por perturbações em fatores transientes associados à biogênese de ribossomos, como reportado para Bop1 (Pestov *et al.,* 2001), WDR12 (Hölzel *et al.,* 2005), nucleofosmina (Kurki *et al.,* 2004), nucleostemina (Dai *et al.,* 2008), TCOF1 (Jones *et al.,* 2008) e hUTP18 (Holzel *et al.,* 2010). Ainda, depleção de proteínas ribossomais componentes das subunidades ribossomais 40S (RPS6 e RPS9) (Lindström & Zhang, 2008; Fumagalli *et al.,* 2009) e 60S (RPL29 e RPL30) (Sun *et al.,* 2010), também mostraram ativação de p53 mediada pela resposta RP-HDM2-p53.

Atualmente, não se sabe exatamente o porquê do envolvimento de várias proteínas ribossomais na regulação da resposta ao estresse nucleolar via HDM2-p53. Isso sugere que essas proteínas, isoladas ou em conjunto, possam atuar na regulação da via utilizando diferentes mecanismos. De acordo com esta

hipótese, tem-se que RPL5 e RPL11 exercem um efeito sinérgico na inibição de HDM2, levando à ativação robusta de p53, muito mais acentuada que o efeito exercido pelas mesmas proteínas isoladamente (Horn & Vousden, 2008).

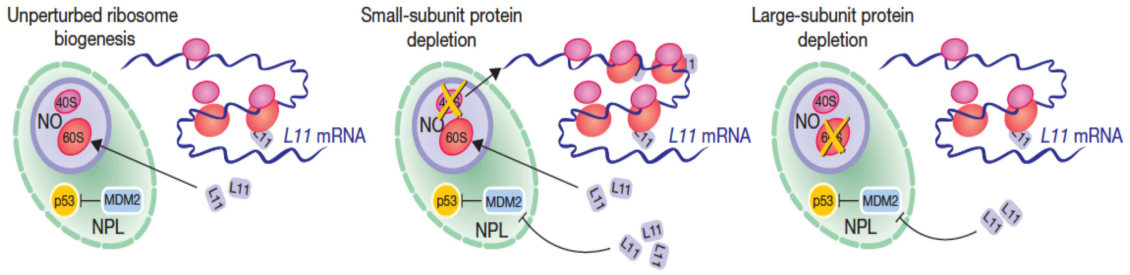

Figura 1.9: Modelo para estabilização de p53 em resposta à deficiência na biogênese de ribossomos. Durante a síntese de ribossomos, RPL11 é incorporada à partícula pré-ribossomal 60S. No entanto, defeitos neste processo ou na maturação dos rRNAs possibilitam que o excesso de RPL11 se ligue à HDM2, inibindo sua atividade de ubiquitina E3 ligase, com consequente estabilização p53. Por outro lado, quando a biogênese da subunidade 40S é deficiente, a síntese da subunidade 60S continua, levando ao aumento da tradução de 5'-TOP mRNA, permitindo, dessa maneira, que o excesso de RPL11 inative HDM2, embora a síntese global de proteínas seja inibida. NPL, nucleoplasma; NO, nucléolo. Figura extraída de (Fumagalli *et al.,* 2009).

De acordo com a função das proteínas ribossomais que interagem com HDM2 no processo de resposta ao estresse ribossomal via RP-HDM2-p53, seria lógico pensar que a depleção dessas proteínas atenuasse a resposta dependente da ativação de p53. Este é o caso para RPL11 (Bhat *et al.,* 2004), RPL5 (Dai & Lu, 2004), RPS7 (Zhu *et al.,* 2009) e RPS3 (Yadavilli *et al.,* 2009), onde a depleção dessas proteínas por RNA de interferência não afeta a estabilidade de p53. Entretanto, este não é o caso da RPL23, pois quando depletada em células em cultura, ativa a resposta de estresse ribossomal dependente de p53, causando parada no ciclo celular (Jin *et al.,* 2004). Essa discrepância de efeitos causados pela depleção de proteínas ribossomais que interagem com HDM2 sobre a ativação e estabilização de p53 sugere que existam respostas estresse-específicas dependente de proteínas ribossomais específicas para monitorar o estresse ribossomal.

1.7. Ribossomopatias

Ribossomopatia é o termo empregado para agrupar o conjunto de doenças genéticas associadas a mutações em genes que codificam proteínas ribossomais ou fatores associados à biogênese de ribossomos (Luft, 2010). Sendo o ribossomo o componente principal da maquinaria de síntese de proteínas nos organismos, é esperado que deficiências na biogênese ou função desta macromolécula levem à letalidade embrionária. No entanto, isso não é verdade e a descoberta de novas ribossomopatias vem aumentando nos últimos anos. Além disso, é surpreendente que deficiências na biogênese ou função dos ribossomos apresentem sintomas diversificados e com certo grau de propensão tecidual, visto que os ribossomos estão presentes em todos os tecidos no corpo (Freed *et al.,* 2010).

Aproximadamente 13 deficiências genéticas associadas à biogênese ou função dos ribossomos já foram descritas (Freed *et al.,* 2010). As ribossomopatias podem ser causadas por deficiências em fatores envolvidos na biogênese de ribossomos bem como por deficiências em componentes integrais dos ribossomos. Dentre as doenças associadas a deficiências em fatores envolvidos na biogênese de ribossomos, podemos destacar: a) *Síndrome de Treacher Collins (TCS)*, causada por mutações em Treacle, uma fosfoproteína nucleolar provavelmente envolvida na transcrição do DNA ribossomal (Valdez *et al.,* 2004) e metilação do rRNA 18S (Gonzales *et al.,* 2005); b) *Infertilidade masculina*, deficiência causada por mutações na proteína UTP14c, uma isoforma de UTP14, componente do processomo SSU, envolvida no processamento do pré-rRNA (Hu *et al.,* 2011), expressa especificamente nos testículos (Rohozinski & Bishop, 2004); c) *Cirrose infantil hereditária dos índios da América do Norte*, doença causada por mutações em UTP4, componente do processomo SSU envolvida no processamento do pré-rRNA (Prieto & McStay, 2007); d) *Síndrome de Bowen-Conradi*, doença letal causada por mutações em EMG1 (Armistead *et al.,* 2009), uma provável metil-transferase envolvida na biogênese da subunidade ribossomal 40S (Liu & Thiele, 2001; Eschrich *et al.,*

2002; Leulliot *et al.,* 2008); e) *Síndrome da alopécia, defeitos neurológicos e endocrinopatia* é uma doença associada a mutações em RBM28, uma proteína envolvida na biogênese da subunidade ribossomal 60S (Nousbeck *et al.,* 2008) e f) *Síndrome de Shwachman-Bodian Diamond (SDS)*, associada a mutações em SBDS, uma proteína envolvida na maturação e exportação da subunidade ribossomal 60S (Ganapathi *et al.,* 2007; Menne *et al.,* 2007).

As deficiências genéticas relacionadas a defeitos em proteínas ribossomais são duas: *Anemia de Diamond-Blackfan (DBA)*, onde mutações nas proteínas RPS15, RPS17, RPS19, RPS24, RPS27A, RPL5, RPL6, RPL11 e RPL35A estão associadas com pelo menos 50% dos casos (Draptchinskaia *et al.,* 1999; Gazda *et al.,* 2006; Cmejla *et al.,* 2007; Farrar *et al.,* 2008; Gazda *et al.,* 2008; Vlachos *et al.,* 2008) e a *Síndrome 5q*$^{-}$, associada à deficiência na proteína ribossomal RPS14 (Boultwood *et al.,* 2002; Ebert *et al.,* 2008).

As ribossomopatias ainda podem ser causadas por deficiência em pequenos complexos ribonucleoprotéicos nucleolares envolvidos na maturação dos rRNAs. Neste contexto, destacam-se a *Hipoplasia cartilagem-cabelo (CHH)*, *Disqueratose congênita (DC)* e *Síndrome de Prader-Willi (PWS)*. A *Hipoplasia cartilagem-cabelo (CHH)* é causada por mutações no gene *RMRP*, o qual codifica para o snoRNA componente do complexo RNase MRP (Ridanpää *et al.,* 2001), envolvido no processamento do pré-rRNA (Welting *et al.,* 2004). A *Disqueratose congênita (DC)* pode ser herdada de maneira recessiva ligada ao X ou autossômica dominante ou recessiva. DC ligada ao X é causada por mutações na disquerina, proteína componente do snoRNP *box H/ACA*, responsável pela pseudo-uridinilação de rRNAs e processamento do pré-rRNA (Heiss *et al.,* 1998). DC autossômica recessiva é causada por mutações nos genes *NHP2* ou *NOP10*, componentes essenciais do *box H/ACA* ou por mutações em *TERT*, transcriptase componente do complexo da telomerase. A forma autossômica dominante é causada por mutações em *TERC*, RNA componente do complexo da telomerase (Savage & Alter, 2009; Walne & Dokal, 2009). Análises em pacientes com DC tem evidenciado tanto encurtamento de telômeros quanto defeitos associados à função e biogênese dos ribossomos (He

et al., 2002; Montanaro *et al.,* 2002; Ruggero *et al.,* 2003; Mochizuki *et al.,* 2004; Yoon *et al.,* 2006). Visto que o complexo da telomerase também é um RNP *box H/ACA* contendo disquerina, estudos adicionais necessitam ser feitos com o objetivo de caracterizar a contribuição específica de cada componente dos RNPs nessa doença. A *Síndrome de Prader-Willi (PWS)* é causada por alterações cromossômicas na região 15q11-q13, região rica em RNAs não-codificadores componentes de diversos RNPs *box C/D*, o quais estão envolvidos com metilação de rRNAs e processamento do pré-rRNA (Reichow *et al.,* 2007).

Além de deficiências em proteínas ribossomais e fatores diretamente envolvidos na biogênese de ribossomos, existem doenças que são modificadas por deficiências em fatores envolvidos na síntese de ribossomos. Este grupo inclui: *Glaucoma primário de ângulo aberto (GPAA)*, doença ainda não associada a um único gene, porém, um dos candidatos é o *WDR36/UTP21*, o qual codifica para a proteína UTP21, componente do processomo SSU (Krogan *et al.,* 2004); e *Modificadores de neurofibromatose tipo 1 (NF1)*, doença causada por deleção do gene *NF1*. Em aproximadamente 5% dos casos ocorrem microdeleções de genes ao redor de *NF1*. Nestes casos, a doença é mais severa. Um dos genes candidatos nessas regiões de microdeleção é o *HCA66/UTP6* (Bartelt-Kirbach *et al.,* 2009), o qual codifica para proteína UTP6, um componente do processo SSU (Krogan *et al.,* 2004).

Embora uma ampla variedade de sintomas esteja associado com as ribossomopatias, não existe um sintoma que seja comum a todas as doenças. No entanto, alguns sintomas são mais frequentes, como por exemplo: deformidades esqueléticas, retardo mental, anemia, deficiência na medula óssea e predisposição ao câncer. A predisposição ao câncer pode ser associada à via de resposta ao estresse nucleolar, onde defeitos na biogênese de ribossomos promovem ativação de p53, como apresentado no tópico anterior. No entanto, a grande questão é: como ocorre o surgimento de sintomas tecido-específicos nas ribossomopatias? A falência da medula óssea pode ser associada à alta taxa de proliferação celular, a qual demanda síntese de proteínas, que por sua vez, exige grande quantidade de ribossomos. Porém, se esta for a explicação, como

explicar o desenvolvimento embrionário, onde todos os tecidos apresentam alta taxa de proliferação celular?

Frente à falta de explicação dos mecanismos por trás da ocorrência de sintomas tecido-específicos em ribossomopatias, faz-se algumas especulações. Talvez a preferência tecidual esteja associada a parceiros de interação tecido-específicos para o gene envolvido, ou mesmo que a expressão desse gene seja regulada de maneira tecido-específica, por meio de *splicing* alternativo ou microRNAs, entre outros. Pode ser também que haja funções extra-ribossomais tecido-específicas para algumas proteínas ribossomais associadas às doenças. A elucidação dos mecanismos envolvidos nas ribossomopatias, principalmente a razão pela qual são apresentados sintomas tecido-específicos, ainda permanece um dos maiores desafios para o futuro.

1.8. Estudo funcional das proteínas humanas NIP7 e FTSJ3 no processamento do pré-rRNA

Saccharomyces cerevisiae tem sido amplamente empregada como modelo biológico no estudo da biogênese de ribossomos em eucariotos. Em geral, assume-se que o mecanismo de síntese de ribossomos seja conservado em Eukarya devido à carência de investigações em outros sistemas eucariotos. No entanto, alguns fatores envolvidos na biogênese de ribossomos em levedura tem apresentado funções distintas em mamíferos (Gelperin *et al.,* 2001; Chen *et al.,* 2003; Léger-Silvestre *et al.,* 2004; Carron *et al.,* 2011).

Em levedura, o pré-rRNA precursor primário é processado inicialmente por uma única via, no sentido 5’ → 3’ até que a região ITS2 seja clivada e a pré-partícula ribossomal 90S seja separada em pré-partículas ribossomais 40S e 60S (Grandi & Rybin, 2002; Nissan *et al.,* 2002; Kopp *et al.,* 2007). Por outro lado, em mamíferos, o pré-rRNA 47S pode ser clivado inicialmente nas regiões 5’ETS, ITS1 ou ITS2, gerando vias de processamento distintas (Bowman *et al.,* 1981; Hadjiolova *et al.,* 1993). As diferentes vias de processamento do pré-rRNA

47S ocorrem simultaneamente em células de mamíferos (Bowman *et al.,* 1981), porém o mecanismo que define a via a ser utilizada pelas células ainda não foi estabelecido. Além disso, a ausência da caracterização proteômica dos complexos pré-ribossomais e a associação desses complexos com pré-rRNAs tem dificultado o entendimento do mecanismo geral de síntese de ribossomos em mamíferos.

A biogênese de ribossomos têm implicações adicionais em organismos multicelulares. Em humanos, por exemplo, cerca de 13 doenças genéticas já foram associadas a defeitos na síntese e/ou função dos ribossomos (Freed *et al.,* 2010). Defeitos na síntese de ribossomos também tem sido associados à ativação de p53, conectando a síntese de ribossomos com o desenvolvimento de tumores (descrito em detalhes no tópico 1.5.). Adicionalmente, foi demonstrado que o ribossomo tem função regulatória em mamíferos, onde mRNAs específicos são traduzidos pelos ribossomos de maneira seletiva durante diferentes estágios do desenvolvimento (Kondrashov *et al.,* 2011). Isso abre novas áreas de estudos no que diz respeito ao ribossomo como partícula regulatória, e não somente como um componente constitutivo da síntese de proteínas.

As diferenças existentes entre levedura e mamíferos no processamento de pré-rRNAs e montagem dos ribossomos, a associação da síntese e função dos ribossomos a doenças genéticas e câncer e o fato do ribossomo ser uma macromolécula com função regulatória, ressaltam a importância do entendimento sistemático do mecanismo de biogênese de ribossomos em mamíferos, principalmente em humanos.

Neste contexto, o objetivo geral do trabalho foi investigar o papel das proteínas NIP7 e FTSJ3 na biogênese de ribossomos em células humanas. Para tal, as proteínas em estudo foram depletadas em diferentes linhagens celulares por meio de técnicas fundamentadas no mecanismo de inibição da expressão gênica por interferência de RNA (RNAi).

No capitulo I, foi demonstrado que a proteína NIP7 humana é necessária para o processamento correto do pré-rRNA 47S, principalmente na via de

maturação do rRNA 18S e consequentemente, para a biogênese da subunidade ribossomal 40S. Por outro lado, em levedura, Nip7p está envolvida no processamento e maturação do rRNA 25S e biogênese da subunidade ribossomal 60S (Zanchin *et al.,* 1997). Com esta observação inesperada surgiu a seguinte questão: NIP7 humana complementa a deficiência de Nip7p em levedura? Em suporte aos resultados observados, foi demonstrado que NIP7 humana não apresenta capacidade de complementar Nip7p em levedura. Com isso, os resultados adicionam NIP7 à lista de fatores com funções divergentes entre levedura e mamíferos.

Na tentativa de obter-se mais informações sobre o mecanismo funcional de NIP7 humana, foi feita uma busca de parceiros de interação para NIP7 humana por meio de ensaio de duplo híbrido em levedura. Os resultados, não publicados, revelaram parceiros de interação diferentes daqueles observados para Nip7p em levedura (Zanchin & Goldfarb, 1999a). A proteína FTSJ3 foi isolada como parceira de interação mais frequente para NIP7. No capítulo II, foi confirmado que NIP7 e FTSJ3 interagem *in vivo* e ainda que essa interação NIP7-FTSJ3 é dependente de RNA. Também foi demonstrado que FTSJ3 é necessária para as clivagens iniciais do pré-rRNA 47S. Sua depleção causa acúmulo do pré-34S, o qual contém o rRNA 18S. O pré-34S é precursor dos pré-rRNAs 26S e 21S, os quais acumulam sob deficiência de NIP7. Consequentemente, FTSJ3 participa do processamento inicial do pré-rRNA 47S, principalmente na via de maturação do rRNA 18S e na biogênese da subunidade ribossomal 40S, assim como NIP7.

Os resultados apresentados sugerem que NIP7 e FTSJ3 possam ser componentes de um mesmo complexo envolvido no processamento inicial do pré-rRNA 47S, principalmente na via de maturação do rRNA 18S e biogênese da subunidade ribossomal 40S. Em suporte à esta hipótese, NIP7 e FTSJ3 já foram isoladas em complexos contendo RPS19 (Orrù *et al.,* 2007), componente integral da subunidade ribossomal 40S e em complexos contendo Par14, proteína envolvida na processamento do pré-rRNA (Fujiyama-Nakamura *et al.,* 2009). Adicionalmente, em busca de melhor entender o mecanismo funcional de

FTSJ3 e NIP7, o capítulo III apresenta a caracterização proteômica de complexos contendo as proteínas FTSJ3 e NIP7. Foi demonstrado que essas proteínas podem associar-se com complexos pré-ribossomais contendo componentes das subunidades ribossomais 40S e 60S, bem como fatores não-ribossomais associados à biogênese de ribossomos, como nucleofosmina e nucleolina, entre outros. Em conclusão, os resultados apresentados apoiam a hipótese de que FTSJ3 e NIP7 possam atuar em associação, como partes de um mesmo complexo, porém, em diferentes passos durante a síntese da subunidade ribossomal 40S em células humanas.

2. OBJETIVOS

O objetivo geral do presente trabalho foi investigar a função das proteínas NIP7 e FTSJ3 na biogênese de ribossomos em células humanas.

Especificamente, os objetivos foram:

✓ Determinar a função das proteínas NIP7 e FTSJ3 no processamento do pré-rRNA e biogênese das subunidades ribossomais.

✓ Avaliar o efeito da depleção de NIP7 e FTSJ3 na taxa de proliferação celular.

✓ Determinar a localização subcelular da proteína FTSJ3, bem como seus domínios FtsJ e Spb1_C.

✓ Verificar o mecanismo de interação entre as proteínas NIP7 e FTSJ3 *in vivo*.

✓ Identificar os componentes de complexos protéicos contendo as proteínas NIP7 e FTSJ3.

3. RESULTADOS

3.1. Capítulo I (Artigo I)

The NIP7 protein is required for accurate pre-rRNA processing in human cells

Luis G. Morello, Cédric Hesling, Patrícia P. Coltri, Beatriz A. Castilho, Ruth Rimokh and Nilson I. T. Zanchin

Nucleic Acids Research, **39**, 648-665 (2011)

648–665 *Nucleic Acids Research, 2011, Vol. 39, No. 2* *Published online 26 August 2010*
doi:10.1093/nar/gkq758

The NIP7 protein is required for accurate pre-rRNA processing in human cells

Luis G. Morello[1], Cédric Hesling[1,2], Patrícia P. Coltri[1,3], Beatriz A. Castilho[3], Ruth Rimokh[2] and Nilson I. T. Zanchin[1,*]

[1]Laboratório Nacional de Biociências, Centro Nacional de Pesquisa em Energia e Materiais, Rua Giuseppe Maximo Scolfaro 10000, CEP13083-970, Campinas SP, Brazil, [2]Institut National de la Santé et de la Recherche Médicale U590, Centre Léon Bérard, Université de Lyon, 69373 Lyon Cedex 08, France and [3]Department of Microbiology, Immunology and Parasitology, Universidade Federal de São Paulo, Rua Botucatu 862, São Paulo, SP 04023-062, Brazil

Received November 15, 2009; Revised August 6, 2010; Accepted August 9, 2010

ABSTRACT

Eukaryotic ribosome biogenesis requires the function of a large number of *trans*-acting factors which interact transiently with the nascent pre-rRNA and dissociate as the ribosomal subunits proceed to maturation and export to the cytoplasm. Loss-of-function mutations in human *trans*-acting factors or ribosome components may lead to genetic syndromes. In a previous study, we have shown association between the SBDS (Shwachman–Bodian–Diamond syndrome) and NIP7 proteins and that downregulation of SBDS in HEK293 affects gene expression at the transcriptional and translational levels. In this study, we show that downregulation of NIP7 affects pre-rRNA processing, causing an imbalance of the 40S/60S subunit ratio. We also identified defects at the pre-rRNA processing level with a decrease of the 34S pre-rRNA concentration and an increase of the 26S and 21S pre-rRNA concentrations, indicating that processing at site 2 is particularly slower in NIP7-depleted cells and showing that NIP7 is required for maturation of the 18S rRNA. The NIP7 protein is restricted to the nuclear compartment and co-sediments with complexes with molecular masses in the range of 40S–80S, suggesting an association to nucleolar pre-ribosomal particles. Downregulation of NIP7 affects cell proliferation, consistently with an important role for NIP7 in rRNA biosynthesis in human cells.

INTRODUCTION

Biogenesis of eukaryotic ribosomes involves synthesis and assembly of four ribosomal RNAs (rRNA) with about 80 ribosomal proteins mediated by more than 170 *trans*-acting factors. A significant amount of the cell energy is devoted to the maturation of three of the four eukaryotic rRNA molecules (18S, 5.8S and 25/28S) which are generated from a single transcript containing the sequences of the mature rRNAs flanked by spacer sequences. During rRNA maturation, the spacer sequences are excised by a series of endo and exonucleolytic cleavages and, at specific positions defined by sequence complementarity to snoRNAs, bases or riboses are modified by methylation and uridines are converted to pseudouridines (1–4). The pre-rRNA processing pathway is best characterized in the *Saccharomyces cerevisiae* model system. In wild-type strains, pre-rRNA maturation follows a 5′ to 3′ processing hierarchy where the 5′ ETS (external transcribed spacer sequence) is cleaved before processing in ITS1 (internal transcribed spacer sequence 1), which in its turn is cleaved before ITS2 (5–7).

Most of the yeast ribosome biogenesis factors have counterparts in higher eukaryotes, although not all the data obtained from the yeast system can be transferred to vertebrates. For instance, pre-rRNA maturation does not follow the 5′ to 3′ processing hierarchy in vertebrates. Instead, the order of processing depends on the species, cell type and physiological state. The mammalian pre-rRNA can be processed by simultaneous alternative pathways (8,9), following an initial cleavage that takes place at the site A′ of the 47S pre-rRNA generating the 45S pre-rRNA. The three major pathways differ in the place of the first processing step in the 45S pre-rRNA. In pathway A, the first cleavage takes place at Site 1, in

*To whom correspondence should be addressed. Tel: +55 19 3521 1144; Fax: +55 19 3521 1089; Email: zanchin@cbmeg.unicamp.br

The authors wish it to be known that, in their opinion, the first two authors should be regarded as joint First Authors.

pathway B, at Site 2c and, in pathway C, at Site 4b (Figure 1). The pathway has continuously been reviewed and novel intermediates and a cleavage site in the 5′-ETS have recently been described for mouse and human cells (10,11).

Expression of genes encoding ribosome biogenesis factors (termed Ribi regulon) is tightly regulated, showing a coordinated response to nutrient supply, physiological conditions or genetic perturbations (12–15). Transcription of this group of genes requires concerted action of the three RNA polymerases which in animals is mediated by the transcription factor Myc (16–19). Synchronized expression of the Ribi regulon involves also feedback regulation by several ribosomal proteins (20–22). Accurate synthesis of ribosomes is critical to all cells. Mutations in *S. cerevisiae* genes required for ribosome biogenesis usually interfere with the order of pre-rRNA processing steps, causing accumulation of aberrant pre-rRNAs or fast degradation of pre-rRNA intermediates. Pre-rRNA processing defects can also lead to imbalance of the 40S/60S subunit ratio or affect subunit export to the cytoplasm. In humans, mutations causing loss of function in genes encoding structural proteins or ribosome biogenesis factors may lead to genetic syndromes. Currently, there are five known syndromes associated with mutations in such genes. A series of mutations in genes encoding both 40S subunit (23–25) and 60S subunit proteins (26–28) have been linked to the

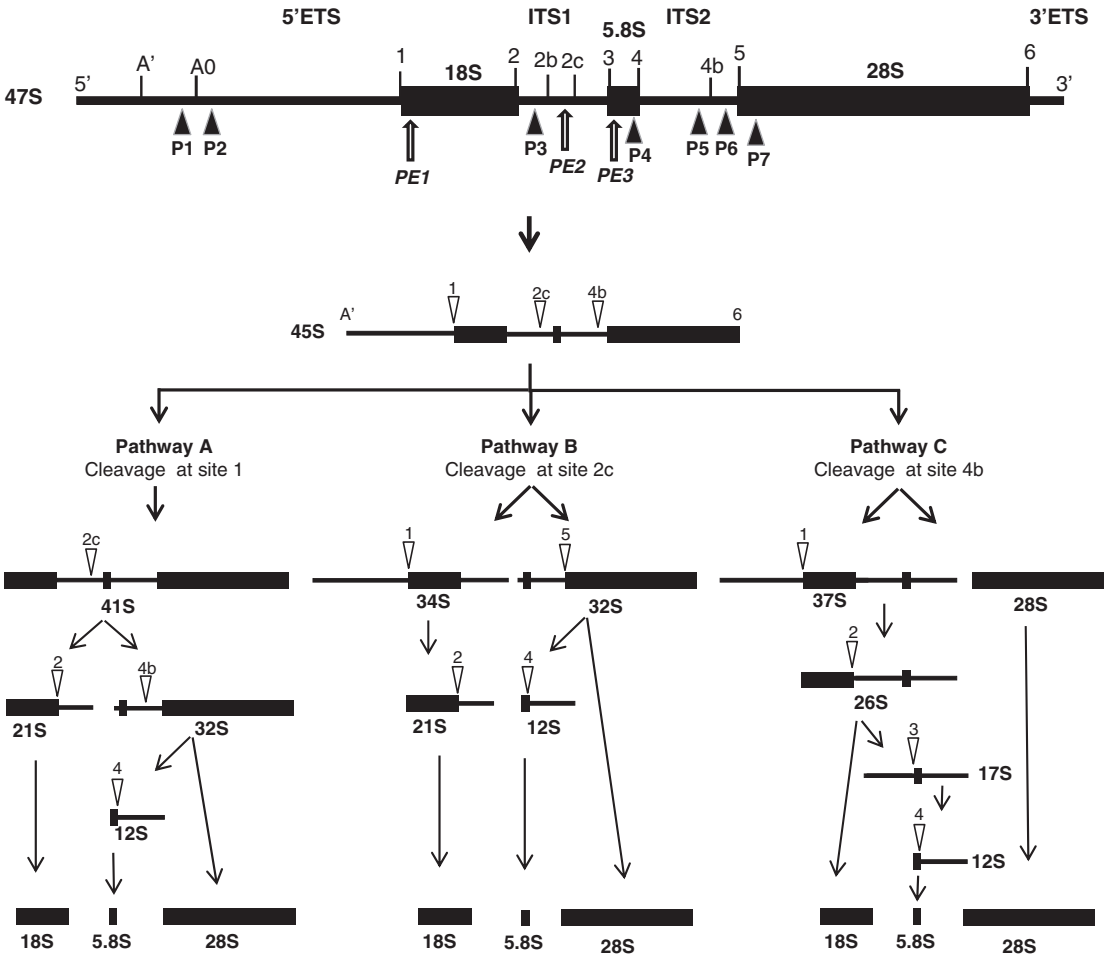

Figure 1. Schematic representation of the human pre-rRNA processing pathways. The 47S pre-rRNA is converted to the 45S pre-rRNA following the initial cleavages at sites A′ in the 5′-ETS and at site 6, at the 3′-end of the mature 28S rRNA. The 45S is processed by three alternative pathways. In pathway A, the first cleavage in 45S takes place at site 1, generating the 41S pre-rRNA whose 5′-end corresponds to the 5′-end of the mature 18S rRNA. The 41S pre-rRNA is subsequently processed at site 2c, separating the 21S pre-rRNA, from the 32S pre-rRNA. The 3′-end of the 21S pre-rRNA is processed to generate the 18S rRNA. The 32S pre-rRNA is cleaved at site 4b, generating the 12S pre-rRNA and the 28S rRNA. Finally, the 3′-end of the 12S pre-rRNA is processed to generate the mature 5.8S rRNA. In pathway B, the first cleavage in 45S takes place at site 2c, generating the 34S and 32S pre-rRNAs. The 34S pre-rRNA is subsequently processed at site 1, generating the 21S pre-rRNA. The 3′-end of the 21S pre-rRNA is processed further to generate the 18S rRNA. The 32S pre-rRNA is processed as described for pathway A. In pathway C, the first cleavage in 45S takes place at site 4b, generating the 37S and the 28S rRNA. The 37S pre-rRNA is subsequently processed at site 1, generating the 26S pre-rRNA, which is subsequently cleaved at site 2 generating the 18S rRNA and the 17S pre-rRNA. This pre-rRNA is processed at site 3 generating the 12S pre-rRNA and the 3′-end of the 12S pre-rRNA is processed to generate the mature 5.8S rRNA. This representation of the pathways was based on the papers published by Bowman *et al.* (8) and Hadjiolova *et al.* (9). Open arrowheads indicate the subsequent cleavage sites. Dark arrowheads (P1–P7) underneath the 47S pre-rRNA indicate the positions of the oligonucleotide probes used in northern blot and the open arrows (PE1–PE3) indicate the oligonucleotide probes used in primer extensions analyses, respectively.

Diamond Blackfan Anemia (DBA). In addition, Dyskeratosis Congenita has been associated with mutations in the X-linked DKC1 gene (29), encoding dyskerin, the pseudouridine synthase component of box H/ACA snoRNP. Deficiency in dyskerin abrogates pseudouridylation of rRNA and affects translation initiation of mRNAs containing internal ribosomal entry sites (IRES) (30,31). Mutations in the RNA component of the RNase MRP have been linked to Cartilage–Hair hypoplasia (CHH) (32). Mutations in the gene encoding the protein treacle are linked to the Treacher Collins syndrome. Treacle interacts with RNA polymerase I and Nop56, a subunit of the box CD snoRNP, and is involved in rRNA methylation (33,34). The Shwachman-Bodian-Diamond syndrome (SDS) is associated to mutations in the SBDS gene (35). Studies using both yeast and human cells have shown that SBDS orthologs are involved in ribosome biosynthesis and function (36–38). Dysregulation of ribosome biosynthesis and translational capacity has also been associated to pathological conditions such as human breast cancer (39).

The *S. cerevisiae* NIP7 protein is required for pre-rRNA processing and ribosome biosynthesis (40). NIP7 orthologs are highly conserved, ranging from 160 to 180 amino-acid residues and sharing a two-domain architecture with the C-terminal region corresponding to the PUA domain (named after pseudouridine synthases and archaeosine-specific transglycosylases) with a predicted RNA-interaction activity (41) that in the case of the *Pyrococcus abyssi* and *S. cerevisiae* NIP7 orthologs was already confirmed (42). The human NIP7 interacts with Nop132 (43), the putative ortholog of the *S. cerevisiae* Nop8p that is also involved in ribosome biogenesis (44). Furthermore, the human NIP7 was found in complexes isolated by affinity-tagged purification of RPS19 (45), a component of the 40S subunit that plays an essential role in its synthesis (23), and of parvulin (Par14), a peptidyl-prolyl *cis–trans* isomerase (PPIase) required for pre-rRNA processing (46). In a previous work, we have detected the interaction of NIP7 with SBDS in the yeast two-hybrid system (47). In addition, an immobilized GST–SBDS fusion protein was able to pull-down NIP7 from HEK293 cell extracts, indicating that both proteins can be part of a multisubunit complex (47).

Although the evidence above points to a role for the human NIP7 protein in ribosome biosynthesis, so far there is no report on the functional analysis of this protein. In this work, we used RNA interference to downregulate NIP7 and investigate its function in human cell lineages. We show that downregulation of NIP7 affects cell proliferation and causes imbalance of the 40S/60S subunit ratio. We also identified defects at the pre-rRNA processing level with a decrease of the 34S pre-rRNA concentration and an increase of the 26S and 21S pre-rRNA concentrations, suggesting that processing at site 2 is particularly slower in NIP7-depleted cells. The results presented in this work suggest that NIP7 is required for accurate processing of the pre-rRNAs leading to 18S rRNA maturation and 40S subunit biogenesis. At least part of the pre-rRNA processing defects caused by NIP7 downregulation have been described for other situations in which ribosome biogenesis was impaired, such as treatment with leptomycin B, which inhibits exportin Crm1/Xpo1 and blocks ribosome subunit export from the nucleus, and for downregulation of 40S biogenesis factors (11). The NIP7 protein is restricted to the nuclear compartment and co-sediments with complexes with molecular masses in the range of 40S–80S suggesting an association to nucleolar pre-ribosomal particles. This work shows that NIP7 plays a critical role in pre-rRNA maturation in human cells.

MATERIALS AND METHODS

Plasmid construction

DNA cloning was performed using the *Escherichia coli* strain DH5α which was maintained in LB medium containing 50 mg ml^{-1} of the required antibiotic used in transformant selection and manipulated according to standard techniques (48). The *NIP7* 540-bp coding sequence was isolated from pTL1-HSNIP7 (47) using the EcoRI/SalI restriction sites and inserted into the pET28a plasmid, generating pET28-HSNIP7. The *NIP7* shRNA target was 21-residue oligonucleotide whose sequence was selected based on the Ambion siRNA Target Finder. The sequences of the oligonucleotides NIP7-shRNA-F and NIP7-shRNA-R used to generate the shRNA against the *NIP7* mRNA and of the oligonucleotides scrambled shRNA-F and scrambled shRNA-R to generate the control scrambled shRNA, scRNA, is given in Table 1. The annealed oligonucleotides were cloned into pMaleficent (49) previously digested with Esp3I/EcoRI, generating pMaleficent-shRNA-HSNIP7 and pMaleficent-scRNA-HSNIP7, respectively.

Cell culture methods and RNA interference strategies

HEK293 cells (ATCC number CRL-1573) were maintained in MEM (Minimum Essential Alfa Medium, Gibco-BRL) supplemented with 10% fetal bovine serum, 100 U.ml^{-1} penicillin and 100 µg.ml^{-1} streptomycin. The cells were cultured at 37°C in a humidified atmosphere with 5% CO_2. To generate permanent cells with downregulation of *NIP7*, we employed a mammalian transposon system designated pMaleficent/pCMVHSB#17 (49). HEK293 transfections were performed by electroporation as described by Klan and Steinhilber (50). Following transfection, HEK293 cells were transferred into six-well plates and kept under geneticin selection (700 µg.ml^{-1}). Proliferation rates of HEK293 derivative cells were determined using the MTT {[3-(4,5-dimethylthiazolyl-2)-2,5-diphenytetrazolium bromide], Sigma} cell proliferation assay as previously described (47). Downregulation of NIP7 in HeLa and MCF10A cells was achieved by using transient transfections of siRNA. For each assay, 1.5×10^5 cells (~60–80%confluence) were harvested in OPTI MEM (Invitrogen) and transfected with 5 or 10 nM siRNA oligonucleotides (NIP7-siRNA-F and NIP7-siRNA-R, Table 1) using 0.5 µl/ml lipofectamine RNAiMax Transfection Reagent (Invitrogen) following the

Table 1. Primers used in this study

Primer name	Sequence
NIP7-shRNA-F	5′ TCC CGA ACC ATG TGT TGA AAT CTG GTT TCA AGA GAA CCA GAT TTC AAC ACA TGG TTC TTT TTT G 3′
NIP7-shRNA-R	5′ AAT TCA AAA AAG AAC CAT GTG TTG AAA TCT GGT TCT CTT GAA ACC AGA TTC AAC ACA TGG TTC 3′
Scrambled shRNA-F	5′ TCC CGA ATT TGT GAT CCA GGA ATG CTT TCA AGA GAA GCA TTC CTG GAT CAC AAA TTC TTT TTT G 3′
Scrambled shRNA-R	5′ AAT TCA AAA AAG AAT TTG TGA TCC AGG AAT GCT TCT CTT GAA AGC ATT CCT GGA TCA CAA ATT C 3′
NIP7-siRNA-F	5′ GCA CCU ACU GUU UCC GUC UGC ACA A 3′
NIP7-siRNA-R	5′ UUG UGC AGA CGG AAA CAG UAG GUG C 3′
Actin-F	5′ TGG ATC AGC AAG CAG GAG TAT G 3′
Actin-R	5′ GCA TTT GCG GTG GAC GAT 3′
NIP7-F	5′ CCG GGT GTA CTA TGT GAG TGA GAA 3′
NIP7-R	5′ TTG TGG GTT TTA GTG AAT TTT CCA 3′
HPRT-F	5′ TGA CCT TGA TTT ATT TTG CAT ACC 3′
HPRT-R	5′ CGA GCA AGA CGT TCA GTC CT 3′
36B4-F	5′ GTG TTC GAC AAT GGC AGC AT 3′
36B4-R	5′ GAC ACC CTC CAG GAA GCG A 3′
P1	5′ CCC CAA GGC ACG CCT CTC AGA TCG CTA GAG AAG GCT TTT C 3′
P2	5′ CCA CGC AAA CGC GGT CGT CGG CAC CGG TCA CGA CTC GGC A 3′
P3	5′ AAG GGG TCT TTA AAC CTC CGC GCC GGA ACG CGC TAG GTA C 3′
P4	5′ GCG TTC GAA GTG TCG ATG ATC AAT GTG TCC TGC AAT TCA C 3′
P5	5′ CGG GAA CTC GGC CCG AGC CGG CTC TCT CTT TCC CTC TCC G 3′
P6	5′ GGG GAG AGG CGA CGG GAG AGA GAG CGC 3′
P7	5′ CTT TTC CTC CGC TGA CTA ATA TGC TTA 3
PE1	5′ GAC ATG CAT GGC TTA ATC TTT GAG ACA AGC 3′
PE2	5′ GTA AAG CCC CCA CCC GAC GGC CGC CG 3′
PE3	5′ CTC GCA GCT AGC TGC GTT CTT CAT CGA C 3′
MM21	5′ CAC AAG CCC ATT TGA CAC TGA 3′
MM30	5′ CGG AAT TCC GTG GGC CTA AGT CAG ATG ATG 3′
MM36	5′ CTC GAG TTA TTC ATC AAA AAT TTG GAT TGG TAT TTC 3′
MM44	5′ CTG CAG CTC GAG TTA CCT TCG TGT ATA TTC TTC TGA TTT TTA TG 3′
MM54	5′ CTC GAG TCA ACT TTC AAG TAC AGA TGG AGC CAC ATA TTC AAA ACC CAG AAA GAC 3′
MM64	5′ AAT TCA AAA AAG AAT TTG TGA TCC AGG AAT GCT TCT CTT GAA AGC ATT CCT GGA TCA CAA ATT C 3′
MM74	5′ TCC CGT ATA ATC TGT TGT ATA GGT CCT TGA TAT CCG GGA CCT ATA CAA CAG ATT ATA TTT TTT CCA ATT TTT TG 3′

manufacturer's instructions. Parallel control transfection assays were performed with scrambled 'AllStars Negative Control siRNA' (Qiagen); Cells were plated and cultured for 12 h in antibiotic free medium. Medium was changed and cells cultured for 36–96 h in complete fresh medium. For proliferation analysis of transfected HeLa and MCF10A cells, triplicates at a density of 1500 cells/well were seeded in 96-wells plates (100 µl/well) and cultured for 4 h in complete medium. At each time point, cells were treated with 10 µl Uptiblue (Interchim) and incubated for 4 h at 37°C. Luminescent quantification was performed using a spectrophotometer (Cytofluor), excitation 590/25 nm; emission 530/25 nm. Background was measured from wells without cells and subtracted from the 530 nm values. Cell-cycle analyses were performed by fluorescence-activated cell sorting (FACS). For these assays, 0.5×10^6 cells were fixed on ice in 70% (v/v) ethanol for 30 min, washed with PBS and the DNA content stained with 20 µg/ml propidium iodide in PBS in the presence of 1 mg/ml RNAse. Cells were analyzed on a FACSCalibur™ (BD Biosciences) equipped with a 488-nm argon laser. The fluorescence was measured through a 575/25 band pass filter. Cells doublets were removed using the FL2-Area and FL2-Width parameters. Data acquisition was performed using CellQuest software (BD Biosciences) and analysis using ModFit software (Verity Software). FACS analyses were performed with the permanent HEK293 derivative cells (SC, which express the scrambled shRNA and, CP4 cells that express the RNAi against the NIP7 mRNA) and with MCF10A cells transiently transfected with either a scrambled siRNA or a NIP7 siRNA 48 h after transfection.

Analysis of NIP7 mRNA levels

NIP7 mRNA downregulation was confirmed by RT–qPCR using oligonucleotides complementary to *NIP7* sequence (NIP7-shRNA-F and NIP7-shRNA-R). One microgram of total RNA was used for cDNA synthesis using the SuperScript II Reverse Transcriptase system (Invitrogen). The mRNA levels were quantified using the SYBR Green® reagent on a 7500 Real Time PCR system (Applied Biosystems). In the case of HEK293 derivative cells, *NIP7* mRNA levels were normalized to the amount of the actin mRNA determined using primers Actin-F and Actin-R. In the case of HeLa and MCF10A cells, *NIP7*

mRNA levels were normalized to the amount of the HPRT and 36B4 mRNAs, respectively, which were determined using primers HPRT-F and HPRT-R or 36B4-F and 36B4-R, respectively. The sequences of all primers used in this work are given in Table 1. The NIP7 protein levels were determined by immunoblotting as described below.

Sucrose gradient and cell fractionation

Polysomes profiles were analyzed on sucrose gradients as previously described (51). The cells were cultivated up to 50% confluence. Following addition of 100 μg.ml^{-1} cycloheximide, 5×10^7 cells were collected and lyzed using 500 μl of polysome buffer (PB) containing 20 mM Tris–HCl pH 7.5, 100 mM NaCl, 10 mM $MgCl_2$, 1 mM DTT, 1% v/v Triton X-100 and 100 μg.ml^{-1} cycloheximide. Extracts were clarified by centrifugation at $20\,000 \times g$ for 10 min at 4°C. Totals of 255 OD_{260} units (300 μl) were loaded onto linear sucrose gradients (15–50%) prepared in PB. Polysomes were separated by centrifugation at 40 000 rpm for 4 h at 4°C using a Beckman SW41 rotor. Gradients were fractionated by monitoring absorbance at 254 nm. Protein precipitation and removal of sucrose for immunoblot analyses was performed as follows: 150 μl of each sucrose gradient fraction were mixed with 600 μl of methanol and subsequently mixed with 150 μl of chloroform; 450 μl of water were added to the mix and centrifuged at $20\,000 \times g$ for 5 min at 4°C. The aqueous layer was discarded and the pellet washed with 650 μl of methanol, followed by centrifugation as described above. The liquid was discarded and the pellet was taken up in protein sample buffer (48) and analyzed by immunoblotting. For isolation of nuclear and cytoplasmic extracts, 2×10^7 cells were washed in ice cold PBS and harvested by centrifugation at $500 \times g$ for 5 min at 4°C. Cells were lyzed in 1 ml LSB (10 mM Tris–HCl pH 7.4, 320 mM sucrose, 2 mM $MgCl_2$, 3 mM $CsCl_2$, 0.4% NP-40, 1 mM DTT) containing a protease inhibitor cocktail (Roche) for 12 min on ice. Subsequently, the lysate was centrifuged at $800 \times g$ for 2 min at 4°C, the supernatant was collected and centrifuged at $20\,000 \times g$ for 10 min and the resulting supernatant was saved as the cytoplasmic extract. The pellet from the $800 \times g$ centrifugation, containing the nuclei, was washed once with LSB and the nuclear proteins extracted in 300 μl HSB (250 mM NaCl, 50 mM Tris–HCl pH 8.0, 5 mM EDTA pH 8.0, 0.5% NP-40) containing a protease inhibitor cocktail (Roche) and 240 U of RNaseOUT (Invitrogen). The suspension was centrifuged at $20\,000 \times g$ for 10 min at 4°C and the supernatant saved as the nuclear fraction. Totals of 10 OD_{260} units of nuclear extracts were fractionated on 15–50% sucrose gradients prepared in polysome buffer as described above. For immunoblotting, aliquots of sucrose gradient fractions were processed as described above.

Immunoblot analysis

Proteins were resolved by SDS–PAGE and transferred to PVDF membranes at 80 mA for 1 h in buffer containing 25 mM Tris–base, 200 mM glycine and 20% methanol. Subsequently, membranes were blocked for 2 h with TBST buffer (20 mM Tris–HCl pH 7.5, 150 mM NaCl, 0.05% Tween 20) containing 5% low fat milk. The blots were incubated at room temperature for 2 h with primary antibodies and for 1 h with secondary antibodies. Polyclonal antisera for the human NIP7 protein were produced in rabbits and used at a 1:5000 dilution. Rabbit polyclonal antibodies for RPS6, cytoskeletal actin and GAPDH (Bethyl Laboratories) were used at a 1:5000 dilution. Mouse monoclonal for Lamin A/C and alpha-tubulin (Santa Cruz Biotechnology) were used at a 1:300 and 1:2500 dilutions, respectively. The secondary antibodies used were horseradish peroxidase-conjugated goat anti-mouse IgG (Calbiochem) and donkey anti-rabbit IgG (GE Healthcare) both at 1:5000 dilutions. The immunoblots were developed using the ECL western blotting analysis system (GE Healthcare).

RNA analysis

Total RNA from HEK293 cells, scRNA and shRNA-NIP7 clones were isolated by Trizol extraction (Invitrogen). RNAs were fractionated by electrophoresis on 1.2% (w/v) agarose/formaldehyde gels, followed by transfer to Hybond nylon membranes (GE Healthcare). Northern blot was performed using [^{32}P]-labeled oligonucleotide probes (P1–P7) complementary to specific regions of the 47S precursor RNA and submitted to autoradiography. The position of the probes were based on the human ribosomal DNA complete repeating unit, Genebank accession number U13369 (version U13369.1, GI:555853). The positions of the probes are as follows: P1 (5′ETS), complementary to nt 1401–1442; P2 (5′ETS), complementary to nt 1786–1825; P3 (ITS1), complementary to nt 6121–6160; P4 (5.8S), complementary to nt 6690–6729; P5 (ITS2), complementary to nt to 7031–7070; P6 (ITS2), complementary to nt 7812–7838 and; P7 (28S), complementary to nt 7971–7997. Primer extension analysis was performed according to Gonzales *et al.* (52) using oligonucleotide probes PE1 (18S), complementary to nt 3685–3714, PE2 (ITS1), complementary to nt 6299–6324 and PE3 (5.8S), complementary to nt 6655–6682 (Table 1). [^{32}P]-labeled-oligonucleotides MM21, MM30, MM36, MM44, MM54, MM64 and MM74 (Table 1) were used as molecular markers corresponding to 21, 30, 36, 44, 54, 64 and 74 nt, respectively. For metabolic labeling of RNA, HEK293 cells cultured on 100-mm plates at ~70–80% confluence were pre-incubated for 30 min in phosphate-free DMEM (GIBCO) supplemented with 10% FCS. Subsequently, [^{32}P]-orthophosphate (15 μCi/ml) was added to the cultures that were incubated for 45 min and the medium was replaced by cold MEM (GIBCO) supplemented with 10% FCS. Cells were collected at time 0, 30, 60 and 120 min after changing the medium. Total RNA was extracted with Trizol (Invitrogen), and 10 μg were separated by electrophoresis on agarose/formaldehyde gels and revealed by autoradiography. RNA was extracted from sucrose gradient fractions as follows: 700 μl of each fraction were transferred to 1.5 ml tubes and 42 μl of a 10% SDS solution was added to obtain a final SDS percentage of 0.6. The suspension

was subjected to two sequential extractions, the first with 700 µl of phenol/chloroform/isoamyl alcohol (25:24:1) and the second with phenol/chloroform (1:1) and the aqueous phase was transferred to a new tube and the RNA precipitated with 700 µl of isopropanol for 1 h at −20°C. The RNA was sedimented by centrifugation (12 000 × *g* for 10 min at 4°C). The RNA pellet was washed with 75% ethanol, air dried and suspended in 10 µl of DEPC-treated water.

Electrophoretic mobility shift assays (EMSA)

For recombinant NIP7 protein production, we used plasmid pET28-HSNIP7, which was constructed by transferring the 540-bp NIP7 coding sequence from plasmid pTL1-HSNIP7 (47) to plasmid pET28a, using the EcoRI/SalI restriction sites. Expression of NIP7 was performed in *E. coli* BL21(DE3) cells transformed with vector pET28-HSNIP7 and incubated in LB medium containing kanamycin (50 µg ml^{-1}) at 25°C. At an OD_{600} of ~0.8, the culture was induced by adding 0.5 mM IPTG and incubating at 25°C for further 4 h. Cells were harvested by centrifugation, suspended in buffer containing 50 mM sodium phosphate pH 7.2, 100 mM NaCl, 10% glycerol and 0.5 mM phenylmethylsulfonyl fluoride (PMSF) and treated with lysozyme (50 µg ml^{-1}) for 30 min on ice. Subsequently, the cells were disrupted by sonication and the histidine-tagged NIP7 purified by metal-chelating affinity chromatography, using a 20–200 mM imidazole gradient for elution. NIP7 was further purified on a heparin–sepharose column using the same buffer as above for binding and a 50 mM to 1 M KCl gradient for elution. For EMSA, 20 pmol of the RNA oligoribonucleotides poly-$A_{(20)}$, poly-$U_{(20)}$ and poly-$AU_{(21)}$, (5′ UUA UUA UUU AUU UAU UAU UUA 3′) were [^{32}P]-labeled using 1 U T4 PNK and 20 µCi [γ^{32}P]-ATP. 0.4 pmol of [^{32}P]-labeled oligoribonucleotide was incubated with the indicated concentrations of NIP7 in buffer A (20 mM Tris–Cl pH 8.0, 5 mM magnesium acetate, 150 mM potassium acetate, 0.2% v/v Triton X-100, 1 mM DTT, 1 mM PMSF) for 30 min at 37°C. Complexes were resolved on 8% polyacrylamide gels using TBE buffer pH 8.0 for electrophoresis and visualized by autoradiography. RNA competition assays were performed with 1, 5 and 10 pmol of either poly-$A_{(20)}$ or poly-$AU_{(21)}$ oligonucleotides.

RESULTS

Knockdown of NIP7

The strategy to generate HEK293 cells knockdown for NIP7 was based on the generation of stably-transfected cells expressing a shRNA targeting the *NIP7* mRNA using pMaleficent as shRNA delivery vector (49). The efficiency of *NIP7* downregulation was determined by analysis of the *NIP7* mRNA and protein levels. Quantitative RT–PCR indicated that the reduction of *NIP7* mRNA levels reached up to 80% of the parental and control cells (Figure 2A). Although the levels of the NIP7 mRNA are similar in clones CP4 and CP6, the reduction in NIP7 protein levels was more efficient in clone CP4 as observed by western blot analysis (Figure 2C). Downregulation of NIP7 in these clones was stable over the period of this study. CP4 cells showed significant reduction of the proliferation rate (Figure 2E).

RNA interference based on transient transfection of siRNA oligoribonucleotides was used to downregulate NIP7 also in MCF10A and HeLa cells. The NIP7 mRNA levels were reduced to levels <10% of control cells (Figure 2B). In siRNA-treated cells, NIP7 protein was below the detection level as determined by immunoblotting. A significant reduction in the proliferation rate of both cell lines was observed following transfection with the NIP7 siRNA (Figure 2F). The reduced proliferation rate prompted us to perform fluorescence-activated cell sorting (FACS) to investigate cell-cycle progression in these cells. In the case of the permanently transfected HEK293 derivative cells, CP4 show the highest number of cells in the G0–G1 phases and the lowest number in the S phase (Table 2). This effect on the cell cycle, despite of being mild, is consistent with the results observed for MCF10A cells. NIP7 downregulation in MCF10A resulted in an increase of cells in the G0–G1 phases with an equivalent reduction of the number of cells in the S phase (Table 2). This result shows that downregulation of NIP7 lead to accumulation of cells in the G1–S transition.

Analysis of polysomes in HEK293 cells depleted of NIP7

Defects in ribosome biogenesis can in some cases be detected by using sucrose density fractionation of polysomes especially when there is an imbalance in the 40S/60S subunit ratio. The CP4 clone, showing lower NIP7 levels, was chosen for further characterization. NIP7-depleted CP4 cells showed significant reduction of 40S ribosomal subunits (Figure 3C and D). This finding is consistent with the cell proliferation assay and suggests that the reduction in growth rate is due to defective 40S subunit biosynthesis.

Analysis of pre-rRNA processing intermediates in NIP7 deficient cells

Steady-state analysis of pre-rRNA processing was assessed by northern blotting using probes complementary to the transcribed spacer sequences and to the mature rRNAs. The boundaries of most pre-rRNAs intermediates relevant to this work have already been mapped (8–11). A set of northern blots was performed with probes P1, P2, complementary to the 5′-ETS upstream and downstream of Site A0, respectively, and with probe P3 complementary to ITS1, upstream Site 2b (Figure 4). A second set of northern blots was performed with probes P4–P7 that are complementary to the 5.8S rRNA to ITS2 upstream and downstream Site 4b and to the 28S rRNA, respectively (Figure 5).

The precursors most affected are the 21S, 26S/A0-2c and 34S with the 21S and 26S/A0-2c pre-rRNAs showing increased levels and the 34S pre-rRNA showing reduced levels in NIP7 deficient cells (Figure 4). The 26S pre-rRNA running slightly faster than the mature 28S rRNA is detected with probes P2 and P3 but not by

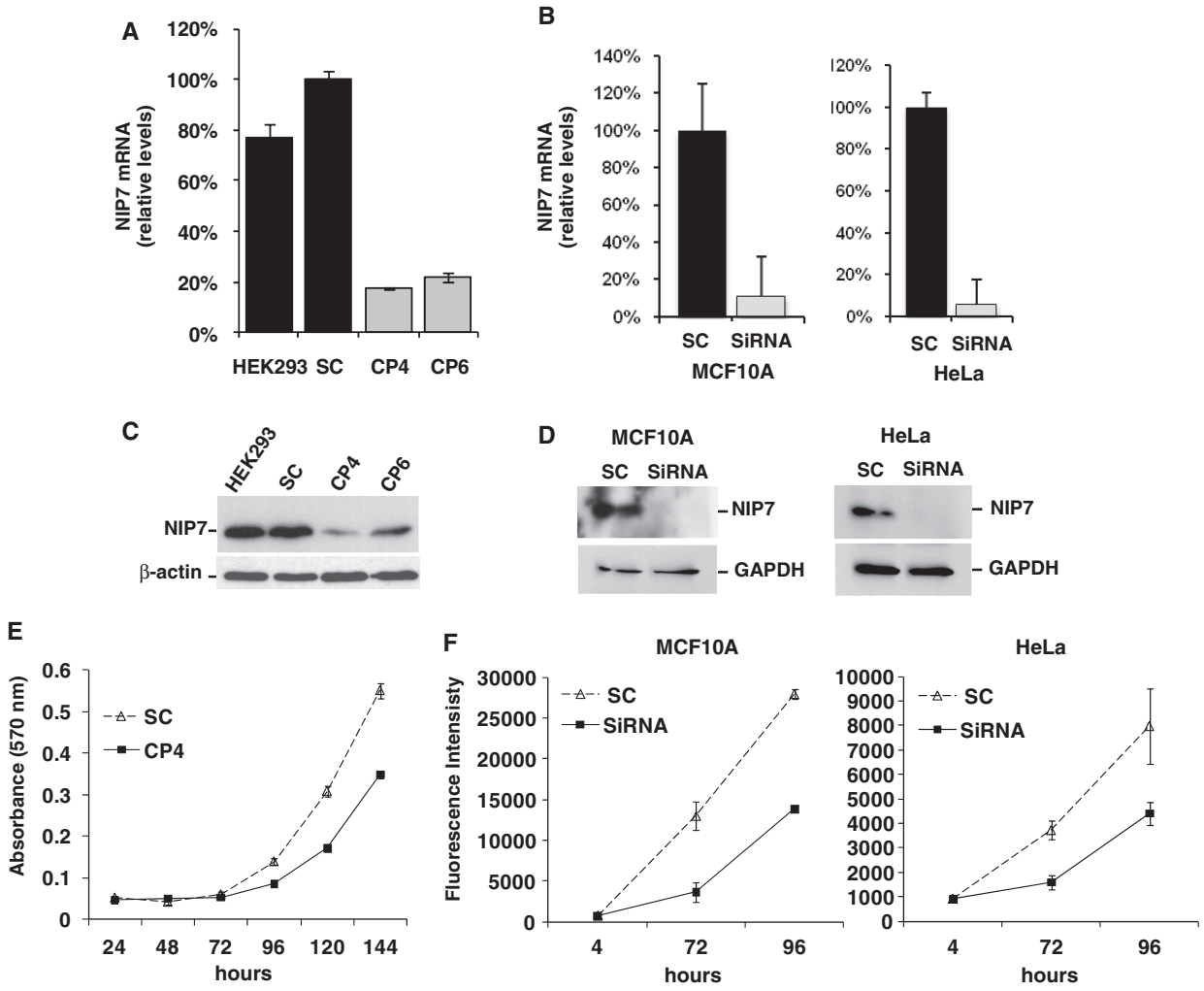

Figure 2. Analysis of NIP7 knockdown. (**A**) NIP7 mRNA levels as determined by quantitative RT–qPCR in HEK293 derivative cells. HEK293, parental cells; SC, cells transfected with a scrambled shRNA; CP4 and CP6, cells transfected with shRNA against the NIP7 mRNA. NIP7 mRNA quantitation was performed using three different RNA extractions from clones CP4 and CP6. (**B**) NIP7 mRNA levels in transiently transfected MCF10A and HeLa cells. SC, control cells transfected with scrambled RNA; SiRNA, cells transfected with siRNA against NIP7. The histogram corresponds to one of the three independent transfections of MFC10A and HeLa cells using three replicates for each cell treatment. The amount of NIP7 mRNA in cells treated with the scrambled shRNA was considered as 100% to calculate its relative levels in the parental cells (HEK293) and in cells expressing the RNAi against the NIP7 mRNA (CP4) or in cells transfected with siRNA against the NIP7 mRNA. (**C**) Immunoblot showing the levels of the NIP7 protein in HEK293 derivative cells β-actin was used as an internal control. (**D**) Immunoblot using antiserum for the NIP7 protein in transiently transfected MCF10A and HeLa cells. (**E**) Proliferation rate of HEK293 derivative cells expressing the scrambled shRNA (SC) and the RNAi against the NIP7 mRNA (CP4) over a 7-day period. (**F**) Proliferation rate of transiently transfected MCF10A and HeLa cells. The graphs correspond to one of the two independent proliferation assays performed using three replicates for each cell treatment.

Table 2. Cell-cycle distribution of NIP7-depleted cells

Cell type	Cell-cycle distribution (%)		
	G0/G1	S	G2
HEK293	49	37	14
HEK293/SC	43	42	15
HEK293/CP4	51	33	16
MCFA10A/SC	47	35	18
MCFA10A/RNAi	73	13	14

Percentage numbers represent the average of three independent experiments.

probe P1 and therefore extends from Sites A0 to 2c (Figure 4B, C and E). We concluded that this pre-rRNA corresponds to the 26S pre-rRNA described by Rouquette and co-workers (11) who defined its extension as from site A0 to a site in ITS1 downstream of nt 5687 and upstream of nt 6613, which must correspond to either Site 2b or 2c. Another precursor named 26S pre-rRNA, extending from Sites 1 to 4b, was described for pathway C [Figure 1, (8)]. However, the possibility that this pre-rRNA is increased was excluded because it was not detected by probes P4 and P5 (Figure 5). Probes P1–P3 can detect both the 34S and

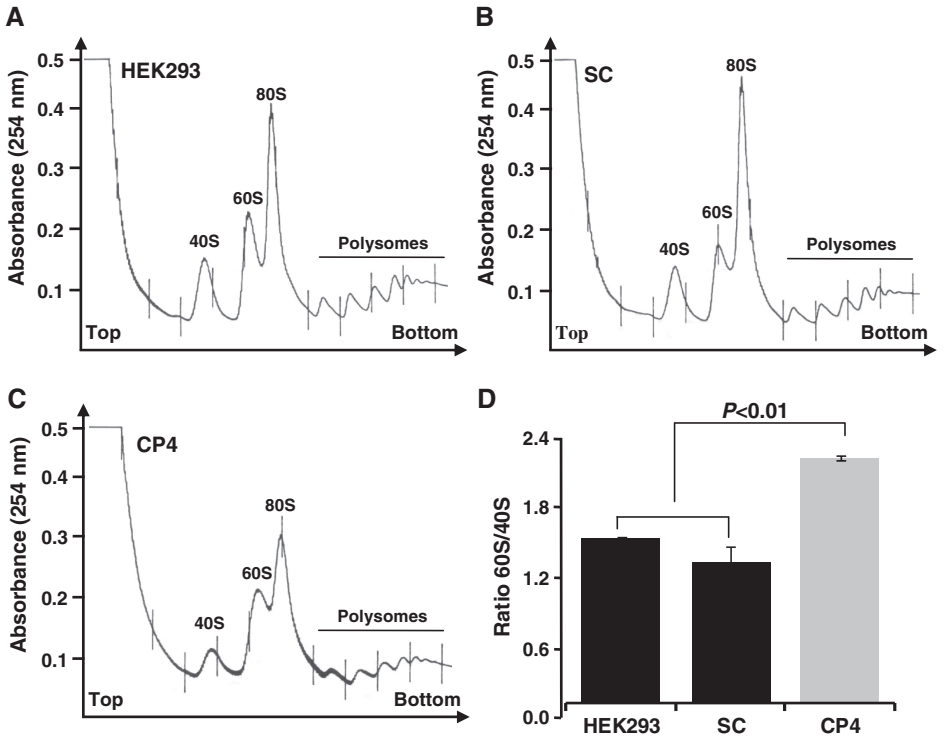

Figure 3. Analysis of polysomes by sucrose density gradient fractionation. (**A**) Polysome profile of HEK293 cells. (**B**) Polysome profile of control cells expressing the scrambled shRNA. (**C**) Polysome profiles of clone CP4 transfected with shRNA targeting the NIP7 mRNA. (**D**) Quantitation of the 60S/40S subunit ratio of HEK293 cells, control scrambled shRNA cells (SC) and of CP4 cells in the polysome profiles shown in A, B and C, respectively. CP4 cells contain a significant lower amount of 40S ribosomal subunits. *P*-value was obtained by using a one-sided Student's *t*-test ($P < 0.01$). Quantitation was based on two independent experiments performed using two replicates.

the 37S pre-rRNAs while probes P4 and P5 can detect both the 37S and the 32S pre-rRNAs (Figures 4 and 5). The 34S and 37S pre-rRNAs, comprising respectively ~6000 and ~7520 nt, may migrate with similar electrophoretic mobility in these gels. In the case of probes P1–P3 (Figure 4), a strong reduction of the signal is observed in this region of the northern blots, indicating that if any 37S pre-rRNA is generated in this cells its concentration is also decreased in NIP7-depleted cells.

A reduction in the concentration of the 32S pre-rRNA can be visually detected in the northern blots with probes P5, P6 and P7 in the NIP7 deficient cell line (Figure 5). The levels of the 41S pre-rRNA are slightly increased in NIP7 deficient cells (Figures 4C, E, 5A–C and F). This pre-rRNA, extending from sites 1 to 6, corresponds to the second largest band detected by probes P3–P6 (Figures 4C, E, 5A–C and F). The levels of the 47S and 45S pre-rRNAs, on the other hand, show a slight decrease in NIP7 deficient cells (Figures 4A–E and 5F).

Accumulation of the 26S/A0-2c pre-rRNA has been described in situations in which there is uncoupling of processing at Sites 1 and 2. Leptomycin B (LMB) inhibits exportin Crm1/Xpo1 and blocks ribosome subunit export from the nucleus. We have analyzed pre-rRNA processing of control cells (SC) and NIP7 shRNA cells (CP4) treated with LMB (Figure 4F). Upon a 4 h LMB treatment, SC cells showed a sharp increase of the 26S/A0-2c pre-rRNA. In CP4 cells, that already contain increased levels of the 26S/A0-2c and 21S pre-rRNAs, LMB treatment has a small effect on the accumulation of the 26S/A0-2c pre-rRNA. Accumulation of the 26S/A0-2c is consistent with slower processing of sites 1 and 2 in NIP7-depleted cells. However, accumulation of the 21S pre-rRNA and of the 41S pre-rRNA indicates that processing at sites 2c/2b and 2 are even slower that at site 1, suggesting that NIP7 is particularly required for processing of the ITS1 sites. Northern blot analysis with probe P3 was performed also with RNA samples from MCF10A cells (Supplementary Data), which detected accumulation of the 21S and 41S pre-rRNAs following downregulation of Nip7, indicating that Nip7 plays an important function in all cell types.

The 37S pre-rRNA (spanning from Sites A′ to 4b) and the 17S pre-rRNA (spanning from Sites 2b to 4b) would be generated only if the pathway C proposed by Bowman and co-workers (8) is indeed taking place in HEK293 cells. Gel electrophoreses used in this work resolved the 28S rRNA (5035 nt) from the 26S/A0-2c pre-rRNA (~4642 nt). Therefore, it would be expected that the 37S pre-rRNA (~7520 nt) would also be separated from the 32S pre-rRNA (6337 bases from sites 3 to 6). However, probes 4 and 5 detected only one band in this region suggesting that HEK293 cells produce low levels of the 37S pre-rRNA. The 17S pre-rRNA could be detected by probes P3, P4 and P5 (Figures 4C, 5A and B) but only

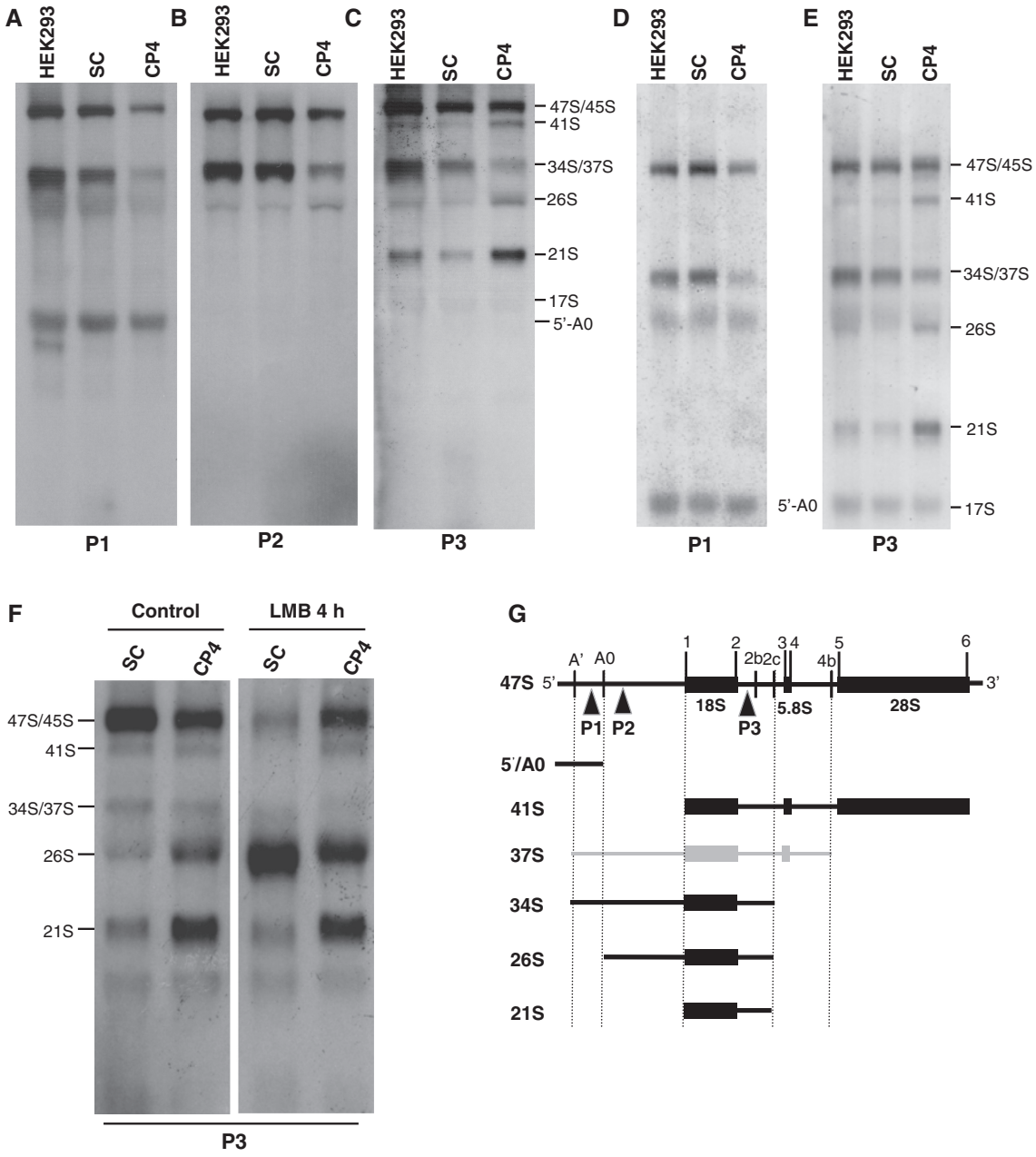

Figure 4. Northern blot analysis of pre-rRNAs detected by using probes complementary to the 5′-ETS and ITS1. (**A**) Northern blot using probe P1 complementary to the 5′-ETS upstream site A0. (**B**) Northern blot using probe P2 complementary to the 5′-ETS downstream site A0. (**C**) Northern blot using probe P3 complementary to ITS1 upstream site 2c. (**D**) and (**E**) Northern blots using probes P1 and P3 of longer electrophoresis runs. (**F**) Northern blot of cells treated with leptomycin B using probe P3 complementary to ITS1 upstream site 2c. (**G**) Structure of the 47S pre-rRNA and pre-rRNA intermediates that are most affected in NIP7-depleted cells. The positions of the probes P1, P2 and P3 used in the northern blots shown in A–D are indicated. HEK293, parental cells; SC, cells transfected with the scrambled shRNA; CP4, cells transfected with shRNA against the NIP7 mRNA.

faint bands are detected in this region. The low levels of both 17S and 37S pre-rRNAs, together with the fact that the 17S immediate upstream precursor, namely the 26S pre-rRNA extending from sites 1 to 4b, was not detected by probes P4 and P5 (Figure 5A and B) are strong indications that pathway C is a minor pathway in HEK293 cells.

An additional band with mobility similar to the 5.8S rRNA is detected with probe P5 ('Asterisk' in Figure 5B). This band might correspond to a fragment comprising from site 4b to an upstream site in ITS2 but only if there would be a cryptic endonucleolytic cleavage site downstream of site 4, which can now be speculated, following the recent discovery of the endonucleolytic activity associated to the exosome, the main *trans*-acting factor responsible for maturation of the 5.8S rRNA 3′-end (53).

Analysis of the pre-rRNA processing kinetics was performed by metabolic labeling with [^{32}P]-orthophosphate

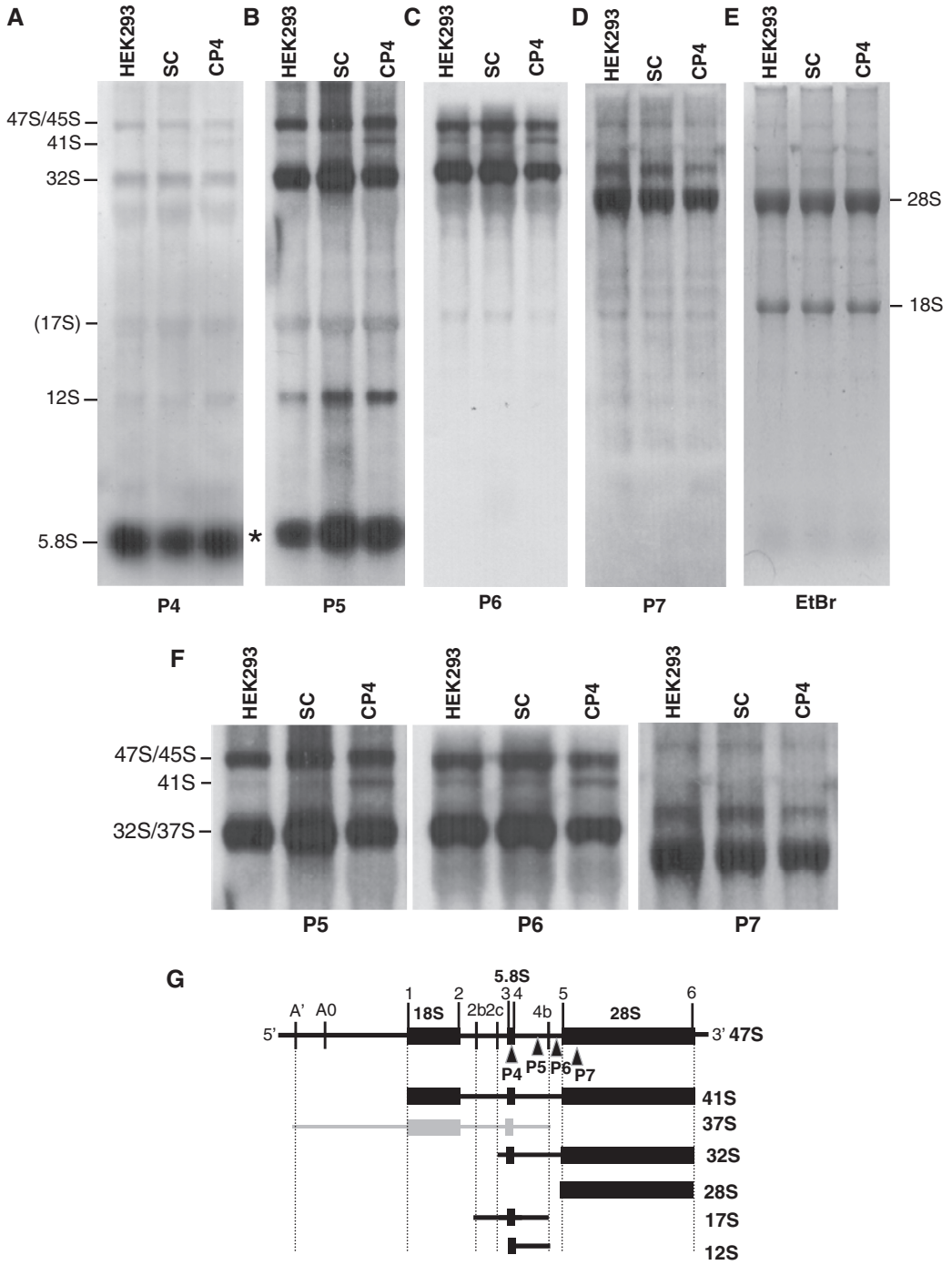

Figure 5. Northern blot analysis of pre-rRNAs detected by using probes complementary to the 5.8S rRNA, ITS2 and the 28S rRNA. (**A**) Northern blot using probe P4 complementary to the 5.8S rRNA. (**B**) Northern blot using probe P5 complementary to ITS2 upstream site 4b. (**C**) Northern blot using probe P6 complementary to ITS2 downstream site 4b. (**D**) Northern blot using probe P7 complementary to the 28S rRNA. (**E**) Ethidium bromide staining of an RNA gel showing the amounts of RNA loaded in each lane. (**F**) Enlarged figures showing the gel region of the high molecular weight pre-rRNAs detected with probes P5, P6 and P7. HEK293, parental cells; SC, cells transfected with the scrambled shRNA; CP4, cells transfected with shRNA against the NIP7 mRNA. (**G**) Structure of the 47S pre-rRNA. The positions of the probes P4, P5, P6 and P7 used in the northern blots shown in A-D are indicated. Asterisk indicates an unidentified band.

(Figure 6). By visual analysis of the autoradiograph, it is possible to observe the 21S pre-rRNA, although faint, in NIP7-depleted cells at the 2 h time point. Quantitation of the bands and calculation of the ratio relative to the amount of the 47S pre-rRNA revealed that formation of the 34S pre-rRNA is reduced and the 21S pre-rRNA is increased in NIP7-depleted cells (Figure 6B), which is consistent with the steady-state analyses, showing a defect in processing of ITS1.

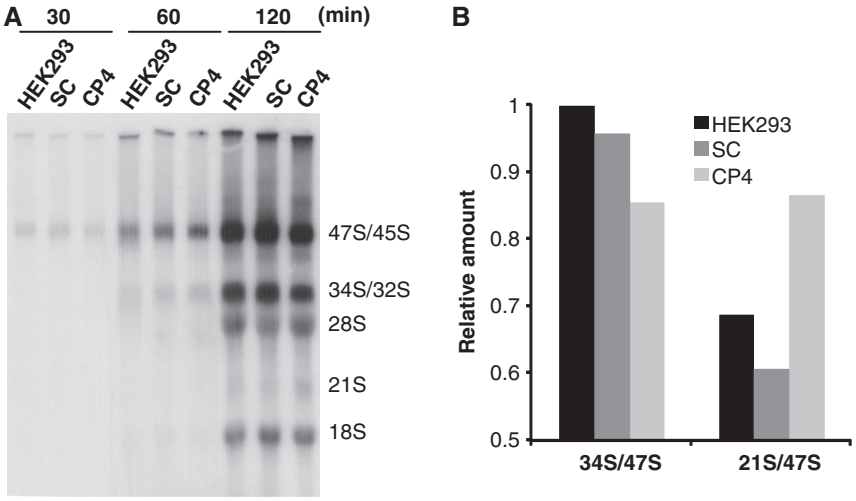

Figure 6. Analysis of pre-rRNA processing kinetics by pulse-chase labeling with ^{32}P-orthophosphate. (**A**) Autoradiography of the RNA samples that were collected every 30 min over a period of 2 h and fractionated by agarose gel electrophoresis. (**B**) Ratio of the 34S and 21S pre-rRNAs relative to the amount of the 47S pre-rRNA. Samples of the 120-min time point were used for quantitation. The 34S/47S ratio in HEK293 cells was taken as 100% to estimate the relative ratio of precursors.

Primer extension analysis of pre-rRNA processing sites in NIP7 deficient cells

Primer extension analyses were performed to examine the 5′-end of rRNA products at the processing sites that appeared to be most affected according to the northern blot analyses (Figure 7). Primer extension with oligonucleotide PE1 complementary to a sequence in the 18S rRNA, 27 bases downstream of the predicted 5′-end of the mature 18S rRNA (Site 1), resulted in products with the expected size (57, 30 nt of the primer PE1 plus 27 nt of extension up to Site 1). Interestingly, however, two bands were observed for all samples, suggesting that the cleavage at site 1 may take place at two adjacent nucleotides. For the parental HEK293 cells and the control cells transfected with the scrambled shRNA, the two bands showed a 1:1 ratio (Figure 7A). NIP7-depleted cells showed different product ratios with a sharp reduction of the longer product (Figure 7A). These discrepancies are consistent with defective processing at site 1 in NIP7-depleted cells. Oligonucleotide PE2 complementary to a sequence in ITS1 (nt 6299–6324 in the pre-rRNA) downstream of probe P3 (complementary to ITS1 nt 6121–6160 in the pre-rRNA) was used to determine the efficiency of cleavage reactions at sites in ITS1. Extension of primer PE2 generated a product of 33 nt (26 nt of the primer and 7 nt of extension), which corresponds to the 5′-end of the pre-rRNAs generated by cleavage at site 2b (Figure 7B). A reduction in the primer extension product is observed in NIP7-depleted cells, corroborating the results of the northern hybridizations which show inhibition of cleavages in ITS1 as a consequence of the reduced levels of NIP7. Oligonucleotide PE3 is complementary to a sequence 32 bases downstream of site 3, the predicted 5′-end of the mature 5.8S rRNA (nt 6655–6682 in the pre-rRNA). Extension of primer PE3 generated two major products, one with 60 nt (28 nt of the primer plus 32 nt of extension), corresponding to the expected size of the product generated by cleavage at site 3 and another one, 8–10 nt longer, designated as 3_L (Figure 7C). In eukaryotes, the 5′-end of the 5.8S rRNA has been described as heterogeneous (54–56) and this result suggests that mammalians may have at least a second form of 5.8S rRNA showing extended 5′-end as observed for *S. cerevisiae* (57). Similarly to the extension of primers PE1 and PE2, knocking down NIP7 expression caused a reduction especially of the longer extension products at site 3. The primer extension results, therefore, confirm the observation described above that lowering NIP7 expression leads to defects in pre-rRNA processing, affecting more strongly processing of the 5′-ETS and ITS1 spacer sequences.

Extension of primer PE3 revealed also three additional products (Figure 7C) that end at positions U7, U14 and A17 of the mature 5.8S rRNA (shorter form). The 5.8S rRNA is known to be methylated at residues U14 and G77, so we can assume that the faint band at the U14 position is a primer extension stop due to methylation. There is no report in the literature about nucleotide or base modification at positions A17 and U7 of the mature 5.8S rRNA. Primer extension stops can be originated when the reverse transcriptase reaches 5′-ends, base/ribose modifications or highly stable secondary structures. The band at position A17 is barely detectable in control cells and increases in NIP7-depleted cells, suggesting that it results from NIP7 deficiency (Figure 7C). In this case it is possible to speculate that the stop was due to premature degradation of the 5.8S rRNA 5′-end in the context of NIP7 deficiency where the aberrant and misprocessed precursors might be directed for degradation. In case of stop at position U7, it is present in control and test cells and is therefore caused by something that is common to the three samples which could be any of the options mentioned above.

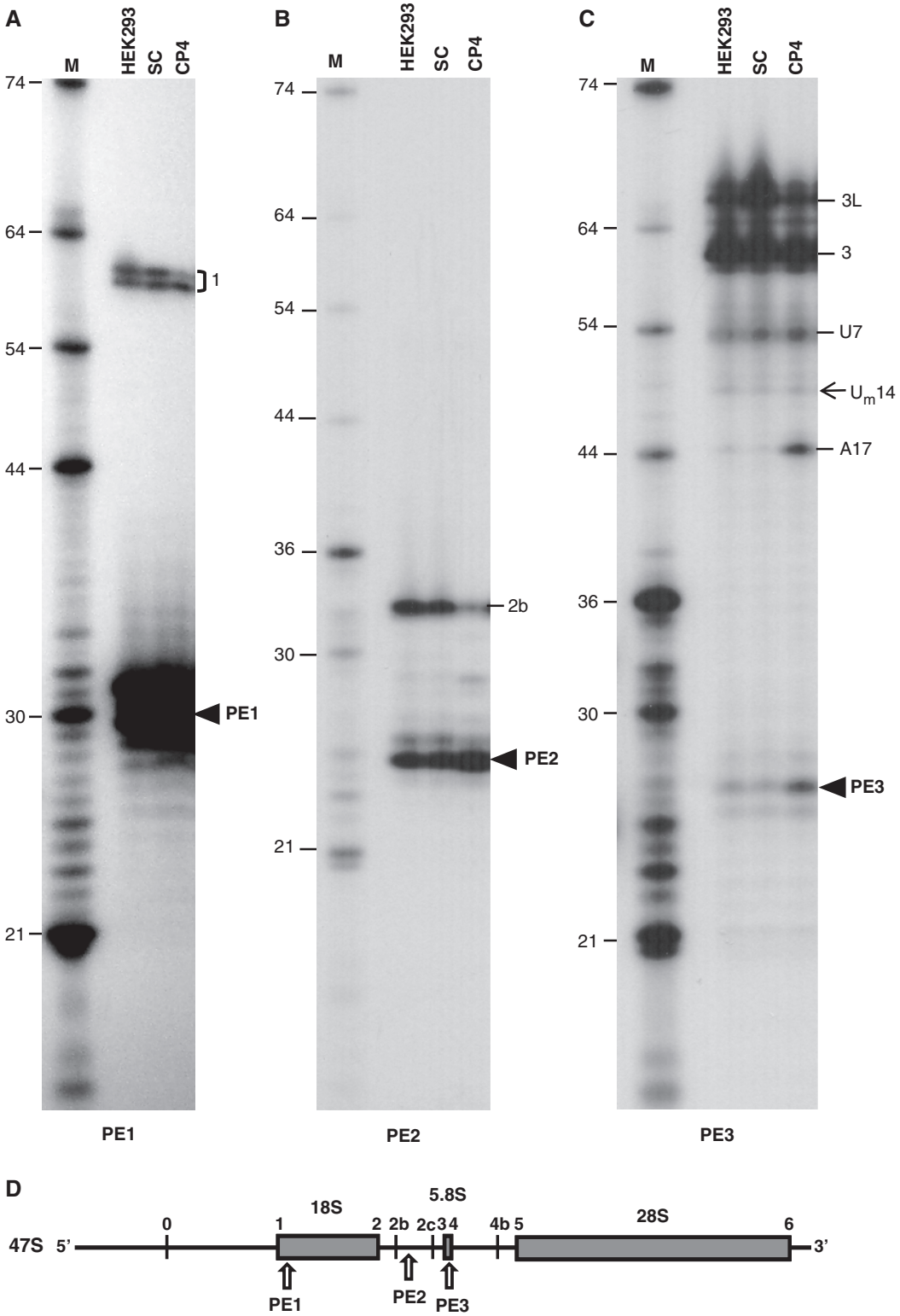

Figure 7. Analysis of primer extension products generated by reverse transcriptase. (**A**) Primer extension products using primer PE1 that is complementary to the 18S rRNA downstream site 1. (**B**) Primer extension products using primer PE2 that is complementary to ITS1 downstream site 2b. (**C**) Primer extension products using primer PE3 that is complementary to the 5.8S rRNA downstream site 3. U_m14 indicates the position of the 2-*O*-methyluridine at position 14 of the 5.8S rRNA. U7 and A17 indicate two unexpected primer extension stops. 1, 2b, 3 and 3L indicate the primer extension products extended to the respective processing sties. Arrowheads indicate the bands corresponding to the primers which were not extended: PE1, 30 nt; PE2, 26 nt and PE3, 28 nt, respectively. HEK293, parental cells; SC, cells transfected with scRNA; CP4, cells transfected with shRNA against the NIP7 mRNA. (**D**) Structure of the 47S pre-rRNA with the indication of the position of the oligonucleotides PE1, PE2 and PE3 used in the primer extension assays shown in A, B and C.

Human NIP7 associates to nuclear pre-ribosomal particles

Western blot analysis of the distribution of NIP7 in sucrose gradient fractions using the regular protocol to isolate polysomal extracts (51) revealed that NIP7 co-sediments in the range of 60S–80S ribosomes (Figure 8B). This result is similar to the distribution of *S. cerevisiae* Nip7p in sucrose gradients (40). However, previous data indicated that human NIP7 is a nucleolar protein (43). Cell fractionation followed by immunoblot analysis can be used to determine protein subcellular localization with a reasonable accuracy that, in some cases, can complement immunofluorescence assays or localization based on fusion to fluorescent proteins. Therefore, cell fractionation experiments were performed and confirmed that NIP7 is restricted to the nuclear compartment (Figure 8C). In a second experiment the sucrose gradient fractionation was performed with nuclear extract. A regular sucrose gradient with whole-cell polysomal extract was performed in parallel so that the positions of the 40S and 60S ribosomal subunits, 80S ribosomes and polysomes of the whole-cell polysomal extracts could serve as reference for sedimentation of the nuclear pre-ribosomal complexes. The fractionation analysis of the nuclear extract on sucrose gradients revealed that NIP7 distribution is highly similar to the profile observed for its distribution in the gradient of the whole-cell extract (Figure 8, compare panels B and D),

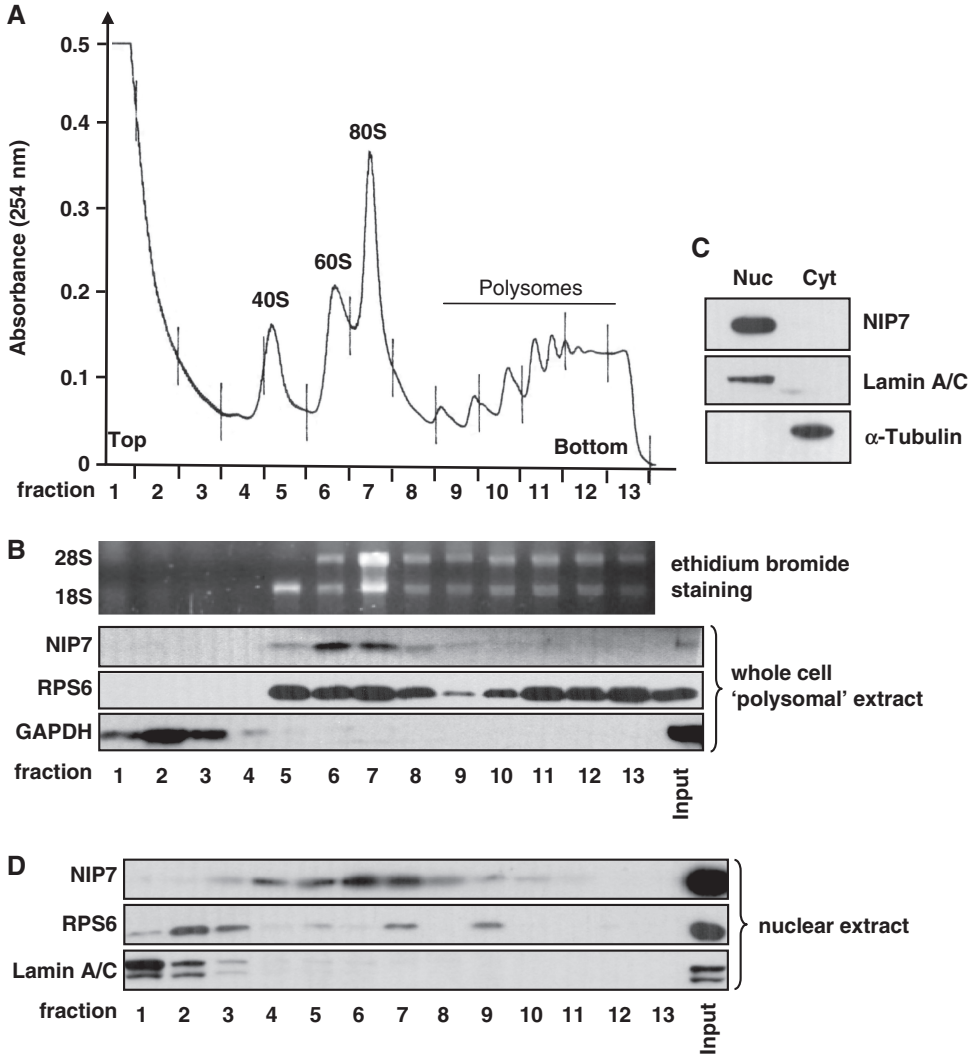

Figure 8. Analysis of NIP7 sedimentation on sucrose density gradients. (**A**) Polysome profile of HEK293 whole-cell polysomal extracts prepared according to Johannes and Sarnow (51). (**B**) Western blot analysis of NIP7 sedimentation on a sucrose density gradient of whole-cell polysomal extracts. 18S and 28S rRNAs and protein RPS6 are shown as references for ribosome and polysome sedimentation. GAPDH was used as reference for proteins not associated to ribosomes. (**C**) Western blots of HEK293 nuclear (Nuc) and cytoplasmic (Cyt) fractions showing NIP7 in the nuclear fraction. Lamin A/C and α-tubulin were used as controls for cell fractionation. (**D**) Western blot analysis of NIP7 following sucrose density gradient fractionation of a nuclear extract. The sucrose density gradients of whole-cell polysomal extract shown in B and nuclear extract shown in D were centrifuged and fractionated in parallel so that the positions of the 40S and 60S ribosomal subunits, 80S ribosomes and polysomes of the whole-cell polysomal extracts served as reference for sedimentation of the nuclear pre-ribosomal complexes. The profile of the nuclear extract is not shown because it is not informative of relevant peak fractions. RPS6 and Lamin A/C were used as references for 40S subunit and free protein sedimentation, respectively.

further suggesting that NIP7 co-sediments with pre-ribosomal particles. The control proteins used in these analyses showed the expected distribution. In the whole-cell extract gradient, RPS6 co-sediments in two major peaks, one between fractions 5 and 8, where the free 40S subunits and 80S ribosomes sediment, and between fractions 10 and 13, associated with polysomes (Figure 8B). In the gradient of nuclear extracts, on the other hand, most of RPS6, sediments in fractions 2 and 3, either as a soluble protein or as part of small complexes (Figure 8D). A smaller fraction of RPS6 sediments in fractions 5–9, indicating that it is associated to pre-ribosomal particles (Figure 8D). Lamin A/C was used as nuclear marker and behaves as a soluble protein in the sucrose gradient of the nuclear extract (Figure 8D). Consistently with the results shown above, NIP7 co-sediments with particles corresponding to pre-ribosomes in nuclear extracts gradients (Figure 8D). Combined, these results strongly indicate that NIP7 binds pre-ribosome particles in the nucleolus, thereby participating in the early pre-rRNA processing reactions.

Human NIP7 interacts with poly-U and poly-AU RNAs *in vitro*

The *S. cerevisiae* and *P. abyssi* Nip7 orthologs interact *in vitro* preferentially with poly-U homopolymers (42) and with poly-AU (J. S. Luz and C. C. Oliveira, personal communication). In order to determine whether recombinant human NIP7 also binds to RNA we initially tested its interaction with poly-U using electrophoretic mobility shift assays under native conditions. These assays showed that human NIP7 binds to polyuridine sequences although with low affinity (Figure 9A). Subsequent experiments showed that the human NIP7 protein binds to poly-AU with higher affinity than to poly-U (Figure 9B). In addition, competition assays were performed with increasing concentrations of unlabeled poly-A and poly-AU oligonucleotides. An excess of poly-A did not show effect on the NIP7–poly-AU interaction while the intensity of the band shift was reduced by increasing concentrations of unlabeled poly-AU oligonucleotides (Figure 9B and C), confirming the specificity of the NIP7–poly-AU interaction. The poly-AU oligonucleotide can form intra and intermolecular base-pairing suggesting that NIP7 might have a higher affinity for structured RNAs.

DISCUSSION

Given the essential function of the *S. cerevisiae NIP7* gene (40), the high conservation of NIP7 orthologs and the association to other ribosome synthesis proteins, we could predict that NIP7 would play an important function in human cells. We applied the RNA interference experimental approach to downregulate NIP7 expression and search for loss-of-function phenotypes. Downregulation of NIP7 in HEK293 cells was efficiently obtained using the transposon-based delivery system described by Heggestad *et al.* (49). Downregulation of NIP7 in HEK293, MCF10A and HeLa cells leads to reduction of cell proliferation rates, with cells accumulating in the G1 phase, indicating that NIP7 plays an important role in all human cells. Downregulation of NIP7 in HEK293 cells affected the levels of 40S ribosomal subunits and caused alterations in pre-rRNA processing which affected mainly the levels of the 34S, 26S and 21S pre-rRNA intermediates. Reduction of the 34S pre-rRNA indicates a slow processing defect at sites 2b and 2c. The increase of the 26S pre-rRNA concentration also correlates with slow processing of site 1 and of sites 2/2b whereas the increase of the 21S pre-rRNA indicates slow processing at sites 2/2b. Primer extension analysis of sites 1, 2b and 3 further supports the northern blot data. At least part of the pre-rRNA processing defects caused by NIP7 depletion have been described for other situations in which ribosome biogenesis was impaired, such as treatment with leptomycin B, which inhibits exportin Crm1/Xpo1 and blocks ribosome subunit export from the nucleus, and for knockdown of 40S biogenesis factors (11). The data obtained in this study indicate that human NIP7 is required primarily for processing of the pre-rRNA intermediates leading to the synthesis of the 18S rRNA and 40S subunit. Taking into account the conditional depletion of yeast Nip7p leads to a deficit of 60S subunits and to accumulation of the 27S pre-rRNA (40), during the course of this work, we have tested whether the human and archaeal *NIP7* orthologs could complement a yeast *Δnip7* mutant strain (Supplementary Figure S1). This analysis showed that neither the human nor the archaeal *NIP7* ortholog can complement a yeast *Δnip7* strain. This finding indicates that although the three orthologs bind structured RNA, and the yeast and human NIP7 are involved in pre-rRNA processing, the function of yeast Nip7p is not fully conserved in human cells.

The interactions of human NIP7 with other proteins are consistent with its role in ribosome biosynthesis. The first interaction described was with Nop132 (43), the putative ortholog of the *S. cerevisiae* Nop8p (44). Tests using the yeast two hybrid system and GST pull-down assays detected association of NIP7 with SBDS, indicating that both proteins may be part of a multisubunit complex (47). Subsequently, human NIP7 was found in association with complexes isolated by affinity-tagged purification of the 40S subunit protein RPS19 (45). This protein was already shown to play an essential role in 40S subunit biosynthesis in human cells (23), consistently with the genetic findings that link mutations in the *RPS19* gene to the DBA (25). Orrù and co-workers (45) described 159 proteins that co-purify with GST-RPS19. Although this complex is heterogeneous, it contains structural components of both the 40S and 60S subunits and a large set of proteins already known to function in ribosome synthesis. NIP7 is also found in complexes isolated by affinity-tagged purification of parvulin (Par14), a peptidyl-prolyl *cis–trans* isomerase (PPIase) reported to function in pre-rRNA processing (46). These large complexes are found mostly in the nucleolus, although some components may be found throughout the whole nucleus, consistently with our data describing NIP7 in the nuclear extracts that sediment in sucrose gradients

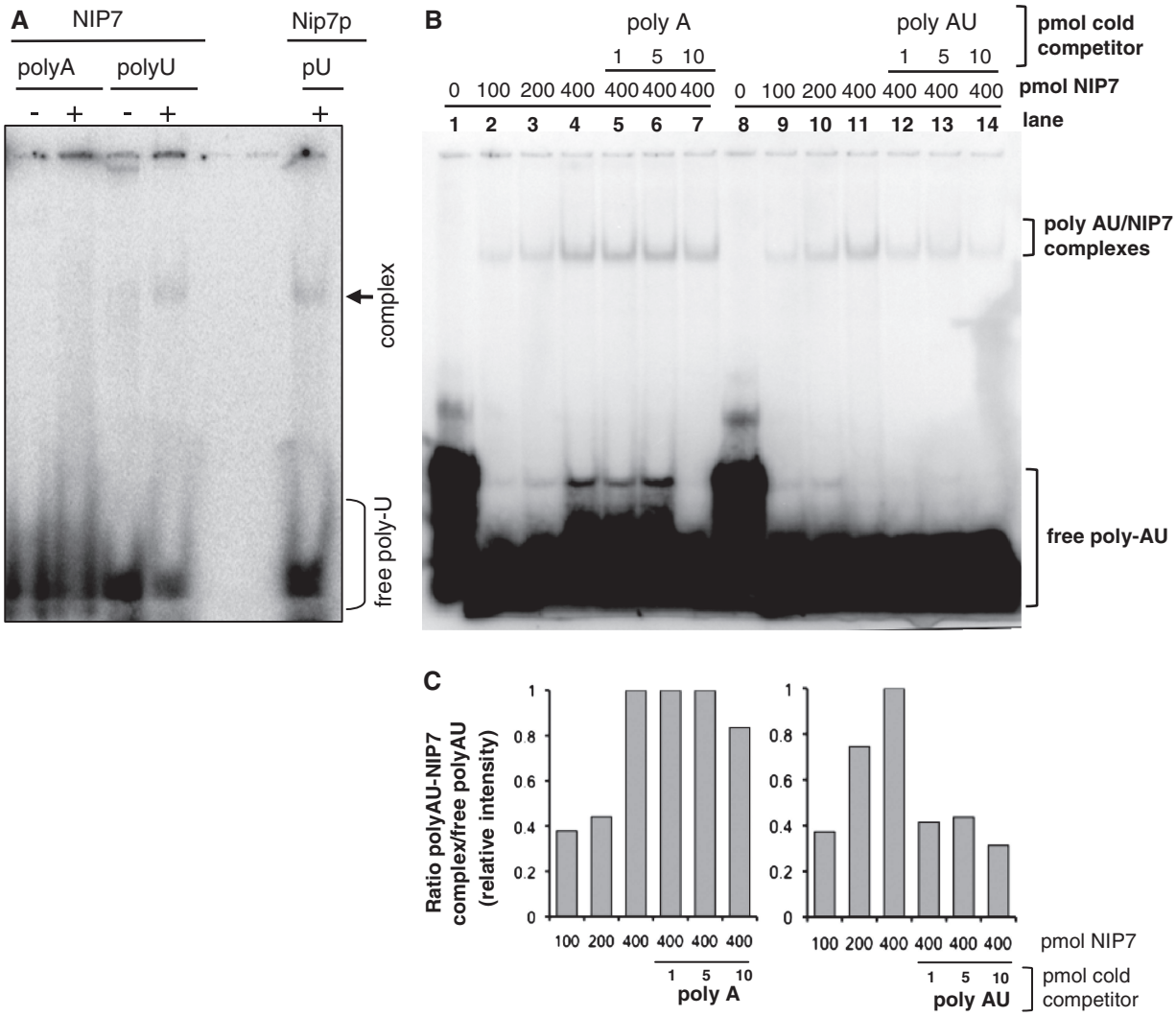

Figure 9. Analysis of NIP7 interaction with RNA *in vitro*. (**A**) Autoradiography of an electrophoretic mobility shift assay to determine the interaction of NIP7 with poly-U. One picomole of [^{32}P]-labeled poly-$A_{(20)}$ (negative control) and poly-$U_{(20)}$ were incubated with 100 pmol of recombinant NIP7. pU indicates the positive control in the assay containing [^{32}P]-labeled poly-$U_{(20)}$ and *S. cerevisiae* Nip7p. The arrow indicates the shifted bands corresponding to the complexes formed by NIP7 and yeast Nip7p with poly-U. (**B**) Autoradiography of an electrophoretic mobility shift assay showing the interaction of NIP7 with poly-AU. A total of 0.4 pmol of a [^{32}P]-labeled 21 mer poly-AU was incubated with 100, 200 and 400 pmol of recombinant NIP7 (lanes 2–4 and 9–11) showing NIP7 concentration dependent complex formation. Parallel competition experiments were performed. In lanes 5–7, 1, 5 and 10 pmol of cold poly-A were used as competitors. No effect of polyA addition is observed on the formation of poly-AU/NIP7 complexes. In lanes 12–14, 1, 5 and 10 pmol of cold poly-AU were used as competitor. As expected, a reduction of poly-AU/NIP7 complex formation is observed. (**C**) Graphs showing the quantitation of the ratio between the amount of polyAU-NIP7 complexes and the amount of free poly-AU of the experiment shown in (B). To calculate the relative intensities, the value of lane 4 was taken as 100% for the binding reactions from lanes 1 to 7 (graph on the left) and the value of lane 11 and taken as 100% for the binding reactions from lanes 8 to 14 (graph on the right).

with molecular masses in the range of 40S–80S ribosomes. During the development of this work, it became clear that the cell extracts used in the sucrose gradient fractionations contained nuclear and nucleolar contaminants probably due to partial leakage of nuclear content during disruption of cells under the hypotonic buffer conditions used or due to partial disruption of nuclei by the 1% v/v Triton detergent that is added to the extraction buffer. Cell fractionation revealed NIP7 only in the nuclear fraction and sucrose gradient fractionation of nuclear extracts indicated that NIP7 co-sediments with high molecular complexes, consistently with its association to pre-ribosomal particles.

Depletion of *S. cerevisiae* Nip7p caused a general defect in pre-rRNA processing, with accumulation of normal (35S and 27S) and of the aberrant (23S) pre-rRNAs and a reduction in the concentration of the mature rRNAs. Despite the global defects on pre-rRNA processing, *S. cerevisiae* Nip7p depletion led to a deficit of 60S subunit (40) and was found in 60S complexes (58). In addition, *S. cerevisiae* Nip7p interacts with a group of proteins involved in ribosome synthesis, including the exosome subunit Rrp43p and the nucleolar proteins Nop8p, Nop53p and Sdo1p (37,44,59,60). These proteins have been implicated to 60S subunit synthesis, although it is important to point out that conditional depletion of the

exosome subunit Rrp43p also led to general defects in pre-rRNA processing resulting in deficit of 40S ribosomal subunits (60). This phenotype is highly unexpected, given that exosome components have previously been reported to be required for excision of the ITS2 segment during maturation of the 3′-end of the 5.8S rRNA, a component of the 60S subunit (61). Further analysis of Rrp43p-depleted cells (60) and of temperature sensitive mutant strains (62) confirmed that deficiency of Rrp43p causes global defects in pre-rRNA processing, making it difficult to distinguish the primary from the secondary defects based only on data obtained from conditional mutants.

Despite the discrepancies between the defects observed in yeast and human NIP7 deficient cells, both human and yeast NIP7 proteins share the ability to bind poly-U *in vitro*, although human NIP7 has shown higher affinity for a poly-AU oligoribonucleotide. NIP7 cognate RNA target sequences have not been identified yet and its preference for binding to poly-U and poly-AU suggests that it might interact with uridine-rich sequences of the pre-rRNA similarly to Rrp5p, which was described to interact with a uridine-rich sequence in the ITS1 of the *S. cerevisiae* pre-rRNA (63). NIP7 orthologs share a two-domain architecture with the C-terminal PUA domain mediating interaction with RNA (42). This domain organization, suggests that NIP7 is an adaptor protein with the C-terminal domain interacting with RNA targets and the N-terminal domain mediating interaction with protein targets.

Saccharomyces cerevisiae NIP7 is part of the Ribi regulon (13,15) and its transcription levels were also shown to correlate with other Ribi regulon genes in response to stress caused by the alkylating agent methyl methanesulfonate (64). In addition, a study based on the analysis of gene expression in response to abrupt changes in environmental conditions has associated *S. cerevisiae* NIP7 to the early repressed ribosomal genes (65). As for the human NIP7 gene, its core promoter contains the 5′-C ACGTG-3′ sequence, also known as E(CG) sequence (66), that is recognized by the Myc:Max heterodimer, indicating that NIP7 is part of the human Ribi regulon proposed to be under control of the Myc transcription factor (16–18).

In conclusion, the data presented in this study show that human NIP7 plays an important role for cell proliferation and implicate NIP7 primarily in the processing of pre-rRNA intermediates leading to maturation of the 18S rRNA and 40S ribosomal subunit biosynthesis. The pre-rRNA processing defects clearly indicate that NIP7 plays a critical role in pre-rRNA processing in human cells. Association of NIP7 to RPS19 complexes (45) helps to explain the pre-RNA processing defects of the 18S rRNA pathway observed in this work for NIP7-depleted cells. We also show evidence that the human NIP7 protein is restricted to the nuclear compartment and that its sedimentation pattern in sucrose gradient fractionation indicates that it is associated to nuclear pre-ribosomal complexes.

SUPPLEMENTARY DATA

Supplementary Data are available at NAR Online.

ACKNOWLEDGEMENTS

The authors are grateful to Carla C. Oliveira for critical reading of the manuscript and discussion during the development of this study. The authors thank Prof. Irene G. H. Lorand-Metze for her support with FACS analyses.

FUNDING

FAPESP (grants CEPID/CBME 98/14138-2 and 06/02083-7) and CNPq (grant 473551/2008-0) to NITZ; FAPESP fellowships (2007/58371-3, 2003/06299-6 and 2006/57653-2 to L.G.M., P.P.C. and C.H.). Funding for open access charge: FAPESP grant Fundação de Amparo à Pesquisa do Estado de São Paulo or from funds from CNPq (Brazilian National Research Council).

Conflict of interest statement. None declared.

REFERENCES

1. Fromont-Racine,M., Senger,B., Saveanu,C. and Fasiolo,F. (2003) Ribosome assembly in eukaryotes. *Gene*, **313**, 17–42.
2. Henras,A., Soudet,K., Gérus,J.M., Lebaron,S., Caizergues-Ferrer,M., Mougin,A. and Henry,Y. (2008) The post-transcriptional steps of eukaryotic ribosome biogenesis. *Cell. Mol. Life Sci.*, **65**, 2334–2359.
3. Peng,W.T., Robinson,M.D., Mnaimneh,S., Krogan,N.J., Cagney,G., Morris,Q., Davierwala,A.P., Grigull,J., Yang,X., Zhang,W. *et al.* (2003) A panoramic view of yeast noncoding RNA processing. *Cell*, **113**, 919–933.
4. Venema,J. and Tollervey,D. (1999) Ribosome synthesis in *Saccharomyces cerevisiae*. *Annu. Rev. Genet.*, **33**, 261–311.
5. Grandi,P., Rybin,V., Bassler,J., Petfalski,E., Strauss,D., Marzioch,M., Schäfer,T., Kuster,B., Tschochner,H., Tollervey,D. *et al.* (2002) 90S pre-ribosomes include the 35S pre-rRNA, the U3 snoRNP, and 40S subunit processing factors but predominantly lack 60S synthesis factors. *Mol. Cell*, **10**, 105–115.
6. Nissan,T.A., Bassler,J., Petfalski,E., Tollervey,D. and Hurt,E. (2002) 60S pre-ribosome formation viewed from assembly in the nucleolus until export to the cytoplasm. *EMBO J.*, **15**, 5539–5547.
7. Tschochner,H. and Hurt,E. (2003) Pre-ribosomes on the road from the nucleolus to the cytoplasm. *Trends Cell Biol.*, **13**, 255–263.
8. Bowman,L.H., Rabin,B. and Schlessinger,D. (1981) Multiple ribosomal RNA cleavage pathways in mammalian cells. *Nucleic Acids Res.*, **9**, 4951–4965.
9. Hadjiolova,K.V., Nicoloso,M., Mazan,S., Hadjiolov,A.A. and Bachellerie,J.-P. (1993) Alternative pre-rRNA processing pathways in human cells and their alteration by cycloheximide inhibition of protein synthesis. *Eur. J. Biochem.*, **212**, 211–215.
10. Kent,T., Lapik,Y.R. and Pestov,D.G. (2009) The 52 external transcribed spacer in mouse ribosomal RNA contains two cleavage sites. *RNA*, **15**, 14–20.
11. Rouquette,J., Choesmel,V. and Gleizes,P.-E. (2005) Nuclear export and cytoplasmic processing of precursors to the 40S ribosomal subunits in mammalian cells. *EMBO J.*, **24**, 2862–2872.
12. Powers,T. and Walter,P. (1999) Regulation of ribosome biogenesis by the rapamycin-sensitive TOR-signaling pathway in *Saccharomyces cerevisiae*. *Mol. Biol. Cell.*, **10**, 987–1000.
13. Gasch,A.P., Spellman,P.T., Kao,C.M., Carmel-Harel,O., Eisen,M.B., Storz,G., Botstein,D. and Brown,P.O. (2000) Genomic expression programs in the response of yeast cells to environmental changes. *Mol. Biol. Cell.*, **11**, 4241–4257.

14. Hannan,K.M., Brandenburger,Y., Jenkins,A., Sharkey,K., Cavanaugh,A., Rothblum,L., Moss,T., Poortinga,G., McArthur,G.A., Pearson,R.B. *et al.* (2003) mTOR-dependent regulation of ribosomal gene transcription requires S6K1 and is mediated by phosphorylation of the carboxy-terminal activation domain of the nucleolar transcription factor UBF. *Mol. Cell. Biol.*, **23**, 8862–8877.
15. Jorgensen,P., Rupeš,I., Sharom,J.R., Schneper,L., Broach,J.R. and Tyers,M. (2004) A dynamic transcriptional network communicates growth potential to ribosome synthesis and critical cell size. *Genes Dev.*, **18**, 2491–2505.
16. Schlosser,I., Hölzel,M., Mürnseer,M., Burtscher,H., Weidle,U.H. and Eick,D. (2003) A role for c-Myc in the regulation of ribosomal RNA processing. *Nucleic Acids Res.*, **31**, 6148–6156.
17. Arabi,A., Wu,S., Ridderstråle,K., Bierhoff,H., Shiue,C., Fatyol,K., Fahlén,S., Hydbring,P., Söderberg,O., Grummt,I. *et al.* (2005) c-Myc associates with ribosomal DNA and activates RNA polymerase I transcription. *Nat. Cell. Biol.*, **7**, 303–310.
18. Grandori,C., Gomez-Roman,N., Felton-Edkins,Z.A., Ngouenet,C., Galloway,D.A., Eisenman,R.N. and White,R.J. (2005) c-Myc binds to human ribosomal DNA and stimulates transcription of rRNA genes by RNA polymerase I. *Nat. Cell. Biol.*, **7**, 311–318.
19. Grewal,S.S., Li,L., Orian,A., Eisenman,R.N. and Edgar,B.A. (2005) Myc-dependent regulation of ribosomal RNA synthesis during Drosophila development. *Nat. Cell. Biol.*, **7**, 295–302.
20. Zhao,Y., Sohn,J.-H. and Warner,J.R. (2003) Autoregulation in the biosynthesis of ribosomes. *Mol. Cell Biol.*, **23**, 699–707.
21. Barna,M., Pusic,A., Zollo,O., Costa,M., Kondrashov,N., Rego,E., Rao,P.H. and Ruggero,D. (2008) Suppression of Myc oncogenic activity by ribosomal protein haploinsufficiency. *Nature*, **456**, 971–975.
22. Dai,M.S. and Lu,H. (2008) Crosstalk between c-Myc and ribosome in ribosomal biogenesis and cancer. *J. Cell. Biochem.*, **105**, 670–677.
23. Choesmel,V., Bacqueville,D., Rouquette,J., Noaillac-Depeyre,J., Fribourg,S., Crétien,A., Leblanc,T., Tchernia,G., da Costa,L. and Gleizes,P.-E. (2007) Impaired ribosome biogenesis in Diamond-Blackfan anemia. *Blood*, **109**, 1275–1283.
24. Cmejla,R., Cmejlova,J., Handrkova,H., Petrak,J. and Pospisilova,D. (2007) Ribosomal protein S17 gene (RPS17) is mutated in Diamond-Blackfan anemia. *Hum. Mutat.*, **28**, 1178–1182.
25. Draptchinskaia,N., Gustavsson,P., Andersson,B., Pettersson,M., Willig,T.N., Dianzani,I., Ball,S., Tchernia,G., Klar,J., Matsson,H. *et al.* (1999) The gene encoding ribosomal protein S19 is mutated in Diamond–Blackfan anaemia. *Nat. Genet.*, **21**, 169–175.
26. Cmejla,R., Cmejlova,J., Handrkova,H., Petrak,J., Petrtylova,K., Mihal,V., Stary,J., Cerna,Z., Jabali,Y. and Pospisilova,D. (2009) Identification of mutations in the ribosomal protein L5 (RPL5) and ribosomal protein L11 (RPL11) genes in Czech patients with Diamond-Blackfan anemia. *Hum. Mutat.*, **30**, 321–327.
27. Farrar,J.E., Nater,M., Caywood,E., McDevitt,M.A., Kowalski,J., Takemoto,C.M., Talbot,C.C. Jr, Meltzer,P., Esposito,D., Beggs,A.H. *et al.* (2008) Abnormalities of the large ribosomal subunit protein, Rpl35a, in Diamond-Blackfan anemia. *Blood*, **11**, 1582–1592.
28. Gazda,H.T., Sheen,M.R., Vlachos,A., Choesmel,V., O'Donohue,M.F., Schneider,H., Darras,N., Hasman,C., Sieff,C.A., Newburger,P.E. *et al.* (2008) Ribosomal protein L5 and L11 mutations are associated with cleft palate and abnormal thumbs in Diamond-Blackfan anemia patients. *Am. J. Hum. Genet.*, **83**, 769–780.
29. Heiss,N.S., Knight,S.W., Vulliamy,T.J., Klauck,S.M., Wiemann,S., Mason,P.J., Poustka,A. and Dokal,I. (1998) X-linked dyskeratosis congenital is caused by mutations in a highly conserved gene with putative nucleolar functions. *Nat. Genet.*, **19**, 32–38.
30. Ruggero,D., Grisendi,S., Piazza,F., Rego,E., Mari,F., Rao,P.H., Cordon-Card,C. and Pandolfi,P.P. (2003) Dyskeratosis congenita and cancer in mice deficient in ribosomal RNA modification. *Science*, **299**, 259–262.
31. Yoon,A., Peng,G., Brandenburger,Y., Zollo,O., Xu,W., Rego,E. and Ruggero,D. (2006) Impaired control of IRES-mediated translation in X-linked dyskeratosis congenital. *Science*, **312**, 902–906.
32. Ridanpaa,M., van Eenennaam,H., Pelin,K., Chadwick,R., Johnson,C., Yuan,B., van Venrooij,W., Pruijn,G., Salmela,R., Rockas,S. *et al.* (2001) Mutations in the RNA component of RNase MRP cause a pleiotropic human disease, cartilage-hair hypoplasia. *Cell*, **104**, 195–203.
33. Gonzales,B., Henning,D., So,R.B., Dixon,J., Dixon,M.J. and Valdez,B.C. (2005) The Treacher Collins syndrome (TCOF1) gene product is involved in pre-rRNA methylation, *Hum. Mol. Genet.*, **14**, 2035–2043.
34. Valdez,B.C., Henning,D., So,R.B., Dixon,J. and Dixon,M.J. (2004) The Treacher Collins syndrome (TCOF1) gene product is involved in ribosomal DNA gene transcription by interacting with upstream binding factor. *Proc. Natl Acad. Sci. USA*, **101**, 10709–10714.
35. Boocock,G.R., Morrison,J.A., Popovic,M., Richards,N., Ellis,L., Durie,P.R. and Rommens,J.M. (2003) Mutations in SBDS are associated with Shwachman–Diamond syndrome. *Nat. Genet.*, **33**, 97–101.
36. Ganapathi,K.A., Austin,K.M., Lee,C.S., Dias,A., Malsch,M.M, Reed,R. and Shimamura,A. (2007) The human Shwachman-Diamond syndrome protein, SBDS, associates with ribosomal RNA. *Blood*, **110**, 1458–1465.
37. Luz,J.S., Georg,R.C., Gomes,C.H., Machado-Santelli,G.M. and Oliveira,C.C. (2009) Sdo1p, the yeast ortholog of Shwachman-Bodian-Diamond syndrome protein binds RNA and interacts with nuclear rRNA processing factors. *Yeast*, **26**, 287–298.
38. Menne,T.F., Goyenechea,B., Sánchez-Puig,N., Wong,C.C., Tonkin,L.M., Ancliff,P.J., Brost,R.L., Costanzo,M., Boone,C. and Warren,A.J. (2007) The Shwachman-Bodian-Diamond syndrome protein mediates translational activation of ribosomes in yeast. *Nat. Genet.*, **39**, 486–495.
39. Belin,S., Beghin,A., Solano-Gonzàlez,E., Bezin,L., Brunet-Manquat,S., Textoris,J., Prats,A.C., Mertani,H.C., Dumontet,C. and Diaz,J.-J. (2009) Dysregulation of ribosome biogenesis and translational capacity is associated with tumor progression of human breast cancer cells. *PLoS ONE*, **4**, e7147.
40. Zanchin,N.I.T., Roberts,P., de Silva,A., Sherman,F. and Goldfarb,D.S. (1997) *Saccharomyces cerevisiae* Nip7p is required for efficient 60S ribosome subunit biogenesis. *Mol. Cell. Biol.*, **17**, 5001–5015.
41. Aravind,L. and Koonin,E. (1999) Novel predicted RNA-binding domains associated with the translation machinery. *J. Mol. Biol.*, **48**, 291–302.
42. Coltri,P.P., Guimarães,B.G., Granato,D.C., Luz,J.S., Teixeira,E., Oliveira,C.C. and Zanchin,N.I.T. (2007) Structural insights into the interaction of the Nip7 PUA domain with polyuridine RNA. *Biochemistry*, **46**, 14177–14187.
43. Sekiguchi,T., Todaka,Y., Wang,Y., Hirose,E., Nakashima,N. and Nishimoto,T. (2004) A novel human nucleolar protein, Nop132, binds to the G proteins, RRAG A/C/D. *J. Biol. Chem.*, **279**, 8343–8350.
44. Zanchin,N.I.T. and Goldfarb,D.S. (1999) Nip7p interacts with Nop8p, an essential nucleolar protein required for 60S ribosome biogenesis, and the exosome subunit Rrp43p. *Mol. Cell. Biol.*, **19**, 1518–1525.
45. Orrù,S., Aspesi,A., Armiraglio,M., Caterino,M., Loreni,F., Ruoppolo,M., Santoro,C. and Dianzani,I. (2007) Analysis of the ribosomal protein S19 interactome. *Mol. Cell. Proteomics*, **6**, 382–393.
46. Fujiyama-Nakamura,S., Yoshikawa,H., Homma,K., Hayano,T., Tsujimura-Takahashi,T., Izumikawa,K., Ishikawa,H., Miyazawa,N., Yanagida,M., Miura,Y. *et al.* (2009) Parvulin (Par14), a peptidyl-prolyl cis-trans isomerase, is a novel rRNA processing factor that evolved in the metazoan lineage. *Mol. Cell. Proteomics*, **8**, 1552–1565.
47. Hesling,C., Oliveira,C.C., Castilho,B.A. and Zanchin,N.I.T. (2007) The Shwachman-Bodian-Diamond syndrome associated protein interacts with HsNip7 and its down-regulation affects gene expression at the transcriptional and translational levels. *Exp. Cell Res.*, **313**, 4180–4195.
48. Sambrook,J., Fritsch,E.J. and Maniatis,T. (1989) *Molecular cloning, A Laboratory Manual*, 2nd edn. Cold Spring Harbor Laboratory Press, Cold Spring Harbor, NY.

49. Heggestad,A.D., Notterpek,L. and Fletcher,B.S. (2004) Transposon based RNAi delivery system for generating knockdown cell lines. *Biochem. Biophys. Res. Commun.*, **316**, 643–650.
50. Klan,N. and Steinhilber,D. (2003) Transient transfection of the human myeloid cell line Mono Mac 6 using electroporation. *Biotechniques*, **34**, 142–147.
51. Johannes,G. and Sarnow,P. (1998) Cap-independent polysomal association of natural mRNAs encoding c-myc, BiP, and eIF4G conferred by internal ribosome entry sites. *RNA*, **12**, 1500–1513.
52. Gonzales,F.A., Zanchin,N.I.T., Luz,J.S. and Oliveira,C.C. (2005) Characterization of *Saccharomyces cerevisiae* Nop17p, a novel Nop58p-interacting protein that is involved in pre-rRNA processing. *J. Mol. Biol.*, **346**, 437–455.
53. Lebreton,A., Tomecki,R., Dziembowski,A. and Séraphin,B. (2008) Endonucleolytic RNA cleavage by a eukaryotic exosome. *Nature*, **456**, 993–996.
54. Bowman,L.H., Goldman,W.E., Goldberg,G.I., Herbert,M.B. and Schiessinger,D. (1983) Location of the initial cleavage sites in mouse pre-rRNA. *Mol. Cell. Biol.*, **3**, 1501–1510.
55. Rubin,G.M. (1974) Three forms of the 5.8S ribosomal RNA species in *Saccharomyces cerevisiae*. *Eur. J. Biochem.*, **41**, 197–202.
56. Smith,S.D., Banerjee,N. and Sitz,T.O. (1984) Gene heterogeneity: a basis for alternative 5.8S rRNA processing. *Biochemistry*, **23**, 3648–3652.
57. Schmitt,M.E. and Clayton,D.A. (1993) Nuclear RNase MRP is required for correct processing of pre-5.8S rRNA in *Saccharomyces cerevisiae*. *Mol. Cell. Biol.*, **13**, 7935–7941.
58. Lebreton,A., Rousselle,J.-C., Lenormand,P., Namane,A., Jacquier,A., Fromont-Racine,M. and Saveanu,C. (2008) 60S ribosomal subunit assembly dynamics defined by semi-quantitative mass spectrometry of purified complexes. *Nucleic Acids Res.*, **36**, 4988–4999.
59. Granato,D.C., Gonzales,F.A., Luz,J.S., Cassiola,F., Machado-Santelli,G.M. and Oliveira,C.C. (2005) Nop53p, an essential nucleolar protein that interacts with Nop17p and Nip7p, is required for pre-rRNA processing in *Saccharomyces cerevisiae*. *FEBS J.*, **272**, 4450–4463.
60. Zanchin,N.I.T. and Goldfarb,D.S. (1999) The exosome subunit Rrp43p is required for the efficient maturation of 5.8S, 18S and 25S rRNA. *Nucleic Acids Res.*, **27**, 1283–1288.
61. Mitchell,P., Petfalski,E., Shevchenko,S., Mann,M. and Tollervey,D. (1997) The exosome: a conserved eukaryotic RNA processing complex containing multiple 3′-5′ exoribonucleases. *Cell*, **91**, 457–466.
62. Oliveira,C.C., Gonzales,F.A. and Zanchin,N.I.T. (2002) Temperature-sensitive mutants of the exosome subunit Rrp43p show a deficiency in mRNA degradation and no longer interact with the exosome. *Nucleic Acids Res.*, **30**, 4186–4198.
63. de Boer,P., Vos,H.R., Faber,A.W., Vos,J.C. and Raué,H.A. (2006) Rrp5p, a trans-acting factor in yeast ribosome biogenesis, is an RNA-binding protein with a pronounced preference for U-rich sequences. *RNA*, **12**, 263–271.
64. Jelinsky,S.A. and Samson,L.D. (1999) Global response of *Saccharomyces cerevisiae* to an alkylating agent. *Proc. Natl Acad. Sci. USA*, **96**, 1486–1491.
65. Chechik,G. and Koller,D. (2009) Timing of gene expression responses to environmental changes. *J. Comput. Biol.*, **16**, 279–290.
66. Brown,S.J., Cole,M.D. and Erives,A.J. (2008) Evolution of the holozoan ribosome biogenesis regulon. *BMC Genomics*, **9**, 442, doi:10.1186/1471-2164-9-442.

Supplemental data

Human NIP7 does not complement yeast *Δnip7* cells

Plasmids used in the complementation assay:

Plasmids YEplac181/GPD-HsNIP7 and YEplac181/GPD-PaNIP7 contain, respectively, the human NIP7 cDNA and the *Pyrococcus abyssi* NIP7 (PaNIP7) coding sequence under the control of the strong constitutive GAPDH (glyceraldehydes-3-phosphate dehydrogenase) promoter. YEplac181/GPD-HsNIP7 was constructed by inserting simultaneously the GAPDH promoter digested with Eco RI and Bam HI and the NIP7 cDNA digested with Bgl II and Sal I into the Eco RI and Sal I restriction sites of plasmid YEplac181 (Gietz and Sugino, 1988) The GAPDH promoter was isolated from plasmid pDN291 (Ng and Walter, 1996). YEplac181/GPD-PaNIP7 was constructed by inserting simultaneously the GAPDH promoter (digested with Eco RI and Bam HI) and the PaNIP7 coding sequence (isolated from pCYTEX-PaNip7 following digestion with Bgl II and Sal I) (Coltri *et al*., 2004) into the Eco RI and Sal I restriction sites of plasmid YEplac181 (Gietz and Sugino, 1988).

Yeast strains:

W303-1a: *MAT***a,** *ade2-1*, *leu2-3*, *112 his3-11,15*, *trp1-1*, *ura3-1*, *can1-100*.

DG439: *MAT***a**, *ade2-1*, *leu2-3,112*, *trp1-1*, *ura3-1*, *nip7::HIS3* p[*URA3 ARSH4 GAL1::HA-NIP7*].

DG440: *MAT***a**, *ade2-1*, *leu2-3,112*, *trp1-1*, *ura3-1*, *nip7::HIS3* p[*LEU2 ARS1 NIP7*].

Yeast transformation:

Yeast strain DG439 (Zanchin *et al*., 1997) was transformed with 5 μg of either YEplac181/GPD-HsNIP7 or YEplac181/GPD-PaNIP7 by using the lithium acetate method as previously described (Ausubel *et al.*, 1998). The cells were plated on YNB minimal medium containing 2% (w/v) galactose and supplemented with adenine and tryptophan. In this medium, the cells are maintained by the NIP7 copy of plasmid p[URA3 ARSH4 GAL1::HA-NIP7] and the DG439 transformants were selected by the Leu^+ phenotype

conferred by the the *LEU2* auxotrophy marker of plasmid YEplac181 (Gietz and Sugino, 1988).

Complementation assay:

The complementation assay was performed by plating the test strains (DG439 transformed with YEplac181/GPD-HsNIP7 and DG439 transformed with YEplac181/GPD-PaNIP7) and the control strains (W303-1a and DG440) on YPD medium. The glucose present in the YPD medium inhibits the *GAL1* promoter, blocking the expression of yeast Nip7p, cloned under the control of the *GAL1* promoter in plasmid YCpHANIP7 (Zanchin *et al.*, 1997). The human NIP7 cDNA and the *P. abyssi* NIP7 coding sequence are under the control of the strong constitutive yeast promoter GAPDH. In this assay, only the control strains were able to grow (supplemental figure 1) showing that neither the human nor the *P. abyssi* NIP7 orthologs can complement the knock out of the yeast *NIP7* gene.

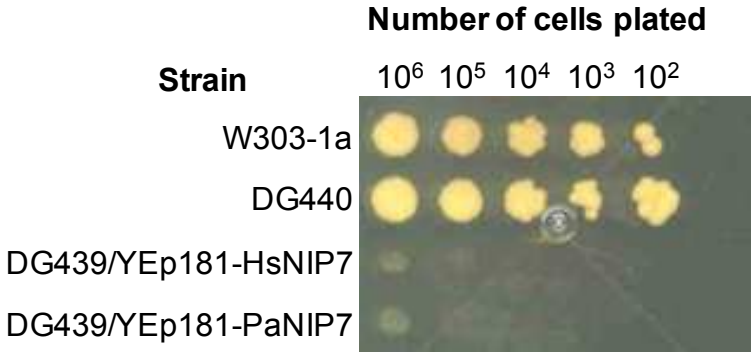

Supplemental figure 1. Assay to test complementation of the yeast *Δnip7* strain by the human and archael Nip7 orthologs.

Northern blot analysis of pre-rRNA processing in MCF10A cells

In order to determine whether downregulation of Nip7 in MCF10A cells affects pre-rRNA processing we performed a Northern blot with probe P3. This probe was selected because it can detect the major processing defects observed in HEK293 cells expressing shRNA against the Nip7 mRNA. MCF10A cells transfection, RNA extraction and Northern hybridization were performed as described in the Materials and Methods section of the manuscript. This analysis revealed an increase of the 41S and 21S pre-rRNAs which is consistent with the pre-RNA processing defects observed for HEK293 cells deficient for Nip7.

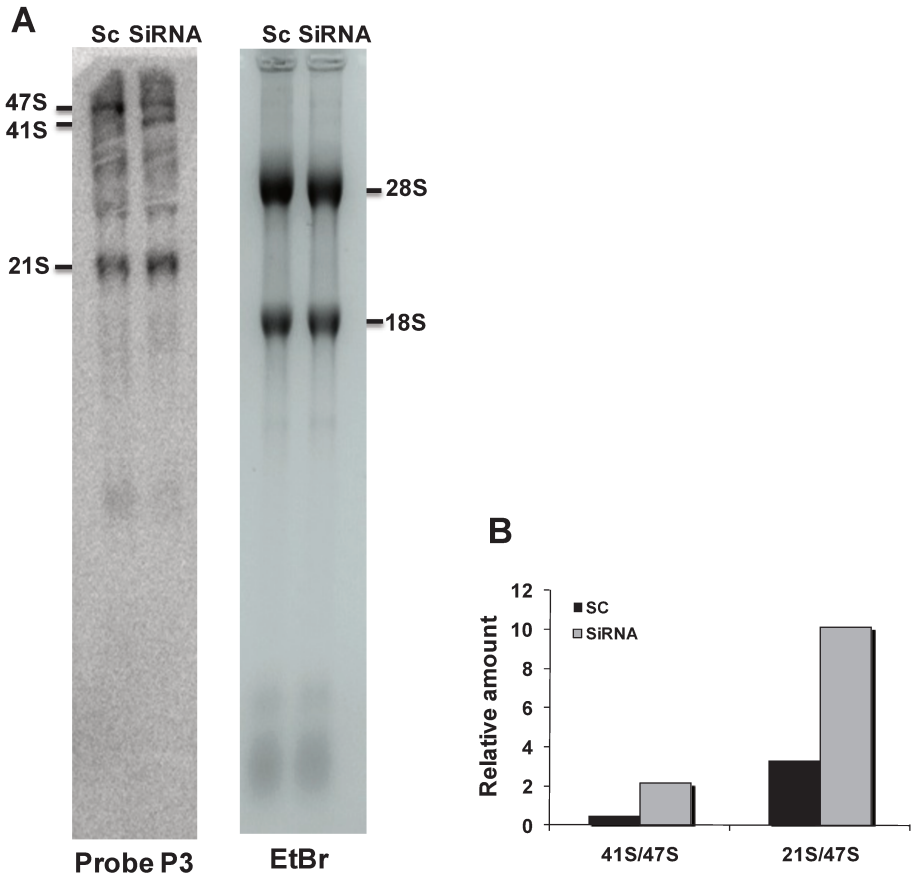

Supplemental figure 2. Norhthern blot analysis of total RNA isolated from MCF10A cells. (**A**) Norhthern blot (left) using probe P3. The right panel shows the membrane stained with ethidium bromide showing equivalent gel loading. (**B**) Quantitation of the bands and calculation of the ratio relative to the amount of the 47S pre-rRNA showing an increase of the 41S and 21S pre-rRNAs in Nip7-depleted cells

References for the supplemental data:

Ausubel,F.M.; Brent,R.; Kingston,R.; Moore,D.D.; Seidman,J.G.; Smith,J.A.; Struha,K. (1998). Current Protocols in Molecular Biology. New York: John Wiley & Sons.

Coltri,P.P., Guimarães,B.G., Oliveira,C.C., Zanchin, N.I. 2004. Expression, crystallization and preliminary X-ray analysis of the *Pyrococcus abyssi* protein homologue of *Saccharomyces cerevisiae* Nip7p. *Acta Crystallogr D Biol Crystallogr.* **60**(Pt 10):1925-1928.

Gietz,R.D., Sugino,A. 1988. New yeast and Escherichia coli shuttle vectors constructed with in vitro mutagenized yeast genes lacking six-base pair restriction sites. *Gene* **74**:527–534.

Ng,D.T., Walter,P. 1996. ER membrane protein complex required for nuclear fusion. *J Cell Biol.* **132**:499-509.

Zanchin,N.I., Roberts,P., DeSilva,A., Sherman,F., Goldfarb,D.S. 1997. *Saccharomyces cerevisiae* Nip7p is required for efficient 60S ribosome subunit biogenesis. *Mol. Cell. Biol*. **17**:5001-5015.

3. RESULTADOS

3.2. Capítulo II (Artigo II)

The Human Nucleolar Protein FTSJ3 Associates with NIP7 and Functions in Pre-rRNA Processing

Luis G. Morello, Patricia P. Coltri, Alexandre J. C. Quaresma, Fernando M. Simabuco, Tereza C. L. Silva, Guramrit Singh, Jeffrey A. Nickerson, Carla C. Oliveira, Melissa J. Moore, Nilson I. T. Zanchin

PLoS ONE, **6**, e29174 (2011)

OPEN ACCESS Freely available online

PLoS one

The Human Nucleolar Protein FTSJ3 Associates with NIP7 and Functions in Pre-rRNA Processing

Luis G. Morello[1,4], Patricia P. Coltri[2], Alexandre J. C. Quaresma[3], Fernando M. Simabuco[1], Tereza C. L. Silva[1], Guramrit Singh[4], Jeffrey A. Nickerson[3], Carla C. Oliveira[2], Melissa J. Moore[4], Nilson I. T. Zanchin[5]*

1 Laboratório Nacional de Biociências, Centro Nacional de Pesquisa em Energia e Materiais, Campinas, São Paulo, Brazil, **2** Department of Biochemistry, University of São Paulo, São Paulo, Brazil, **3** Department of Cell Biology and Cancer Center, University of Massachusetts Medical School, Worcester, Massachusetts, United States of America, **4** Department of Biochemistry and Molecular Pharmacology and Howard Hughes Medical Institute, University of Massachusetts Medical School, Worcester, Massachusetts, United States of America, **5** Instituto Carlos Chagas, Fundação Instituto Oswaldo Cruz, Curitiba, Paraná, Brazil

Abstract

NIP7 is one of the many trans-acting factors required for eukaryotic ribosome biogenesis, which interacts with nascent pre-ribosomal particles and dissociates as they complete maturation and are exported to the cytoplasm. By using conditional knockdown, we have shown previously that yeast Nip7p is required primarily for 60S subunit synthesis while human NIP7 is involved in the biogenesis of 40S subunit. This raised the possibility that human NIP7 interacts with a different set of proteins as compared to the yeast protein. By using the yeast two-hybrid system we identified FTSJ3, a putative ortholog of yeast Spb1p, as a human NIP7-interacting protein. A functional association between NIP7 and FTSJ3 is further supported by colocalization and coimmunoprecipitation analyses. Conditional knockdown revealed that depletion of FTSJ3 affects cell proliferation and causes pre-rRNA processing defects. The major pre-rRNA processing defect involves accumulation of the 34S pre-rRNA encompassing from site A′ to site 2b. Accumulation of this pre-rRNA indicates that processing of sites A0, 1 and 2 are slower in cells depleted of FTSJ3 and implicates FTSJ3 in the pathway leading to 18S rRNA maturation as observed previously for NIP7. The results presented in this work indicate a close functional interaction between NIP7 and FTSJ3 during pre-rRNA processing and show that FTSJ3 participates in ribosome synthesis in human cells.

Citation: Morello LG, Coltri PP, Quaresma AJC, Simabuco FM, Silva TCL, et al. (2011) The Human Nucleolar Protein FTSJ3 Associates with NIP7 and Functions in Pre-rRNA Processing. PLoS ONE 6(12): e29174. doi:10.1371/journal.pone.0029174

Editor: Grzegorz Kudla, University of Edinburgh, United Kingdom

Received August 12, 2011; **Accepted** November 22, 2011; **Published** December 16, 2011

Funding: This work was supported by FAPESP (grant 06/02083-7) and CNPq (grant 473551/2008-0) to NITZ. LGM, PPC, and FMS were recipients of FAPESP fellowships (2007/58371-3, 2003/06299-6 and 2008/57110-4). The funders had no role in study design, data collection and analysis, decision to publish, or preparation of the manuscript.

Competing Interests: The authors have declared that no competing interests exist.

* E-mail: nilson.zanchin@pq.cnpq.br

Introduction

Synthesis of eukaryotic ribosomes takes place mainly in the nucleolus, a specialized cell compartment within the nucleus, where RNA polymerase I transcribes a large polycistronic ribosomal RNA, the 47S pre-rRNA. This pre-rRNA contains the 18S, 5.8S and 28S rRNAs flanked by the 5′ and 3′ external spacer sequences (5′ ETS and 3′ ETS) and by the internal spacer sequences 1 (ITS1) and 2 (ITS2). It is processed into the 18S, 5.8S and 28S mature rRNAs by a series of endo- and exonucleolytic cleavages and covalent nucleotide modifications concomitantly with assembling of ribosomal proteins to form the ribosomal particles. Pre-rRNA cleavages and modifications, which include base and ribose methylation and uridine isomerization to pseudouridine at specific sites, are mediated by trans-acting factors. These factors bind to nascent pre-ribosomal particles and dissociate as their function is accomplished along this high-energy consuming process [1–5]. Approximately 200 eukaryotic pre-ribosome trans-acting factors have already been identified based on protein interaction and genetic and biochemical analyses [5].

In *Saccharomyces cerevisiae*, mutations in genes required for ribosome biogenesis usually interfere with the order of pre-rRNA processing steps, causing accumulation of aberrant pre-rRNAs or fast degradation of pre-rRNA intermediates. Ribosome synthesis defects eventually lead to imbalance of the 40S/60S subunit ratio or affect subunit export to the cytoplasm. Ribosome synthesis and function have additional implications for multicellular organisms, especially for humans, where over fifteen genetic diseases have already been linked to mutations in genes that affect ribosome structure or synthesis [6]. These genes can be divided into three major groups. One group includes permanent components of ribosomes both from the small (RPS7, RPS14, RPS17, RPS19, RPS24) and large (RPL5, RPL11, RPL35A) subunits. A second group encodes trans-acting protein factors required for synthesis of both the small (UTP14c, CIRH1A, EMG1, WDR36, HCA66) and large (RBM28, SBDS) subunits. And, a third group includes components of small ribonucleoproteins involved in pre-rRNA cleavage (RMRP), pseudouridylation (DKC1, NOP10, NHP2) and methylation (TCOF1, HBII-85 – deleted Box C/D cluster) and in rDNA transcription (TCOF1) [7]. These genetic diseases underscore the importance of accurate ribosome synthesis and function for normal cellular function.

S. cerevisiae has been widely used as a model system to identify trans-acting factors and to study the ribosome synthesis mechanism. Although the general mechanism is conserved in all eukaryotes, several key differences between yeast and mammalians have emerged. In wild type *S.cerevisiae* strains, processing of the 35S

pre-rRNA follows a 5′ to 3′ processing hierarchy where the 5′ ETS is cleaved before processing of ITS1, which in its turn is cleaved before ITS2 [2,8,9]. The mammalian 47S pre-rRNA, on the other hand, is initially converted to a 45S pre-rRNA that is processed by three simultaneous alternative pathways, depending on the site where the first cleavage occurs. In pathway A, the first cleavage at site 1 removes the complete 5′ ETS. In pathway B, the first cleavage takes place at site 2c in ITS1. In pathway C, the first site to be cleaved is 4b in the ITS2 [10,11].

Most ribosome biogenesis factors have initially been characterized in *S. cerevisiae* and it has been widely assumed that their function is conserved in human cells. However, recent studies have shown that conditional depletion of human ribosome synthesis factors produce phenotypes significantly different from those observed in yeast. Bystin and hTsr1, the human orthologs of yeast Enp1 and Tsr1, respectively, are required for the maturation of the 18S rRNA and synthesis of the 40S subunit. However, conditional knockdown of these proteins in HEK293 lead to defects in pre-rRNA processing and 40S subunit export that are distinct from those reported for the yeast orthologs [12–15]. In *S. cerevisiae*, Nip7p depletion causes a profound effect on 60S subunit formation, leading to accumulation of unprocessed 27S pre-rRNA and to a deficit of 60S subunits [16]. Consistently with this, yeast Nip7p interacts with the Nop8p, Nop53p, Sdo1p proteins that are involved in 60S subunit synthesis [17–20]. Nip7p interacts also with Rrp43p, an exosome subunit involved in exonucleolytic maturation of the 3′-end of the 5.8S rRNA [18,21]. In contrast to yeast, NIP7 knockdown in human cells leads to 40S ribosome deficiency. Pre-rRNA processing defects were detected in human cells depleted of NIP7, which include decrease of the 34S pre-rRNA and an increase of the 26S and 21S pre-rRNA concentrations [22].

The different phenotypes observed for conditional depletion of the yeast and human NIP7 proteins raised the possibility that the human NIP7 interacts with a different set of partners. To better understand the essential role played by NIP7 in ribosome biogenesis in human cells [22], and to elucidate the basis of functional difference displayed by NIP7 in yeast and humans, we performed a yeast two-hybrid screen to identify human proteins that interact with NIP7. We have identified FTSJ3 as a NIP7-interacting protein. FTSJ3 shows sequence similarity to the yeast protein Spb1. Both contain a putative RNA-methyl-transferase domain (FtsJ) in the N-terminal region and a conserved uncharacterized domain (Spb1_C) in the C-terminal region. Spb1 was shown to be required for 60S subunit synthesis in yeast [23] and to mediate methylation of the conserved G_{2922} that is located within the A loop of the catalytic center of the ribosome [24,25]. A second line of evidence supporting the hypothesis that human NIP7 and FTSJ3 function in association during ribosome biogenesis as part of the same pre-ribosomal complexes comes from studies where both NIP7 and FTSJ3 were copurified by affinity purification of parvulin (Par14) [26–28].

The evidence mentioned above prompted us to further characterize the physical and functional interaction between NIP7 and FTSJ3. We describe in this study a functional association between NIP7 and FTSJ3 based on colocalization and coimmunoprecipitation analyses. We show also that FTSJ3 is required for pre-rRNA processing and cell proliferation, acting in the pathway leading to 18S rRNA maturation as observed previously for NIP7. Specifically, the cells depleted of FTSJ3 accumulate the 34S pre-rRNA, encompassing from site A′ to site 2b, indicating that processing of sites A0, 1 and 2 is inhibited in absence of FTSJ3.

Results

Isolation of FTSJ3 as a NIP7-interacting partner

Human NIP7 plays an essential role in ribosome biogenesis and functions in close association with the SBDS protein [22,29]. NIP7 knockdown in human cell lines leads to 40S ribosome deficiency with concomitant decrease of the 34S pre-rRNA concentration and an increase of the 26S and 21S pre-rRNA concentrations [22]. Increase of the 26S pre-rRNA indicates uncoupling of processing at sites A0 and 1 and increase of the 21S pre-rRNA indicates that processing at site 2 is particularly slower in NIP7-depleted cells. These defects are in contrast with those observed upon conditional depletion of Nip7p in yeast cells, which accumulate unprocessed 27S pre-rRNA and show a deficit of 60S subunits [16]. Given these observations, we hypothesized that the yeast and human NIP7 proteins display differential protein-protein interactions. To test such a hypothesis, we undertook a yeast two-hybrid screen to identify human NIP7-interacting proteins. The screen was performed using a l*ex*A-NIP7 fusion protein as bait to screen a human fetal brain cDNA library (Clontech HL4028AH). 121 positive clones were isolated from over 3×10^6 yeast transformants. 50 positive clones were sequenced and ten of them (20%) encode FTSJ3, a putative ortholog of yeast Spb1p. FTSJ3 is an 847 amino acid protein containing a putative RNA-methyl-transferase domain (FtsJ, residues 22–202) and a Spb1_C domain (residues 640–847). The cDNAs isolated in the yeast-two hybrid screen encode both full-length and truncated proteins starting at residues 291, 373 and 433 (Fig. 1A). Expression of the two-hybrid reporters *HIS*3 (Fig. 1B) and *lacZ* (data not shown) confirmed interactions between NIP7 and FTSJ3 (full-length protein or its truncations) isolated in the screen. These results suggest that the FTSJ3 region comprising from residue 433 to the C-terminus mediates the interaction with NIP7. In order to confirm the interaction identified using the yeast two-hybrid system we performed pull-down assays using recombinant proteins produced in *E. coli*. The assay was performed with GST-FSTJ3 immobilized on glutathione-sepharose beads and purified histidine-tagged NIP7. As expected, NIP7 was retained in the bound fraction in the GST-FTSJ3 binding reaction (Fig. 1C, upper panel, lane 3) but not in the control reaction (Fig. 1C, lower panel, lane 3). The NIP7-FTSJ3 interaction observed both in the yeast two-hybrid and in the pull-down assay using recombinant proteins indicated that these proteins interact directly in vivo. However, we know from a previous study that NIP7 can bind to unspecific RNAs in vitro [22]. FTSJ3 possesses a putative RNA-methyl-transferase domain in the N-terminal region and a large intrinsically disordered region encompassing the central region and the conserved Spb1_C domain in the C-terminal region. These features indicate that FTSJ3 might also be an RNA-binding protein, raising the possibility that the interaction between NIP7 and FTSJ3 might as well take place through an RNA molecule. To test this possibility, a binding reaction was performed after treating the immobilized GST-FTSJ3 with RNase A. Interestingly, the interaction was abolished by the RNase A treatment (Fig. 1C, upper panel, lane 4). Addition of excess yeast total RNA to the binding reaction recovers NIP7 binding to GST-FTSJ3 (Fig. 1C, upper panel, lane 5). Treatment with RNase A after the addition of excess total RNA decreased the recovery of NIP7 interacting with FTSJ3 (Fig. 1C, upper panel, lane 6). These findings indicate that the interaction between recombinant NIP7 and FTSJ3 in vitro is mediated by binding to RNA molecules bound nonspecifically to both proteins.

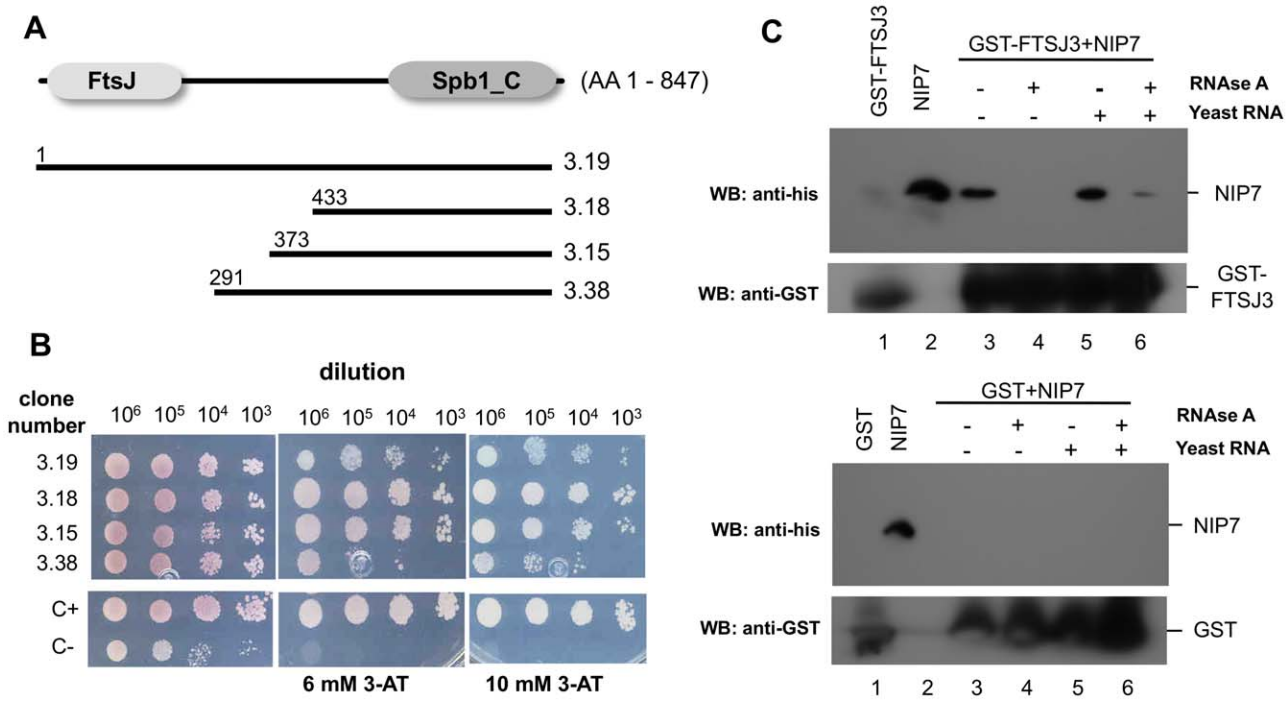

Figure 1. Isolation and validation of FTSJ3 as a bona-fide interaction partner of NIP7. (**A**) Diagram of the FTSJ3 protein (adapted from PFAM database) and cDNA clones showing positive interaction with NIP7 in the yeast two-hybrid system. Conserved domains, FtsJ and Spb1_C, are shown in grey boxes. Bars represent the length of each cDNA isolated in the yeast two-hybrid screen. The first amino acid encoded by the truncated cDNAs is indicated on the left. (**B**) Dilution-based growth assays of yeast cells tested for *HIS3* expression as a reporter of two-hybrid interactions between NIP7 and human cDNAs indicated on the left (top panel). A positive control for two-hybrid interaction (C+, yeast strain L40 expressing *lex*A-Nip7p and AD-Nop8p) and negative control (C−, yeast strain L40 expressing *lex*A-NIP7 and GAL4AD) are shown in the bottom panel. Dilutions of cells are shown on the top and 3-aminotriazole concentrations employed are indicated on the bottom. (**C**) Interaction assays using recombinant His-NIP7 and GST-FTSJ3. GST-FSTJ3 (upper panel) and GST (lower panel) were immobilized on gluthathione-sepharose beads and the indicated samples (+) were treated with RNase. Subsequently, purified His-NIP7 was added to the binding reactions. Yeast total RNA was also added to the indicated samples (+). Bound His-NIP7 was detected by immunoblotting using an anti-histidine antibody. Immunoblotting using a GST antibody was used to detect GST-FTSJ3 as indicated. RNase A treatment abolishes His-NIP7-GST-FTSJ3 interaction.
doi:10.1371/journal.pone.0029174.g001

HEK293 endogenous NIP7 coprecipitates with FLAG-FTSJ3 through RNA

The finding that the interaction between recombinant NIP7 and FTSJ3 is abolished by RNase treatment is intriguing and indicates that their interaction is also mediated by RNA in human cells. To test this possibility, we generated a stably transfected HEK293 derivative cell line that expresses N-terminally FLAG-tagged full-length FTSJ3 from a tetracycline-inducible promoter (Fig. 2A, B). A HEK293 cell line stably expressing an unrelated 3PGDH protein similarly fused to the FLAG-tag was used as a control. Following induction with tetracycline, we immunoprecipitated the FLAG-tagged proteins to test if endogenous NIP7 coimmunoprecipitated with FLAG-FTSJ3. NIP7 was detected in immunoprecipitates of FTSJ3 only when FLAG-FTSJ3 was induced with tetracycline prior to immunoprecipitation (IP) (Fig. 2C). Incubation of the extracts with RNase abolishes the coimmunoprecipitation of NIP7 with FLAG-FTSJ3, revealing that their biochemical association in HEK293 cells is dependent upon RNA (Fig. 2D). This finding strongly indicates that NIP7-FTSJ3 interaction in HEK293 cells does not take place by direct contact but is bridged by an RNA molecule. Alternatively, a molecular rearrangement caused by NIP7 binding to RNA is required for its interaction with FTSJ3.

Previous studies using sucrose density gradient fractionation showed that NIP7 cosediments with particles corresponding to pre-ribosomes [22]. Analysis of FTSJ3 sedimentation on sucrose density gradients revealed that a fraction of FTSJ3 overlaps with NIP7 in the range of the 40S–60S ribosome subunits although part of FTSJ3 is found in the soluble fractions (Fig. 2E). This result indicates that FTSJ3 and NIP7 are not components of a permanent complex but interact transiently with pre-ribosomal complexes during ribosome synthesis. This is consistent with the findings described below that FTSJ3 knockdown is required affects mainly the early processing steps while NIP7 is required for the late processing steps leading to 18S rRNA synthesis.

FTSJ3 colocalizes with NIP7 in the nucleolus

To evaluate the potential functional association of NIP7 and FTSJ3 in vivo, we determined their subcelullar localization using exogenously expressed fluorescent fusion proteins and immunolocalization of the endogenous proteins. HeLa cells expressing NIP7 fused C-terminally to EGFP and RFP-tagged FTSJ3 were visualized by confocal microscopy for intrinsic fluorescence of the fusion proteins. Both exogenous proteins colocalized to the nucleolus (Fig. 3A). This colocalization of the two proteins to the nucleolus was independently confirmed by double staining of U2OS cells with antibodies against FTSJ3 and NIP7 (Fig. 3B).

The conserved domains found in FTSJ3 are represented in Fig. 3C. FTSJ3 contains a putative nuclear localization signal in its carboxy-terminal region (residues 808–847) that is part of the conserved Spb1_C domain. It is likely that this region of the protein is responsible for its localization to the nucleus, and perhaps the

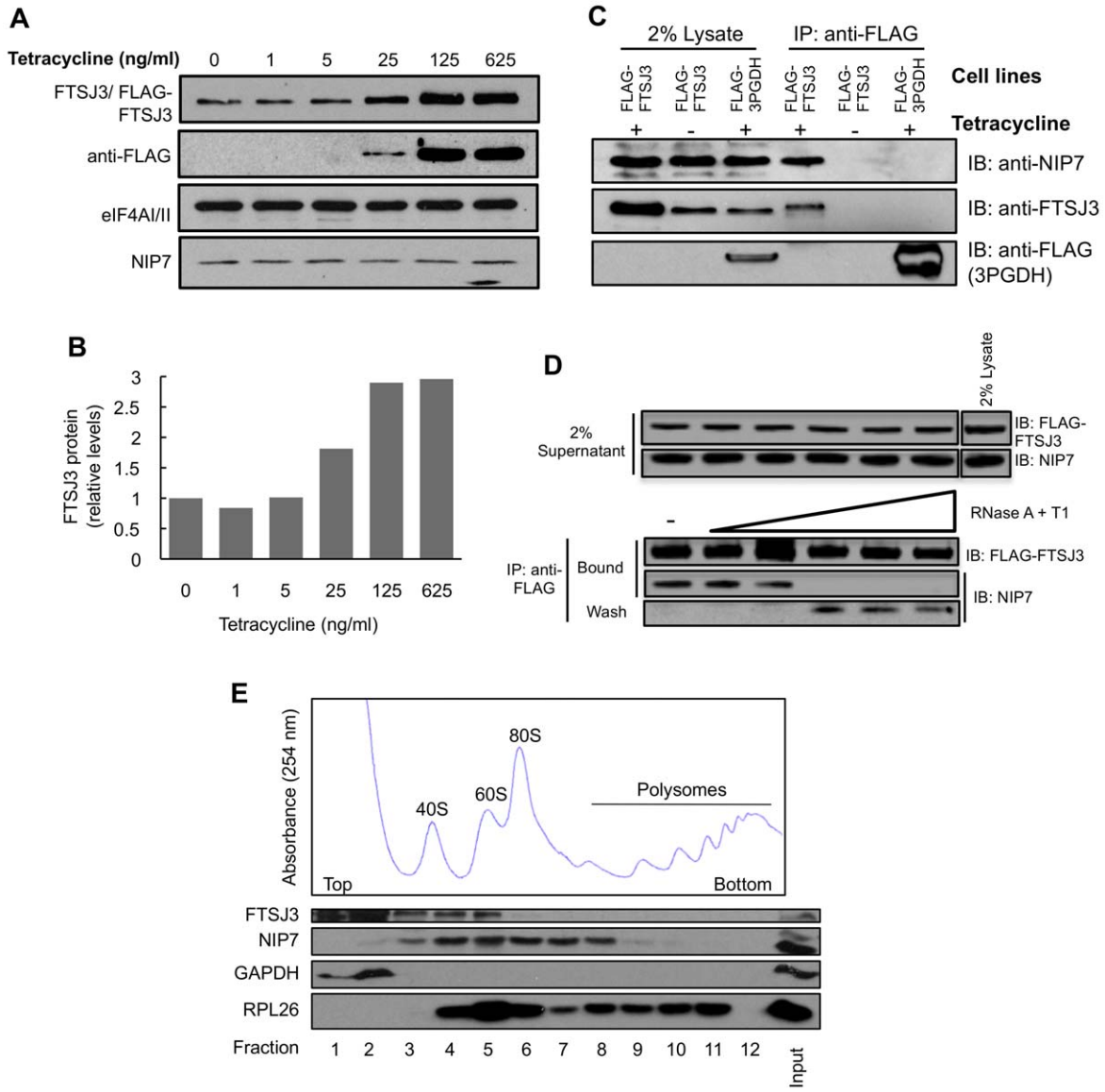

Figure 2. NIP7 associates with FTSJ3 in vivo in an RNA-dependent manner. (**A**) Analysis by western blot of FLAG-FTSJ3 induction in stably transfected HEK293 Flp-In T-Rex cells with increasing concentrations of tetracycline. Both endogenous and recombinant FLAG-FTSJ3 were detected by using antibody specific to FTSJ3. FLAG-FTSJ3 expression was confirmed by using antibody against the FLAG peptide. eIF4AI/II was used as a gel loading control. NIP7 levels are not affected by over-expression of FLAG-FTSJ3. (**B**) FTSJ3 relative levels as determined by band quantification using ImageJ software and normalized to eIF4AI/II. (**C**) Coimmunoprecipitation of NIP7 with FLAG-FTSJ3. FLAG-tagged FTSJ3 and 3PGDH were immunoprecipitated from extracts of stably transfected HEK293 Flp-In T-Rex cell lines using anti-FLAG (IP) followed by immunoblotting (IB) with anti-NIP7, anti-FTSJ3 and anti-FLAG. Parallel controls were performed using cells without induction and with cells stably transfected with FLAG-3PGDH. NIP7 is detected in the immunoprecitipation with FLAG-FTSJ3 (panel IP:anti-FLAG, lane + tetracycline) (**D**) FLAG-FTSJ3 was immunoprecipitated with anti-FLAG from cell extracts of stably transfected HEK293 Flp-In T-Rex treated with increasing concentrations of the RNases A and T1 and immunoblotted with antibodies for NIP7 and FTSJ3. RNase treatment abolishes NIP7 coimmunoprecipitation with FLAG-FTSJ3. (**E**) Analysis of FTSJ3 sedimentation. Cell extracts of HEK293 Flp-In T-Rex cells were fractionated by sucrose density gradient centrifugation and the fractions analyzed by immunoblotting using antibodies for the indicated proteins. FTSJ3 sedimentation overlaps with NIP7 in the range of the 40S–60S ribosome subunits. GAPDH was used as reference for soluble proteins and RPL26 as reference for 60S, 80S and polysome sedimentation.
doi:10.1371/journal.pone.0029174.g002

nucleolus. To test this, we assessed the subcellular localization of the Spb1_C domain (FTSJ3 residues 640–847) and FtsJ domain (residues 22–202), and compared those to the localization of the full-length protein. As seen in Figure 3D, cells transfected with FLAG-Spb1_C display nucleolar staining, similar to the cells that express FLAG-tagged full-length FTSJ3. In contrast, FLAG-FtsJ localized to the cytoplasm (Fig. 3D). These results suggest that Spb1_C domain mediates nucleolar localization of FTSJ3. Cell fractionation followed by immunoblot analysis showed that FTSJ3 is restricted to the nuclear compartment, which is consistent with its nucleolar localization (Fig. 3E). These findings further indicate a functional association between NIP7 and FTSJ3.

FTSJ3 depletion affects NIP7 binding kinetics

If FTSJ3 and NIP7 function in close association in an RNP structure in the nucleolus, depletion of FTSJ3 might interfere with

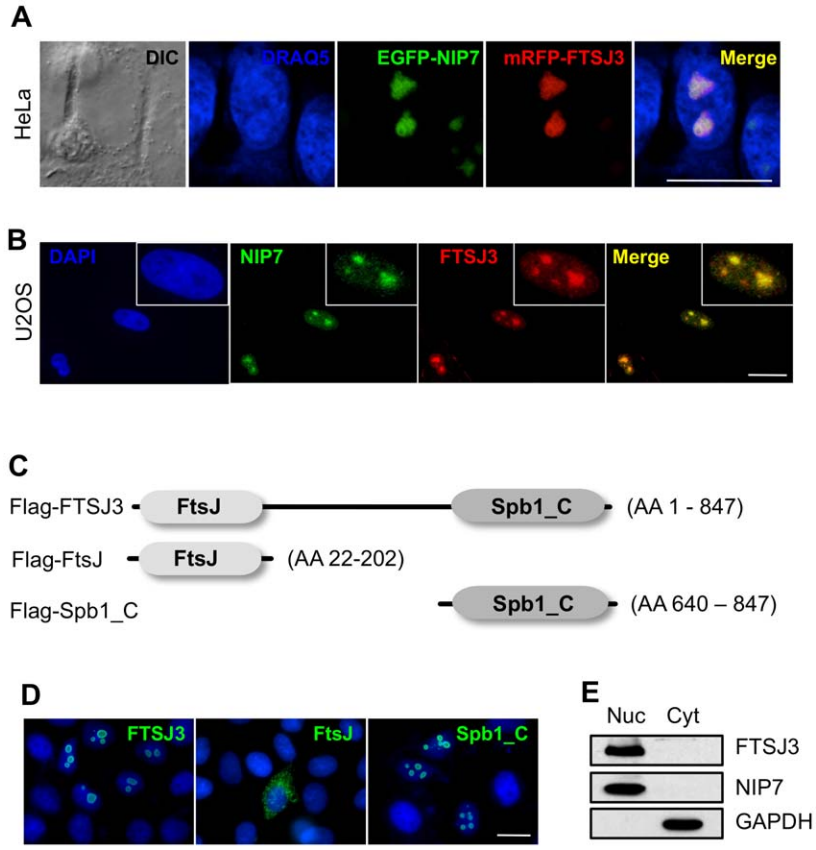

Figure 3. FTSJ3 colocalizes with NIP7 in the nucleolus. (**A**) Transient expression of EGFP-NIP7 and mRFP-FTSJ3 in HeLa cells. Both fusion proteins are observed in the nucleolus 48 hours post transfection. Nuclei were counterstained in blue with DRAQ5. (**B**) Immunofluorescent localization of endogenous NIP7 and FTSJ3 in U2OS cells. NIP7 and FTSJ3 were detected using secondary antibodies conjugated to Alexa Fluor 488 (green) and 568 (red), respectively. Nuclei were counterstained with DAPI. Boxes show an enlarged nucleus (**C**) Diagram of the FTSJ3 protein indicating the two conserved domains, FtsJ and Spb1_C (adapted from PFAM data base). (**D**) Subcellular localization of FLAG-tagged FTSJ3 and FtsJ and Spb1_C domains in transiently transfected HeLa cells. The FLAG-tagged proteins were immunostained with anti-FLAG followed by FITC-conjugated secondary IgG. Nuclei were counterstained with DAPI. The panel shows overlays of DAPI counterstaining and immunostaining. Scale bars represent 30 μm. (**E**) Western blots of HeLa nuclear (Nuc) and cytoplasmic (Cyt) preparations showing FTSJ3 in the nuclear fraction. NIP7 and GAPDH were used as controls for nuclear and cytoplasmic fractions, respectively.
doi:10.1371/journal.pone.0029174.g003

the kinetics of NIP7 binding to the nucleolar architecture. To address this question, we first generated stable HEK293 cell lines expressing a short-hairpin RNA (shRNA) targeting FTSJ3 mRNA, or scrambled shRNA as a control [30]. Western blots in Figure 4A and B (quantification in Fig. 4C and D) show that upon induction of the FTSJ3-targeting shRNA with doxycycline, the FTSJ3 protein levels are reduced to 18% of the control levels. Using these cells, we tested if there is a change in the immobile fraction of NIP7 in the nucleolus by measuring the fluorescence recovery after photobleaching (FRAP) of EGFP-NIP7 in the nucleolus. FRAP is used to measure the dynamics of molecular mobility, including diffusion, transport or movement of fluorescently labeled molecules. By subtracting the mobile fraction during a given time, it can also be used to determine the immobile labeled fraction. In this work, we used FRAP to determine the fraction of EGFP-NIP7 that is immobile in the nucleolus both in control and in FTSJ3 knockdown cells. As compared to the control (scrambled+Dox), the recovery of NIP7 fluorescence in the photobleached area (or nucleolus) was faster under FTSJ3 knockdown conditions (shRNA+Dox) (Fig. 5A). Quantification of fluorescent protein levels revealed that in the presence of FTSJ3, NIP7 was more tightly bound at the nucleolus, with the immobile fraction representing approximately 30% of the measured protein amounts (Fig. 5B). However, when FTSJ3 was depleted, the NIP7 dynamics changed, with a significant reduction in the protein's immobile fraction (~4.3%, $p<0.001$) (Fig. 5B) probably caused. This analysis indicates that NIP7 binding to pre-ribosomes in the nucleolus is compromised in absence of FTSJ3 and is consistent with a close relationship of the proteins during ribosome biogenesis.

Analysis of pre-rRNA processing intermediates in FTSJ3 knockdown cells

Our observation of FTSJ3 interaction with NIP7, its nucleolar localization and sequence similarity to yeast Spb1 points to a role for FTSJ3 in pre-rRNA maturation in human cells. To investigate whether FTSJ3 is involved in pre-rRNA processing, we measured the steady-state levels of pre-rRNA intermediates in FTSJ3 knockdown cells. Initially, we analyzed pre-RNA processing using a HEK293 derivative cell line expressing a doxycycline-inducible shRNA that targets the FTSJ3 mRNA. Northern blots using total RNA extracted from these cells with probes complementary to the external and internal transcribed spacer sequences of the pre-rRNAs (Fig. 6) show a concomitant rise in steady-state levels of the 34S pre-rRNA in cells in which FTSJ3 knockdown was induced with increasing amounts of doxycycline for 3 days (Fig. 6B and C).

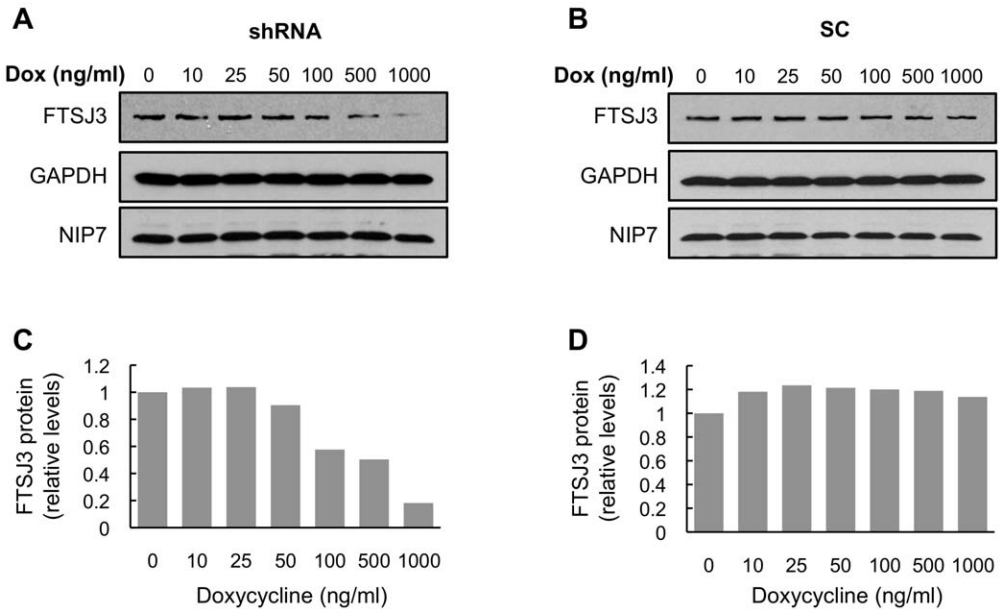

Figure 4. Analysis of FTSJ3 knockdown by RNA interference using the pFRT-U6tetO inducible system. (**A, B**) Western blot analysis to determine FTSJ3 levels in HEK293 Flp-In T-Rex cells expressing either a small hairpin RNAs targeting FTSJ3 (shRNA) or a scrambled control (SC) 72 h after induction with doxycycline (Dox). FTSJ3 levels decrease upon induction of the shRNA with doxycycline in dose-dependent manner. NIP7 levels are not affected by depletion of FTSJ3. (**C, D**) FTSJ3 relative levels were determined by band quantification using ImageJ software and normalized to GAPDH, which was used as an internal control. FTSJ3 was reduced to 20% of its original levels in cells treated with doxycycline at 1000 ng/ml.
doi:10.1371/journal.pone.0029174.g004

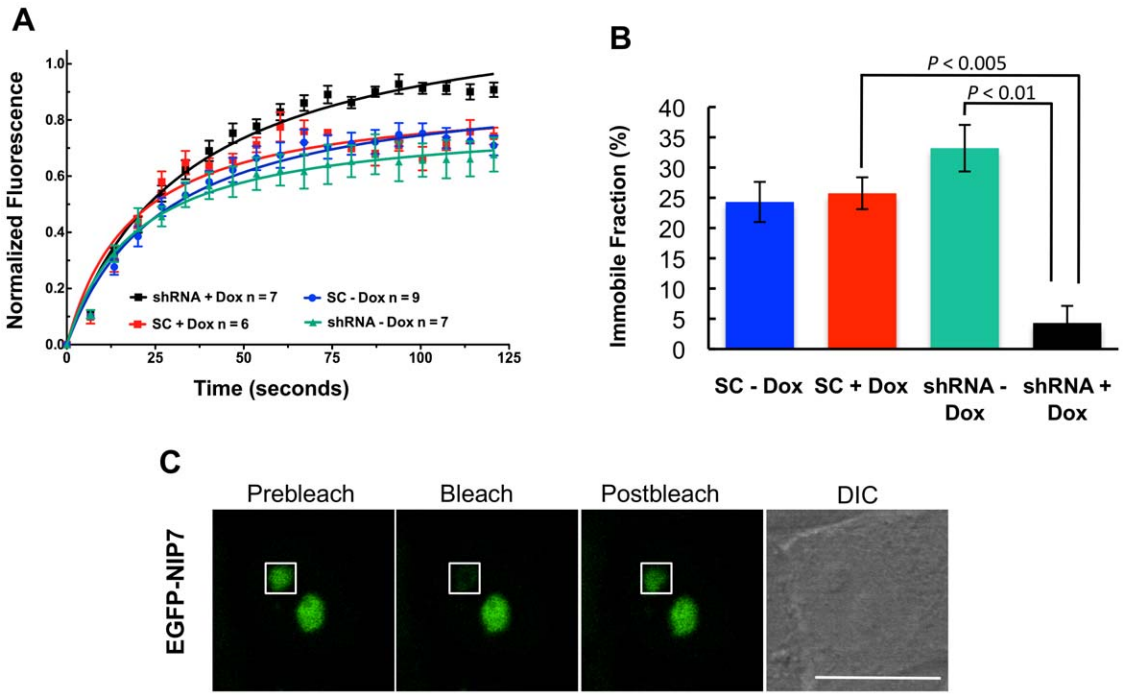

Figure 5. NIP7 shows different binding kinetics at the nucleolus under FTSJ3 depletion. (**A**) Fluorescence recovery after photobleaching (FRAP) was measured for EGFP-NIP7 in HEK293 Flp-In T-Rex cells expressing either a shRNA targeting FTSJ3 or a scrambled control (SC) and induced (+) or not (−) with doxycycline (Dox). The graph shows normalized mean fluorescence recovery curves over time calculated for EGFP-NIP7 at the nucleolus. Means were plotted with standard errors for each time point. (**B**) Graph of the 120-seconds time point postbleach. Data are representative of two independent experiments with at least 6 cells analyzed in each experiment. *P*-value was obtained by using a one-sided Student's t-test. (**C**) Images of a representative cell showing EGFP-NIP7 fluorescence before photobleaching (prebleach), immediately after photobleaching (bleach), and after 120 seconds when the fluorescence has already recovered (postbleach). The white box indicates the region of interest used in the analysis. The scale bar represents 30 μm.
doi:10.1371/journal.pone.0029174.g005

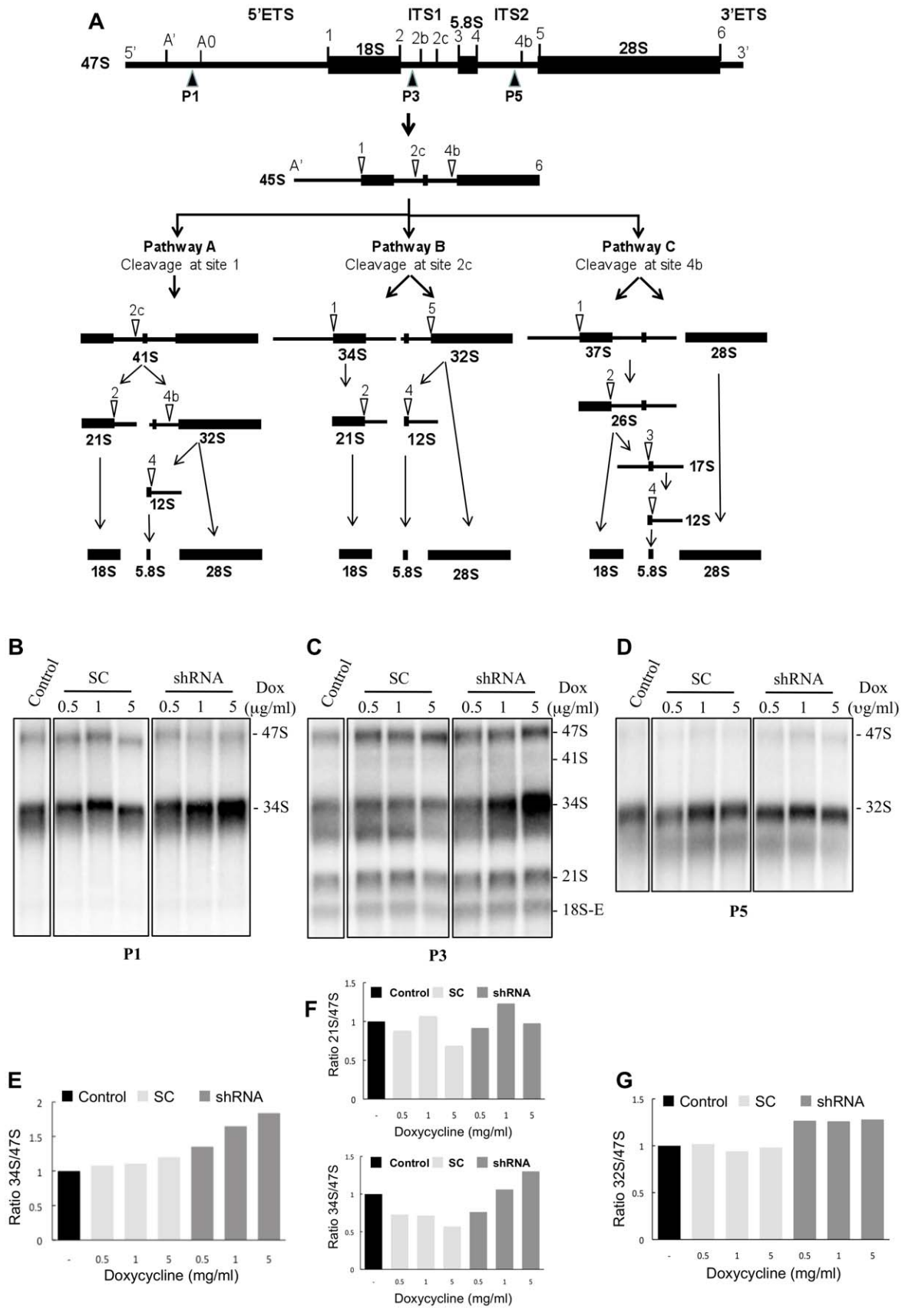

Figure 6. Analysis of pre-rRNAs intermediates in HEK293 Flp-In T-Rex cells expressing a shRNA targeting the FTSJ3 mRNA. (**A**) Diagram of the human pre-rRNA processing pathways. The 47S pre-rRNA is converted to the 45S pre-rRNA following the initial cleavages at sites A′ in the 5′-ETS and at site 6, at the 3′-end of the mature 28S rRNA. The 45S is processed by three alternative pathways, which is determined by the

location of the first cleavage, leading to the mature rRNAs 18S, 5.8S and 28S. For additional details, see Morello et al. [22]. Open arrowheads indicate the sequential cleavage sites. Dark arrowheads (P1, P3 and P5) underneath the 47S pre-rRNA indicate the positions of the oligonucleotide probes used in Northern blotting. (**B**) Northern blot using probe P1 complementary to the 5′-ETS upstream site A0. (**C**) Northern blot using probe P3 complementary to ITS1 upstream site 2b. (**D**) Northern blot using probe P5 complementary to ITS2 upstream site 4b. (**E**–**G**) Graphs representing the ratio between the indicated intermediate pre-rRNA and the 47S pre-rRNA of the Northern blots shown in B (**E**), C (**F**) and D (**G**). Bands were quantified by using ImageQuant software. For Northern blots, RNA was isolated form HEK293 Flp-In T-Rex cells expressing either a shRNA targeting FTSJ3 (shRNA) or a scrambled control (SC) induced with the indicated concentrations of doxycycline (Dox) during 3 days. The control lane corresponds to the cell line expressing a shRNA targeting FTSJ3 not induced (−) with doxycycline.
doi:10.1371/journal.pone.0029174.g006

A slight increase in the 21S pre-RNA levels can also be observed. Accumulation of the 34S pre-rRNA is detected by probes P1 and P3 showing that it encompasses from site A′ to site 2b which indicates that processing of sites A0, 1 and 2 are slower in cells depleted of FTSJ3. In comparison, no change in the levels of intermediates leading to 28S and 5.8S mature rRNAs was observed upon FTSJ3 knockdown (Fig. 6D). These findings indicate that FTSJ3 functions in the pathway leading to 18S rRNA maturation and 40S subunit synthesis and are consistent with a functional interaction with NIP7, which is also required for 18S pre-rRNA and 40S subunit formation [22].

To confirm the results obtained with FTSJ3 knockdown using the doxycycline-inducible shRNA in HEK293 cells, we analyzed also the pre-RNA processing defects in HEK293 and HeLa cells transiently transfected with a siRNA directed to a different region of the FTSJ3 mRNA. FTSJ3 was efficiently knocked down in both cell lines (Fig. 7A). Northern blot analysis using probe 3, complementary to ITS1, revealed and increase of the 34S pre-RNA (Fig. 7B,C), which is consistent with the data obtained for the FTSJ3 knock down using the doxycycline-inducible shRNA.

Conditional knockdown of FTSJ3 affects HEK293 cell proliferation rate

Since downregulation of FTSJ3 affects NIP7 binding kinetics in the nucleolus and alters the balance of the pre-rRNA processing pathways causing an increase of the 34S pre-rRNA, we tested whether FTSJ3 knockdown affects cell proliferation. Cells expressing the FTSJ3-targeting shRNA showed a doxycycline dose-dependent reduction of the proliferation rate over 120 hours (Fig. 8A), whereas the proliferation of control cells expressing the scrambled RNA was not affected (Fig. 8B). This result indicates that prolonged depletion of FTSJ3 affects overall cellular physiology, reducing the proliferation rate. Nucleolar chemical stress and defective ribosome synthesis have been shown to trigger stress responses involving p53 which block cell cycle progression [31–35]. Fluorescence-activated cell sorting (FACS) analyses, however, did not reveal significant differences in the cell cycle stage of HEK293 cells expressing the shRNA targeting FTSJ3 as compared to the control cells expressing the scrambled control even though the cell proliferation rate of cells expressing the shRNA was reduced to nearly 50% of the proliferation rate of the control cells (Fig. 8C–E). The levels of p53 were similar in both test and control cells indicating that the reduced proliferation caused by FTSJ3 knockdown may not be related to activation of p53 and induction of apoptosis.

Discussion

We have previously shown that the human NIP7 is involved in the pre-RNA processing pathway leading to 40S ribosomal subunit synthesis [22]. At the pre-rRNA processing level, human NIP7 knockdown leads to decrease of 34S pre-rRNA and increase of the 26S and 21S pre-rRNA concentrations. This imbalance in pre-rRNA concentrations is caused by uncoupling of processing at sites A0 and 1 and slower processing at site 2 in NIP7-depleted cells [22]. Despite of structure conservation, knockdown of human NIP7 affects 40S subunit formation while knockdown of yeast Nip7p leads to a deficit of 60S subunits showing that NIP7 acts at

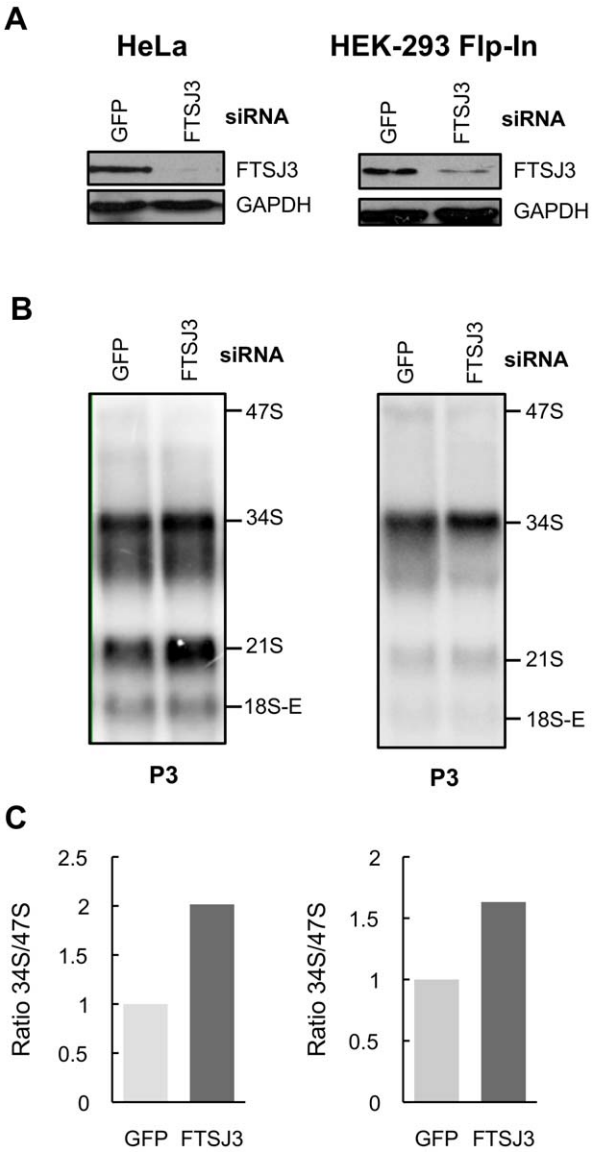

Figure 7. Analysis of pre-rRNAs intermediates in HeLa and HEK293 Flp-In T-Rex cells transiently transfected with a siRNA targeting the FTSJ3 mRNA. (**A**) Western blot analysis to determine FTSJ3 levels 72 h following siRNA transfection. (**B**) Northern blot using probe P3 complementary to ITS1 upstream site 2b. (**C**) Graphs representing the ratio between the 34S and 47S pre-rRNA of the Northern blots shown in B. Bands were quantified by using ImageQuant software. Control cells were transfected with siRNA targeting the GFP mRNA.
doi:10.1371/journal.pone.0029174.g007

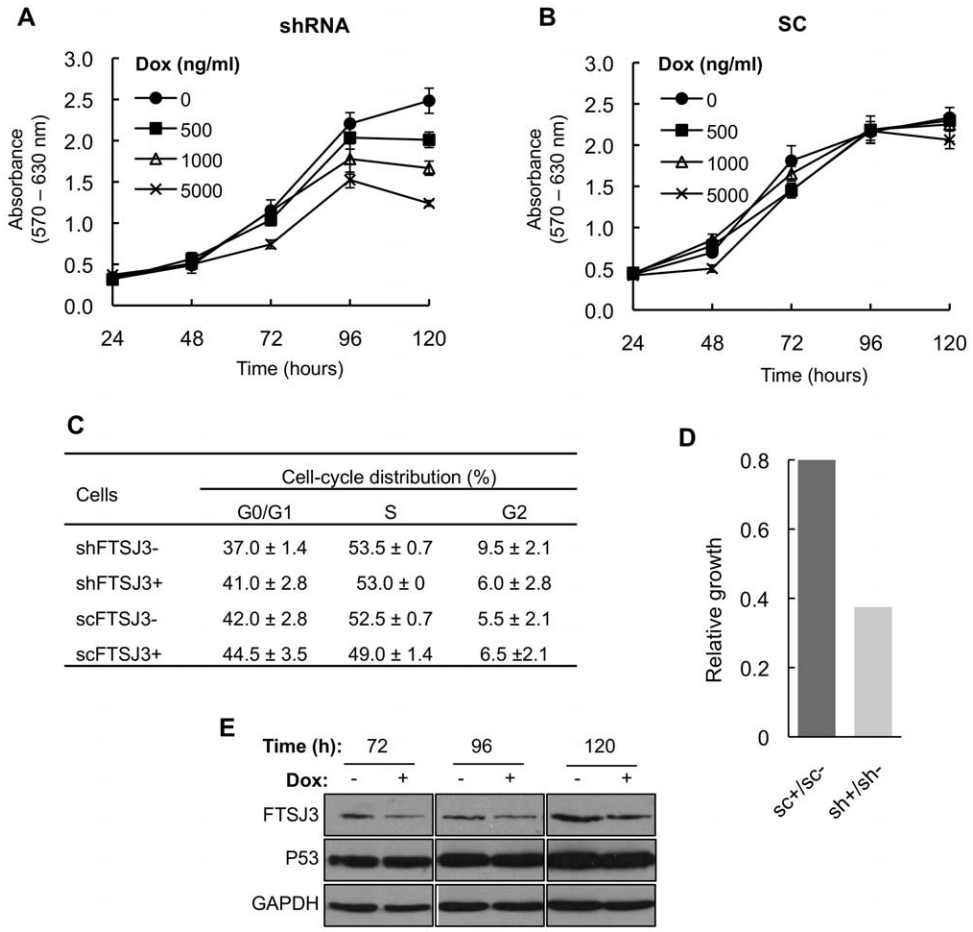

Cells	Cell-cycle distribution (%)		
	G0/G1	S	G2
shFTSJ3-	37.0 ± 1.4	53.5 ± 0.7	9.5 ± 2.1
shFTSJ3+	41.0 ± 2.8	53.0 ± 0	6.0 ± 2.8
scFTSJ3-	42.0 ± 2.8	52.5 ± 0.7	5.5 ± 2.1
scFTSJ3+	44.5 ± 3.5	49.0 ± 1.4	6.5 ±2.1

Figure 8. Analysis of cell proliferation over a 5-day period of induction with doxycycline (Dox). (**A**) Proliferation rate of cells expressing the shRNA targeting FTSJ3. (**B**) Proliferation rate of cells expressing the scrambled control SC RNA. (The graphs represent one of four independent assays performed using four technical replicates for each cell treatment). Induction of the shRNA targeting FTSJ3 leads to a reduction in cell proliferation. (**C**) Cell cycle analysis by fluorescence-activated cell sorting (FACS). FACS analyses were performed with HEK293 Flp-In T-Rex cells stably transfected with the pFRT-U6tetO plasmid expressing either a shRNA targeting FTSJ3 (shRNA) or a scrambled control (SC) and induced (+) or not (−) with 5 μg/ml of doxycycline for 5 days. (**D**) Relative growth rate differences between cells expressing the scrambled control scRNA (sc+/sc−) and cell expressing the shRNA targeting the FTSJ3 mRNA (sh+/sh−) induced (+) or not (−) with doxycycline for the 120 h time point. (**E**) Immunoblot analysis showing the levels of the FTSJ3 and p53 proteins in cells expressing either the shRNA targeting the FTSJ3 mRNA or the scrambled control induced (+) or not (−) with doxycycline. GAPDH was used as a gel loading control. The levels of FTSJ3 are reduced as expected and the levels of p53 are not affected.

doi:10.1371/journal.pone.0029174.g008

a different step of rRNA synthesis in these organisms [22,36]. This finding raised the question whether the human and yeast orthologs share the same set of interacting partners. In this work, we have begun to test this hypothesis by employing the yeast two-hybrid system, which has widely been used to study protein interactions. Interestingly, FTSJ3 was isolated as one of the most frequent human NIP7-interacting candidate. This finding was intriguing because FTSJ3 is a putative ortholog of *S. cerevisiae* Spb1, which has previously been implicated in 60S subunit synthesis [23]. However, both studies describing protein composition of human pre-rRNA complexes [26,27] along with the experimental evidence presented in this work on NIP7 and FTSJ3 interactions and their functional analysis are consistent with a major role for these proteins in the 40S biogenesis pathway in human cells. This is in contrast to the function of yeast Nip7p and Spb1 mainly in the pathway leading to 60S subunit synthesis.

In addition to the 60S synthesis defects caused by conditional depletion of yeast Nip7p, it has been found in pre-60S complexes [28,37–39]. Similarly, Spb1 was shown to be required for 60S subunit synthesis in yeast [23] and to associate with pre-60S subunits [9,28,39]. So far, there is no report describing yeast Nip7p and Spb1 in pre-40S complexes [28,40,41]. Human NIP7 and FTSJ3, however, are found in complexes isolated by affinity purification of RPS19, a structural component of the mature 40S subunit [27]. Consistently with a function in 40S subunit synthesis, depletion of NIP7 and FTSJ3 was described to affect nuclear accumulation of RPS2-YFP, a small subunit reporter protein, but has little effect on the nuclear accumulation of a large subunit reporter protein, RPL29-GFP [42]. NIP7 and FTSJ3 are also found in association with parvulin and nucleolin complexes [26,28,43]. In these cases, association with a particular pre-ribosomal particle is less clear. Parvulin is present in both pre-40S and pre-60S complexes [26] while nucleolin has been proposed to function in the first step of pre-rRNA cleavage [44]. Complexes isolated by affinity purification of both parvulin and nucleolin contain trans-acting factors required for synthesis of both the 60S and 40S subunits [26,28]. Association of NIP7 and FTSJ3 with parvulin and nucleolin complexes further supports their close

functional association and might also suggest that at some point during assembly they both join pre-ribosomal complexes prior to separation of the pre-40S and pre-60S complexes.

The experimental data on subcellular localization and interaction analysis support a close functional relation between FTSJ3 and NIP7. Endogenous NIP7 and FTSJ3 and transiently transfected EGFP-NIP7 and mRFP-FTSJ3 fusion proteins are detected in the nucleolus (Fig. 3). In addition, FRAP analyses have shown that knockdown of FTSJ3 affects NIP7 binding dynamics in the nucleolus. We also showed FTSJ3 Spb1_C domain is responsible for nucle(ol)ar localization of FTSJ3. A GST pull-down assay performed with recombinant proteins indicated that they could interact directly. However, assays using bacterial expressed proteins and immunoprecipitation of FLAG-tagged FTSJ3 from HEK293 cell lysates showed that its interaction with NIP7 is mediated by RNA since incubation with RNase abolished the interaction in both cases (Figs. 1–2). NIP7 shows a conserved two-domain architecture and, for the *S. cerevisiae* and *P. abyssi* orthologs, the C-terminal PUA domain (after *P*seudo-*U*ridine synthases and *A*rchaeosine-specific transglycosylases) mediates RNA interaction [36]. The PUA domain is conserved in the human NIP7 and is likely responsible for the RNA-binding activity of NIP7 [22]. Structure predictions indicate that except for the putative RNA-methyl-transferase domain (residues 22–202) FTSJ3 contains a large intrinsically disordered region, roughly from amino acid 300 onwards until the C-terminus, which also includes the conserved uncharacterized domain (Spb1_C). We could not identify any RNA binding motifs in this region using different prediction algorithms, and the basis of FTSJ3's RNA binding remains an open question. Intrinsically disordered regions have higher flexibility and provide also larger binding interfaces when compared to folded proteins of the same size, allowing them to fit a variety of different binding partners [45]. The predicted structure of FTSJ3 is therefore compatible with NIP7 interaction mediated by an RNA molecule acting as a third partner.

The reduction in the proliferation rate of FTSJ3-knockdown cells shows that it plays an important cellular function (Fig. 8). Reduced proliferation arises most probably from defective pre-rRNA processing in absence of FTSJ3. FTSJ3 acts in the pathway leading to 18S formation (Figs. 6–7), the same pathway that requires NIP7 function [22]. However, our data argues for FTSJ3 function at distinct processing steps of this pathway as compared to NIP7. Accumulation of the 21S pre-rRNA is evidence for slower maturation of the 3′-end of the 18S rRNA (site 2) in NIP7-knockdown cells [22]. In mammalian cells, the cleavages of sites A0 and 1 in the 5′ ETS are coupled and defects that uncouple these cleavages lead to an increase of the 26S pre-rRNA, which is the case observed for NIP7 depletion [22]. Cells depleted of FTSJ3, on the other hand, accumulate unprocessed 34S pre-rRNA, which results from slower processing of the 5′ ETS sites A0, 1 and from slower processing of site 2 (Figs. 6–7). This finding indicates that FTSJ3 acts at earlier processing steps relative to NIP7. Recently, O'Donohue and co-workers [46] described the identification of two functional groups of 40S ribosomal proteins. One group, termed initiation-RPS, is required for the initial processing steps while the second group, termed progression-RPS is required for the late steps of 18S rRNA synthesis. Knockdown of individual members of the initiation-RPS group leads to a strong accumulation of the 34S pre-rRNAs, which results from inhibition of the 5′ ETS sites A0 and 1 and of the ITS1 site 2. On the other hand, knockdown of members of the progression-RPS group, show accumulation of the 26S, 21S and 18S-E pre-rRNAs [46]. A comparison of these defects with those caused by FTSJ3 and NIP7 depletion suggests that FTSJ3 acts during the stage of initiation-RPS while NIP7 acts during the stage of progression-RPS.

This work raised an intriguing question regarding the functional homology between *S. cerevisiae* Spb1 and human FTSJ3 which share 33% overall amino acid sequence identity and 52% similarity. Spb1 depletion causes decrease of the 27SA2 and 20S pre-rRNAs, appearance of a 23S aberrant pre-rRNA and accumulation of unprocessed 35S pre-rRNA [23]. In addition, Spb1 deficiency leads to formation of halfmer polysomes and deficit of 60S subunits [23]. Spb1 knockdown does not affect global rRNA methylation [23] but it is required for site-specific methylation at residue Gm_{2922} located in the catalytic center of the ribosome [24,25]. Differences in specific pre-rRNA processing steps in *S. cerevisiae* and humans may be more common than initially thought. A recent study has shown that conditional knockdown of the human orthologs of yeast Enp1 and Tsr1, bystin and hTsr1 in HEK293 cells leads to defects in pre-rRNA processing and 40S subunit export that are distinct from those reported for the yeast orthologs [12–15]. Our findings regarding FTSJ3 and NIP7 function in 18S rRNA maturation in this and previous work add to the growing list of differences in yeast and human rRNA processing pathways [22]. Whereas our work on the role of NIP7 and FTSJ3 in pre-rRNA processing sheds new light on the mechanism of ribosome biogenesis in human cells, it also portends presence of other yet to be discovered differences in ribosome biogenesis pathways in yeast and mammals.

Materials and Methods

Plasmid construction and bacterial strains

Plasmids construction and cloning procedures are briefly summarized below. pTL1-NIP7 was generated by replacing the ampicilin *E. coli* selection marker of vector pBTM-NIP7 [17] to kanamycin. Plasmid pACT-NOP8 has been described previously [17]. The human NIP7 540 bp coding sequence was isolated from pTL1-HsNip7 [29] using the EcoRI/SalI restriction sites and inserted into the pET28a and pEGFP-C2 plasmids, generating pET28-HsNip7 and pEGFP-HsNip7, respectively. pACT-FTSJ3 was isolated in a yeast two-hybrid screen using the human NIP7 as bait (see below). The polylinker of pmRFP was modified to adjust the reading frame to that of the *FTSJ3* cDNA isolated from pACT-FTSJ3. pmRFP was modified by inserting a polylinker into the HindIII/SalI restriction sites, generating plasmid pmRFPL. The *FTSJ3* coding sequence was isolated from pACT-FTSJ3 using the EcoRI/XhoI restriction sites and inserted into pGEX-5X2 (GE Healthcare), generating plasmid pGEX-FTSJ3. Subsequently, the *FTSJ3* cDNA was isolated from pGEX-FTSJ3 and inserted into pmRFPL using the EcoRI/NotI restriction sites, generating pmRFPL-FTSJ3. The full-length FTSJ3 cDNA and its FtsJ (amino acids 22 to 202) and Spb1_C (amino acids 640 to 847) domains were cloned into pcDNA 3.1(+) containing a FLAG-tag upstream of the modified multiple cloning site (pcDNA-FLAG) using the EcoRI/XbaI restriction sites, generating the plasmids pcDNA-FLAG-FTSJ3, pcDNA-FLAG-FtsJ and pcDNA-FLAG-Spb1_C, respectively. FTSJ3 was also cloned into pcDNA5/FRT/TO containing a FLAG-tag upstream of the multiple cloning site (pcDNA5/FRT/TO-FLAG) using the HindIII/XhoI restriction sites, generating the plasmid pcDNA5/FRT/TO-FLAG-FTSJ3. *Escherichia coli* strains DH5α and BL21(DE3) were maintained in LB medium containing 50 mg/ml of the required antibiotic used in transformant selection and manipulated according to standard techniques [47]. The targets for *FTSJ3* small hairpin RNA (shRNA) were a 19-residue oligonucleotide whose sequence was selected based on the Dharmacon siDESIGN Center (Thermo

Scientific/Dharmacon RNAi Technologies). It corresponds to nucleotides 993–1011 of the FTSJ3 mRNA target sequence (accession number NM_017647.2). The loop sequence (TTCAAGAGA) used to generate the hairpin was previously described by Ambion siRNA Target Finder. The oligonucleotide sequences to generate the shRNA against the *FTSJ3* mRNA correspond to LGM7 (5′ GAT CGC TAC TAA ACT GGA GAA CAA TTC AAG AGA TTG TTC TCC AGT TTA GTA GTT TTT TGT AC 3′) and LGM8 (5′ AAA AAA CTA CTA AAC TGG AGA ACA ATC TCT TGA ATT GTT CTC CAG TTT AGT AGC 3′) and the control-scrambled sequence (SC) corresponds to LGM9 (5′ GAT CGC AAT AGC TAG CTG AAA CAA TTC AAG AGA TTG TTT CAG CTA GCT ATT GTT TTT TGT AC 3′) and LGM10 (5′ AAA AAA CAA TAG CTA GCT GAA ACA ATC TCT TGA ATT GTT TCA GCT AGC TAT TGC 3′). The annealed oligonucleotides were cloned into pFRT-U6tetO [30] previously digested with BglII/KpnI, generating pFRT-U6tetO-shRNA-FTSJ3 and pFRT-U6tetO-SC-FTSJ3, respectively.

Yeast two-hybrid assays

The yeast host strain L40 [*MAT*a *his3*D*200*,*trp1-901*,*leu2-3*,*311*,*ade2*,*lys2801am URA3*::(*lexAop*)$_8$-*lacZ LYS2*::(*lexAop*)$_4$-*HIS3*] [48] used in the two-hybrid analyses contains both yeast *HIS3* and *E. coli lac*Z genes as reporters for two-hybrid interaction integrated into the genome. An L40 derivative strain bearing plasmid pTL1-HsNip7, encoding a DNA-binding (DBD, *lexA*) fusion protein was transformed with a human fetal brain cDNA library constructed in the pACT2 vector (Clontech HL4028AH) using a PEG/lithium acetate mediated protocol (Matchmaker Yeast Protocol Handbook, Clontech). Transformants showing positive interaction were selected on YNB plates supplemented with adenine and 6 mM 3-AT (3-amino-triazol, Sigma). Subsequently, positive clones ($His3^+$) were subjected to a second round of selection based on the activation of the reporter gene *lac*Z, using X-Gal filter assays. Plasmid pACT2 was rescued from the positive clones and the NIP7-interacting proteins identified by DNA sequencing followed by BLAST analyses (http://www.ncbi.nlm.nih.gov/BLAST/). The L40 strain expressing the yeast proteins Nip7p fused to the DNA binding domain of *lex*A (pTL1-NIP7) and Nop8p fused to activation domain of *GAL4* (pACT-NOP8) was used as a positive control in yeast two-hybrid assays [17]. The L40 strain bearing plasmid pTL1-HsNip7 and pACT2 was used as a negative control.

Cell culture methods and shRNA-mediated knockdown

HEK293 Flp-In T-Rex (Invitrogen), HeLa (ATCC) and U2OS (ATCC) cells were maintained in high-glucose (4.5 g/l) Dulbecco's modified Eagle's medium supplemented with 2 mM glutamine, 10% fetal bovine serum and 100 U/ml penicillin and 100 μg/ml streptomycin. HEK293 Flp-In T-Rex cells were cultivated with tetracycline-free fetal bovine serum (GIBCO). The cells were cultured at 37°C in a humidified atmosphere with 5% CO_2. Transfections were performed with Lipofectamine 2000 (Invitrogen), according to procedures described by the manufacturer. HEK293/Flp-In/FLAG-FTSJ3 and HEK293/Flp-In/FLAG-3PGDH are cell lines derivative of HEK293 Flp-In T-Rex (Invitrogen) that were generated as follows: HEK293 Flp-In T-Rex cells at 60% estimated confluency in 10-cm plates were cotransfected with pcDNA5/FRT/TO-FLAG-FTSJ3 (1 μg) and pOG44 (9 μg) encoding the Flp recombinase, generating the stably transfected HEK293/Flp-In/FLAG-FTSJ3 cell line. Two days after transfection, cells were diluted 1:10 and 1:5 in 10-cm plates and the incubation medium was supplemented with 100 μg/ml hygromycin B. The medium was replaced every two days. Resistant colonies were pooled and maintained in medium described above that was supplemented with 50 μg/ml hygromycin B. Transgene expression was induced by adding tetracycline at the indicated concentrations (0.001 to 0.625 μg/ml) to the cultures. The HEK293/Flp-In/FLAG-3PGDH cell line was generated in the same way. To generate polyclonal stable FTSJ3 knockdown cell lines, we stably transfected HEK293 Flp-In T-Rex cells with pFRT-U6tetO [30] that expressed shRNA targeting FTSJ3 mRNA (nucleotides 1568–1586), or scrambled shRNA as a control as described above. To verify depletion, FTSJ3 protein levels were assayed by immunoblotting as described below. Proliferation rates were determined by using the MTT-based CellTiter 96 Non-Radioactive Cell Proliferation Assay (Promega). Medium with inducer was replaced every two days for FTSJ3 knockdown experiments. For fluorescence assays, 1×10^5 cells were seeded on sterile 18 mm coverslips, and for live cell experiments, 3×10^5 cells were seeded on sterile 40 mm coverslips. Cell-cycle analyses were performed by fluorescence-activated cell sorting (FACS). For these assays, 0.5×10^6 cells were fixed on ice in 70% (v/v) ethanol for 30 min, washed with PBS and the DNA content stained with 20 mg/ml propidium iodide in PBS in the presence of 1 mg/ml RNAse. Cells were analyzed on a FACSCalibur TM (BD Biosciences) equipped with a 488-nm argon laser. The fluorescence was measured through a 575/25 band pass filter. Cells doublets were removed using the FL2-Area and FL2-Width parameters. Data acquisition was performed using CellQuest software (BD Biosciences) and analysis using ModFit software (Verity Software). FACS analyses were performed with HEK293 Flp-In T-Rex cells stably transfected with the pFRT-U6tetO plasmid expressing either a shRNA targeting FTSJ3 (shRNA) or a scrambled control (SC) and induced (+) or not (−) with 5 μg/ml of doxycycline for 5 days and harvested at ~50% confluency.

Transient transfection

HEK293 Flp-In T-Rex and HeLa cells at 60% estimated confluency in 10-cm plates were transiently trasfected with 50 nM of siRNA duplexes against FTSJ3 by using DharmaFECT Duo Transfection Reagent (Dharmacon) according to the manufacture's instructions. The accession number of the FTSJ3 mRNA target sequence is NM_017647.2 The oligoribonucleotides used to generate the siRNAs duplexes were purchased from SIGMA (SASI_Hs01_00197929). Their sequences are 5′ GCC UUA UUG UGG GAG UGG A_dT_dT 3′ (oligo 1307693, sense) and 5′ UCC ACU CCC ACA AUA AGG C_dT_dT 3′ (oligo 1307694, anti-sense) and correspond to nucleotides 280 to 298 in the FTSJ3 target mRNA. Parallel control transfection assays were performed with 50 nM of siRNA duplexes against GFP (sense 5′ CUU GAC UUC AGC ACG CGU CUU 3′ and anti-sense 5′ GAC GCG UGC UGA AGU CAA GUU 3′). 72 hours after transfections, the cells were harvested and $1/10^{th}$ was used for protein analysis and $9/10^{th}$ processed for RNA analysis.

Immunoblot analysis and antibodies

Proteins were resolved by SDS–PAGE and immunoblot was performed as described previously [22]. Primary antibodies and their dilutions to detect respective proteins were as follows: chicken polyclonal anti-FTSJ3 (Sigma) (1:80,000), rabbit polyclonal anti-NIP7 (Abcam) (1:4,000), rabbit polyclonal anti-eIF4AI/II (Santa Cruz Biotechnology) (1:2,500), rabbit polyclonal anti-GAPDH (Abcam) (1:8,000), rabbit polyclonal anti-RPL26 (1:2,500) (Bethyl Laboratories), mouse monoclonal anti-FLAG M2 HRP-conjugated (Sigma) (1:1,000), mouse monoclonal anti-polyhistidine (Sigma) (1:5,000). Secondary antibodies were horseradish peroxidase-

conjugated goat anti-mouse IgG (Thermo Scientific), goat anti-rabbit IgG (Thermo Scientific) and rabbit anti-chicken/turkey IgG (Sigma). The immunoblots were developed using the ECL western blotting analysis system (Thermo Scientific).

Interaction assays using recombinant proteins

GST-FTSJ3 and His-NIP7 fusion proteins and GST used in control experiments were expressed in *E. coli* BL21(DE3) using the conditions described previously for His-NIP7 [22]. His-NIP7 was purified by metal-chelating chromatography as previously described [22]. GST-FTSJ3 and GST were isolated from IPTG-induced bacterial cell extracts as described below: bacterial cells were suspended in PBS buffer pH 7.5 (140 mM NaCl; 2.7 mM KCl; 10 mM Na_2HPO_4; 1.8 mM KH_2PO_4), containing 1 mM DTT, 1 mM PMSF, 0.5% (v/v) NP40 and 5% (v/v) glycerol. The cells were lysed by lysozyme treatment and sonication and extracts cleared by centrifugation. The extracts were incubated with glutathione-sepharose beads (GE Healthcare) for 1 hour at 4°C and the beads washed with 10 volumes of PBS buffer containing 1 mM DTT and 1 mM PMSF. Glutathione-sepharose beads containing either GST-FTSJ3 or GST were treated with RNAse A (100 U/ml) or with a mock-buffered solution for 30 min at 4°C. Subsequently the solution containing RNase A was removed and the beads washed once with 10 volumes of PBS buffer. 20 µg of His-NIP7 was added to the binding reactions and incubated for 2 h at 4°C. To the indicated samples, 5 µg of yeast total RNA were also added to the binding reactions. Subsequently the sepharose beads were washed with 10 volumes of PBS buffer with or without RNAse (as indicated) and the proteins analyzed by immunoblotting using mouse antibodies directed against the poly-histidine tag (Sigma) and rabbit antibodies to GST (Sigma).

Cell fractionation

For isolation of nuclear and cytoplasmic extracts, 1×10^7 cells were washed in ice-cold PBS and harvested by centrifugation at 500 *g* for 5 minutes at 4°C. Cells were lyzed in 1 ml of hypotonic cell lysis buffer [20 mM Tris–HCl, pH 7.5; 10 mM NaCl; 15 mM MgCl2; 1 mM EDTA; 0.5% (v/v) NP40; 0.1% (v/v) Triton X-100; complete EDTA-free protease inhibitor cocktail (Roche)] for 10 minutes on ice. Subsequently, NaCl was added to 150 mM final concentration and incubated on ice for 5 minutes. The lysate was centrifuged at 2,800 *g* for 10 minutes at 4°C, the supernatant was collected and cleared at 20,000 *g* for 10 minutes and the resulting supernatant was saved as the cytoplasmic extract. The pellet from the 2,800 *g* centrifugation, containing the nuclei, was washed once with hypotonic cell lysis buffer and the nuclear proteins extracted with 300 µl of denaturing buffer [hypotonic lysis buffer containing 1% (w/v) SDS]. The suspension was centrifuged at 20,000 *g* for 10 minutes at 4°C and the supernatant saved as the nuclear fraction.

Co-immunoprecipitation assays

HEK293/Flp-In/FLAG-FTSJ3 and HEK293/Flp-In/FLAG-3PGDH cell lines were induced for 18–20 hours with 25 and 100 ng/ml of tetracycline, respectively. Cells from a 10-cm plate at 90% estimated confluency were suspended in 1 ml of hypotonic cell lysis buffer [20 mM Tris-HCl, pH 7.5; 15 mM NaCl; 10 mM EDTA; 0.5% (v/v) NP40; 0.5 mM DTT; complete EDTA-free protease inhibitor cocktail (Roche)] and incubated on ice for 10 minutes. NaCl was added to 150 mM final concentration and the lysate sonicated 10 times (2 second bursts) at 40% amplitude with at least 10 second intervals on ice. The cell lysate was cleared by centrifugation at 15,000 *g*. Subsequently, 50 µl of anti-FLAG M2 magnetic beads (Sigma) were added per ml of cell lysate and incubated in 1.5 ml centrifugation tubes on a rotating wheel for 2 hours at 4°C. The magnetic beads were harvested on a magnetic particle collector and supernatants were removed from the bead-bound material. The beads were washed 4 times with 1 ml of isotonic wash buffer (IsoWB) [20 mM Tris-HCl, pH 7.5; 150 mM NaCl; 0.5% (v/v) NP 40, complete EDTA-free protease inhibitor cocktail (Roche)] and suspended in 50 µl of IsoWB. For RNA-dependent protein interaction experiments, RNase A + T1 cocktail (AM2286 – Ambion) was titrated down (2.5 U RNase A and 100 U RNase T1, 0.25 U RNase A and 10 U RNase T1, 0.025 U RNase A and 1 U RNase T1, 0.0025 U RNase A and 0.1 U RNase T1 and 0.00025 U RNase A and 0.01 U RNase T1), and the bead suspension incubated in a water bath at 37°C for 10 minutes, and subsequently cooled for 5 minutes on ice. The supernatant was saved and beads were washed 3 times with 1 ml of IsoWB and suspended in 50 µl of SDS-PAGE loading buffer [47]. Proteins were detected by immunoblotting as described above.

Immunocytochemistry and confocal microscopy

Immunofluorescent localization experiments to detect endogenous NIP7 and FTSJ3 were performed using U2OS cells as previously described [49]. Briefly, after washing in cold Hanks Balanced Salt Solution (HBSS) (GibcoBRL, Paisley, UK), cells were permeabilized in 0.5% Triton X-100 in CSK buffer (10 mM PIPES, pH 6.8; 300 mM sucrose; 100 mM NaCl; 3 mM $MgCl_2$; 1 mM EGTA) for 5 minutes and subsequently fixed on ice with CSK buffer containing 4% formaldehyde for 50 minutes. U2OS cells were eventually stained with antibodies against NIP7 (Abcam) and FSTJ3 (Sigma), raised in rabbit and chicken, respectively, and with secondary goat anti-rabbit IgG conjugated with Alexa Fluor 488 (Invitrogen) and goat anti-chicken IgG conjugated with Alexa Fluor 568 (Invitrogen), both diluted 1:100. Finally, the coverslips were analyzed on an inverted fluorescence microscope (Leica CTR6000). For immunolocalization of FLAG-tagged proteins, HeLa cells transfected with plasmids pcDNA-FLAG-FTSJ3, pcDNA-FLAG-FtsJ or pcDNA-FLAG-Spb1_C seeded on 18 mm coverslips were fixed in 4% paraformaldehyde in PBS, and permeabilized with 0.5% (v/v) Triton X-100 in PBS. Cells were subsequently incubated for 30 minutes in blocking buffer [0.2% (v/v) Triton X-100 and 3% (w/v) low fat milk in PBS], followed by incubation with mouse anti-FLAG M2 (Sigma) diluted 1:100 in the same buffer for 1 hour at 37°C. Cells were washed three times with PBS containing 0.2% (v/v) Triton X-100 and incubated 1 hour at 37°C in blocking buffer with 1:100 secondary anti-mouse coupled to FITC (Invitrogen). Finally, cells were washed as described above, counterstained in DAPI and mounted in PBS:glycerol (1:1). Images were obtained with a Nikon Eclipse E600 microscope and digital images were processed using the Cool-SNAPPro digital system (Media Cybernetics). For confocal microscopy, HeLa cells seeded on 18 mm coverslips were cotransfected with plasmids ecoding EGFP-NIP7 and mRFP-FTSJ3. 48 hours post transfection, cells were fixed with 4% paraformaldehyde for 20 minutes, permeabilized with 0.25% Triton X-100 in PBS for 10 minutes and mounted in ProLong Gold (Invitrogen) containing DRAQ5. The subcellular localization of EGFP- and mRFP- fusion proteins was monitored by fluorescence on a Leica confocal microscope (Leica Microsystems, Exton, PA).

Fluorescence recovery after photobleaching (FRAP)

FRAP assays were performed at 37°C as previously described [49,50]. Leica Confocal Software (Leica Microsystems, Exton, PA) was used to measure the intensity of fluorescence in the bleached

region of interest and in the whole nucleus at each time point. Any remaining fluorescence in the bleached area after the bleach was normalized to zero. To calculate the relative fluorescence intensity (Irel) in the bleached area we used three alternative equations. The first one used the equation: Irel, $t = N_0 * I_f / N_t * I_0$ [51]. The second approach used the equation: Irel, $t = (I_t * (N_0/N_t)) - (I_{pbl} * (N_0/N_{pbl}))/(I_0 - (I_{pbl} * (N_0/N_{pbl}))$. For both equations: N_0 was the total nuclear fluorescence before bleaching, N_{pbl} was the total nuclear fluorescence in the first image taken after the bleach, N_t was the total nuclear fluorescence at time t, I_0 was the fluorescence in the bleach zone before the bleach, I_t was the fluorescence in the bleach zone at time t, and I_{pbl} the fluorescence in the bleach zone in the first image taken after the bleach. Recovery curves were drawn using Graphpad Prism 5. Curve-fitting was performed as described previously [52]. Individual time points are presented as means with error bars showing standard errors. Several equations were tested, but the best fit for these photobleach recoveries was obtained using an exponential association curve: $F(t) = Fmax\ (1 - e^{-kt})$. All half times of recovery and immobile fractions were calculated from a best fit to this equation.

Polysome profile analysis

Polysome profiles were analyzed on sucrose gradients essentially as previously described [22,53]. Briefly, HEK293 Flp-In T-Rex cells stably transfected with the pFRT-U6tetO plasmid expressing either a shRNA targeting FTSJ3 (shRNA) or a scrambled control (SC) were induced (+) or not (−) with 5 μg/ml of doxycycline for 3 days and harvested at ~50% confluency. Following addition of 100 μg/ml cycloheximide, 5×10^7 cells were collected and lyzed using 500 μl of polysome buffer (PB) containing 20 mM Tris-HCl pH, 7.5; 100 mM NaCl; 10 mM $MgCl_2$; 1 mM DTT; 1% (v/v) Triton X-100 and 100 μg/ml cycloheximide. Extracts were clarified by centrifugation at 20,000 *g* for 10 minutes at 4°C. Totals of 35 OD_{260} units were loaded onto linear sucrose gradients (10–50%) prepared in PB. Polysomes were separated by centrifugation at 40,000 rpm for 4 hours at 4°C using a Beckman SW41 rotor. Gradients were fractionated by monitoring absorbance at 254 nm. Protein precipitation and removal of sucrose for immunoblot analyses was performed as follows: 150 μl of each sucrose gradient fraction were mixed with 600 μl of methanol and subsequently mixed with 150 μl of chloroform; 450 μl of water were added to the mix and centrifuged at 20,000 *g* for 5 min at 4°C. The aqueous layer was discarded and the pellet washed with 650 μL of methanol, followed by centrifugation as described above. The liquid was discarded and the pellet was taken up in protein sample buffer and analyzed by immunoblotting.

RNA analysis

Total RNA from HEK293/Flp-In/shRNA-FTSJ3 and HEK293/Flp-In/SC-FTSJ3 cell lines and from HeLa and HEK293 Flp-In T-Rex cells transiently transfected with siRNAs was isolated by TRI Reagent RT (Molecular Research Center, Inc.). RNA samples were fractionated by electrophoresis on 1.0% (w/v) agarose/formaldehyde gels, followed by transfer to Biotrans(+) nylon membranes (MP Biomedicals). Membranes were hybridized with [^{32}P]-labeled oligonucleotide probes P1 (5′ CCC CAA GGC ACG CCT CTC AGA TCG CTA GAG AAG GCT TTT C 3′), P3 (5′ AAG GGG TCT TTA AAC CTC CGC GCC GGA ACG CGC TAG GTA C 3′) and P5 (5′ CGG GAA CTC GGC CCG AGC CGG CTC TCT CTT TCC CTC TCC G 3′) as described previously (Morello et al., 2011), for 16 hours in ExpressHyb solution (BD Biosciences). Northern blots were visualized and quantified using a Storm 840 Phosphorimager (Molecular Dynamics).

Acknowledgments

We thank Adriana Franco Paes Leme (LNBio, CNPEM) for her support during the development of this work.

Author Contributions

Conceived and designed the experiments: LGM PPC AJCQ FMS NITZ. Performed the experiments: LGM PPC CCO AJCQ FMS TCLS. Analyzed the data: LGM PPC AJCQ FMS TCLS GS JAN CCO MJM NITZ. Contributed reagents/materials/analysis tools: JAN MJM CCO NITZ. Wrote the paper: LGM PPC CCO NITZ.

References

1. Fromont-Racine M, Senger B, Saveanu C, Fasiolo F (2003) Ribosome assembly in eukaryotes. Gene 313: 17–42.
2. Tschochner H, Hurt E (2003) Pre-ribosomes on the road from the nucleolus to the cytoplasm. Trends Cell Biol 13: 255–263.
3. Henras A, Soudet K, Gérus JM, Lebaron S, Caizergues-Ferrer M, et al. (2008) The post-transcriptional steps of eukaryotic ribosome biogenesis. Cell Mol Life Sci 65: 2334–2359.
4. Strunk BS, Karbstein K (2009) Powering through ribosome assembly. RNA 15: 2083–2104.
5. Kressler D, Hurt E, Bassler J (2010) Driving ribosome assembly. Biochim Biophys Acta 1803: 673–683.
6. Freed EF, Bleichert F, Dutca LM, Baserga SJ (2010) When ribosomes go bad: diseases of ribosome biogenesis. Mol Biosyst 6: 481–493.
7. Valdez BC, Henning D, So RB, Dixon J, Dixon MJ (2004) The Treacher Collins syndrome (TCOF1) gene product is involved in ribosomal DNA gene transcription by interacting with upstream binding factor. Proc Natl Acad Sci USA 101: 10709–10714.
8. Grandi P, Rybin V, Bassler J, Petfalski E, Strauss D, et al. (2002) 90S pre-ribosomes include the 35S pre-rRNA, the U3 snoRNP, and 40S subunit processing factors but predominantly lack 60S synthesis factors. Mol Cell 10: 105–115.
9. Nissan TA, Bassler J, Petfalski E, Tollervey D, Hurt E (2002) 60S pre-ribosome formation viewed from assembly in the nucleolus until export to the cytoplasm. EMBO J 15: 5539–5547.
10. Bowman LH, Rabin B, Schlessinger D (1981) Multiple ribosomal RNA cleavage pathways in mammalian cells. Nucleic Acids Res 9: 4951–4965.
11. Hadjiolova KV, Nicoloso M, Mazan S, Hadjiolov AA, Bachellerie J-P (1993) Alternative pre-rRNA processing pathways in human cells and their alteration by cycloheximide inhibition of protein synthesis. Eur J Biochem 212: 211–215.
12. Gelperin D, Horton L, Beckman J, Hensold J, Lemmon SK (2001) Bms1p, a novel GTP-binding protein, and the related Tsr1p are required for distinct steps of 40S ribosome biogenesis in yeast. RNA 7: 1268–1283.
13. Chen W, Bucaria J, Band DA, Sutton A, Sternglanz R (2003) Enp1, a yeast protein associated with U3 and U14 snoRNAs, is required for pre-rRNA processing and 40S subunit synthesis. Nucleic Acids Res 31: 690–699.
14. Leger-Silvestre I, Milkereit P, Ferreira-Cerca S, Saveanu C, Rousselle JC, et al. (2004) The ribosomal protein Rps15p is required for nuclear exit of the 40S subunit precursors in yeast. EMBO J 23: 2336–2347.
15. Carron C, O'Donohue MF, Choesmel V, Faubladier M, Gleizes PE (2010) Analysis of two human pre-ribosomal factors, bystin and hTsr1, highlights differences in evolution of ribosome biogenesis between yeast and mammals. Nucleic Acids Res 39: 280–291.
16. Zanchin NIT, Roberts P, de Silva A, Sherman F, Goldfarb DS (1997) *Saccharomyces cerevisiae* Nip7p is required for efficient 60S ribosome subunit biogenesis. Mol Cell Biol 17: 5001–5015.
17. Zanchin NIT, Goldfarb DS (1999a) Nip7p interacts with Nop8p, an essential nucleolar protein required for 60S ribosome biogenesis, and the exosome subunit Rrp43p. Mol Cell Biol 19: 1518–1525.
18. Zanchin NIT, Goldfarb DS (1999b) The exosome subunit Rrp43p is required for the efficient maturation of 5.8S, 18S and 25S rRNA. Nucleic Acids Res 27: 1283–1288.
19. Granato DC, Gonzales FA, Luz JS, Cassiola F, Machado-Santelli GM, et al. (2005) Nop53p, an essential nucleolar protein that interacts with Nop17p and Nip7p, is required for pre-rRNA processing in Saccharomyces cerevisiae. FEBS J 272: 4450–4463.
20. Luz JS, Georg RC, Gomes CH, Machado-Santelli GM, Oliveira CC (2009) Sdo1p, the yeast ortholog of Shwachman-Bodian-Diamond syndrome protein binds RNA and interacts with nuclear rRNA processing factors. Yeast 26: 287–298.

21. Mitchell P, Petfalski E, Shevchenko S, Mann M, Tollervey D (1997) The exosome: a conserved eukaryotic RNA processing complex containing multiple 3′-5′ exoribonucleases. Cell 91: 457–466.
22. Morello LG, Hesling C, Coltri PP, Castilho BA, Rimokh R, et al. (2011) The NIP7 protein is required for accurate pre-rRNA processing in human cells. Nucleic Acids Res 39: 648–665.
23. Kressler D, Rojo M, Linder P, Cruz J (1999) Spb1p is a putative methyltransferase required for 60S ribosomal subunit biogenesis in *Saccharomyces cerevisiae*. Nucleic Acids Res 27: 4598–608.
24. Bonnerot C, Pintard L, Lutfalla G (2003) Functional redundancy of Spb1p and a snR52-dependent mechanism for the 2′-O-ribose methylation of a conserved rRNA position in yeast. Mol Cell 12: 1309–1315.
25. Lapeyre B, Purushothaman SK (2004) Spb1p-directed formation of Gm2922 in the ribosome catalytic center occurs at a late processing stage. Mol Cell 16: 663–669.
26. Fujiyama-Nakamura S, Yoshikawa H, Homma K, Hayano T, Tsujimura-Takahashi T, et al. (2009) Parvulin (Par14), a peptidyl-prolyl cis-trans isomerase, is a novel rRNA processing factor that evolved in the metazoan lineage. Mol Cell Proteomics 8: 1552–1565.
27. Orrù S, Aspesi A, Armiraglio M, Caterino M, Loreni F, et al. (2007) Analysis of the Ribosomal Protein S19 Interactome. Mol Cell Proteomics 6: 382–393.
28. Takahashi N, Yanagida M, Fujiyama S, Hayano T, Isobe T (2003) Proteomic snapshot analyses of preribosomal ribonucleoprotein complexes formed at various stages of ribosome biogenesis in yeast and mammalian cells. Mass Spectrom Rev 22: 287–317.
29. Hesling C, Oliveira CC, Castilho BA, Zanchin NIT (2007) The Shwachman-Bodian-Diamond syndrome associated protein interacts with HsNip7 and its down-regulation affects gene expression at the transcriptional and translational levels. Exp Cell Res 313: 4180–4195.
30. Aagaard L, Amarzguioui M, Sun G, Santos LC, Ehsani A, et al. (2007) A facile lentiviral vector system for expression of doxycycline-inducible shRNAs: knockdown of the pre-miRNA processing enzyme Drosha. Mol Ther 15: 938–945.
31. Boulon S, Westman BJ, Hutten S, Boisvert FM, Lamond AI (2010) The nucleolus under stress. Mol Cell 40: 216–227.
32. Rubbi CP, Milner J (2003) Disruption of the nucleolus mediates stabilization of p53 in response to DNA damage and other stresses. EMBO J 22: 6068–7607.
33. Hölzel M, Orban M, Hochstatter J, Rohrmoser M, Harasim T, et al. (2010a) Defects in 18 S or 28 S rRNA processing activate the p53 pathway. J Biol Chem 285: 6364–6370.
34. Hölzel M, Burger K, Mühl B, Orban M, Kellner M, et al. (2010b) The tumor suppressor p53 connects ribosome biogenesis to cell cycle control: a double-edged sword. Oncotarget 1: 43–47.
35. Sun XX, Wang YG, Xirodimas DP, Daí MS (2010) Perturbation of 60 S ribosomal biogenesis results in ribosomal protein L5- and L11-dependent p53 activation. J Biol Chem 285: 25812–25821.
36. Coltri PP, Guimarães BG, Granato DC, Luz JS, Teixeira E, et al. (2007) Structural insights into the interaction of the Nip7 PUA domain with polyuridine RNA. Biochemistry 46: 14177–14187.
37. Horsey EW, Jakovljevic J, Miles TD, Harnpicharnchai P, Woolford JL, Jr. (2004) Role of the yeast Rrp1 protein in the dynamics of pre-ribosome maturation. RNA 10: 813–827.
38. Miles TD, Jakovljevic J, Horsey EW, Harnpicharnchai P, Tang L, et al. (2005) Ytm1, Nop7, and Erb1 form a complex necessary for maturation of yeast 66S preribosomes. Mol Cell Biol 25: 10419–10432.
39. Lebreton A, Rousselle J-C, Lenormand P, Namane A, Jacquier A, et al. (2008) 60S ribosomal subunit assembly dynamics defined by semi-quantitative mass spectrometry of purified complexes. Nucleic Acids Res 36: 4988–4999.
40. Dragon F, Gallagher JE, Compagnone-Post PA, Mitchell BM, Porwancher KA, et al. (2002) A large nucleolar U3 ribonucleoprotein required for 18S ribosomal RNA biogenesis. Nature 417: 967–970.
41. Schäfer T, Strauss D, Petfalski E, Tollervey D, Hurt E (2003) The path from nucleolar 90S to cytoplasmic 40S pre-ribosomes. EMBO J 22: 1370–1380.
42. Wild T, Horvath P, Wyler E, Widmann B, Badertscher L, et al. (2010) A protein inventory of human ribosome biogenesis reveals an essential function of exportin 5 in 60S subunit export. PLoS Biol 8: e1000522.
43. Fujiyama S, Yanagida M, Hayano T, Miura Y, Isobe T, et al. (2002) Isolation and proteomic characterization of human parvulin associating preribosomal ribonucleoprotein complexes. J Biol Chem 277: 23773–23780.
44. Ginisty H, Amalric F, Bouvet P (1998) Nucleolin functions in the first step of ribosomal RNA processing. EMBO J 17: 1476–1486.
45. Fink AL (2005) Natively unfolded proteins. Curr Opin Struct Biol 15: 35–41.
46. O'Donohue MF, Choesmel V, Faubladier M, Fichant G, Gleizes PE (2010) Functional dichotomy of ribosomal proteins during the synthesis of mammalian 40S ribosomal subunits. J Cell Biol 190: 853–866.
47. Sambrook J, Fritsch EJ, Maniatis T Molecular cloning, a laboratory manual 2nd ed., Cold Spring Harbor Laboratory Press, Cold Spring Harbor, NY.
48. Hollenberg SM, Sternglanz R, Cheng PF, Weintraub H (1995) Identification of a new family of tissue-specific basic helix-loop-helix protein with a two-hybrid system. Mol Cell Biol 15: 3813–3822.
49. Wagner S, Chiosea S, Nickerson JA (2003) The spatial targeting and nuclear matrix binding domains of SRm160. Proc Natl Acad Sci U S A 100: 3269–3274.
50. Kota KP, Wagner SR, Huerta E, Underwood JM, Nickerson JA (2008) Binding of ATP to UAP56 is necessary for mRNA export. J Cell Sci 121: 1526–1537.
51. Phair RD, Misteli T (2000) High mobility of proteins in the mammalian cell nucleus. Nature 404: 604–609.
52. Liu F, Wagner S, Campbell RB, Nickerson JA, Schiffer CA, et al. (2005) PTEN enters the nucleus by diffusion. J Cell Biochem 96: 221–234.
53. Johannes G, Sarnow P (1998) Cap-independent polysomal association of natural mRNAs encoding c-myc, BiP, and eIF4G conferred by internal ribosome entry sites. RNA 12: 1500–1513.

3. RESULTADOS

3.3. Capítulo III (Artigo III)

Proteomic Characterization of the Human FTSJ3 Pre-ribosomal Complexes

Fernando M. Simabuco, Luis G. Morello, Annelize Zambon Barbosa Aragão, Adriana Franco Paes Leme and Nilson I. T. Zanchin

Journal of Proteome Research, **11**, 3112−3126 (2012)

Journal of proteome research

Article

pubs.acs.org/jpr

Proteomic Characterization of the Human FTSJ3 Preribosomal Complexes

Fernando M. Simabuco,[†] Luis G. Morello,[†] Annelize Zambon Barbosa Aragão,[†] Adriana Franco Paes Leme,[†] and Nilson I. T. Zanchin*[,‡]

[†]Laboratório Nacional de Biociências, Centro Nacional de Pesquisa em Energia e Materiais, Rua Giuseppe Maximo Scolfaro 10000, P.O. Box 6192, CEP 13083-970, Campinas SP, Brazil

[‡]Instituto Carlos Chagas, Fundação Instituto Oswaldo Cruz/FIOCRUZ, Rua Prof. Algacyr Munhoz Mader 3775, CEP 81350-010, Curitiba, Paraná, Brazil

ABSTRACT: In eukaryotes, ribosome biogenesis involves excision of transcribed spacer sequences from the preribosomal RNA, base and ribose covalent modification at specific sites, assembly of ribosomal proteins, and transport of subunits from the nucleolus to the cytoplasm where mature ribosomes engage in mRNA translation. The biochemical reactions throughout ribosome synthesis are mediated by factors that associate transiently to the preribosomal complexes. In this work, we describe the complexes containing the human protein FTSJ3. This protein functions in association with NIP7 in ribosome synthesis and contains a putative RNA-methyltransferase domain (FtsJ) in the N-terminal region and two uncharacterized domains in the central (DUF3381) and C-terminal (Spb1_C) regions. FLAG-tagged FTSJ3 coimmunoprecipitates both RPS and RPL proteins, ribosome synthesis factors, and proteins whose function in ribosome synthesis has not been demonstrated yet. A similar set of proteins coimmunoprecipitates with the Spb1_C domain, suggesting that FTSJ3 interaction with the preribosome complexes is mediated by the Spb1_C domain. Approximately 50% of the components of FTSJ3 complexes are shared by complexes described for RPS19, Par14, nucleolin, and NOP56. A significant number of factors are also found in complexes described for nucleophosmin, SBDS, ISG20L2, and NIP7. These findings provide information on the dynamics of preribosome complexes in human cells.

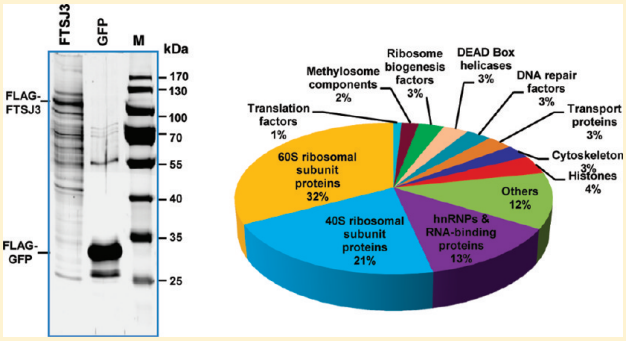

KEYWORDS: *ribosome synthesis mechanism, preribosome complexes, ribosome synthesis factors, Spb1-C domain protein*

INTRODUCTION

Synthesis of eukaryotic ribosomes takes place mainly in the nucleolus, a specialized cell compartment within the nucleus, where RNA polymerase I transcribes a large polycistronic preribosomal RNA (pre-rRNA), that contains the 18S, 5.8S, and 25S/28S rRNAs. Synthesis of the mature rRNAs includes a series of endo- and exonucleolytic cleavages to remove the spacer sequences. In addition, the rRNAs undergo covalent modifications that include base and ribose methylation and uridine isomerization to pseudouridine at specific sites. In parallel with processing and modification, the rRNAs are assembled with ribosomal proteins, and the ribosomal subunits are exported to the cytoplasm where they undergo the final steps of maturation and eventually engage in mRNA translation. Pre-rRNA cleavages and modifications are mediated by trans-acting factors that bind to nascent preribosomal particles and dissociate as their function is accomplished.[1−5] Approximately 200 trans-acting factors that function in ribosome synthesis have already been identified on the basis of protein interaction and genetic analyses.[5]

The yeast *Saccharomyces cerevisiae* has been widely used as a model system to identify trans-acting factors and to study the ribosome synthesis mechanism. Proteomic approaches have been used to characterize preribosomal particles in *S. cerevisiae*. A 90S preribosome complex was described as the initial complex formed during ribosome synthesis.[6,7] It contains the 35S pre-rRNA, the U3 small nucleolar RNA (snoRNA), and a set of nonribosomal proteins that are required for synthesis and nuclear export of the 40S subunit.[6] It contains also 40S ribosomal proteins but lacks most 60S subunit proteins, indicating that 60S proteins and synthesis factors bind later in the process.[6] The U3 snoRNA and its approximately 30 associated proteins form a subcomplex termed the small subunit (SSU) processome, which acts in the synthesis of the 18S rRNA.[8] Cleavage in the internal transcribed spacer 1 (ITS1) generates the pre-40S and pre-60S complexes. The pre-40S complex contains fewer ribosome synthesis factors as compared to the 90S complex, indicating that nonribosomal

Received: November 6, 2011
Published: April 30, 2012

dx.doi.org/10.1021/pr201106n | *J. Proteome Res.* 2012, 11, 3112−3126

proteins dissociate during transition from the 90S to the pre-40S complex.[7] Pull-down assays with different synthesis factors revealed specific composition both for the early and intermediate nucleolar pre-40S complexes and for the late cytoplasmic pre-40S complexes.[7] About 50 nonribosomal proteins have been identified in 60S precomplexes.[9−12] The composition of the pre-60S complex changes according to the stage of synthesis and cell compartment as determined by proteomic analysis of complexes isolated in pull-down assays using different tagged 60S synthesis factors or different conditional mutants.[9−12]

Although the general mechanism of ribosome synthesis is conserved in all eukaryotes, several key differences between yeast and mammalians have emerged. In wild type *S. cerevisiae* strains, processing of the 35S pre-rRNA follows a 5′ to 3′ processing hierarchy, where the 5′ external transcribed spacer (5′ ETS) is cleaved before processing of the ITS1, which in its turn is cleaved before ITS2.[6,9] The mammalian 47S pre-rRNA, on the other hand, is initially converted to a 45S pre-rRNA that is processed by simultaneous alternative pathways.[13] In pathway 1, there are concomitant cleavages at sites A0 and A1, removing the complete 5′ ETS, whereas in pathway 2, processing starts in ITS1 at site 2. In pathway 1, the 41S pre-rRNA is cleaved at site 2 into 21S and 32S pre-rRNAs. The 21S is successively processed to sites C and E to generate the 18S rRNA, and the 32S pre-rRNA is processed in ITS2, generating the 12S pre-rRNA and the 28S rRNA. The 12S is processed at site 4a into 7S and then at site 4′ to generate the 5.8S rRNA. In pathway 2, the 30S is matured either directly into 21S by simultaneous processing at sites A0 and 1, or through the formation of a 26S pre-rRNA intermediate.

Ribosome synthesis factors that perform catalytic functions in pre-rRNA cleavage, methylation, and pseudouridylation are conserved in *Archaea*, yeast, and mammals. However, recent studies have demonstrated that the phenotypes shown by conditional depletion of certain human ribosome synthesis factors differ significantly from the phenotypes observed in yeast. This is the case of Bystin and hTsr1, the human orthologs of yeast Enp1 and Tsr1, respectively. In yeast, Enp1 is required for the maturation of the 18S rRNA and synthesis of the 40S subunit, but conditional knockdown of Bystin in HEK293 cells leads to formation of a new RNA precursor.[14,15] Conditional depletion of hTsr1 causes 40S particles to be partially retained in the nucleus, while yeast Tsr1 is dispensable for 40S subunit nuclear exit.[15,16] A significant difference has been described also for the yeast and human NIP7 orthologs. While conditional knockdown of yeast Nip7 affects mainly the synthesis of 60S subunits, knockdown of human NIP7 affects the 18S processing pathway and 40S subunit synthesis.[17,18] In a previous study, we found that human NIP7 interacts with FTSJ3 in the yeast two hybrid assay.[19] FTSJ3 shows sequence similarity to the yeast protein Spb1, which contains a putative RNA-methyl-transferase domain (FtsJ) in the N-terminal region, an uncharacterized domain in the central region (DUF3381, residues 226−407) and a conserved uncharacterized domain (Spb1_C) in the C-terminal region. Spb1 was already shown to be required for 60S subunit synthesis in yeast[20] and to mediate methylation of the conserved G_{2922} that is located within the A loop of the catalytic center of the ribosome.[21,22] In contrast to yeast Spb1, and consistently with the data obtained for human NIP7,[18] human FTSJ3 is required for processing of the pre-rRNA intermediates in the pathway leading to 18S rRNA maturation.[19] Ribosome synthesis and function have additional implications for humans since over 15 genetic diseases have already been linked to mutations in genes that code for ribosomal proteins and ribosome synthesis factors.[23] Therefore, despite the general similarities between the yeast and human ribosome synthesis, it is important to determine the molecular mechanisms that are specific to pre-rRNA processing and the unique features that underlie ribosome function in human cells.

Although only a few studies on the proteomic characterization of human preribosome complexes have been published to date, they provide important information on the dynamics of ribosome synthesis in human cells. A review of the literature data published so far suggests the existence of three major types of complexes regarding the content of ribosomal proteins. One type of complex contains ribosomal proteins of both the 40S and 60S subunits with a higher ratio of 40S proteins, such as the complexes isolated by affinity-purification of RPS19.[24] A second type contains ribosomal proteins of both the 40S and 60S subunits but with a higher ratio of 60S proteins as for example the complexes described for nucleolin[25] and nucleophosmin.[26,27] The second type of complex may include also parvulin (Par14)[28] and NOP56.[29] They probably contain pre-rRNAs that are not cleaved in ITS1. Alternatively, these ribosome synthesis factors may function in the synthesis of both ribosomal subunits. The third type of complex is highly enriched in 60S ribosomal proteins and includes SBDS[30] and ISG20L2.[31] The composition of the latter complex suggests that these factors play a role that is specific to the synthesis of the 60S ribosomal subunit.

Proteomic studies have shown that FTSJ3 associates with complexes isolated by affinity purification of Par14,[28] RPS19,[24] and nucleolin.[32] FTSJ3 displays the same structural arrangement as Spb1. Secondary structure prediction indicates that the Spb1_C C-terminal domain is intrinsically disordered. In this work, we describe the preribosome complexes isolated by affinity purification of human FTSJ3. In addition, we provide evidence that the intrinsically disordered Spb1_C domain of FTSJ3 plays a role in macromolecular interactions.

METHODS AND MATERIALS

Plasmid Construction

The full-length FTSJ3 cDNA (accession number NM_017647.3) and its FtsJ (amino acids 22−202) and Spb1_C (amino acids 640−847) domains, and the NIP7 cDNA (accession number NM_016101) were cloned into pcDNA 3.1 (+) containing a FLAG-tag upstream of the modified multiple cloning site (pcDNA-FLAG) using the *Eco*RI/*Xba*I restriction sites, generating the plasmids pcDNA-FLAG-FTSJ3, pcDNA-FLAG-FtsJ, pcDNA-FLAG-Spb1_C, and pcDNA-FLAG-NIP7, respectively. A pcDNA-FLAG-GFP plasmid was used as control for expression of a nonrelated protein in the immunoprecipitation assays.

Cell Culture Methods

HEK293 cells were maintained in high-glucose (4.5 g/L) Dulbecco's modified Eagle's medium supplemented with 10% fetal bovine serum, 100 U/mL of penicillin, and 100 μg/mL of streptomycin. The cells were cultured at 37 °C in a humidified atmosphere with 5% CO_2. Transfections were performed with Lipofectamine PLUS (Invitrogen). Briefly, five 150-mm plates with cells growing at ∼80% confluency were washed with serum-free medium and incubated for 3 h with a mixture of Lipofectamine PLUS and plasmid DNA using the amounts

dx.doi.org/10.1021/pr201106n | J. Proteome Res. 2012, 11, 3112−3126

recommended by the manufacturer. Subsequently, the serum-free medium was changed to complete medium, and the cells were incubated further for 48 h.

Immunoprecipitation Using Anti-FLAG Antibody Coupled with Agarose Beads

HEK293 cells with FLAG-tagged proteins were washed twice with PBS and harvested by pipetting up and down in PBS. Cells were suspended in lysis buffer (50 mM Tris.HCl, pH 7.4, 150 mM NaCl, 1 mM EDTA, 1% Triton X-100) containing a protease inhibitor cocktail (Roche). Lysates were incubated for 15 min on ice and centrifuged at 12000*g* for 10 min. Supernatants were collected, diluted 1:1 in lysis buffer, and incubated overnight at 4 °C with anti-FLAG agarose-coupled beads (Sigma) under mild agitation. Subsequently, the beads were washed five times with ice-cold TBS (50 mM Tris-HCl, pH 7.5, 150 mM NaCl) and eluted with 150 ng/μL of FLAG peptide (Sigma) at 4 °C for 2 h under moderate agitation. Supernatants were collected and stored at −20 °C for analysis by mass spectrometry and immunoblotting.

Immunoblot Analysis and Antibodies

Proteins were resolved by SDS−PAGE and immunoblots were performed as described previously.[19] Primary antibodies and their dilutions were as follows: mouse monoclonal anti-FLAG (Sigma) (1:5000), goat polyclonal anti-PRMT5 (Santa Cruz Biotechnology) (1:1000), mouse monoclonal anti-NPM (Sigma) (1:2000), mouse monoclonal anti-hnRNPQ (Santa Cruz Biotechnology) (1:1000). Secondary antibodies were horseradish peroxidase-conjugated goat antimouse IgG (Calbiochem) and goat antirabbit IgG (Calbiochem). Immunoblots were developed using the ECL Plus Western blotting detection system (GE Healthcare).

Trypsin Digestion and Mass Spectrometry Analysis

Following immunoprecipitation, the eluates were reduced, alkylated, and digested with trypsin as previously described.[33] After digestion, the peptides were suspended in 20 μL of 0.1% formic acid, and 4.5 μL aliquots were separated by C18 (100 μm × 100 mm) RP-nanoUPLC (nanoAcquity, Waters) coupled with a Q-Tof Ultima mass spectrometer (Waters) with nanoelectrospray source at a flow rate of 0.6 μL/min. The gradient was 2−90% acetonitrile in 0.1% formic acid over 45 min. The nanoelectrospray voltage was set to 3.5 kV and a cone voltage of 30 V, and the source temperature was 100 °C. The instrument was operated in the "top three" mode, in which one MS spectrum is acquired followed by MS/MS of the top three most-intense peaks detected. After MS/MS fragmentation, the ion was placed on exclusion list for 60S.

Data Analysis

The spectra were acquired using software MassLynx v.4.1, and the raw data files were converted to a peak list format (mgf) without summing the scans by the software Mascot Distiller v.2.3.2.0, 2009 (Matrix Science), allowing the label-free analysis, and searched against Human International Protein Database (IPI) v. 3.72 (86392 sequences; 35093930 residues) using engine Mascot v.2.3.01 (Matrix Science), with carbamidomethylation as fixed modifications, oxidation of methionine as variable modification, one trypsin missed cleavage, and a tolerance of 0.1 Da for both precursor and fragment ions. Only peptides with a minimum of five amino acid residues that showed significant threshold ($p < 0.05$) in Mascot-based score were considered as a product of peptide cleavage. The peptide was considered as unique when it differs in at least 1 amino acid residue; covalently modified peptides, including N- or C-terminal elongation (i.e., missed cleavages), counted as unique, and different charge states of the same peptide and modifications were not counted as unique. For each identified protein, the number of spectral counts and unique peptides were assessed.

RESULTS AND DISCUSSION

Identification of FTSJ3-Interacting Proteins

Human FTSJ3 shows sequence similarity to the yeast protein Spb1, a protein that has already been shown to function in ribosome biogenesis.[29] Both proteins share a structural arrangement containing a putative RNA-methyl-transferase domain (FtsJ, residues 22−202) in the N-terminal region and two conserved uncharacterized domains, DUF3381 (residues 226−407), located in the central region, and Spb1_C (residues 640−828) located in the C-terminal region. Previous studies have shown that FTSJ3 associates with preribosomal complexes isolated by affinity purification of parvulin (Par14),[25] RPS19,[21] and nucleolin.[32] Knock down experiments showing that FTSJ3 is required for accurate pre-rRNA processing[19] further support its role in ribosome biogenesis. Little information is currently available on the human preribosome complex composition. The fact that three processing pathways act simultaneously may indicate that the dynamics of complex formation during ribosome synthesis in mammalian cells is different from the one observed in *S. cerevisiae*. Therefore, proteomics characterization of FTSJ3 affinity-purified complexes may provide information on the ribosome synthesis mechanism in human cells. To determine the FTSJ3 interactome in HEK293 cells, we performed immunoprecipitation experiments with FLAG-tagged FTSJ3 on a FLAG-peptide affinity resin, which showed specific copurification of a large number of proteins (Figure 1B). LC−MS/MS analysis of trypsin-digested proteins that copurified with FLAG-FTSJ3 identified 98 proteins, including 21 40S subunit proteins, 33 60S subunit proteins, and 44 proteins of various functional categories that included 10 heterogeneous nuclear ribonucleoproteins (hnRNPs) (Table 1). None of those proteins were found in a control immunoprecipitation, performed in the same conditions for a FLAG-GFP protein (data not shown). The proteins nucleophosmin (NPM), hnRNPQ, and arginine methyltransferase 5 (PRMT5) were selected to confirm interaction with FTSJ3 by immunoblotting. All of the proteins tested coimmunoprecipitated with FLAG-FTSJ3 (Figure 2).

In the *Saccharomyces* Genome Database (http://www.yeastgenome.org/), there is a list of 25 proteins described to interact with yeast Spb1, the ortholog of human FTSJ3. A comparison of the set of Spb1-interacting proteins with the 98 proteins identified in the pulldown with FLAG-FTSJ3 showed that they share only one ortholog, which, incredibly, is Nip7/NIP7. This finding, although as unpredictable as it appears, is in agreement with the different phenotypes observed for conditional depletion of Nip7 and Spb1 in yeast and for downregulation of NIP7 and FTSJ3 in human cells.

Identification of Proteins Interacting with the Spb1_C domain of FTSJ3

Spb1_C is a conserved domain of unknown function found in the C-terminal region of all eukaryotic orthologs of yeast Spb1. Structure predictions indicate that except for the putative RNA-methyl-transferase domain (residues 22−202), FTSJ3 contains a large intrinsically disordered region, roughly from amino acid

dx.doi.org/10.1021/pr201106n | J. Proteome Res. 2012, 11, 3112−3126

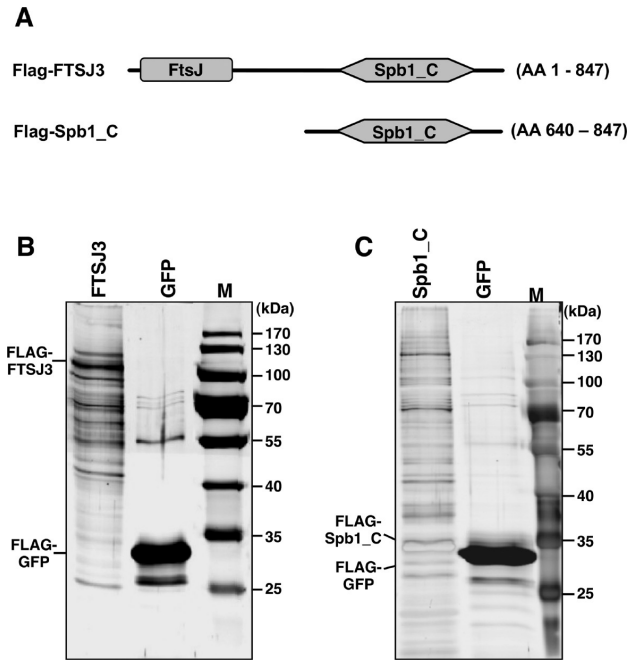

Figure 1. Immuno-affinity purification of the FLAG-FTSJ3 and FLAG-Spb1_C fusion proteins. (A) Diagram of the FTSJ3 and Spb1_C proteins fused to the FLAG tag. The conserved FtsJ and Spb1_C domains are indicated. (B) and (C), SDS-PAGE analysis of proteins copurifying with FLAG-FTSJ3 and FLAG-Spb1_C, respectively. FLAG-tagged GFP was used as a negative control. The FLAG-tagged proteins were expressed transiently in HEK293 and purified with a FLAG antibody immobilized on agarose beads (Sigma). Following electrophoresis, the gels were silver stained.

300 onward up to the C-terminus, which also includes the conserved uncharacterized domain Spb1_C. Intrinsically disordered regions have higher flexibility and provide also larger binding interfaces when compared to folded proteins of the same size, allowing them to fit a variety of different binding partners.[34] Preribosome complexes depend upon multiple macromolecular interactions, and the Spb1_C domain displays the features of a candidate to mediate macromolecular interactions. Theoretical predictions did identify RNA binding motifs in the Spb1_C domain. However, intrinsically disordered regions can mediate both protein−protein and protein−RNA interactions.[35]

To test whether the Spb1_C domain interacts with preribosome complexes, the Spb1_C region of FTSJ3 (residues 640−847) containing the FLAG-tag in the N-terminal region was expressed in HEK293 cells and purified using FLAG-peptide affinity beads. SDS-PAGE analysis revealed a large number of proteins copurifying with FLAG-Spb1_C (Figure 1C), and 55 of them were identified by LC−MS/MS analysis (Table 1). Again, none of those proteins were found in the control immunoprecipitation, performed in the same conditions for a FLAG-GFP protein (data not shown). Although the number of proteins identified in the FLAG-Spb1_C immunoprecipitation is smaller, it contains proteins belonging to the same categories of those identified in the FLAG-FTSJ3 immunoprecipitation. The proteins identified comprise 15 proteins of the 40S subunit, 22 proteins of the 60S subunit, and 18 nonribosomal proteins. The specific interactions of nucleophosmin, hnRNPQ, and PRMT5 with FLAG-Spb1_C were confirmed by immunoblotting (Figure 2).

Analysis of Proteins Copurifying with FLAG-NIP7

NIP7 and FTSJ3 are both nucleolar proteins that function in association in ribosome synthesis, but the pre-rRNA processing defects caused by RNAi knockdown of these proteins suggest that they are required for different cleavages of the pre-rRNAs leading to 18S maturation and 40S subunit formation.[18,19] In order to complement the analysis of the complexes formed by these two proteins, we performed pulldown and mass spectrometry analyses also for FLAG-NIP7. This fusion protein was transiently expressed in HEK293, and the pulldown assays were performed as described for FLAG-FTSJ3 and FLAG-Spb1_C. FLAG-NIP7 turned out to be less efficient than FLAG-FTSJ3 and FLAG-Spb1_C to copurify preribosomal complexes. Nevertheless, we could identify 40 proteins that copurified specifically in the FLAG-NIP7 pulldown. Twenty-two of these proteins (Table 1) are also found in the FLAG-FTSJ3 and FLAG-Spb1_C pulldowns, including 12 ribosomal proteins and three characterized ribosome synthesis factors. The remainder (TUBA1C, TUBB2C, TUBB3, TUBB6, TUBA8, ACTA2, PPM1B, HSPA7, HSPD1, KIFC3, KIF11, SCYL2, STK38, ATP5A1, PRDX1, TXN, PI4K2A, CCDC105) are most probably contaminants resulting from unspecific binding to FLAG-NIP7.

Functional Classes of the Proteins Associated with Affinity-Purified FLAG-FTSJ3, FLAG-Spb1_C, and FLAG-NIP7 Complexes

The proteins copurifying with FLAG-FTSJ3 and FLAG-Spb1_C were classified according to their molecular function (Figure 3, Table 1). From the 98 proteins copurifying with FLAG-FTSJ3, 54 (55%) are ribosomal protein components of mature ribosomes. Twenty-one proteins belong to the 40S subunit proteins and represent a ratio of approximately 65.6% of the protein components found in a mature 40S subunit. The 33 RPL proteins identified in the complex represents approximately 86.8% of the protein components found in a mature 60S subunit. The 44 nonribosomal proteins found in the complex comprise factors with both demonstrated and putative function in ribosome synthesis, components of heterogeneous nuclear ribonucleoproteins and proteins that may have an indirect function in ribosome synthesis, and a few proteins that may not be functionally connected with ribosome synthesis. Among the ribosome synthesis factors whose function in ribosome synthesis has been already demonstrated are the proteins nucleolin,[36] nucleophosmin (NPM),[26,27,37] the RNA helicases DDX5[38] and DDX21,[39] and PRMT5.[40] Interestingly, 10 components of hnRNPs were identified in the FLAG-FTSJ3 immunoprecipitation assay. An equivalent number of hnRNPs associated to preribosomes has been described only for the complexes isolated by affinity purification of the 40S subunit protein RPS19.[24] The presence of hnRNPs is intriguing. However, proteomics studies have already described the presence of 15 hnRNPs in the nucleolus,[41−43] indicating that this class of proteins may be regular components of the nucleolar compartment. Other functional classes of proteins such as transport proteins are also found scattered in immunoprecipitation assays of other ribosome synthesis factors. Histones are abundant proteins in nucleolar extract preparations[43] and their association to preribosomes as well as the association of transcription factors is most probably indirect.

Although a smaller number of proteins were identified in the immunoprecipitation with FLAG-Spb1_C, they belong to the same functional categories of those that were copurified with

dx.doi.org/10.1021/pr201106n | J. Proteome Res. 2012, 11, 3112−3126

Table 1. Identification of Full-Length FTSJ3 protein, Spb1_C Domain, and NIP7-Interacting Proteins by Mass Spectrometry after Tag-Immunoprecipitation

Protein name	Bait protein			Gene symbol	IPI accession number	Yeast homolog
	FLAG-FTSJ3*	FLAG-Spb1_C*	FLAG-NIP7*			
40S ribosomal subunit proteins						
40S ribosomal protein S2	7/7	5/2	2/1	RPS2	IPI00013485	RPS2
40S ribosomal protein S3	1/1			RPS3	IPI00011253	RPS3
40S ribosomal protein S3A	6/6	7/4		RPS3A	IPI00419880	RPS1B
40S ribosomal protein S4, X isoform	4/4			RPS4X	IPI00217030	RPS4A
40S ribosomal protein S5	1/1		5/1	RPS5	IPI00008433	RPS5
40S ribosomal protein S6	4/4	6/4		RPS6	IPI00021840	RPS6A
40S ribosomal protein S7		3/2		RPS7	IPI00013415	RPS7A
40S ribosomal protein S8	5/5	6/5		RPS8	IPI00216587	RPS8A
40S ribosomal protein S9	7/7	7/5	3/2	RPS9	IPI00221088	RPS9A
40S ribosomal protein S10	1/1			RPS10	IPI00008438	RPS10A
40S ribosomal protein S11	1/1	2/2		RPS11	IPI00025091	RPS11A
40S ribosomal protein S13	3/3	6/2		RPS13	IPI00221089	RPS13
40S ribosomal protein S14	2/2	5/3		RPS14	IPI00026271	RPS14A
40S ribosomal protein S15A	1/1			RPS15A	IPI00221091	RPS22A
40S ribosomal protein S16	2/2	3/2		RPS16	IPI00221092	RPS16B
40S ribosomal protein S18	3/3	3/2		RPS18	IPI00013296	RPS18B
40S ribosomal protein S19	5/5	1/1		RPS19	IPI00215780	RPS19A
40S ribosomal protein S25	3/3	3/2	2/1	RPS25	IPI00012750	RPS25A
40S ribosomal protein S23	1/1	2/2		RPS23	IPI00218606	RPS23A
Isoform 1 of 40S ribosomal protein S24	1/1			RPS24	IPI00029750	RPS24A
Ribosomal protein S30 precursor	1/1	2/1		FAU	IPI00973736	RPS30B
60S ribosomal subunit proteins						
60S ribosomal protein L3	7/7	3/2	1/1	RPL3	IPI00550021	RPL3
60S ribosomal protein L4	5/5	4/4		RPL4	IPI00003918	RPL4A
60S ribosomal protein L6	4/4	9/5		RPL6	IPI00790342	RPL6A
60S ribosomal protein L7A	6/6	10/7	4/2	RPL7A	IPI00299573	RPL8B
60S ribosomal protein L8	1/1	3/2		RPL8	IPI00012772	RPL2B
60S ribosomal protein L10A	3/3			RPL10A	IPI00412579	RPL1A
60S ribosomal protein L10-like	1/1			RPL10L	IPI00064765	RPL10
60S ribosomal protein L11 (isoform 1)	2/2	4/3		RPL11	IPI00376798	RPL11B
60S ribosomal protein L12 (isofomr 1)	1/1	5/3		RPL12	IPI00024933	RPL12A
60S ribosomal protein L13	5/5	9/4		RPL13	IPI00465361	RPL13A
60S ribosomal protein L14	3/3	2/2		RPL14	IPI00555744	RPL14A
60S ribosomal protein L15	3/3			RPL15	IPI00470528	YL10
60S ribosomal protein L17	1/1			RPL17	IPI00413324	unknown
60S ribosomal protein L18	2/2	4/3	1/1	RPL18	IPI00215719	RPL18B
60S ribosomal protein L18A	5/5			RPL18A	IPI00026202	RPL20B
60S ribosomal protein L19	2/2	1/1		RPL19	IPI00025329	RPL19B
60S ribosomal protein L21		3/3		RPL21	IPI00247583	RPL21A
60S ribosomal protein L22	2/2	2/2		RPL22	IPI00219153	RPL22A
60S ribosomal protein L23	3/3			RPL23	IPI00010153	RPL23B
60S ribosomal protein L23A	1/1	3/1	2/1	RPL23A	IPI00021266	RPL25
60S ribosomal protein L24	3/3	2/2		RPL24	IPI00306332	RPL24A
60S ribosomal protein L26	4/4	6/4		RPL26	IPI00027270	RPL26A
60S ribosomal protein L27	1/1	2/2		RPL27	IPI00219155	RPL27B
60S ribosomal protein L27A	3/3	7/4	2/1	RPL27A	IPI00456758	RPL28
60S ribosomal protein L28	2/2			RPL28	IPI00182533	unknown
60S ribosomal protein L30	2/2	1/1		RPL30	IPI00219156	RPL30
60S ribosomal protein L31	2/2	4/2	3/2	RPL31	IPI00026302	RPL31A
60S ribosomal protein L35A	1/1			RPL35A	IPI00029731	RPL33B
60S ribosomal protein L36	2/2			RPL36	IPI00216237	RPL36B
60S ribosomal protein L36A-like	1/1			RPL36AL	IPI00056494	RPL42A
60S acidic ribosomal protein P0	1/1			RPLP0	IPI00008530	RPP0
60S acidic ribosomal protein P1	2/2	2/1	3/1	RPLP1	IPI00008527	RPP1A
60S acidic ribosomal protein P2	2/2	1/1	2/1	RPLP2	IPI00008529	RPP2B
Ribosome biogenesis factors						
rRNA methyltransferase 3	30/28	23/8		FTSJ3	IPI00217686	SPB1
Nucleolin	11/11	11/6	10/4	NCL	IPI00604620	NSR1
Nucleophosmin (isoform 2)	7/7	3/1	1/1	NPM1	IPI00220740	Unknown
60S ribosome subunit biogenesis protein NIP7 homolog			32/7	NIP7	IPI00007175	NIP7
DEAD Box helicases						
ATP-dependent RNA helicase DDX5	3/3	2/1		DDX5	IPI00017617	DBP2
Nucleolar RNA helicase 2, isoform 1 (DDX21)	4/3			DDX21	IPI00015953	unknown
ATP-dependent RNA helicase DDX50	2/1			DDX50	IPI00031554	MRH4
DNA repair factors						
X-ray repair cross-complementing protein 5	4/4			XRCC5	IPI00220834	YKU80
X-ray repair cross-complementing protein 6	2/2	1/1		XRCC6	IPI00644712	YKU70
Poly [ADP-ribose] polymerase 1	4/4			PARP1	IPI00449049	unknown
Translation factors						
Eukaryotic translation initiation factor 4B	1/1	4/3	19/8	EIF4B	IPI00012079	TIF3
Methylosome components						
Protein arginine N-methyltransferase 5 (isoform b)	2/2	30/14	46/15	PRMT5	IPI00064328	HSL7
Methylosome protein 50	1/1	5/4	20/8	WDR77	IPI00012202	unknown
Methylosome subunit pICln			2/1	CLNS1A	IPI00004795	unknown

dx.doi.org/10.1021/pr201106n | J. Proteome Res. 2012, 11, 3112–3126

Table 1. continued

RNA-binding proteins						
Heterogeneous nuclear ribonucleoprotein A0	1/1			HNRNPA0	IPI00011913	unknown
Heterogeneous nuclear ribonucleoprotein A1 (isoform A1-B)	4/4			HNRNPA1	IPI00215965	unknown
Heterogeneous nuclear ribonucleoprotein D0 (isoform 1)	5/4			HNRNPD	IPI00028888	unknown
Heterogeneous nuclear ribonucleoprotein F	3/2			HNRNPF	IPI00003881	unknown
Heterogeneous nuclear ribonucleoprotein K (isoform 1)	2/2	3/2		HNRNPK	IPI00216049	unknown
Heterogeneous nuclear ribonucleoprotein M (isoform 1)	1/1			HNRNPM	IPI00171903	GBP2
Heterogeneous nuclear ribonucleoprotein A/B (isoform 1)	3/3	1/1		HNRNPAB	IPI00106509	unknown
Heterogeneous nuclear ribonucleoprotein D-like (isoform 1)	3/3			HNRPDL	IPI00011274	unknown
Isoform 2 of Heterogeneous nuclear ribonucleoprotein Q	4/4			SYNCRIP	IPI00402182	unknown
Heterogeneous nuclear ribonucleoprotein U (short isoform)	8/8	8/4	4/3	HNRNPU	IPI00479217	unknown
Signal recognition particle 14 kDa protein	1/1			SRP14	IPI00293434	unknown
Isoform 1 of Serine/arginine-rich splicing factor 7	2/2			SRSF7	IPI00003377	unknown
Nuclease-sensitive element-binding protein 1		1/1		YBX1	IPI00031812	unknown
Transport proteins						
Insulin-like growth factor 2 mRNA-binding protein 1	1/1	3/2		IGF2BP1	IPI00008557	unknown
THO complex subunit 4	1/1			THOC4	IPI01010794	unknown
Exportin-2 (isoform 1)	1/1			CSE1L	IPI00022744	CSE1
Histones						
Histone H1x	1/1			H1FX	IPI00021924	unknown
Histone H2B type 2-E	2/2			HIST2H2BE	IPI00003935	unknown
Histone H1.2	4/4			HIST1H1C	IPI00217465	unknown
Histone H1.3		16/5	5/3	HIST1H1D	IPI00217466	unknown
Cytoskeleton						
Tubulin alpha-4A chain	1/1			TUBA4A	IPI00007750	TUB1
Actin, cytoplasmic 1	2/2			ACTB	IPI00021439	ACT1
Beta-actin-like protein 2	2/2		10/2	ACTBL2	IPI00003269	unknown
Others						
TBP-associated factor 2N (isoform short)	1/1			TAF15	IPI00020194	unknown
Thyroid hormone receptor-associated protein 3		8/7		TRAP150	IPI00104050	unknown
Heat shock 70 kDa protein 1A/1B	8/8	9/6		HSPA1A/1B	IPI00304925	SSA4
Kinesin-like protein KIF11	1/1	40/25	101/35	KIF11	IPI00305289	KIP1
Enhancer of rudimentary homolog		3/2		ERH	IPI00029631	unknown
Leucine-rich repeat-containing protein 59	4/4			LRRC59	IPI00396321	unknown
Interleukin enhancer-binding factor 2	2/2			ILF2	IPI00005198	unknown
Interleukin enhancer-binding factor 3 (isoform 5)	2/2			ILF3	IPI00219330	unknown
ADP/ATP translocase 2	2/2			SLC25A5	IPI00007188	unknown
ADP/ATP translocase 4	2/2			SLC25A31	IPI00010420	PET9
28S ribosomal protein S34, mitochondrial	1/1			MRPS34	IPI00169413	unknown
Cardiotrophin-like cytokine factor 1	2/1			CLCF1	IPI00294405	unknown

*Number of spectral counts/unique peptides.

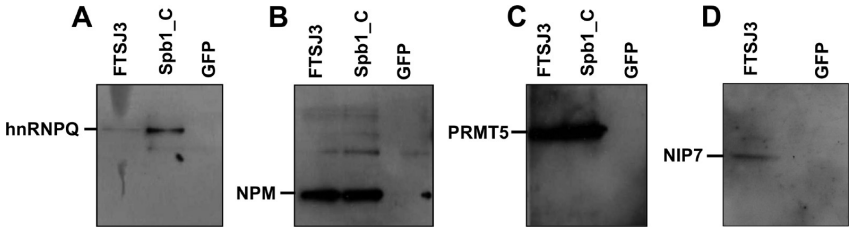

Figure 2. Identification of proteins coimmunoprecipitating with FLAG-FTSJ3 and FLAG-Spb1_C by immunoblotting. FLAG-FTSJ3 and FLAG-Spb1_C and the control protein FLAG-GFP were immunoprecipitated with an antibody for the FLAG epitope. The immunoprecipitates were analyzed by Western blotting using antibodies for hnRNPQ (A), nucleophosmin (B), PRMT5 (C), and NIP7 (D).

the full-length FTSJ3 (Table 1). This is an important finding because it shows that FTSJ3 interaction with preribosome complexes is mediated by the Spb1_C domain. The FLAG-NIP7 pulldown revealed a surprisingly low number of ribosomal proteins and ribosome synthesis factors. Possibly, the FLAG tag may affect its incorporation into the preribosome complexes, or the FLAG tag in this construction is not accessible for interaction with the antibody. Despite the low number of proteins copurifying with FLAG-NIP7, they are consistent with the functional role proposed for this protein. In addition to the 12 ribosomal proteins (four RPS and eight RPL proteins), proteins that were already shown to function in ribosome synthesis were also found in this analysis. They include nucleolin,[36] nucleophosmin (NPM),[26,27,37] and PRMT5.[40] The methylsome components PRMT5 and WDR77 copurified with both the FLAG-FTSJ3, FLAG-Spb1_C complexes. FLAG-NIP7 copurified PRMT5, WDR77, and an additional component, CLNS1A (Table 1). The Ftsj domain implicates FTSJ3 in RNA methylation. Copurification of methylsome components with both FTSJ3 and NIP7 might raise a new working hypothesis as to determine whether these proteins function in association.

Analysis of the Ribosomal Protein Content of Complexes Affinity-Purified with Ribosome Synthesis Factors and RPS19

In an attempt to evaluate the composition and dynamics of human preribosome complexes, we have compared the proteins identified in the FTSJ3 immunoprecipitation with complexes isolated with one ribosomal protein and six ribosome synthesis factors, which have been described in the literature so far (Table 2, Figure 3). For this comparison, the proteins were grouped according to the functional categories used to classify the proteins purified in the FLAG-FTSJ3 assay (Table 2). The names of the functional categories used in this paper have already been described in previous studies.[24,28,29] Despite the

dx.doi.org/10.1021/pr201106n | J. Proteome Res. 2012, 11, 3112–3126

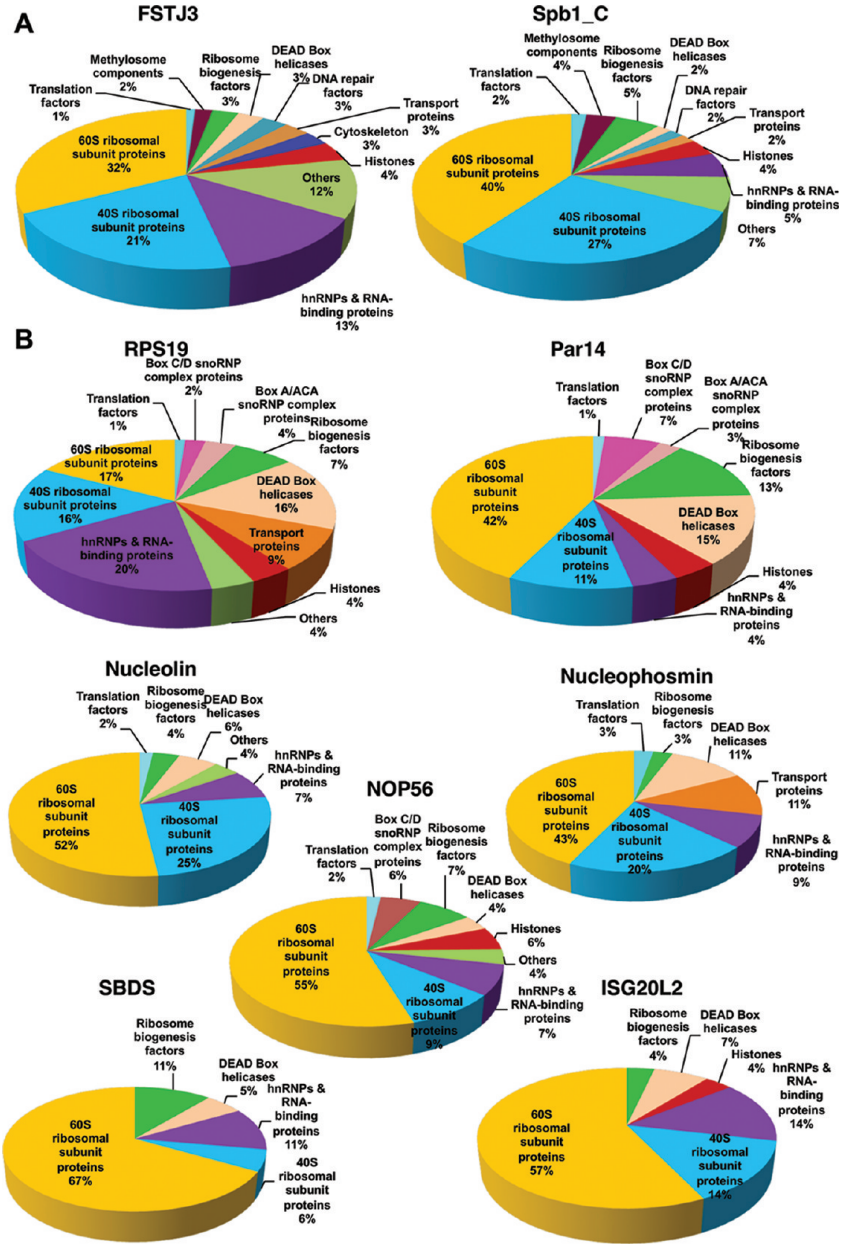

Figure 3. Comparison of the functional classes of the proteins identified by interaction with FLAG-FTSJ3 and FLAG-Spb1_C. (A) Functional categories of the proteins that coimmunoprecipitate with FLAG-FTSJ3 and FLAG-Spb1_C identified in this work as described in the Table 1. (B) Functional categories of the proteins identified by interaction analyses with the ribosomal protein RPS19 and with the ribosome biogenesis factors Nucleolin,[32] Nucleophosmin (NPM),[23,24] Parvulin (Par14),[25] SBDS,[27] NOP56,[26] and ISG20L2,[28] according to the classes described in Table 2.

fact that these experiments were performed under different conditions, the ratio of proteins in each category allows for some important observations on the composition of the complexes that are compatible with the function proposed for each of the proteins used as bait in the pull-down and immunoprecipitation assays.

Ribosomal subunit proteins are the most abundant proteins found in these complexes. Initially, we analyzed the ribosomal protein content to determine whether there was a correlation between the protein composition of each complex and the stage of ribosome synthesis or with the protein localization in the structural domains of mature ribosomes. The first comparison was performed with the FTSJ3 (83 proteins, this study), RPS19[24] (81 proteins), and Par14[28] (75 proteins) assays, since they contain a larger and similar number of total proteins identified. As it can be seen in Table 2, these complexes share different sets of ribosomal proteins. FTSJ3 contains the largest number of ribosomal proteins, comprising 21 small subunit proteins and 33 large subunit proteins. In the RPS19 assay, there are 13 small subunit proteins, while in the in the Par14 assay there are only 8. Conversely, in the RPS19 assay there are only 14 large subunit proteins, whereas in the Par14 assay there are 33. The ribosomal proteins in the FTSJ3 pulldown that are common to the RPS19 and Par14 pulldowns are shown in Figure 4. Regarding the ribosomal protein content, FTSJ3, RPS19, and Par14 are most probably part of different preribosome complexes.

dx.doi.org/10.1021/pr201106n | J. Proteome Res. 2012, 11, 3112–3126

Table 2. Comparison of FTSJ3-interacting Proteins with Components of Proteins Complexes Described for the 40S Subunit Protein RPS19[24] and for the Ribosome Synthesis Factors Parvulin (Par14),[28] Nucleolin,[25] NOP56,[29] NPM,[26,27] SBDS,[30] and ISG20L2[31]

Protein name	FTSJ3	RPS19[21]	Par14[25]	NCL[22]	NOP56[26]	NPM	SBDS[27]	ISG20L2[28]
40S ribosomal subunit proteins								
40S ribosomal protein S2	ok	ok	ok	ok	ok			
40S ribosomal protein S3	ok	ok		ok			ok	
40S ribosomal protein S3A	ok		ok	ok	ok	ok[23,24]		
40S ribosomal protein S4x	ok	ok	ok	ok				
40S ribosomal protein S5	ok	ok				ok[24]		
40S ribosomal protein S6	ok	ok	ok	ok		ok[23,24]		ok
40S ribosomal protein S7	ok	ok		ok		ok[24]		
40S ribosomal protein S8	ok	ok	ok		ok			
40S ribosomal protein S9	ok		ok	ok	ok	ok[23]		ok
40S ribosomal protein S10	ok	ok						
40S ribosomal protein S11	ok		ok			ok[23]		
40S ribosomal protein S13	ok			ok		ok[23]		
40S ribosomal protein S14	ok	ok		ok				
40S ribosomal protein S15A	ok			ok				
40S ribosomal protein S16	ok	ok		ok	ok			
40S ribosomal protein S18	ok			ok				
40S ribosomal protein S19	ok	n/a		ok				
40S ribosomal protein S23	ok	ok						ok
40S ribosomal protein S24	ok	ok						
40S ribosomal protein S25	ok		ok					
40S ribosomal protein S26		ok						ok
Ribosomal protein S30 precursor (FAU)	ok							
60S ribosomal subunit proteins								
60S ribosomal protein L3	ok	ok	ok	ok	ok		ok	
60S ribosomal protein L4	ok	ok	ok	ok	ok	ok[24]	ok	ok
60S ribosomal protein L5			ok	ok	ok		ok	ok
60S ribosomal protein L5B						ok[24]		
60S ribosomal protein L6	ok	ok	ok	ok	ok		ok	ok
60S ribosomal protein L7		ok	ok	ok	ok	ok[23,24]	ok	ok
60S ribosomal protein L7A	ok	ok	ok	ok		ok[23]	ok	ok
60S ribosomal protein L8	ok	ok	ok		ok	ok[23]	ok	ok
60S ribosomal protein L9		ok		ok	ok			
60S ribosomal protein L10			ok	ok	ok			
60S ribosomal protein L10A	ok	ok	ok	ok	ok			ok
60S ribosomal protein L10L	ok							
60S ribosomal protein L11	ok			ok	ok	ok[23]		
60S ribosomal protein L12	ok			ok	ok	ok[23]	ok	
60S ribosomal protein L13	ok		ok	ok	ok	ok[23]	ok	
60S ribosomal protein L13A			ok	ok	ok	ok[24]		
60S ribosomal protein L14	ok	ok	ok	ok	ok		ok	
60S ribosomal protein L15	ok		ok	ok	ok			
60S ribosomal protein L17	ok		ok	ok	ok			
60S ribosomal protein L18	ok		ok	ok	ok	ok[23]	ok	ok
60S ribosomal protein L18A	ok		ok	ok	ok			ok
60S ribosomal protein L19	ok		ok					
60S ribosomal protein L21	ok		ok	ok	ok	ok[23]		ok
60S ribosomal protein L22	ok					ok[24]		ok
60S ribosomal protein L23	ok				ok			
60S ribosomal protein L23A	ok		ok	ok	ok			ok
60S ribosomal protein L24	ok	ok						ok
60S ribosomal protein L26	ok		ok	ok	ok	ok[23]		
60S ribosomal protein L27	ok		ok	ok	ok	ok[24]		ok
60S ribosomal protein L27A	ok	ok	ok	ok	ok			
60S ribosomal protein L28	ok		ok			ok[23]		
60S ribosomal protein L29			ok					
60S ribosomal protein L30	ok		ok	ok	ok			
60S ribosomal protein L31	ok		ok		ok			ok
60S ribosomal protein L32			ok					
60S ribosomal protein L35			ok	ok	ok			
60S ribosomal protein L35A	ok		ok		ok			
60S ribosomal protein L36	ok		ok	ok				
60S ribosomal protein L36A-L	ok							
60S acidic ribosomal protein P0	ok	ok	ok	ok	ok		ok	
60S acidic ribosomal protein P1	ok	ok						
60S acidic ribosomal protein P2	ok	ok	ok					ok

dx.doi.org/10.1021/pr201106n | J. Proteome Res. 2012, 11, 3112–3126

Table 2. continued

Ribosome Biogenesis & Nucleolar Proteins								
Nucleolin	ok	ok	ok	ok	ok		ok	ok
Nucleophosmin	ok		ok	ok	ok	n/a	ok	
rRNA methyltransferase 3 (FTSJ3)	ok	ok	ok					
60S ribosome subunit biogenesis protein NIP7		ok	ok					
Nucleolar protein Nol1		ok	ok					
Nucleolar protein Nol10		ok						
Pescadillo homolog 1, BRCT domain		ok	ok					
Block of proliferation 1 (Bop1)			ok			ok[24]		
WD repeat domain 12 (WDR12)			ok					
BRIX1			ok		ok			
Peter pan (Ssf1 homolog)			ok		ok			
Box C/D snoRNP complex proteins								
Nucleolar protein Nop5/58			ok		ok			
Nucleolar protein Nop5A/56		ok	ok		ok			
Fibrillarin		ok	ok		ok			
NHP2 non-histone chromosome protein 2-like 1			ok		ok			
WD repeats and SOF1 domain containing			ok					
Box A/ACA snoRNP complex proteins								
Nucleolar protein NolA3		ok	ok					
Nucleolar protein NolA1		ok						
dyskeratosis congenita 1, dyskerin homolog		ok	ok					
DEAD Box helicases								
ATP-dependent RNA helicase A DDX1						ok[23,24]		
RNA helicase DDX3X		ok						
ATP-dependent RNA helicase DDX5	ok	ok	ok	ok		ok[24]		
ATP-dependent RNA helicase A DDX9		ok	ok	ok	ok	ok[23,24]		
RNA helicase DDX15		ok	ok					
RNA helicase DDX17		ok						
RNA helicase DDX18		ok	ok					
Nucleolar RNA helicase 2 (DDX21, DDX26, DDX56)	ok	ok	ok	ok	ok	ok[23]	ok	
RNA helicase DDX24		ok	ok					
RNA helicase DDX27			ok					ok
RNA helicase DDX30		ok	ok					
RNA helicase DDX36		ok						
RNA helicase DDX41		ok						
RNA helicase DDX48			ok					
ATP-dependent RNA helicase DDX50	ok	ok	ok					ok
RNA helicase DDX54		ok						
Translation								
Eukaryotic translation initiation factor 4B	ok							
Eukaryotic translation initiation factor 2				ok				
Eukaryotic translation elongation factor 1		ok	ok		ok			
Eukaryotic translation elongation factor 2					ok	ok[24]		
RNA binding proteins								
Heterogeneous nuclear ribonucleoprotein A0	ok							
Heterogeneous nuclear ribonucleoprotein A1	ok	ok		ok	ok	ok[24]		ok
Heterogeneous nuclear ribonucleoprotein A2/B1		ok						ok
Heterogeneous nuclear ribonucleoprotein A3		ok						
Heterogeneous nuclear ribonucleoprotein C		ok						
Heterogeneous nuclear ribonucleoprotein D0	ok							
Heterogeneous nuclear ribonucleoprotein D2		ok						
Heterogeneous nuclear ribonucleoprotein F	ok	ok						
Heterogeneous nuclear ribonucleoprotein G		ok						
Heterogeneous nuclear ribonucleoprotein K	ok							
Heterogeneous nuclear ribonucleoprotein M	ok		ok	ok	ok		ok	
Heterogeneous nuclear ribonucleoprotein N		ok						
Heterogeneous nuclear ribonucleoprotein A/B	ok							
Heterogeneous nuclear ribonucleoprotein D-like	ok							
Heterogeneous nuclear ribonucleoprotein Q	ok	ok		ok				
Heterogeneous nuclear ribonucleoprotein R		ok						
Heterogeneous nuclear ribonucleoprotein U	ok	ok	ok	ok	ok		ok	
Heterogeneous nuclear ribonucleoprotein H2						ok[24]		
Signal recognition particle 14 kDa protein	ok				ok			

dx.doi.org/10.1021/pr201106n | J. Proteome Res. 2012, 11, 3112–3126

Table 2. continued

Splicing factor 3B1		ok						
Splicing factor 3B2		ok						
Splicing factor 3B3		ok						
Serine/arginine-rich splicing factor 1 (ASF/SF2)			ok					ok
Serine/arginine-rich splicing factor 3								ok
Serine/arginine-rich splicing factor 7	ok							
Serine/arginine-rich splicing factor 9		ok						
Serine/arginine-rich splicing factor 10		ok						
Cleavage and polyadenylation specificity factor subunit 6						ok[24]		
Transport factors								
Insulin-like growth factor 2 mRNA-binding protein 1	ok	ok					ok	
Insulin-like growth factor 2 mRNA-binding protein 3		ok						
THO complex subunit 4	ok							
Importin 4		ok						
Importin 7		ok						
Exportin-1 (Crmp1)		ok				ok[24]		
Exportin-2	ok	ok						
Exportin-5		ok						
Nuclear export factor (Epbl)						ok[24]		
Nuclear pore complex protein Nup50						ok[24]		
Nuclear pore glycoprotein p62						ok[24]		
Histones								
Histone H1x (H1FX)	ok				ok			
Histone H1b (HIST1H1B)		ok	ok				ok	
Histone H1.2 (HIST1H1C)	ok	ok	ok				ok	
Histone H1.3 (**HIST1H1D**)	ok	ok			ok			
Histone H2B type 2-E (HIST2H2BE)	ok		ok		ok			ok
Others								
Nuclease-sensitive element-binding protein 1	ok	ok						
Kinesin-like protein KIF11	ok			ok				
Interleukin enhancer-binding factor 2		ok			ok			
Interleukin enhancer-binding factor 3	ok	ok		ok	ok			
Total number of proteins compared	**83**	**81**	**75**	**52**	**54**	**41**	**21**	**28**

The RPS19 complex contains the larger 40S/60S ribosomal protein ratio, which is compatible with its requirement for 40S subunit formation. RNAi-mediated knockdown and naturally occurring mutations in RPS19 impairs 18S rRNA synthesis, formation of 40S subunits, and export of pre-40S particles to the cytoplasm.[44] Orrù and co-workers[24] propose that the identification of ribosomal proteins belonging to the small and the large subunits suggests that the RPS19 complex corresponds to the 90S preribosome described for yeast,[6] which contains the pre-rRNA prior to cleavage of ITS1. However, from the eight protein complexes compared in Table 2, RPS19 is the only structural component of mature ribosomes. This suggests that the 60S subunit proteins copurifying with RPS19 may be better explained by the fact that, together with preribosomes and mature 40S subunits, RPS19 can pulldown also 80S ribosomes. Data from our own group show that FTSJ3 knockdown affects mainly processing of the 18S rRNA precursors.[19] In FTSJ3 complex, the presence of a large number of ribosomal proteins belonging to both subunits indicates that it copurifies complexes that are at an initial stage, containing the pre-RNA before its cleavage in ITS1. Despite the low number of 40S subunit proteins in the Par14 complex, Par14 was reported to cosediment with both pre-40S and pre-60S complexes, and its knockdown reduces the rate of processing of the 47S pre-rRNA equally affecting production of both the 18 and 28S rRNAs.[28]

We analyzed next the ribosomal protein content of the nucleolin and NOP56 assays. From the 52 proteins found in the nucleolin assay,[22] 40 are ribosomal proteins, 13 belonging to the small subunit and 27 to the large subunit. In the case of NOP56, from the 54 proteins identified, 29 are 60S subunit proteins and 5 are small subunit proteins.[29] Most of the ribosomal proteins found in the nucleolin and Par14 are found in the FTSJ3 complex (Figure 4). Nucleolin was reported to act in the initial step of pre-rRNA processing in mouse cells[36] and is a component of the SSU processome in yeast cells.[45] These studies implicate nucleolin in the initial step of 47S cleavage in the 5′ ETS. However, nucleolin has been implicated in a wide variety of cellular processes[46,47] and may play more roles in ribosome biogenesis in addition to the first 47S pre-rRNA cleavage. NOP56 (also named NOP5A) is a protein component of box C/D snoRNPs that contain also fibrillarin, NOP5/NOP58, and nonhistone chromosome protein 2-like 1.[29] Box C/D snoRNPs catalyze methylation of pre-rRNAs and rRNAs and are not expected to bind preferentially to a determined pre-rRNA region. However, the complex isolated by NOP56 affinity-purification is highly enriched with 60S subunit proteins (Table 2). It is unclear why there are fewer 40S proteins in the NOP56 complex since in rRNA pull-down assays both the 40S and 60S rRNAs copurify with NOP56 with similar efficiency.[29]

A relatively small number of proteins was described for ISG20L2[31] (28 proteins, 4 small subunit proteins, and 16 large subunit proteins) and SBDS[30] (21 proteins, one small subunit protein, and 12 large subunit proteins). ISGL20L2 is required for maturation of the 5.8S rRNA,[31] which is consistent with the

dx.doi.org/10.1021/pr201106n | J. Proteome Res. 2012, 11, 3112–3126

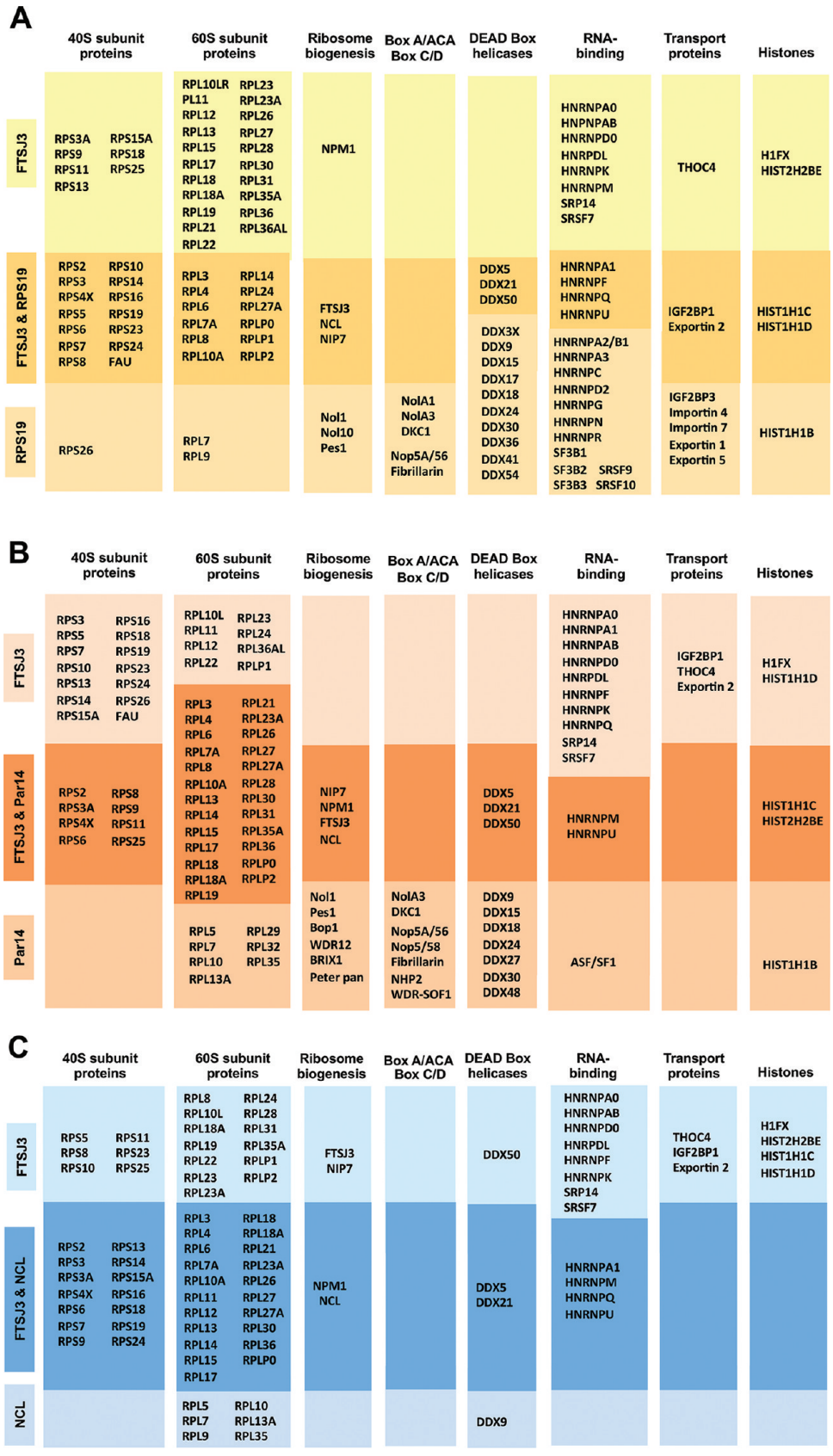

Figure 4. continued

dx.doi.org/10.1021/pr201106n | J. Proteome Res. 2012, 11, 3112–3126

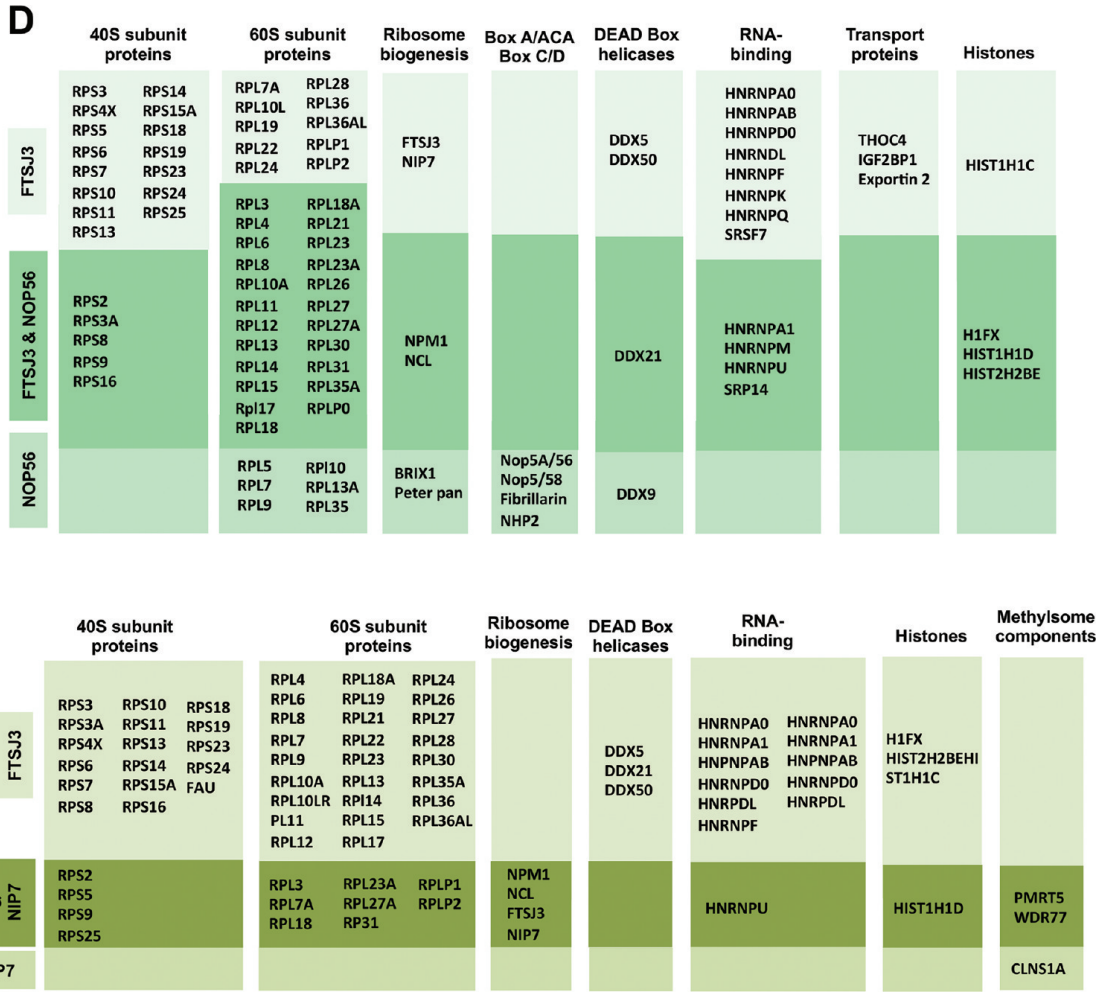

Figure 4. Comparison of the categories of proteins of the FTSJ3 complex with the components of the complexes isolated by affinity-purification of RPS19, Parvulin (Par14), nucleolin (NCL), and NOP56. (A) FTSJ3 × RPS19. (B) FTSJ3 × Par14. (C) FTSJ3 × nucleolin. (D) FTSJ3 × NOP56. (E) FTSJ3 × NIP7.

higher number of 60S ribosomal proteins found in its complex. SBDS and the GTPase elongation factor-like 1 (EFL1) act together to catalyze dissociation of the eukaryotic initiation factor 6 (eIF6) from newly synthesized ribosomes, allowing them to engage in translation.[48] SBDS has also been reported to be required for accurate maturation of 60S subunits and assembly of 80S ribosomes.[49] Therefore, the enrichment of 60S ribosomal proteins in SBDS affinity-purified complexes is consistent with its molecular function in the late steps of synthesis and translation activation of 60S subunits.

Nucloephosmin has been implicated in diverse cellular processes such as ribosome biogenesis, centrosome duplication, protein chaperoning, and transcriptional control. Its implication in ribosome synthesis was initially attributed to its RNase activity[50] showing preferential endoribonucleolytic activity toward the ITS2 region of the pre-rRNA.[51] Subsequent studies have shown that nucleophosmin associates with complexes containing ribosomal proteins and RNA helicases[26] and that it is required for nuclear export of RPL5[37] and ribosome subunits.[27] The fact that NPM mediates nuclear export of 40S and 60S subunits can explain the presence of ribosomal proteins belonging to both subunits in complexes purified by coimmunoprecipitation with nucleophosmin.

Preribosome complexes are best characterized in the yeast *S. cerevisiae* model system. We compared the composition of the complexes isolated with the human ribosome synthesis factors and could not establish a direct correlation with the 90S complex,[6] neither with the pre-40S[7,8] nor 60S[9−11] complexes. Processing of the 47S pre-RNA in mammals takes place by simultaneous pathways, making it difficult to establish the intermediary complexes that are formed during ribosome assembly in mammal cells. The 40S subunit has been described as formed by the structural domains, head, platform, and body. The 60S subunit is divided into central protuberance, L1 stalk, and P stalk. We used the structure of the yeast ribosome[52] as reference to compare with the ribosomal protein content of the complexes described in Table 2. We found that the ribosomal proteins are scattered throughout the three domains of both the 40S and 60S subunits. At least in the complexes studied in this work, ribosomal protein binding to pre-rRNA seems not to follow a sequential order defined by domain architecture of the mature ribosome subunits.

dx.doi.org/10.1021/pr201106n | J. Proteome Res. 2012, 11, 3112−3126

Analysis of the Nonribosomal Proteins Found in Complexes Affinity-Purified with Ribosome Synthesis Factors and RPS19

The RPS19 and Par14 complexes contain a large number of nonribosomal proteins with 22 nonribosomal proteins common to both complexes (Table 2, Figure 3). The set of common nonribosomal proteins includes 10 ribosome synthesis factors and eight DEAD box helicases, respectively, two of which have already been demonstrated to function in ribosome synthesis. The FTSJ3 complex contains a surprisingly low number of characterized ribosome synthesis factors, including nucleolin, nucleophosmin, DDX5, DDX21, and possibly also DDX50. So far, only the RNA helicases DDX5[38] and DDX21[39] have been demonstrated to act on ribosome biogenesis in human cells. These helicases may act on a large number of RNA substrates, and the features that provide substrate specificity are not well established. Nevertheless, their high enrichment in the RPS19 (13 DDX helicases) (Table 2[24]) and Par14 (11 DDX helicases) (Table 2[28]) complexes also suggests that the still uncharacterized DDX helicases may play specific functions in ribosome biogenesis.

In the FTSJ3 assay, the second largest group of proteins includes the heterogeneous nuclear ribonucleoproteins (10 hnRNPs). Eleven hnRNPs proteins are found also in the RPS19 complex (Table 2[24]), although only hnRNPA1, hnRNPF, hnRNPQ, and hnRNPU are common to both complexes (Figure 4). RPS19 contains a large number of both hnRNPs (11) and DEAD box helicases (13), while FTSJ3 contains a large number of hnRNPs (10) and low number of DEAD helicases (3), and Par14 contains a large number of DEAD box helicases (10) and a low number of hnRNPs (2) (Figure 4). These differences in hnRNPs and DEAD box helicases content in the RPS19, FTSJ3, and Par14 pulldown assays most probably represent different preribosome complexes that are formed during ribosome synthesis and is consistent with the analysis made in the previous section based on the ribosome protein content in each complex.

Several hnRNPS are found also in other complexes, especially in the nucleolin and NOP56 with four members each (Table 2). hnRNPA1, hnRNPM, and hnRNPU were the most frequent hnRNPs found in these complexes. So far, only Nop3p, the yeast ortholog of hnRNPU, was shown to be essential for ribosome biogenesis, participating in 60S subunit maturation.[53] hnRNPs display natural ability to bind to RNA and it is not possible to rule out that they may bind to naked regions of the pre-rRNA during preparation of the extracts during isolation of the complexes. However, hnRNPs have already been described as part of the proteomic component of the nucleolus.[41−43] This finding, together with the fact the hnRNPs are highly enriched in the RPS19 and FTSJ3 complexes (Figure 4), suggests that hnRNPs may not be technical contaminants of the preparations. However, despite this evidence, their direct role in pre-rRNA processing and ribosome biogenesis in mammalian cells remains to be proven.

The complexes copurifying with nucleolin, NOP56, nucleophosmin, SBDS, and ISGL20 contain a low number of ribosome synthesis factors. The NOP56 complex contains the four protein components of the box C/D snoRNP, as expected, in addition to BRIX1, Peter Pan, nucleolin, nucleophosmin, DDX5, and DDX21 (Table 2[29]). Interestingly nucleolin and nucleophosmin are the ribosome synthesis factors found in most preribosome complexes described so far, including the FLAG-NIP7 complex (Tables 1 and 2). The SBDS-co-purifying complex contrasts with the late pre-40S complexes. A pull-down analysis of proteins copurifying with hRio2 revealed 40S subunit proteins and the factors hTsr1, hLtv1, hEnp1, hNob1, and hDim2, which are required for late pre-40S ribosome maturation.[54] hRIO2 binds directly to Crmp1/exportin-1 and acts to release of hDim2, hLtv1, and hNob1 from cytoplasmic 40S precursors.[54] Among the nonribosomal proteins, a group of transport factors was found in the FTSJ3, RPS19, and nucleophosmin complexes, while no transport factor was found in the complexes enriched with 60S ribosomal proteins (Table 2).

Another group of proteins that consistently copurified with preribosome complexes involves the histones H1FX, HIST1H1B, HIST1H1C, HIST1H1D, HIST2H2BE. The functional relationship between the ribosome and these proteins is not presently understood. Histones are abundant proteins in nucleolar extracts,[43] and their presence in the pull down assays may result from unspecific binding. However, we cannot rule out completely the possibility that since the initial phase of pre-rRNA synthesis and complex assembly is cotranscriptional, histones may be copurified because they are associated to the initial complexes.

In conclusion, we showed that FTSJ3 can associate to preribosome complexes that contain both 40S and 60S ribosomal proteins in addition to a set of nonribosomal proteins, some of them with a function in ribosome synthesis already described. We provide evidence that a group of hnRNPs associated specifically to the preribosome complexes copurified with FTSJ3. We provide also evidence for a function for the Spb1_C domain in macromolecular interactions. In addition, the comparison of the human preribosome complexes described in the literature provides elements to understand the steps involved in ribosome synthesis in human cells.

■ AUTHOR INFORMATION

Corresponding Author

*Tel.: 55 41 2104-3225. Fax: 55 41 3316-3267. E-mail: nizanchin@fiocruz.br.

Notes

The authors declare no competing financial interest.

■ ACKNOWLEDGMENTS

We thank Armando Moraes Ventura (ICB-USP), who provided the antibodies for NPM and PMRT5. This work was supported by FAPESP (Grant 06/02083-7) and CNPq (Grants 473551/2008-0 and 479779/2010-4) to NITZ. FMS and LGM were recipients of FAPESP fellowships (2007/58371-3, 2003/06299-6, and 2008/57110-4).

■ REFERENCES

(1) Fromont-Racine, M.; Senger, B.; Saveanu, C.; Fasiolo, F. Ribosome assembly in eukaryotes. *Gene* **2003**, *313*, 17−42.

(2) Tschochner, H.; Hurt, E. Pre-ribosomes on the road from the nucleolus to the cytoplasm. *Trends Cell Biol.* **2003**, *13*, 255−263.

(3) Henras, A.; Soudet, K.; Gérus, J. M.; Lebaron, S.; Caizergues-Ferrer, M.; Mougin, A.; Henry, Y. The post-transcriptional steps of eukaryotic ribosome biogenesis. *Cell. Mol. Life Sci.* **2008**, *65*, 2334−2359.

(4) Strunk, B. S.; Karbstein, K. Powering through ribosome assembly. *RNA* **2009**, *15*, 2083−2104.

(5) Kressler, D.; Hurt, E.; Bassler, J. Driving ribosome assembly. *Biochim. Biophys. Acta* **2010**, *1803*, 673−683.

(6) Grandi, P.; Rybin, V.; Bassler, J.; Petfalski, E.; Strauss, D.; et al. 90S pre-ribosomes include the 35S pre-rRNA, the U3 snoRNP, and 40S subunit processing factors but predominantly lack 60S synthesis factors. *Mol. Cell* **2002**, *10*, 105−115.
(7) Schäfer, T.; Strauss, D.; Petfalski, E.; Tollervey, D.; Hurt, E. The path from nucleolar 90S to cytoplasmic 40S pre-ribosomes. *EMBO J.* **2003**, *22*, 1370−1380.
(8) Dragon, F.; Gallagher, J. E.; Compagnone-Post, P. A.; Mitchell, B. M.; Porwancher, K. A.; et al. A large nucleolar U3 ribonucleoprotein required for 18S ribosomal RNA biogenesis. *Nature* **2002**, *417*, 967−970.
(9) Nissan, T. A.; Bassler, J.; Petfalski, E.; Tollervey, D.; Hurt, E. 60S pre-ribosome formation viewed from assembly in the nucleolus until export to the cytoplasm. *EMBO J.* **2002**, *15*, 5539−5547.
(10) Saveanu, C.; Namane, A.; Gleizes, P. E.; Lebreton, A.; Rousselle., J. C.; et al. Sequential protein association with nascent 60S ribosomal particles. *Mol. Cell. Biol.* **2003**, *23*, 4449−4460.
(11) Miles, T. D.; Jakovljevic, J.; Horsey, E. W.; Harnpicharnchai, P.; Tang, L.; Woolford, J. L., Jr. Ytm1, Nop7, and Erb1 form a complex necessary for maturation of yeast 66S preribosomes. *Mol. Cell. Biol.* **2005**, *25*, 10419−10432.
(12) Lebreton, A.; Rousselle, J.-C.; Lenormand, P.; Namane, A.; Jacquier, A.; et al. 60S ribosomal subunit assembly dynamics defined by semi-quantitative mass spectrometry of purified complexes. *Nucleic Acids Res.* **2008**, *36*, 4988−4999.
(13) Mullineux, S. T.; Lafontaine, D. L. Mapping the cleavage sites on mammalian pre-rRNAs: Where do we stand? *Biochimie* **2012**, DOI: j.biochi.2012.02.001.
(14) Chen, W.; Bucaria, J.; Band, D. A.; Sutton, A.; Sternglanz, R. Enp1, a yeast protein associated with U3 and U14 snoRNAs, is required for pre-rRNA processing and 40S subunit synthesis. *Nucleic Acids Res.* **2003**, *31*, 690−699.
(15) Carron, C.; O'Donohue, M. F.; Choesmel, V.; Faubladier, M.; Gleizes, P. E. Analysis of two human pre-ribosomal factors, bystin and hTsr1, highlights differences in evolution of ribosome biogenesis between yeast and mammals. *Nucleic Acids Res.* **2011**, *39*, 280−291.
(16) Léger-Silvestre, I.; Milkereit, P.; Ferreira-Cerca, S.; Saveanu, C.; Rousselle, J. C.; et al. The ribosomal protein Rps15p is required for nuclear exit of the 40S subunit precursors in yeast. *EMBO J.* **2004**, *23*, 2336−2347.
(17) Zanchin, N. I. T.; Roberts, P.; de Silva, A.; Sherman, F.; Goldfarb, D. S. *Saccharomyces cerevisiae* Nip7p is required for efficient 60S ribosome subunit biogenesis. *Mol. Cell. Biol.* **1997**, *17*, 5001−5015.
(18) Morello, L. G.; Hesling, C.; Coltri, P. P.; Castilho, B. A.; Rimokh, R.; Zanchin, N. I. T. The NIP7 protein is required for accurate pre-rRNA processing in human cells. *Nucleic Acids Res.* **2011**, *39*, 648−665.
(19) Morello, L. G.; Coltri, P. P.; Quaresma, A. J.; Simabuco, F. M.; Silva, T. C.; et al. The human nucleolar protein FTSJ3 associates with NIP7 and functions in pre-rRNA processing. *PLoS One* **2011**, *6*, e29174.
(20) Kressler, D.; Rojo, M.; Linder, P.; Cruz, J. Spb1p is a putative methyltransferase required for 60S ribosomal subunit biogenesis in *Saccharomyces cerevisiae*. *Nucleic Acids Res.* **1999**, *27*, 4598−4608.
(21) Bonnerot, C.; Pintard, L.; Lutfalla, G. Functional redundancy of Spb1p and a snR52-dependent mechanism for the 2′-O-ribose methylation of a conserved rRNA position in yeast. *Mol. Cell* **2003**, *12*, 1309−1315.
(22) Lapeyre, B.; Purushothaman, S. K. Spb1p-directed formation of Gm2922 in the ribosome catalytic center occurs at a late processing stage. *Mol. Cell* **2004**, *16*, 663−669.
(23) Freed, E. F.; Bleichert, F.; Dutca, L. M.; Baserga, S. J. When ribosomes go bad: diseases of ribosome biogenesis. *Mol. Biosyst.* **2010**, *6*, 481−493.
(24) Orrù, S.; Aspesi, A.; Armiraglio, M.; Caterino, M.; Loreni, F.; Ruoppolo, M.; Santoro, C.; Dianzani, I. Analysis of the ribosomal protein S19 interactome. *Mol. Cell. Proteomics* **2007**, *6*, 382−393.
(25) Yanagida, M; Shimamoto, A; Nishikawa, K; Furuichi, Y; Isobe, T; Takahashi, N. Isolation and proteomic characterization of the major proteins of the nucleolin-binding ribonucleoprotein complexes. *Proteomics* **2001**, *1*, 1390−1404.
(26) Lindström, M. S.; Zhang, Y. Ribosomal protein S9 is a novel B23/NPM-binding protein required for normal cell proliferation. *J. Biol. Chem.* **2008**, *283*, 15568−15576.
(27) Maggi, L. B., Jr; Kuchenruether, M.; Dadey, D. Y.; Schwope, R. M.; Grisendi, S.; et al. Nucleophosmin serves as a rate-limiting nuclear export chaperone for the Mammalian ribosome. *Mol. Cell. Biol.* **2008**, *28*, 7050−7065.
(28) Fujiyama-Nakamura, S.; Yoshikawa, H.; Homma, K.; Hayano, T.; Tsujimura-Takahashi, T.; et al. Parvulin (Par14), a peptidyl-prolyl cis-trans isomerase, is a novel rRNA processing factor that evolved in the metazoan lineage. *Mol. Cell. Proteomics* **2009**, *8*, 1552−1565.
(29) Hayano, T.; Yanagida, M.; Yamauchi, Y.; Shinkawa, T.; Isobe., T.; Takahashi, N. Proteomic analysis of human Nop56p-associated pre-ribosomal ribonucleoprotein complexes. Possible link between Nop56p and the nucleolar protein treacle responsible for Treacher Collins syndrome. *J. Biol. Chem.* **2003**, *278*, 34309−34319.
(30) Ball, H. L.; Zhang, B.; Riches, J. J.; Gandhi, R.; Li, J.; Rommens, J. M.; Myers, J. S. Shwachman-Bodian Diamond syndrome is a multi-functional protein implicated in cellular stress responses. *Hum. Mol. Genet.* **2009**, *18*, 3684−3695.
(31) Couté, Y.; Kindbeiter, K.; Belin, S.; Dieckmann, R.; Duret, L.; Bezin, L.; Sanchez, J. C.; Diaz, J. J. ISG20L2, a novel vertebrate nucleolar exoribonuclease involved in ribosome biogenesis. *Mol. Cell. Proteomics.* **2008**, *7*, 546−559.
(32) Takahashi, N.; Yanagida, M.; Fujiyama, S.; Hayano, T.; Isobe, T. Proteomic snapshot analyses of preribosomal ribonucleoprotein complexes formed at various stages of ribosome biogenesis in yeast and mammalian cells. *Mass Spectrom. Rev.* **2003**, *22*, 287−317.
(33) Paes Leme, A. F.; Sherman, N. E.; Smalley, D. M.; Sizukusa, L. O.; Oliveira, A. K.; et al. Hemorrhagic activity of HF3, a snake venom metalloproteinase: insights from the proteomic analysis of mouse skin and blood plasma. *J. Proteome Res.* **2011**, *11*, 279−291.
(34) Fink, A. L. Natively unfolded proteins. *Curr. Opin. Struct. Biol.* **2005**, *15*, 35−41.
(35) Wright, P. E.; Dyson, H. J. Intrinsically unstructured proteins: re-assessing the protein structure-function paradigm. *J. Mol. Biol.* **1999**, *293*, 321−331.
(36) Ginisty, H.; Amalric, F.; Bouvet, P. Nucleolin functions in the first step of ribosomal RNA processing. *EMBO J.* **1998**, *17*, 1476−1486.
(37) Yu, Y.; Maggi, L. B., Jr; Brady, S. N.; Apicelli, A. J.; Dai, M. S.; Lu, H.; Weber, J. D. Nucleophosmin is essential for ribosomal protein L5 nuclear export. *Mol. Cell. Biol.* **2006**, *26*, 3798−809.
(38) Jalal, C.; Uhlmann-Schiffler, H.; Stahl, H. Redundant role of DEAD box proteins p68 (Ddx5) and p72/p82 (Ddx17) in ribosome biogenesis and cell proliferation. *Nucleic Acids Res.* **2007**, *35*, 3590−3601.
(39) Henning, D.; So, R. B.; Jin, R.; Lau, L. F.; Valdez, B. C. Silencing of RNA helicase II/Gualphainhibits mammalian ribosomal RNA production. *J. Biol. Chem.* **2003**, *278*, 52307−52314.
(40) Ren, J.; Wang, Y.; Liang, Y.; Zhang, Y.; Bao, S.; Xu, Z. Methylation of ribosomal protein S10 by protein-arginine methyl-transferase 5 regulates ribosome biogenesis. *J. Biol. Chem.* **2010**, *285*, 12695−12705.
(41) Ahmad, Y.; Boisvert, F. M.; Gregor, P.; Cobley, A.; Lamond, A. I. NOPdb: Nucleolar Proteome Database—2008 update. *Nucleic Acids Res.* **2009**, D181−D184.
(42) Lam, Y. W.; Evans, V. C.; Heesom, K. J.; Lamond, A. I.; Matthews, D. A. Proteomics analysis of the nucleolus in adenovirus-infected cells. *Mol. Cell. Proteomics* **2010**, *9*, 117−130.
(43) Jarboui, M. A.; Wynne, K.; Elia, G.; Hall, W. W.; Gautier, V. W. Proteomic profiling of the human T-cell nucleolus. *Mol. Immunol.* **2011**, *49*, 441−452.

(44) Choesmel, V.; Bacqueville, D.; Rouquette, J.; Noaillac-Depeyre, J.; Fribourg, S.; et al. Impaired ribosome biogenesis in Diamond–Blackfan anemia. *Blood* **2007**, *109*, 1275–1283.
(45) Turner, A. J.; Knox, A. A.; Prieto, J. L.; McStay, B.; Watkins, N. J. A novel small-subunit processome assembly intermediate that contains the U3 snoRNP, nucleolin, RRP5, and DBP4. *Mol. Cell. Biol.* **2009**, *29*, 3007–3017.
(46) Tuteja, R.; Tuteja, N. Nucleolin: a multifunctional major nucleolar phosphoprotein. *Crit. Rev. Biochem. Mol. Biol.* **1998**, *33*, 407–436.
(47) Mongelard, F.; Bouvet, P. Nucleolin: a multiFACeTed protein. *Trends Cell Biol.* **2007**, *17*, 80–86.
(48) Finch, A. J.; Hilcenko, C.; Basse, N.; Drynan, L. F.; Goyenechea, B.; et al. Uncoupling of GTP hydrolysis from eIF6 release on the ribosome causes Shwachman–Diamond syndrome. *Genes Dev.* **2011**, *25*, 917–929.
(49) Wong, C. C.; Traynor, D.; Basse, N.; Kay, R. R.; Warren, A. J. Defective ribosome assembly in Shwachman–Diamond syndrome. *Blood* **2011**, *118*, 4305–4312.
(50) Herrera, J. E.; Savkur, R.; Olson, M. O. The ribonuclease activity of nucleolar protein B23. *Nucleic Acids Res.* **1995**, *23*, 3974–3979.
(51) Savkur, R. S.; Olson, M. O. Preferential cleavage in pre-ribosomal RNA by protein B23 endoribonuclease. *Nucleic Acids Res.* **1998**, *26*, 4508–4515.
(52) Ben-Shem, A.; Garreau de Loubresse, N.; Melnikov, S.; Jenner, L.; Yusupova, G; Yusupov, M. The structure of the eukaryotic ribosome at 3.0 Å resolution. *Science* **2011**, *334*, 1524–1529.
(53) Russell, I. D.; Tollervey, D. NOP3 is an essential yeast protein which is required for pre-rRNA processing. *J. Cell Biol.* **1992**, *119*, 737–747.
(54) Zemp, I.; Wild, T.; O'Donohue, M. F.; Wandrey, F.; Widmann, B.; et al. Distinct cytoplasmic maturation steps of 40S ribosomal subunit precursors require hRio2. *J. Cell. Biol.* **2009**, *185*, 1167–1180.

dx.doi.org/10.1021/pr201106n | *J. Proteome Res.* 2012, 11, 3112–3126

4. DISCUSSÃO

4.1. Mecanismo de interação e co-localização de NIP7 e FTSJ3

A interação de NIP7 humana com outras proteínas é consistente com sua função na biogênese de ribossomos. Primeiramente, foi demonstrado que NIP7 humana tem localização nucleolar e que interage com Nop132 (Sekiguchi *et al.,* 2004), provável ortóloga de Nop8p (Zanchin & Goldfarb, 1999a). Testes utilizando o sistema de duplo-híbrido em levedura e ensaios de imunoprecipitação detectaram a associação entre NIP7 e SBDS, indicando que ambas as proteínas poderiam ser componentes de um mesmo complexo (Hesling *et al.,* 2007). Subsequentemente, NIP7 foi encontrada em associação com complexos contendo a proteína RPS19 (Orrù *et al.,* 2007), proteína ribossomal que desempenha função essencial na biogênese da subunidade ribossomal 40S em células humanas (Choesmel & Bacqueville, 2007). NIP7 também foi encontrada em associação com complexos contendo a proteína parvulina (Par14), uma peptidil-prolil *cis-trans* isomerase (PPIase) envolvida no processamento do pré-rRNA (Fujiyama-Nakamura *et al.,* 2009). Estas observações são consistentes com nossos resultados, mostrando que NIP7 é restrita à fração nuclear (Figura 8C – artigo I) e que sedimenta com complexos de massa molecular compatíveis com partículas pré-ribossomais, na faixa de 40-80S (Figura 8 – artigo I).

Os dados experimentais de localização subcelular e análises de interação apoiam a relação funcional entre FTSJ3 e NIP7 (Figuras 1, 2 e 3 – artigo II). FTSJ3 e NIP7 endógenas, bem como as proteínas fusionadas mRFP-FTSJ3 e EGFP-NIP7 apresentaram localização nucleolar (Figura 3A e B – artigo II). Além disso, experimentos de FRAP (*Fluorescence Recovery After Photobleaching*), mostraram que a depleção de FTSJ3 afeta a taxa de difusão de EGFP-NIP7 no nucléolo (Figura 5 – artigo II). Nós também demonstramos que o domínio Spb1_C é responsável pela localização nucle(ol)ar da FTSJ3 (Figura 3D – artigo II). Experimentos iniciais de duplo-híbrido (Figura 1A e B – artigo II) e de *pull-*

down da proteína recombinante GST-FTSJ3 (dado não mostrado) indicaram que FTSJ3 e NIP7 poderiam interagir de forma direta. Entretanto, ensaios utilizando proteínas recombinantes expressas em bactérias (Figura 1C – artigo II), bem como imunoprecipitação de FLAG-FTSJ3 a partir de extratos de células HEK293 (Figura 2C e D – artigo II) revelaram que a interação FTSJ3-NIP7 é dependente de RNA, desde que a incubação com RNase, em ambos os casos, aboliu esta interação.

NIP7 apresenta um domínio conservado na região C-terminal (PUA – *P*seudo-*U*ridine synthases and *A*rchaeosine-specific transglycosylases) que promove a interação com RNA (Coltri *et al.,* 2007). O domínio PUA é conservado na NIP7 humana e é provavelmente responsável pela atividade de ligação de NIP7 a moléculas de RNA (Figura 9 – artigo I). A predição estrutural de FTSJ3 indica que a proteína é majoritariamente desestruturada, com exceção do provável domínio de RNA-metil-transferase FtsJ (resíduos 22-202). Análises de predição feitas com diferentes algoritmos não revelaram motivos de ligação à RNA em FTSJ3, de forma que a base para a ligação de FTSJ3 ao RNA permanece uma questão aberta. Sabe-se que regiões desestruturada tem alta flexibilidade e fornecem ampla interface de interação, permitindo a elas que acomodem uma variedade de diferentes parceiros de ligação (Fink, 2005). Neste contexto, a região desestruturada truncada de FTSJ3 (resíduos 433-847), incluindo o domínio conservado Spb1_C, porém de função não conhecida, mostrou-se suficiente para suportar a interação FTSJ3-NIP7 (Figura 1A e B – artigo II). Portanto, os resultados sugerem que essa região predita desestruturada em FTSJ3 seja compatível com a interação com NIP7 mediada por uma molécula de RNA atuando como um terceiro componente (Figura 4.1).

4.2. Função de NIP7 e FTSJ3 no processamento de pre-rRNA e síntese de ribossomos

Nip7p é uma proteína essencial em levedura, onde já foi demonstrada sua

participação no processamento do pré-rRNA, principalmente na clivagem do precursor 27S e consequentemente, na formação da subunidade ribossomal 60S (Zanchin *et al.,* 1997). Análises *in silico* revelaram que o gene *NIP7* é conservado ao longo da evolução, com ortólogos preditos desde Archaea a eucariotos superiores. Neste contexto, a hipótese inicial do trabalho sugeriria que NIP7 humana participasse da formação da subunidade ribossomal 60S. Então, nós depletamos NIP7 em células humanas por meio da técnica de interferência de RNA (Figura 2A, B, C e D – artigo I) objetivando a busca de fenótipos associados à perda de função do gene.

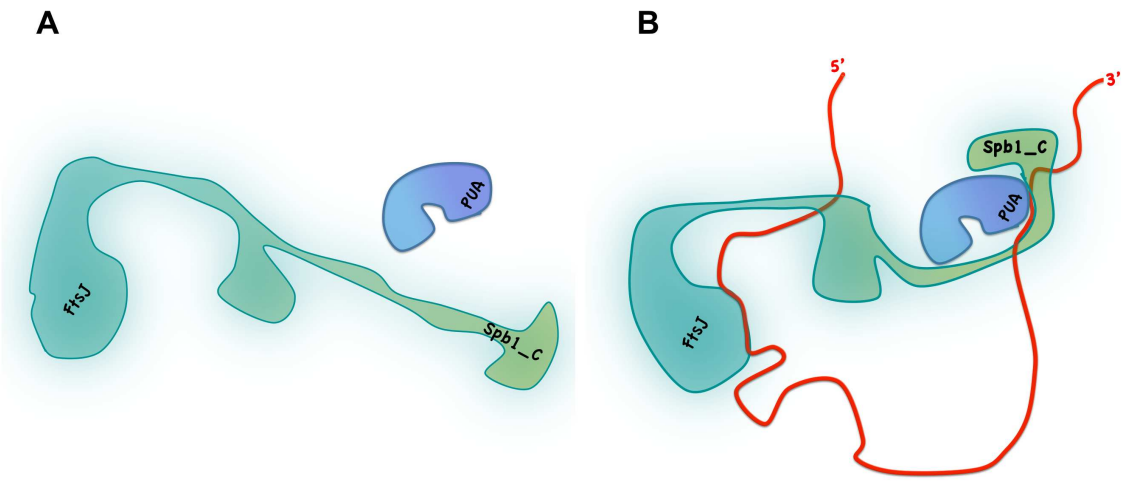

Figura 4.1: Modelo proposto de interação entre FTSJ3 e NIP7 mediado por RNA. A) Modelo proposto para as proteínas livres. **B**) modelo proposto para as proteínas em associação. Neste modelo, a região desestruturada de FTSJ3 adquiriria uma organização para acomodar a parceira de interação NIP7, na presença de uma molécula de RNA. A molécula de RNA, eventualmente, interagiria com o provável domínio de RNA-metil-transferase FtsJ. O modelo propõe uma interação entre NIP7, a partir do seu domínio PUA, e FTSJ3, a partir da sua região desestruturada C-terminal, incluindo o domínio Spb1_C. O modelo de interação NIP7-FTSJ3 tem como base os resultados de interação de NIP7 com RNA e de interação entre NIP7 e FTSJ3 apresentados neste trabalho. A proteína FTSJ3 está representada em tons de verde e seus domínios, FtsJ e Spb1_C, indicados na própria figura. NIP7 está representada em tons de azul com seu domínio PUA indicado. O RNA está representado em vermelho. As proteínas estão representadas com tamanho proporcional, relativo uma à outra. FTSJ3 está representada de acordo com predição estrutural realizada com a plataforma I-TASSER (Roy *et al.,* 2010).

Em nível de processamento do pré-rRNA, a depleção de NIP7 em células humanas afeta principalmente os precursores relacionados à via de maturação do rRNA 18S, diminuindo os níveis do pré-rRNA 34S e aumentando os níveis dos pré-rRNAs 26S e 21S (Figura 4 e 6 – artigo I) (Figura 4.2). Esse desequilíbrio nas concentrações dos pré-rRNAs é causado pelo desacoplamento das clivagens nos sítios A0 e 1 e atraso no processamento do sítio 2 em células deficientes em NIP7 (Figura 7 – artigo I). Parte dos defeitos no processamento do pré-rRNA causados pela depleção de NIP7 já foram descritos previamente em situações onde a biogênese de ribossomos foi perturbada (Rouquette *et al.,* 2005).

Células deficientes em FTSJ3 também revelaram a necessidade da proteína na via de maturação do rRNA 18S (Figuras 6 e 7 – artigo II), a mesma via que exige a atuação de NIP7 (artigo I). Entretanto, os resultados obtidos sugerem que FTSJ3 atue em passos distintos daqueles observados para NIP7.

O acúmulo do pré-rRNA 21S em células deficientes em NIP7 (Figuras 4 e 6 – artigo I) é evidência da maturação atrasada da extremidade 3' do rRNA 18S. Em mamíferos, as clivagens dos sítios A0 e 1, na região 5'ETS são acopladas e defeitos que desacoplem estas clivagens levam ao aumento nos níveis do pré-rRNA 26S, caso observado em células deficientes em NIP7 (Figura 4B, C e E – artigo I). Células depletadas para FTSJ3, por outro lado, acumulam o pré-rRNA 34S, resultante de processamento lento dos sítios A0 e 1 e mais lento ainda no sitio 2 (Figuras 6 e 7 – artigo II) (Figura 4.2). Esses resultados indicam que FTSJ3 atua em passos anteriores à função de NIP7 no processamento do pré-rRNA. Recentemente, O'Donohue e colaboradores (2010) descreveram dois grupos funcionais de proteínas ribossomais componentes da subunidade ribossomal 40S. Um grupo chamado RPS-iniciação, necessário para os passos iniciais do processamento do pré-rRNA, e outro grupo, chamado RPS-progressão, necessário em passos tardios na formação do rRNA 18S. Depleção individual de componentes do grupo RPS-iniciação leva ao acúmulo acentuado do pré-rRNA 34S, resultante da inibição das clivagens nos sítios A0 e 1 na região 5'ETS e sítio 2, na região ITS1. Por outro lado, depleção de membros do

grupo RPS-progressão causa acúmulo do pré-rRNA 26S, 21S e 18S-E (O'Donohue *et al.,* 2010). Uma comparação destes fenótipos com aqueles observados em nossos experimentos utilizando células deficientes em FTSJ3 e NIP7 sugerem que FTSJ3 participe do estágio RPS-iniciação ao passo que NIP7 atuaria durante os estágios de RPS-progressão.

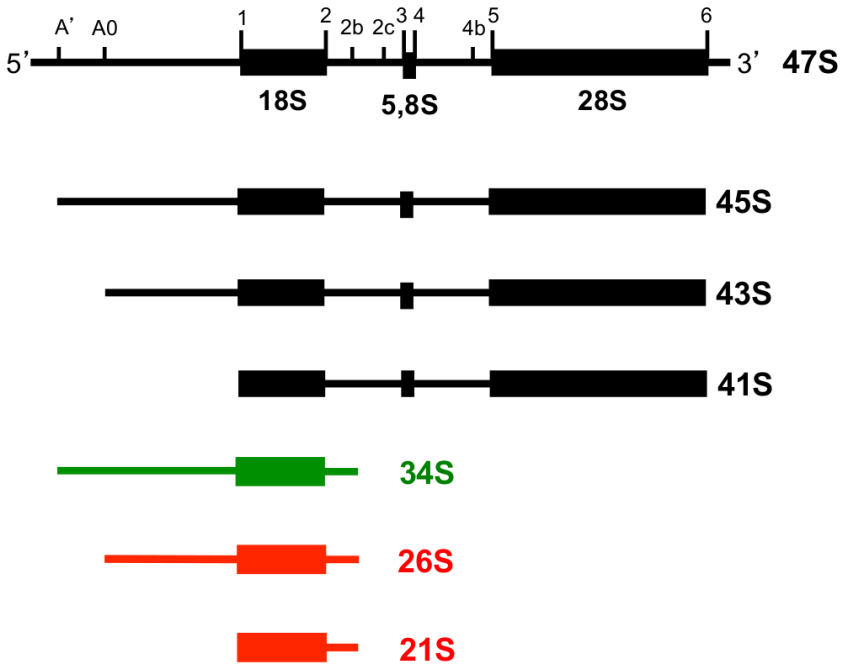

Figura 4.2: Estrutura do pré-rRNA 47S mostrando os principais sítios de clivagens e destacando os intermediários na via de maturação do rRNA 18S. Em verde está destacado o pré-34S, acumulado em células deficientes em FTSJ3 e diminuído em células deficientes em NIP7. Em vermelho estão destacados os intermediários 26S e 21S, ambos acumulados em células deficientes em NIP7.

4.3. Diferenças funcionais entre NIP7 e FTSJ3 e suas respectivas ortólogas de levedura Nip7p e Spb1p

Os resultados obtidos no presente trabalho indicam que a NIP7 humana é necessária primariamente para o processamento correto de pré-rRNAs intermediários associados à via de síntese do rRNA 18S e consequentemente, à formação da subunidade ribossomal 40S. Levando-se em consideração que a

depleção condicional de Nip7p em levedura afeta o processamento do pré-rRNA 27S e a formação da subunidade ribossomal 60S (Zanchin *et al.,* 1997), nós avaliamos a capacidade de NIP7 humana em complementar a deficiência de Nip7p em levedura (*Δnip7*). Esta análise revelou que a proteína NIP7 humana não apresenta capacidade para complementar levedura deficiente em Nip7p (Figura suplementar 1 – artigo I). Apesar das discrepâncias entre as funções propostas para NIP7 em levedura e células humanas, ambas apresentam capacidade de se ligar em sequências de RNA ricas em U (poli-U) *in vitro* (Figura 9 – artigo I, (Coltri *et al.,* 2007)), embora NIP7 humana tenha mostrado maior afinidade por sequências poli-AU (Figura 9 – artigo I). A sequência-alvo de RNA endógeno para NIP7 ainda não foi identificada, porém sua afinidade por poli-U e poli-AU sugere que NIP7 poderia interagir com sequências do pré-rRNA ricas em uridina, similarmente à Rrp5p, a qual foi descrita interagindo com sequências ricas em uridina na região ITS1 do pré-rRNA em *S. cerevisiae* (de Boer *et al.,* 2006). Embora os resultados apresentados mostrem a participação de NIP7 humana na biogênese de ribossomos, a função de Nip7p em levedura não é completamente conservada em células humanas.

Frente à divergência de funções encontrada para a proteína NIP7 em levedura e células humanas e visto que NIP7 humana não complementa levedura deficiente em Nip7p, nós nos indagamos se NIP7 humana e Nip7p de levedura associam-se com os mesmos parceiros de interação. Esta hipótese foi inicialmente testada em sistema de duplo-híbrido em levedura, o qual já foi amplamente empregado em estudos de interação protéica, utilizando-se NIP7 humana como isca. FTSJ3 foi isolada como um dos parceiros de interação mais frequente para NIP7 (Figura 1B – artigo II). O resultado é intrigante, pois FTSJ3 é a provável ortóloga da proteína Spb1p de *S. cerevisiae*, a qual foi previamente associada à formação da subunidade ribossomal 60S (Kressler *et al.,* 1999). Entretanto, a caracterização proteômica de complexos pré-ribossomais em células humanas (Orrù *et al.,* 2007; Fujiyama-Nakamura *et al.,* 2009), juntamente com evidências experimentais apresentadas neste trabalho (artigos I e II), são consistentes com a atuação de NIP7 e FTSJ3 na biogênese da subunidade

ribossomal 40S em células humanas. Isto contrasta com a função das proteínas Nip7p e Spb1p em levedura, as quais estão envolvidas principalmente na formação da subunidade ribossomal 60S (Zanchin *et al.,* 1997; Kressler *et al.,* 1999).

Este trabalho gerou uma questão intrigante a respeito da homologia de função entre as proteínas Spb1p de *S. cerevisiae* e FTSJ3 humana, visto que FTSJ3 apresenta 33% de identidade e 52% de similaridade com Spb1p. A depleção de Spb1p causa decréscimo nos níveis dos pré-rRNAs 27SA2 e 20S, surgimento de um intermediário aberrante, o pré-rRNA 23S e acúmulo do precursor primário 35S (Kressler *et al.,* 1999). Além disso, a deficiência em Spb1p leva ao surgimento de *halfmers* nos polissomos e decréscimo nos níveis da subunidade ribossomal 60S (Kressler *et al.,* 1999). A análise de metilação revelou que a depleção de Spb1p não afeta os níveis de metilação global dos rRNAs (Kressler *et al.,* 1999), porém Spb1p catalisa a metilação sítio-específica do nucleotídeo Gm_{2922} do rRNA 25S, localizado no centro catalítico do ribossomo (Bonnerot *et al.,* 2003; Lapeyre & Purushothaman, 2004).

Diferenças em passos específicos do processamento do pré-rRNA em *S. cerevisiae* e humanos pode ser mais comum do que inicialmente pensado. Um estudo recente mostrou que, em células humanas, a depleção condicional de bystin e hTsr1, ortólogos das proteínas Enp1 e Tsr1 em *S. cerevisiae*, leva a defeitos no processamento do pré-rRNA e na exportação da subunidade ribossomal 40S distintos daqueles relatados em levedura (Gelperin *et al.,* 2001; Chen *et al.,* 2003; Léger-Silvestre *et al.,* 2004; Carron *et al.,* 2011). Nossas observações a respeito da função de FTSJ3 e NIP7 na maturação do rRNA 18S adiciona estas proteínas na lista crescente de diferenças no processamento do pré-rRNA em levedura e humanos. Este trabalho, além de fornecer novas informações sobre o mecanismo de biogênese de ribossomos em células humanas, ele também propõe que a biogênese de ribossomos não seja tão conservada entre levedura e mamíferos como pensado anteriormente, principalmente no que diz respeito ao processamento do pré-rRNA.

4.4. Consequências da deficiência em NIP7 e FTSJ3 para a proliferação celular

Inicialmente, foi detectado que a depleção de NIP7 em células humanas inibe a proliferação celular (Figura 2E e F – artigo I) causando bloqueio do ciclo celular em fase G1 (Tabela 2 – artigo I). Em seguida, foi demonstrado que NIP7 participa da biogênese de ribossomos em células humanas, onde a deficiência em NIP7 prejudica a formação da subunidade ribossomal 40S (Figura 3 – artigo I). Dessa forma, a deficiência em NIP7 poderia ativar p53 via resposta ao estresse nucleolar (RP-HDM2-p53) (Pestov *et al.,* 2001). No entanto, a ativação/estabilização de p53 não foi testada nos ensaios de depleção da NIP7.

A depleção de FTSJ3 em células humanas também afeta negativamente a proliferação celular, sugerindo que FTSJ3 desempenhe importante função celular (Figura 8A e B – artigo II). Porém, a inibição de cerca de 50% na taxa de proliferação celular em células deficientes em FTSJ3 (Figura 8A e D – artigo II) não é totalmente explicada pelo nível do bloqueio do ciclo celular em fase G1 e/ou intensidade da ativação/estabilização de p53 (Figura 8C e E – artigo II). Portanto, essa redução na taxa de proliferação celular tem influência adicional de sinalização celular ao estresse, provavelmente derivada do processamento defectivo do pré-rRNA na ausência de FTSJ3.

A proteína p53 é um supressor tumoral envolvido em diversas vias de sinalização celular. Interessantemente, na última década foi demonstrado que a integridade do processo de síntese de ribossomos em mamíferos é monitorada pela via de resposta RP-HDM2-p53 (Pestov *et al.,* 2001). Neste caso, o estresse nucleolar proveniente da perturbação da síntese de ribossomos causa um desequilíbrio na estequeometria dos componentes de ambas as subunidades ribossomais, de forma que as proteínas ribossomais (RP) livres, ou seja, não incorporadas às subunidades ribossomais, possam então interagir com HDM2, inibindo sua atividade, o que resultaria na estabilização de p53.

Atualmente, não se sabe ao certo o porquê do envolvimento de diferentes proteínas ribossomais na regulação da resposta ao estresse nucleolar via

HDM2-p53. Uma hipótese é que diferentes proteínas poderiam exercer um efeito sinérgico na ativação de p53 (Horn & Vousden, 2008) e a outra hipótese é de que existam respostas estresse-específicas dependente de proteínas ribossomais específicas para monitorar o estresse ribossomal.

4.5. Complexos pré-ribossomais associados a FTSJ3 e NIP7

Em levedura, Nip7p participa da formação da subunidade ribossomal 60S (Zanchin *et al.,* 1997) e já foi descrita em associação com partículas pré-ribossomais 60S (Takahashi *et al.,* 2003; Horsey *et al.,* 2004; Miles *et al.,* 2005; Lebreton *et al.,* 2008a). Similarmente, foi demonstrado que Spb1p é necessária para a formação da subunidade ribossomal 60S (Kressler *et al.,* 1999) e que associa-se com partículas pré-ribossomais 60S (Nissan *et al.,* 2002; Takahashi *et al.,* 2003; Lebreton *et al.,* 2008a). Até o momento, não há relatos de Nip7p e Spb1p em complexos pré-ribossomais 40S (Dragon *et al.,* 2002; Schäfer *et al.,* 2003; Takahashi *et al.,* 2003). Por outro lado, os resultados apresentados neste trabalho indicam que NIP7 e FTSJ3 participem da síntese da subunidade ribossomal 40S em células humanas.

Consistente com nossas observações, NIP7 e FTSJ3 foram encontradas em complexos purificados a partir da proteína RPS19, um componente integral da subunidade ribossomal 40S (Orrù *et al.,* 2007). Além disso, foi demonstrado que a depleção de NIP7 e FTSJ3 causa acúmulo de RPS2-YFP no núcleo, uma proteína repórter para a síntese da subunidade ribossomal 40S, ao passo que RPL29-GFP, proteína repórter para a formação da subunidade ribossomal 60S, permanece praticamente inalterada nessas condições (Wild *et al.,* 2010). NIP7 e FTSJ3 também foram encontradas em associação com complexos contendo parvulina (Par14) e nucleolina (NCL) (Fujiyama *et al.,* 2002; Takahashi *et al.,* 2003; Fujiyama-Nakamura *et al.,* 2009). Nestes casos, a associação com uma subunidade ribossomal em particular é menos clara. Par14 está presente em ambos os complexos ribossomais pré-40S e pré-60S (Fujiyama-Nakamura *et al.,*

2009), ao passo que NCL atua na primeira clivagem do pré-rRNA (Ginisty *et al.,* 1998). A presença de ambas as proteínas, NIP7 e FTSJ3, em complexos purificados a partir de componentes ribossomais ou fatores envolvidos na biogênese de ribossomos, suporta a associação funcional entre essas proteínas, sugerindo que em algum momento durante a biogênese de ribossomos, ambas se juntam em complexos pré-ribossomais antes da separação das partículas pré-40S e pré-60S.

O fato de que três vias de processamento do pré-rRNA ocorrem simultaneamente em células humanas sugere que a dinâmica de formação de complexos pré-ribossomais durante a síntese de ribossomos em mamíferos seja diferente daqueles observados em *S. cerevisiae*. Dessa forma, a caracterização proteômica de complexos purificados por afinidade contendo as proteínas FTSJ3 e NIP7 pode fornecer informações sobre o mecanismo de síntese de ribossomos em células humanas. Neste contexto, para ampliar o conjunto de informações sobre o mecanismo funcional destas proteínas, complexos contendo as proteínas recombinantes FLAG-NIP7 e FLAG-FTSJ3, bem como o domínio FLAG-Spb1_C, foram purificados por afinidade e caracterizados de acordo com seus conteúdos protéicos (artigo III)..

Ensaios de imunoprecipitação de complexos contendo a proteína recombinante FLAG-FTSJ3 co-precipitaram um total de 98 proteínas (Tabela 1 – artigo III). Das 98 proteínas co-purificadas, 54 (55%) representam proteínas ribossomais, sendo 21 componentes da subunidade ribossomal 40S e 33 componentes da subunidade ribossomal 60S (Tabela 1 – artigo III), o que representa 65.5% e 86.8% do total de proteínas nestas subunidades, respectivamente. As 44 proteínas não-ribossomais encontradas nos complexos compreendem fatores envolvidos na biogênese de ribossomos, componentes de complexos ribonucleoprotéicos nucleares heterogêneos (hnRNPS), proteínas que podem atuar indiretamente na síntese de ribossomos e poucas proteínas que não puderam ser funcionalmente conectadas à síntese de ribossomos (Tabela 1 – artigo III). Dentre os fatores envolvidos na síntese de ribossomos já descritos, estão as proteínas nucleolina (Ginisty *et al.,* 1998), nucleofosmina (Yu

et al., 2006; Lindström & Zhang, 2008; Maggi *et al.,* 2008), PRMT5 (Ren *et al.,* 2010) e as RNA helicases DDX5 (Jalal *et al.,* 2007) e DDX21 (Henning *et al.,* 2003). Notavelmente, 10 componentes de hnRNPs foram identificados em complexos com FLAG-FTSJ3. Um número equivalente de hnRNPs associados com complexos pré-ribossomais foi descrito para complexos contendo a proteína RPS19 (Orrù *et al.,* 2007). A presença de hnRNPs nestes complexos é intrigante, embora 15 deles tenham sido encontrados no nucléolo (Ahmad *et al.,* 2009; Lam *et al.,* 2010; Jarboui *et al.,* 2011), indicando que esta classe de proteínas possa ser componente regular do compartimento nucleolar.

Embora um número menor de proteínas tenha sido identificado em complexos contendo o domínio FLAG-Spb1_C, estas pertencem às mesmas classes funcionais daquelas co-purificadas com FLAG-FTSJ3 (Tabela 1 – artigo III). Complexos contendo FLAG-NIP7 apresentaram um número ainda menor de proteínas ribossomais e fatores associados à síntese de ribossomos (Tabela 1 – artigo III). Provavelmente, o peptídeo FLAG afeta a incorporação de FLAG-NIP7 nos complexos pré-ribossomais, ou, nesta construção, o FLAG pode não ser acessível para interação com anticorpo anti-FLAG. Apesar do baixo número de proteínas co-purificadas com FLAG-NIP7, elas são consistentes com a atuação na síntese de ribossomos proposta para esta proteína. Além de 12 proteínas ribossomais, componentes de ambas as subunidades 40S e 60S, foram também identificados fatores envolvidos na síntese de ribossomos. Estes incluem a nucleolina (Ginisty *et al.,* 1998), nucleofosmina (Yu *et al.,* 2006; Lindström & Zhang, 2008; Maggi *et al.,* 2008) e PRMT5 (Ren *et al.,* 2010).

Componentes do metilossomo, PRMT5 e WDR77, foram co-purificados em complexos com ambas as proteínas FLAG-FTSJ3 e FLAG-Spb1_C. Além de PRMT5 e WDR77, complexos contendo FLAG-NIP7 co-purificaram CLNS1A, um outro componente do metilossomo. A co-purificação de componentes do metilossomo com FTSJ3 e NIP7 gera a hipótese de que estas proteínas podem funcionar em associação.

Na tentativa de avaliar a composição e a dinâmica de complexos pré-ribossomais em células humanas, nós comparamos as proteínas identificadas

em complexos contendo FTSJ3 com complexos descritos na literatura, purificados a partir de proteína ribossomal (RPS19) e a partir de fatores envolvidos na síntese de ribossomos (nucleolina, nucleofosmina, Par14, NOP56, SBDS e ISG20L2) (Tabela 2 e Figura 3 – artigo III). Para esta comparação, as proteínas foram organizadas de acordo com as categorias funcionais usadas para classificar as proteínas identificadas no complexo contendo FLAG-FTSJ3 (Tabela 1 – artigo III). O número de proteínas utilizadas nesta análise foram: 83 para o ensaio com FTSJ3 (obtidas neste estudo); 81 para o ensaio com RPS19 (Orrù *et al.,* 2007); 75 para Par14 (Fujiyama-Nakamura *et al.,* 2009); 54 para NOP56 (Hayano *et al.,* 2003); 52 para nucleolina (Yanagida *et al.,* 2001); 41 para nucleofosmina (Lindström & Zhang, 2008; Maggi *et al.,* 2008); 28 para ISG20L2 (Couté *et al.,* 2008) e 21 para SBDS (Ball *et al.,* 2009). Embora os experimentos tenham sido executados em diferentes condições e um número diferente de proteínas tenham sido identificadas, a razão de proteínas em cada categoria permite algumas observações importantes sobre a composição dos complexos, o que é compatível com a função proposta para cada proteína utilizada como alvo nos ensaios de purificação.

Considerando-se o conteúdo de proteínas ribossomais, o complexo contendo RPS19 apresenta uma maior razão 40S/60S, o que é compatível com sua participação na formação da subunidade ribossomal 40S. Depleção de RPS19 e mutações naturais que ocorrem neste gene afetam a síntese do rRNA 18S, a formação da subunidade ribossomal 40S e a exportação da partícula ribossomal pré-40S para o citoplasma (Choesmel & Bacqueville, 2007). (Orrù *et al.,* 2007) e colaboradores propuseram que a identificação de proteínas ribossomais pertencentes às subunidades ribossomais maior e menor sugerem que o complexo contendo RPS19 corresponde à partícula pré-ribossomal 90S, descrita para levedura, a qual contém o pré-rRNA antes de ser clivado na região ITS1. Dos oito complexos comparados na Tabela 2 – artigo III, RPS19 é a única componente integral do ribossomo. Portanto, as proteínas co-purificadas com RPS19 pertencentes à subunidade ribossomal 60S podem ser explicadas pelo fato de que RPS19, além de pré-partículas ribossomais e da subunidade

ribossomal 40S, ela poderia co-precipitar o ribossomo 80S, contendo ambas as subunidades ribossomais 40S e 60S.

Entre todos os complexos analisados com relação ao conteúdo de proteínas ribossomais, o complexo contendo FTSJ3 é o mais similar ao complexo contendo RPS19 (Figura 3 – artigo III). A presença de um grande número de proteínas ribossomais pertencentes a ambas às subunidades ribossomais indica que FTSJ3 co-purifica complexos pré-ribossomais em estágio inicial de formação, contendo o pré-rRNA antes de ser clivado na região ITS1. Ainda, complexos para RPS19 e para FTSJ3 contém grande número de hnRNPs, 13 e 10, respectivamente (Tabela 2 e Figura 4A – artigo III, (Orrù *et al.,* 2007)). Vários hnRNPs também são encontrados em outros complexos, principalmente com nucleolina e NOP56 (4 hnRNPs em cada complexo) (Tabela 2 e Figura 4C e D – artigo III, (Yanagida *et al.,* 2001; Hayano *et al.,* 2003). Até o momento, apenas Nop3p, ortóloga de hnRNPU em levedura, mostrou-se essencial para a síntese de ribossomos, participando na formação da subunidade ribossomal 60S (Russell & Tollervey, 1992). hnRNPs apresentam habilidade natural de se ligar em RNAs, portanto, não se pode excluir a hipótese de que eles possam se ligar no pré-rRNA durante a preparação dos extratos e purificação dos complexos. Entretanto, hnRNPs já foram descritos como componentes do proteoma nucleolar (Ahmad *et al.,* 2009; Lam *et al.,* 2010; Jarboui *et al.,* 2011). Essas observações, associadas ao fato de que hnRNPs são altamente enriquecidos, de maneira específica, em complexos contendo RPS19 e FTSJ3, sugerem que hnRNPs podem não ser contaminantes das preparações. Porém, apesar das evidências, a atuação direta de hnRNPs no processamento do pré-rRNA e biogênese de ribossomos em mamíferos ainda permanece por ser provada.

Dentro do grupo das RNA helicases, até o momento, apenas as RNA helicases DDX5 e DDX21 foram descritas como fatores envolvidos na biogênese de ribossomos em células humanas (Henning *et al.,* 2003; Jalal *et al.,* 2007). Estas helicases podem atuar em uma ampla gama de substratos de RNA e o mecanismo que especifica o substrato ainda não foi bem estabelecido. Apesar

disso, o enriquecimento dessas proteínas apenas em complexos contendo RPS19 (13 helicases DDX) (Tabela 2 e Figura4A – artigo III, (Orrù *et al.,* 2007)) e Par14 (11 helicases DDX) (Tabela 2 e Figura 4B – artigo III, (Fujiyama-Nakamura *et al.,* 2009)) também sugere que helicases DDX ainda não caracterizadas podem apresentar funções específicas na biogênese de ribossomos.

A nucleolina foi descrita como componente do processomo SSU em levedura (Turner *et al.,* 2009) e como fator envolvido nas clivagens iniciais do pré-rRNA em células de camundongo (Ginisty *et al.,* 1998). Considerando-se o envolvimento da nucleolina nos passos iniciais da clivagem do pré-rRNA 47S, na região 5'ETS, não está claro o porquê de complexos contendo nucleolina apresentarem alta quantidade de proteínas componentes da subunidade ribossomal 60S. Entretanto, a nucleolina já foi associada a diversos processos celulares (Tuteja & Tuteja, 1998; Mongelard & Bouvet, 2007) e pode ser que ela atue em outros passos na biogênese de ribossomos e não só na primeira clivagem do pré-rRNA 47S. A nucleofosmina também é associada a diversos processos celulares como biogênese de ribossomos, duplicação do centrossomo, enovelamento de proteínas e controle transcricional. Sua atuação na síntese de ribossomos foi inicialmente atribuída à sua atividade de RNase (Herrera *et al.,* 1995) mostrando atividade endorribonucleolítica preferencial na região ITS2 do pré-rRNA (Savkur & Olson, 1998). Subsequentemente, estudos mostraram que a nucleofosmina associa-se com complexos contendo proteínas ribossomais e RNA helicases (Lindström & Zhang, 2008) e que é necessária para a exportação nuclear da RPL5 (Yu *et al.,* 2006) e subunidades ribossomais (Maggi *et al.,* 2008). O fato de que nucleofosmina participa da exportação nuclear das subunidades ribossomais 40S e 60S pode explicar a presença de proteínas ribossomais pertencentes a ambas as subunidades em complexos purificados por afinidade à nucleofosmina. Interessantemente, nucleolina e nucleofosmina são proteínas não-ribossomais envolvidas na biogênese de ribossomos encontradas na maioria dos complexos pré-ribossomais descritos, incluindo complexos contendo FLAG-FTSJ3 e FLAG-NIP7 (Tabela 1 – artigo III).

A maioria das proteínas identificadas em complexos contendo ISG20L2 foram também encontradas em complexos contendo Par14 (Tabela 2 – artigo III), indicando que essas duas proteínas podem agir nos mesmos passos da biogênese de ribossomos. Entretanto, Par14 co-sedimenta com ambos os complexos ribossomais pré-40S e pré-60S e a depleção de Par14 reduz a taxa de processamento do pré-rRNA 47S, afetando igualmente a produção de ambos os rRNAs 18S e 28S (Fujiyama-Nakamura *et al.,* 2009). ISG20L2, por outro lado, é necessária para a maturação do rRNA 5,8S (Couté *et al.,* 2008), o que é consistente com a alta quantidade de proteínas ribossomais da subunidade 60S encontradas em seus complexos.

NOP56 é uma proteína componente de snoRNPs *box C/D*, os quais contém ainda fibrilarina, NOP5/NOP58 e NHP2 (Hayano *et al.,* 2003). snoRNPs *box C/D* catalisam reações de metilação em rRNAs, não sendo esperado ligação preferencial em uma região específica do pré-rRNA. No entanto, complexos isolados por afinidade contendo NOP56 são altamente enriquecidos com proteínas ribossomais da subunidade 60S (Tabela 2 – artigo III, (Hayano *et al.,* 2003)). Não está claro o porquê de ter menos proteínas da subunidade ribossomal 40S em complexos contendo NOP56, uma vez que experimentos de *pull-down* de rRNA co-purificam rRNAs de ambas as subunidades ribossomais com eficiência similar, juntamente com NOP56 (Hayano *et al.,* 2003).

SBDS e a GTPase EFL1 atuam juntas na dissociação do fator de iniciação da tradução 6 (eIF6) dos novos ribossomos sintetizados, permitindo que eles sejam engajados na tradução (Finch *et al.,* 2011). SBDS também já foi descrita como envolvida na formação da subunidade ribossomal 60S e associação das subunidades ribossomais na formação do ribossomo funcional 80S (Wong *et al.,* 2011). Dessa forma, o enriquecimento de proteínas ribossomais da subunidade 60S em complexos contendo SBDS é consistente com sua função molecular na síntese da subunidade ribossomal 60S e ativação da tradução. Complexos co-purificados com SBDS contrastam com complexos pré-40S tardios, como aqueles contendo hRio2. Análises de complexos contendo hRio2 revelaram proteínas ribossomais da subunidade 40S e os fatores hTsr1, hLtv1, hEnp1,

hNob1 e hDim2, os quais são necessários na maturação tardia da pré-partícula ribossomal 40S (Zemp *et al.,* 2009). hRio2 liga-se diretamente a Crmp1/exportin-1 e atua na liberação dos fatores hDim2, hLtv1 e hNob1 das partículas pré-ribossomais 40S no citoplasma (Zemp *et al.,* 2009). Entre as proteínas não ribossomais, um conjunto de proteínas envolvidas com o transporte foi identificado em complexos isolados a partir da FTSJ3, da RPS19 e da nucleofosmina, ao passo que nenhuma proteína associada a transporte foi identificada em complexos enriquecidos com proteínas da subunidade ribossomal 60S (Tabela 2 – artigo III).

Um outro grupo de proteínas co-purificadas de maneira consistente com complexos pré-ribossomais compreende as histonas H1FX, HIST1H1B, HIST1H1C, HIST1H1D, HIST2H2BE (Tabela 2 – artigo III). A relação funcional entre ribossomos e estas proteínas não está estabelecida. Histonas são abundantes em extratos nucleolares (Jarboui *et al.,* 2011) e sua presença em complexos pré-ribossomais purificados pode ser resultado de interações inespecíficas. Entretanto, não podemos descartar completamente a possibilidade de que histonas possam interagir com complexos pré-ribossomais iniciais, visto que a montagem dos complexos iniciais ocorre de forma co-transcricional à síntese do pré-rRNA.

5. CONCLUSÕES

Em geral, os resultados apresentados neste trabalho comprovam a relação funcional entre FTSJ3 e NIP7 no processamento do pré-rRNA 47S em células humanas. Os fenótipos observados em células deficientes em FTSJ3 e NIP7 indicam que essas proteínas são necessárias, principalmente, na via de maturação do rRNA 18S e consequentemente, na formação da subunidade ribossomal 40S. Ainda, a associação de FTSJ3 e NIP7 com complexos contendo proteínas ribossomais e fatores não-ribossomais envolvidos na biogênese de ribossomos corroboram o envolvimento das proteínas na síntese de ribossomos em células humanas.

Especificamente, pode-se concluir que:

- Depleção de NIP7 inibe a proliferação celular, causando bloqueio na transição do ciclo celular (G0/G1 → S);
- NIP7 está envolvida na formação da subunidade ribossomal 40S;
- NIP7 participa da maturação do rRNA 18S, afetando o processamento do pré-rRNA nas regiões 5'ETS e ITS1;
- NIP7 é restrita ao compartimento nuclear e associa-se com complexos de massa molecular compatíveis com complexos pré-ribossomais;
- NIP7 liga-se a RNA, preferencialmente em sequências ricas em AU;
- NIP7 humana não tem capacidade de complementar levedura deficiente em Nip7p.
- A associação entre FTSJ3 e NIP7 é dependente de RNA;
- FTSJ3 co-sedimenta com NIP7 em fracionamento em gradiente de sacarose;
- FTSJ3 é restrita ao compartimento nuclear e co-localiza com NIP7 no nucléolo em células humanas;
- O domínio Spb1_C é responsável pela localização nucle(ol)ar de FTSJ3;
- FTSJ3 afeta a difusão de NIP7 no nucléolo, onde, na ausência de FTSJ3, NIP7 torna-se mais dinâmica;

• FTSJ3 participa da maturação do rRNA 18S, afetando as clivagens iniciais na região 5'ETS do pré-rRNA;

• Depleção de FTSJ3 inibe a proliferação celular;

• FTSJ3 e NIP7 associam-se com complexos pré-ribossomais contendo proteínas das subunidades ribossomais 40S e 60S e também fatores envolvidos na biogênese de ribossomos;

• A interação de FTSJ3 com complexos pré-ribossomais é provavelmente mediada pelo domínio Spb1_C;

• hnRNPs são co-purificados de maneira específica com complexos contendo FTSJ3.

6. REFERÊNCIAS BIBLIOGRÁFICAS

Adachi, K., Soeta-Saneyoshi, C., Sagara, H., and Iwakura, Y. (2007). Crucial Role of Bysl in Mammalian Preimplantation Development as an Integral Factor for 40S Ribosome Biogenesis. Molecular and Cellular Biology *27*, 2202–2214.

Ahmad, Y., Boisvert, F.M., Gregor, P., Cobley, A., and Lamond, A.I. (2009). NOPdb: Nucleolar Proteome Database--2008 update. Nucleic Acids Res. *37*, D181–D184.

Allmang, C., Kufel, J., Chanfreau, G., Mitchell, P., Petfalski, E., and Tollervey, D. (1999a). Functions of the exosome in rRNA, snoRNA and snRNA synthesis. The EMBO Journal *18*, 5399–5410.

Allmang, C., Mitchell, P., Petfalski, E., and Tollervey, D. (2000). Degradation of ribosomal RNA precursors by the exosome. Nucleic Acids Res. *28*, 1684–1691.

Allmang, C., Petfalski, E., Podtelejnikov, A., Mann, M., Tollervey, D., and Mitchell, P. (1999b). The yeast exosome and human PM-Scl are related complexes of 3“ --> 5” exonucleases. Genes & Development *13*, 2148–2158.

Ansel, K.M., Pastor, W.A., Rath, N., Lapan, A.D., Glasmacher, E., Wolf, C., Smith, L.C., Papadopoulou, N., Lamperti, E.D., Tahiliani, M., et al. (2008). Mouse Eri1 interacts with the ribosome and catalyzes 5.8S rRNA processing. Nat Struct Mol Biol *15*, 523–530.

Armistead, J., Khatkar, S., Meyer, B., Mark, B.L., Patel, N., Coghlan, G., Lamont, R.E., Liu, S., Wiechert, J., Cattini, P.A., et al. (2009). Mutation of a Gene Essential for Ribosome Biogenesis, EMG1, Causes Bowen-Conradi Syndrome. The American Journal of Human Genetics *84*, 728–739.

Ashcroft, M., Taya, Y., and Vousden, K.H. (2000). Stress signals utilize multiple pathways to stabilize p53. Molecular and Cellular Biology *20*, 3224–3233.

Bachellerie, J.-P., Cavaille, J., and Hüttenhofer, A. (2002). The expanding snoRNA world. Biochimie *84*, 775–790.

Balakin, A.G., Smith, L., and Fournier, M.J. (1996). The RNA world of the nucleolus: two major families of small RNAs defined by different box elements with related functions. Cell *86*, 823–834.

Ball, H.L., Zhang, B., Riches, J.J., Gandhi, R., Li, J., Rommens, J.M., and Myers, J.S. (2009). Shwachman-Bodian Diamond syndrome is a multi-functional protein implicated in cellular stress responses. Human Molecular Genetics *18*, 3684–3695.

Ban, N., Nissen, P., Hansen, J., Moore, P.B., and Steitz, T.A. (2000). The

complete atomic structure of the large ribosomal subunit at 2.4 Å resolution. Science *289*, 905.

Bartelt-Kirbach, B., Wuepping, M., Dodrimont-Lattke, M., and Kaufmann, D. (2009). Expression analysis of genes lying in the NF1 microdeletion interval points to four candidate modifiers for neurofibroma formation. Neurogenetics *10*, 79–85.

Ben-Shem, A., Jenner, L., Yusupova, G., and Yusupov, M. (2010). Crystal Structure of the Eukaryotic Ribosome. Science *330*, 1203–1209.

Bhat, K.P., Itahana, K., Jin, A., and Zhang, Y. (2004). Essential role of ribosomal protein L11 in mediating growth inhibition-induced p53 activation. The EMBO Journal *23*, 2402–2412.

Bonnerot, C., Pintard, L., and Lutfalla, G. (2003). Functional redundancy of Spb1p and a snR52-dependent mechanism for the 2'-O-ribose methylation of a conserved rRNA position in yeast. Molecular Cell *12*, 1309–1315.

Boultwood, J., Fidler, C., Strickson, A.J., Watkins, F., Gama, S., Kearney, L., Tosi, S., Kasprzyk, A., Cheng, J.-F., Jaju, R.J., et al. (2002). Narrowing and genomic annotation of the commonly deleted region of the 5q- syndrome. Blood *99*, 4638–4641.

Bowman, L.H., Rabin, B., and Schlessinger, D. (1981). Multiple ribosomal RNA cleavage pathways in mammalian cells. Nucleic Acids Res. *9*, 4951–4966.

Briggs, M.W., Burkard, K.T., and Butler, J.S. (1998). Rrp6p, the yeast homologue of the human PM-Scl 100-kDa autoantigen, is essential for efficient 5.8 S rRNA 3' end formation. J. Biol. Chem. *273*, 13255–13263.

Brown, J.W.S., Echeverria, M., and Qu, L.H. (2003). Plant snoRNAs: functional evolution and new modes of gene expression. Trends Plant Sci. *8*, 42–49.

Carron, C., O'Donohue, M.F., Choesmel, V., Faubladier, M., and Gleizes, P.E. (2011). Analysis of two human pre-ribosomal factors, bystin and hTsr1, highlights differences in evolution of ribosome biogenesis between yeast and mammals. Nucleic Acids Res. *39*, 280–291.

Castle, C.D., Cassimere, E.K., Lee, J., and Denicourt, C. (2010). Las1L Is a Nucleolar Protein Required for Cell Proliferation and Ribosome Biogenesis. Molecular and Cellular Biology *30*, 4404–4414.

Cavaille, J., Nicoloso, M., and Bachellerie, J.-P. Targeted ribose methylation of RNA in vivo directed by tailored antisense RNA guides. Nature *383*, 732–735.

Chen, D., Zhang, Z., Li, M., Wang, W., Li, Y., Rayburn, E.R., Hill, D.L., Wang, H., and Zhang, R. (2007). Ribosomal protein S7 as a novel modulator of p53-MDM2

interaction: binding to MDM2, stabilization of p53 protein, and activation of p53 function. Oncogene *26*, 5029–5037.

Chen, W., Bucaria, J., Band, D.A., Sutton, A., and Sternglanz, R. (2003). Enp1, a yeast protein associated with U3 and U14 snoRNAs, is required for pre-rRNA processing and 40S subunit synthesis. Nucleic Acids Res. *31*, 690–699.

Choesmel, V., and Bacqueville, D. (2007). Impaired ribosome biogenesis in Diamond-Blackfan anemia. ….

Cmejla, R., Cmejlova, J., Handrkova, H., Petrak, J., and Pospisilova, D. (2007). Ribosomal protein S17 gene (RPS17) is mutated in Diamond-Blackfan anemia. Hum. Mutat. *28*, 1178–1182.

Coltri, P.P., Guimarães, B.G., Granato, D.C., Luz, J.S., Teixeira, E.C., Oliveira, C.C., and Zanchin, N.I.T. (2007). Structural insights into the interaction of the Nip7 PUA domain with polyuridine RNA. Biochemistry *46*, 14177–14187.

Couté, Y., Kindbeiter, K., Belin, S., Dieckmann, R., Duret, L., Bezin, L., Sanchez, J.-C., and Diaz, J.-J. (2008). ISG20L2, a novel vertebrate nucleolar exoribonuclease involved in ribosome biogenesis. Mol. Cell Proteomics *7*, 546–559.

Crick, F. (1970). Central dogma of molecular biology. Nature *227*, 561–563.

Dai, M.-S., and Lu, H. (2004). Inhibition of MDM2-mediated p53 ubiquitination and degradation by ribosomal protein L5. J. Biol. Chem. *279*, 44475–44482.

Dai, M.-S., Zeng, S.X., Jin, Y., Sun, X.-X., David, L., and Lu, H. (2004). Ribosomal protein L23 activates p53 by inhibiting MDM2 function in response to ribosomal perturbation but not to translation inhibition. Molecular and Cellular Biology *24*, 7654–7668.

Dai, M.S., Sun, X.X., and Lu, H. (2008). Aberrant Expression of Nucleostemin Activates p53 and Induces Cell Cycle Arrest via Inhibition of MDM2. Molecular and Cellular Biology *28*, 4365–4376.

de Boer, P., Vos, H.R., Faber, A.W., Vos, J.C., and Raué, H.A. (2006). Rrp5p, a trans-acting factor in yeast ribosome biogenesis, is an RNA-binding protein with a pronounced preference for U-rich sequences. Rna *12*, 263–271.

Decatur, W.A., and Fournier, M.J. (2002). rRNA modifications and ribosome function. Trends in Biochemical Sciences *27*, 344–351.

Dennis, P.P., Omer, A., and Lowe, T. (2001). A guided tour: small RNA function in Archaea. Mol Microbiol *40*, 509–519.

Donati, G., Brighenti, E., Vici, M., Mazzini, G., Treré, D., Montanaro, L., and

Derenzini, M. (2011). Selective inhibition of rRNA transcription downregulates E2F-1: a new p53-independent mechanism linking cell growth to cell proliferation. Journal of Cell Science *124*, 3017–3028.

Dragon, F., Gallagher, J.E.G., Compagnone-Post, P.A., Mitchell, B.M., Porwancher, K.A., Wehner, K.A., Wormsley, S., Settlage, R.E., Shabanowitz, J., Osheim, Y., et al. (2002). A large nucleolar U3 ribonucleoprotein required for 18S ribosomal RNA biogenesis. Nature *417*, 967–970.

Draptchinskaia, N., Gustavsson, P., Andersson, B., Pettersson, M., Willig, T.N., Dianzani, I., Ball, S., Tchernia, G., Klar, J., Matsson, H., et al. (1999). The gene encoding ribosomal protein S19 is mutated in Diamond-Blackfan anaemia. Nat. Genet. *21*, 169–175.

Ebert, B.L., Pretz, J., Bosco, J., Chang, C.Y., Tamayo, P., Galili, N., Raza, A., Root, D.E., Attar, E., Ellis, S.R., et al. (2008). Identification of RPS14 as a 5q- syndrome gene by RNA interference screen. Nature *451*, 335–339.

el-Deiry, W.S. (1998). Regulation of p53 downstream genes. Semin. Cancer Biol. *8*, 345–357.

Elela, S.A., Igel, H., and Ares, M. (1996). RNase III cleaves eukaryotic preribosomal RNA at a U3 snoRNP-dependent site. Cell *85*, 115–124.

Eschrich, D., Buchhaupt, M., Kötter, P., and Entian, K.-D. (2002). Nep1p (Emg1p), a novel protein conserved in eukaryotes and archaea, is involved in ribosome biogenesis. Curr. Genet. *40*, 326–338.

Farrar, J.E., Nater, M., Caywood, E., McDevitt, M.A., Kowalski, J., Takemoto, C.M., Talbot, C.C., Meltzer, P., Esposito, D., Beggs, A.H., et al. (2008). Abnormalities of the large ribosomal subunit protein, Rpl35a, in Diamond-Blackfan anemia. Blood *112*, 1582–1592.

Fatica, A., Oeffinger, M., Dlakić, M., and Tollervey, D. (2003). Nob1p is required for cleavage of the 3' end of 18S rRNA. Molecular and Cellular Biology *23*, 1798–1807.

Finch, A.J., Hilcenko, C., Basse, N., Drynan, L.F., Goyenechea, B., Menne, T.F., Gonzalez Fernandez, A., Simpson, P., D'Santos, C.S., Arends, M.J., et al. (2011). Uncoupling of GTP hydrolysis from eIF6 release on the ribosome causes Shwachman-Diamond syndrome. Genes & Development *25*, 917–929.

Fink, A.L. (2005). Natively unfolded proteins. Current Opinion in Structural Biology *15*, 35–41.

Freed, E.F., Bleichert, F., Dutca, L.M., and Baserga, S.J. (2010). When ribosomes go bad: diseases of ribosome biogenesis. Mol. BioSyst. *6*, 481.

Fromont-Racine, M., Senger, B., Saveanu, C., and Fasiolo, F. (2003). Ribosome assembly in eukaryotes. Gene *313*, 17–42.

Fujiyama, S., Yanagida, M., Hayano, T., Miura, Y., Isobe, T., Fujimori, F., Uchida, T., and Takahashi, N. (2002). Isolation and proteomic characterization of human Parvulin-associating preribosomal ribonucleoprotein complexes. J. Biol. Chem. *277*, 23773–23780.

Fujiyama-Nakamura, S., Yoshikawa, H., Homma, K., Hayano, T., Tsujimura-Takahashi, T., Izumikawa, K., Ishikawa, H., Miyazawa, N., Yanagida, M., Miura, Y., et al. (2009). Parvulin (Par14), a peptidyl-prolyl cis-trans isomerase, is a novel rRNA processing factor that evolved in the metazoan lineage. Mol. Cell Proteomics *8*, 1552–1565.

Fumagalli, S., Di Cara, A., Neb-Gulati, A., Natt, F., Schwemberger, S., Hall, J., Babcock, G.F., Bernardi, R., Pandolfi, P.P., and Thomas, G. (2009). Absence of nucleolar disruption after impairment of 40S ribosome biogenesis reveals an rpL11-translation-dependent mechanism of p53 induction. Nature *11*, 501–508.

Ganapathi, K.A., Austin, K.M., Lee, C.-S., Dias, A., Malsch, M.M., Reed, R., and Shimamura, A. (2007). The human Shwachman-Diamond syndrome protein, SBDS, associates with ribosomal RNA. Blood *110*, 1458–1465.

Ganot, P., Bortolin, M.L., and Kiss, T. (1997). Site-specific pseudouridine formation in preribosomal RNA is guided by small nucleolar RNAs. Cell *89*, 799–809.

Gautier, T., Berges, T., Tollervey, D., and Hurt, E. (1997). Nucleolar KKE/D repeat proteins Nop56p and Nop58p interact with Nop1p and are required for ribosome biogenesis. Molecular and Cellular Biology *17*, 7088.

Gazda, H.T., Grabowska, A., Merida-Long, L.B., Latawiec, E., Schneider, H.E., Lipton, J.M., Vlachos, A., Atsidaftos, E., Ball, S.E., Orfali, K.A., et al. (2006). Ribosomal protein S24 gene is mutated in Diamond-Blackfan anemia. The American Journal of Human Genetics *79*, 1110–1118.

Gazda, H.T., Sheen, M.R., Vlachos, A., Choesmel, V., O'Donohue, M.-F., Schneider, H., Darras, N., Hasman, C., Sieff, C.A., Newburger, P.E., et al. (2008). Ribosomal Protein L5 and L11 Mutations Are Associated with Cleft Palate and Abnormal Thumbs in Diamond-Blackfan Anemia Patients. The American Journal of Human Genetics *83*, 769–780.

Gelperin, D., Horton, L., Beckman, J., Hensold, J., and Lemmon, S.K. (2001). Bms1p, a novel GTP-binding protein, and the related Tsr1p are required for distinct steps of 40S ribosome biogenesis in yeast. Rna *7*, 1268–1283.

Gilkes, D.M., Chen, L., and Chen, J. (2006). MDMX regulation of p53 response to ribosomal stress. The EMBO Journal *25*, 5614–5625.

Ginisty, H., Amalric, F., and Bouvet, P. (1998). Nucleolin functions in the first step of ribosomal RNA processing. The EMBO Journal *17*, 1476–1486.

Ginisty, H., Serin, G., Ghisolfi-Nieto, L., Roger, B., Libante, V., Amalric, F., and Bouvet, P. (2000). Interaction of nucleolin with an evolutionarily conserved pre-ribosomal RNA sequence is required for the assembly of the primary processing complex. J. Biol. Chem. *275*, 18845–18850.

Gonzales, B., Henning, D., So, R.B., Dixon, J., Dixon, M.J., and Valdez, B.C. (2005). The Treacher Collins syndrome (TCOF1) gene product is involved in pre-rRNA methylation. Human Molecular Genetics *14*, 2035–2043.

Grandi, P., and Rybin, V. (2002). ScienceDirect - Molecular Cell : 90S Pre-Ribosomes Include the 35S Pre-rRNA, the U3 snoRNP, and 40S Subunit Processing Factors but Predominantly Lack 60S Synthesis Factors. Molecular Cell.

Granneman, S., Gallagher, J.E.G., Vogelzangs, J., Horstman, W., Van Venrooij, W.J., Baserga, S.J., and Pruijn, G.J.M. (2003). The human Imp3 and Imp4 proteins form a ternary complex with hMpp10, which only interacts with the U3 snoRNA in 60–80S ribonucleoprotein complexes. Nucleic Acids Res. *31*, 1877–1887.

Grimm, T., Hölzel, M., Rohrmoser, M., Harasim, T., Malamoussi, A., Gruber-Eber, A., Kremmer, E., and Eick, D. (2006). Dominant-negative Pes1 mutants inhibit ribosomal RNA processing and cell proliferation via incorporation into the PeBoW-complex. Nucleic Acids Res. *34*, 3030–3043.

Gustafson, W.C., Taylor, C.W., Valdez, B.C., Henning, D., Phippard, A., Ren, Y., Busch, H., and Durban, E. (1998). Nucleolar protein p120 contains an arginine-rich domain that binds to ribosomal RNA. Biochem. J. *331 (Pt 2)*, 387–393.

Hadjiolova, K.V., NICOLOSO, M., Mazan, S., Hadjiolov, A.A., and Bachellerie, J.P. (1993). Alternative pre-rRNA processing pathways in human cells and their alteration by cycloheximide inhibition of protein synthesis. Eur. J. Biochem. *212*, 211–215.

Haindl, M., Harasim, T., Eick, D., and Muller, S. (2008). The nucleolar SUMO-specific protease SENP3 reverses SUMO modification of nucleophosmin and is required for rRNA processing. EMBO Rep *9*, 273–279.

Haupt, Y., Maya, R., Kazaz, A., and Oren, M. (1997). Mdm2 promotes the rapid degradation of p53. Nature *387*, 296–299.

Hayano, T., Yanagida, M., Yamauchi, Y., Shinkawa, T., Isobe, T., and Takahashi, N. (2003). Proteomic analysis of human Nop56p-associated pre-ribosomal ribonucleoprotein complexes. Possible link between Nop56p and the nucleolar protein treacle responsible for Treacher Collins syndrome. J. Biol.

Chem. *278*, 34309–34319.

Hayes, F., and Vasseur, M. (1976). Processing of the 17-S Escherichia coli precursor RNA in the 27-S pre-ribosomal particle. Eur. J. Biochem. *61*, 433–442.

He, J., Navarrete, S., Jasinski, M., Vulliamy, T., Dokal, I., Bessler, M., and Mason, P.J. (2002). Targeted disruption of Dkc1, the gene mutated in X-linked dyskeratosis congenita, causes embryonic lethality in mice. Oncogene *21*, 7740–7744.

Heindl, K., and Martinez, J. (2010). Nol9 is a novel polynucleotide 5'-kinase involved in ribosomal RNA processing. The EMBO Journal *29*, 4161–4171.

Heiss, N.S., Knight, S.W., Vulliamy, T.J., Klauck, S.M., Wiemann, S., Mason, P.J., Poustka, A., and Dokal, I. (1998). X-linked dyskeratosis congenita is caused by mutations in a highly conserved gene with putative nucleolar functions. Nat. Genet. *19*, 32–38.

Hennelly, S.P., Antoun, A., Ehrenberg, M., Gualerzi, C.O., Knight, W., Lodmell, J.S., and Hill, W.E. (2005). A time-resolved investigation of ribosomal subunit association. J. Mol. Biol. *346*, 1243–1258.

Henning, D., So, R.B., Jin, R., Lau, L.F., and Valdez, B.C. (2003). Silencing of RNA helicase II/Gualpha inhibits mammalian ribosomal RNA production. J. Biol. Chem. *278*, 52307–52314.

Henras, A.K., Soudet, J., Gérus, M., Lebaron, S., Caizergues-Ferrer, M., Mougin, A., and Henry, Y. (2008). The post-transcriptional steps of eukaryotic ribosome biogenesis. Cell. Mol. Life Sci. *65*, 2334–2359.

Henríquez, R., Blobel, G., and Aris, J.P. (1990). Isolation and sequencing of NOP1. A yeast gene encoding a nucleolar protein homologous to a human autoimmune antigen. J. Biol. Chem. *265*, 2209–2215.

Henry, Y., Wood, H., Morrissey, J.P., Petfalski, E., Kearsey, S., and Tollervey, D. (1994). The 5' end of yeast 5.8S rRNA is generated by exonucleases from an upstream cleavage site. The EMBO Journal *13*, 2452–2463.

Herrera, J.E., Savkur, R., and Olson, M.O. (1995). The ribonuclease activity of nucleolar protein B23. Nucleic Acids Res. *23*, 3974–3979.

Hesling, C., Oliveira, C.C., Castilho, B.A., and Zanchin, N.I.T. (2007). The Shwachman-Bodian-Diamond syndrome associated protein interacts with HsNip7 and its down-regulation affects gene expression at the transcriptional and translational levels. Exp. Cell Res. *313*, 4180–4195.

Hollstein, M., Rice, K., Greenblatt, M.S., Soussi, T., Fuchs, R., Sørlie, T., Hovig, E., Smith-Sørensen, B., Montesano, R., and Harris, C.C. (1994). Database of

p53 gene somatic mutations in human tumors and cell lines. Nucleic Acids Res. *22*, 3551–3555.

Holzel, M., Orban, M., Hochstatter, J., Rohrmoser, M., Harasim, T., Malamoussi, A., Kremmer, E., Langst, G., and Eick, D. (2010). Defects in 18 S or 28 S rRNA Processing Activate the p53 Pathway. Journal of Biological Chemistry *285*, 6364–6370.

Hong, B., Brockenbrough, J.S., Wu, P., and Aris, J.P. (1997). Nop2p is required for pre-rRNA processing and 60S ribosome subunit synthesis in yeast. Molecular and Cellular Biology *17*, 378–388.

Horn, H.F., and Vousden, K.H. (2008). Cooperation between the ribosomal proteins L5 and L11 in the p53 pathway. Oncogene *27*, 5774–5784.

Horsey, E.W., Jakovljevic, J., Miles, T.D., Harnpicharnchai, P., and Woolford, J.L. (2004). Role of the yeast Rrp1 protein in the dynamics of pre-ribosome maturation. Rna *10*, 813–827.

Hölzel, M., Rohrmoser, M., Schlee, M., Grimm, T., Harasim, T., Malamoussi, A., Gruber-Eber, A., Kremmer, E., Hiddemann, W., Bornkamm, G.W., et al. (2005). Mammalian WDR12 is a novel member of the Pes1-Bop1 complex and is required for ribosome biogenesis and cell proliferation. The Journal of Cell Biology *170*, 367–378.

Hsiao, C., Mohan, S., Kalahar, B.K., and Williams, L.D. (2009). Peeling the Onion: Ribosomes Are Ancient Molecular Fossils. Molecular Biology and Evolution *26*, 2415–2425.

Hu, L., Wang, J., Liu, Y., Zhang, Y., Zhang, L., Kong, R., Zheng, Z., Du, X., and Ke, Y. (2011). A Small Ribosomal Subunit (SSU) Processome Component, the Human U3 Protein 14A (hUTP14A) Binds p53 and Promotes p53 Degradation. Journal of Biological Chemistry *286*, 3119–3128.

Idol, R.A., Robledo, S., Du, H.-Y., Crimmins, D.L., Wilson, D.B., Ladenson, J.H., Bessler, M., and Mason, P.J. (2007). Cells depleted for RPS19, a protein associated with Diamond Blackfan Anemia, show defects in 18S ribosomal RNA synthesis and small ribosomal subunit production. Blood Cells, Molecules, and Diseases *39*, 35–43.

Jalal, C., Uhlmann-Schiffler, H., and Stahl, H. (2007). Redundant role of DEAD box proteins p68 (Ddx5) and p72/p82 (Ddx17) in ribosome biogenesis and cell proliferation. Nucleic Acids Res. *35*, 3590–3601.

Jarboui, M.A., Wynne, K., Elia, G., Hall, W.W., and Gautier, V.W. (2011). Proteomic profiling of the human T-cell nucleolus. Molecular Immunology *49*, 441–452.

Jin, A., Itahana, K., O'Keefe, K., and Zhang, Y. (2004). Inhibition of HDM2 and activation of p53 by ribosomal protein L23. Molecular and Cellular Biology *24*, 7669–7680.

Johnson, A.W. (1997). Rat1p and Xrn1p are functionally interchangeable exoribonucleases that are restricted to and required in the nucleus and cytoplasm, respectively. Molecular and Cellular Biology *17*, 6122–6130.

Jones, N.C., Lynn, M.L., Gaudenz, K., Sakai, D., Aoto, K., Rey, J.-P., Glynn, E.F., Ellington, L., Du, C., Dixon, J., et al. (2008). Prevention of the neurocristopathy Treacher Collins syndrome through inhibition of p53 function. Nat Med *14*, 125–133.

Kaczanowska, M., and Rydén-Aulin, M. (2007). Ribosome biogenesis and the translation process in Escherichia coli. Microbiol. Mol. Biol. Rev. *71*, 477–494.

Kass, S., and Craig, N. (1987). Primary processing of mammalian rRNA involves two adjacent cleavages and is not species specific. Molecular and Cellular Biology.

Kass, S., Tyc, K., Steitz, J.A., and Sollner-Webb, B. (1990). The U3 small nucleolar ribonucleoprotein functions in the first step of preribosomal RNA processing. Cell *60*, 897–908.

Kent, T., Lapik, Y.R., and Pestov, D.G. (2009). The 5' external transcribed spacer in mouse ribosomal RNA contains two cleavage sites. Rna *15*, 14–20.

King, T.H., Liu, B., McCully, R.R., and Fournier, M.J. (2003). Ribosome structure and activity are altered in cells lacking snoRNPs that form pseudouridines in the peptidyl transferase center. Molecular Cell *11*, 425–435.

Kiss, T. (2001). Small nucleolar RNA-guided post-transcriptional modification of cellular RNAs. The EMBO Journal *20*, 3617–3622.

Kiss-László, Z., Henry, Y., Bachellerie, J.P., Caizergues-Ferrer, M., and Kiss, T. (1996). Site-specific ribose methylation of preribosomal RNA: a novel function for small nucleolar RNAs. Cell *85*, 1077–1088.

Kondrashov, N., Pusic, A., Stumpf, C.R., Shimizu, K., Hsieh, A.C., Xue, S., Ishijima, J., Shiroishi, T., and Barna, M. (2011). Ribosome-Mediated Specificity in Hox mRNA Translation and Vertebrate Tissue Patterning. Cell *145*, 383–397.

Kopp, K., Gasiorowski, J., Chen, D., Gilmore, R., Norton, J., Wang, C., Leary, D., Chan, E., Dean, D., and Huang, S. (2007). Pol I transcription and pre-rRNA processing are coordinated in a transcription-dependent manner in mammalian cells. Mol. Biol. Cell *18*, 394–403.

Kressler, D., Hurt, E., and Bassler, J. (2010). Driving ribosome assembly.

Biochim. Biophys. Acta *1803*, 673–683.

Kressler, D., Rojo, M., Linder, P., and Cruz, J. (1999). Spb1p is a putative methyltransferase required for 60S ribosomal subunit biogenesis in Saccharomyces cerevisiae. Nucleic Acids Res. *27*, 4598–4608.

Krogan, N.J., Peng, W.-T., Cagney, G., Robinson, M.D., Haw, R., Zhong, G., Guo, X., Zhang, X., Canadien, V., Richards, D.P., et al. (2004). High-definition macromolecular composition of yeast RNA-processing complexes. Molecular Cell *13*, 225–239.

Kubbutat, M.H., Jones, S.N., and Vousden, K.H. (1997). Regulation of p53 stability by Mdm2. Nature *387*, 299–303.

Kurki, S., Peltonen, K., Latonen, L., Kiviharju, T.M., Ojala, P.M., Meek, D., and Laiho, M. (2004). Nucleolar protein NPM interacts with HDM2 and protects tumor suppressor protein p53 from HDM2-mediated degradation. Cancer Cell *5*, 465–475.

la Cruz, de, J., Kressler, D., Rojo, M., Tollervey, D., and Linder, P. (1998). Spb4p, an essential putative RNA helicase, is required for a late step in the assembly of 60S ribosomal subunits in Saccharomyces cerevisiae. Rna *4*, 1268–1281.

Lafontaine, D., Delcour, J., Glasser, A.L., Desgrès, J., and Vandenhaute, J. (1994). The DIM1 gene responsible for the conserved m6(2)Am6(2)A dimethylation in the 3'-terminal loop of 18 S rRNA is essential in yeast. J. Mol. Biol. *241*, 492–497.

Lafontaine, D., Vandenhaute, J., and Tollervey, D. (1995). The 18S rRNA dimethylase Dim1p is required for pre-ribosomal RNA processing in yeast. Genes & Development *9*, 2470–2481.

Lafontaine, D.L., Bousquet-Antonelli, C., Henry, Y., Caizergues-Ferrer, M., and Tollervey, D. (1998). The box H + ACA snoRNAs carry Cbf5p, the putative rRNA pseudouridine synthase. Genes & Development *12*, 527–537.

Lam, Y.W., Evans, V.C., Heesom, K.J., Lamond, A.I., and Matthews, D.A. (2010). Proteomics analysis of the nucleolus in adenovirus-infected cells. Mol. Cell Proteomics *9*, 117–130.

Lapeyre, B., and Purushothaman, S.K. (2004). Spb1p-directed formation of Gm2922 in the ribosome catalytic center occurs at a late processing stage. Molecular Cell *16*, 663–669.

Lapik, Y.R., Fernandes, C.J., Lau, L.F., and Pestov, D.G. (2004). Physical and Functional Interaction between Pes1 and Bop1 in Mammalian Ribosome Biogenesis. Molecular Cell *15*, 17–29.

Lebaron, S., Froment, C., Fromont-Racine, M., Rain, J.-C., Monsarrat, B., Caizergues-Ferrer, M., and Henry, Y. (2005). The splicing ATPase prp43p is a component of multiple preribosomal particles. Molecular and Cellular Biology *25*, 9269–9282.

Lebreton, A., Rousselle, J.-C., Lenormand, P., Namane, A., Jacquier, A., Fromont-Racine, M., and Saveanu, C. (2008a). 60S ribosomal subunit assembly dynamics defined by semi-quantitative mass spectrometry of purified complexes. Nucleic Acids Res. *36*, 4988–4999.

Lebreton, A., Tomecki, R., Dziembowski, A., and Séraphin, B. (2008b). Endonucleolytic RNA cleavage by a eukaryotic exosome. Nature *456*, 993–996.

Leulliot, N., Bohnsack, M.T., Graille, M., Tollervey, D., and Van Tilbeurgh, H. (2008). The yeast ribosome synthesis factor Emg1 is a novel member of the superfamily of alpha/beta knot fold methyltransferases. Nucleic Acids Res. *36*, 629–639.

Léger-Silvestre, I., Milkereit, P., Ferreira-Cerca, S., Saveanu, C., Rousselle, J.-C., Choesmel, V., Guinefoleau, C., Gas, N., and Gleizes, P.-E. (2004). The ribosomal protein Rps15p is required for nuclear exit of the 40S subunit precursors in yeast. The EMBO Journal *23*, 2336–2347.

Li, Z., and Deutscher, M.P. (1995). The tRNA processing enzyme RNase T is essential for maturation of 5S RNA. Proc. Natl. Acad. Sci. U.S.a. *92*, 6883–6886.

Li, Z., Pandit, S., and Deutscher, M.P. (1999a). Maturation of 23S ribosomal RNA requires the exoribonuclease RNase T. Rna *5*, 139–146.

Li, Z., Pandit, S., and Deutscher, M.P. (1999b). RNase G (CafA protein) and RNase E are both required for the 5' maturation of 16S ribosomal RNA. The EMBO Journal *18*, 2878–2885.

Lindström, M.S., and Zhang, Y. (2008). Ribosomal protein S9 is a novel B23/NPM-binding protein required for normal cell proliferation. J. Biol. Chem. *283*, 15568–15576.

Liu, P.C., and Thiele, D.J. (2001). Novel stress-responsive genes EMG1 and NOP14 encode conserved, interacting proteins required for 40S ribosome biogenesis. Mol. Biol. Cell *12*, 3644–3657.

Loar, J.W., Seiser, R.M., Sundberg, A.E., Sagerson, H.J., Ilias, N., Zobel-Thropp, P., Craig, E.A., and Lycan, D.E. (2004). Genetic and biochemical interactions among Yar1, Ltv1 and Rps3 define novel links between environmental stress and ribosome biogenesis in Saccharomyces cerevisiae. Genetics *168*, 1877–1889.

Lohrum, M.A., and Vousden, K.H. (2000). Regulation and function of the p53-related proteins: same family, different rules. Trends in Cell Biology *10*, 197–202.

Lohrum, M.A.E., Ludwig, R.L., Kubbutat, M.H.G., Hanlon, M., and Vousden, K.H. (2003). Regulation of HDM2 activity by the ribosomal protein L11. Cancer Cell *3*, 577–587.

Luft, F. (2010). The rise of a ribosomopathy and increased cancer risk. J Mol Med *88*, 1–3.

Lygerou, Z., Allmang, C., Tollervey, D., and Seraphin, B. (1996). Accurate processing of a eukaryotic precursor ribosomal RNA by ribonuclease MRP in vitro. Science *272*, 268–270.

Maden, B.E. (1990). The numerous modified nucleotides in eukaryotic ribosomal RNA. Prog. Nucleic Acid Res. Mol. Biol. *39*, 241–303.

Maggi, L.B., Kuchenruether, M., Dadey, D.Y.A., Schwope, R.M., Grisendi, S., Townsend, R.R., Pandolfi, P.P., and Weber, J.D. (2008). Nucleophosmin Serves as a Rate-Limiting Nuclear Export Chaperone for the Mammalian Ribosome. Molecular and Cellular Biology *28*, 7050–7065.

Marechal, V., Elenbaas, B., Piette, J., Nicolas, J.C., and Levine, A.J. (1994). The ribosomal L5 protein is associated with mdm-2 and mdm-2-p53 complexes. Molecular and Cellular Biology *14*, 7414–7420.

McMahon, M., Ayllón, V., Panov, K.I., and O'Connor, R. (2010). Ribosomal 18 S RNA processing by the IGF-I-responsive WDR3 protein is integrated with p53 function in cancer cell proliferation. J. Biol. Chem. *285*, 18309–18318.

Menne, T.F., Goyenechea, B., Sánchez-Puig, N., Wong, C.C., Tonkin, L.M., Ancliff, P.J., Brost, R.L., Costanzo, M., Boone, C., and Warren, A.J. (2007). The Shwachman-Bodian-Diamond syndrome protein mediates translational activation of ribosomes in yeast. Nat. Genet. *39*, 486–495.

Miles, T.D., Jakovljevic, J., Horsey, E.W., Harnpicharnchai, P., Tang, L., and Woolford, J.L. (2005). Ytm1, Nop7, and Erb1 form a complex necessary for maturation of yeast 66S preribosomes. Molecular and Cellular Biology *25*, 10419–10432.

Milkereit, P., Gadal, O., Podtelejnikov, A., Trumtel, S., Gas, N., Petfalski, E., Tollervey, D., Mann, M., Hurt, E., and Tschochner, H. (2001). Maturation and intranuclear transport of pre-ribosomes requires Noc proteins. Cell *105*, 499–509.

Mitchell, P., Petfalski, E., and Tollervey, D. (1996). The 3' end of yeast 5.8S rRNA is generated by an exonuclease processing mechanism. Genes & Development *10*, 502–513.

Mitchell, P., Petfalski, E., Shevchenko, A., Mann, M., and Tollervey, D. (1997). The exosome: a conserved eukaryotic RNA processing complex containing multiple 3“-->5” exoribonucleases. Cell *91*, 457–466.

Mochizuki, Y., He, J., Kulkarni, S., Bessler, M., and Mason, P.J. (2004). Mouse dyskerin mutations affect accumulation of telomerase RNA and small nucleolar RNA, telomerase activity, and ribosomal RNA processing. Proc. Natl. Acad. Sci. U.S.a. *101*, 10756–10761.

Mongelard, F., and Bouvet, P. (2007). Nucleolin: a multiFACeTed protein. Trends in Cell Biology *17*, 80–86.

Montanaro, L., Chillà, A., Treré, D., Pession, A., Govoni, M., Tazzari, P.L., and Derenzini, M. (2002). Increased mortality rate and not impaired ribosomal biogenesis is responsible for proliferative defect in dyskeratosis congenita cell lines. J. Invest. Dermatol. *118*, 193–198.

Natsume, T., Yamauchi, Y., Nakayama, H., Shinkawa, T., Yanagida, M., Takahashi, N., and Isobe, T. (2002). A direct nanoflow liquid chromatography-tandem mass spectrometry system for interaction proteomics. Anal. Chem. *74*, 4725–4733.

Newman, D.R., Kuhn, J.F., Shanab, G.M., and Maxwell, E.S. (2000). Box C/D snoRNA-associated proteins: two pairs of evolutionarily ancient proteins and possible links to replication and transcription. Rna *6*, 861–879.

Ni, J., Tien, A.L., and Fournier, M.J. (1997). Small nucleolar RNAs direct site-specific synthesis of pseudouridine in ribosomal RNA. Cell *89*, 565–573.

Nissan, T.A., Baßler, J., Petfalski, E., and Tollervey, D. (2002). 60S pre-ribosome formation viewed from assembly in the nucleolus until export to the cytoplasm. The EMBO Journal *21*, 5539–5547.

Nousbeck, J., Spiegel, R., Ishida-Yamamoto, A., Indelman, M., Shani-Adir, A., Adir, N., Lipkin, E., Bercovici, S., Geiger, D., van Steensel, M.A., et al. (2008). Alopecia, neurological defects, and endocrinopathy syndrome caused by decreased expression of RBM28, a nucleolar protein associated with ribosome biogenesis. Am. J. Hum. Genet. *82*, 1114–1121.

O'Day, C.L., Chavanikamannil, F., and Abelson, J. (1996). 18S rRNA processing requires the RNA helicase-like protein Rrp3. Nucleic Acids Res. *24*, 3201–3207.

O'Donohue, M.F., Choesmel, V., Faubladier, M., Fichant, G., and Gleizes, P.E. (2010). Functional dichotomy of ribosomal proteins during the synthesis of mammalian 40S ribosomal subunits. The Journal of Cell Biology *190*, 853–866.

Oeffinger, M., Dlakić, M., and Tollervey, D. (2004). A pre-ribosome-associated HEAT-repeat protein is required for export of both ribosomal subunits. Genes & Development *18*, 196–209.

Ofengand, J., and Bakin, A. (1997). Mapping to nucleotide resolution of pseudouridine residues in large subunit ribosomal RNAs from representative

eukaryotes, prokaryotes, archaebacteria, mitochondria and chloroplasts. J. Mol. Biol. *266*, 246–268.

Ofengand, J., and Fournier, M.J. (1998). The pseudouridine residues of rRNA: number, location, biosynthesis, and function. Modification and Editing of RNA 229–253.

Ofir-Rosenfeld, Y., Boggs, K., Michael, D., Kastan, M.B., and Oren, M. (2008). Mdm2 regulates p53 mRNA translation through inhibitory interactions with ribosomal protein L26. Molecular Cell *32*, 180–189.

Oren, M. (2003). Decision making by p53: life, death and cancer. Cell Death Differ. *10*, 431–442.

Orrù, S., Aspesi, A., Armiraglio, M., Caterino, M., Loreni, F., Ruoppolo, M., Santoro, C., and Dianzani, I. (2007). Analysis of the ribosomal protein S19 interactome. Mol. Cell Proteomics *6*, 382–393.

Parker, K.A., Bruzik, J.P., and Steitz, J.A. (1988). An in vitro interaction between the human U3 snRNP and 28S rRNA sequences near the alpha-sarcin site. Nucleic Acids Res. *16*, 10493–10509.

Pestov, D.G., Strezoska, Z., and Lau, L.F. (2001). Evidence of p53-Dependent Cross-Talk between Ribosome Biogenesis and the Cell Cycle: Effects of Nucleolar Protein Bop1 on G1/S Transition. Molecular and Cellular Biology *21*, 4246–4255.

Prieto, J.-L., and McStay, B. (2007). Recruitment of factors linking transcription and processing of pre-rRNA to NOR chromatin is UBF-dependent and occurs independent of transcription in human cells. Genes & Development *21*, 2041–2054.

Qu, L.H., Henras, A., Lu, Y.J., Zhou, H., Zhou, W.X., Zhu, Y.Q., Zhao, J., Henry, Y., Caizergues-Ferrer, M., and Bachellerie, J.P. (1999). Seven novel methylation guide small nucleolar RNAs are processed from a common polycistronic transcript by Rat1p and RNase III in yeast. Molecular and Cellular Biology *19*, 1144–1158.

Reichow, S.L., Hamma, T., Ferré-D'Amaré, A.R., and Varani, G. (2007). The structure and function of small nucleolar ribonucleoproteins. Nucleic Acids Res. *35*, 1452–1464.

Ren, J., Wang, Y., Liang, Y., Zhang, Y., Bao, S., and Xu, Z. (2010). Methylation of ribosomal protein S10 by protein-arginine methyltransferase 5 regulates ribosome biogenesis. J. Biol. Chem. *285*, 12695–12705.

Ridanpää, M., van Eenennaam, H., Pelin, K., Chadwick, R., Johnson, C., Yuan, B., vanVenrooij, W., Pruijn, G., Salmela, R., Rockas, S., et al. (2001). Mutations

in the RNA component of RNase MRP cause a pleiotropic human disease, cartilage-hair hypoplasia. Cell *104*, 195–203.

Rohozinski, J., and Bishop, C.E. (2004). The mouse juvenile spermatogonial depletion (jsd) phenotype is due to a mutation in the X-derived retrogene, mUtp14b. Proc. Natl. Acad. Sci. U.S.a. *101*, 11695–11700.

Romanova, L., Grand, A., Zhang, L., Rayner, S., Katoku-Kikyo, N., Kellner, S., and Kikyo, N. (2009). Critical role of nucleostemin in pre-rRNA processing. J. Biol. Chem. *284*, 4968–4977.

Rouquette, J., Choesmel, V., and Gleizes, P.-E. (2005). Nuclear export and cytoplasmic processing of precursors to the 40S ribosomal subunits in mammalian cells. The EMBO Journal *24*, 2862–2872.

Rout, M.P., Aitchison, J.D., Suprapto, A., Hjertaas, K., Zhao, Y., and Chait, B.T. (2000). The yeast nuclear pore complex: composition, architecture, and transport mechanism. The Journal of Cell Biology *148*, 635–651.

Roy, A., Kucukural, A., and Zhang, Y. (2010). I-TASSER: a unified platform for automated protein structure and function prediction. Nat Protoc *5*, 725–738.

Roy, M.K., Singh, B., Ray, B.K., and Apirion, D. (1983). Maturation of 5-S rRNA: ribonuclease E cleavages and their dependence on precursor sequences. Eur. J. Biochem. *131*, 119–127.

Rubbi, C.P., and Milner, J. (2003). Disruption of the nucleolus mediates stabilization of p53 in response to DNA damage and other stresses. The EMBO Journal *22*, 6068–6077.

Rudra, D., and Warner, J.R. (2004). What better measure than ribosome synthesis? Genes & Development *18*, 2431–2436.

Ruggero, D., Grisendi, S., Piazza, F., Rego, E., Mari, F., Rao, P.H., Cordon-Cardo, C., and Pandolfi, P.P. (2003). Dyskeratosis congenita and cancer in mice deficient in ribosomal RNA modification. Science *299*, 259–262.

Russell, I.D., and Tollervey, D. (1992). NOP3 is an essential yeast protein which is required for pre-rRNA processing. The Journal of Cell Biology *119*, 737–747.

Savage, S.A., and Alter, B.P. (2009). Dyskeratosis congenita. Hematol. Oncol. Clin. North Am. *23*, 215–231.

Savkur, R.S., and Olson, M.O. (1998). Preferential cleavage in pre-ribosomal RNA byprotein B23 endoribonuclease. Nucleic Acids Res. *26*, 4508–4515.

Schäfer, T., Strauss, D., Petfalski, E., Tollervey, D., and Hurt, E. (2003). The path from nucleolar 90S to cytoplasmic 40S pre-ribosomes. The EMBO Journal *22*,

1370–1380.

Schilders, G., Raijmakers, R., Raats, J.M.H., and Pruijn, G.J.M. (2005). MPP6 is an exosome-associated RNA-binding protein involved in 5.8S rRNA maturation. Nucleic Acids Res. *33*, 6795–6804.

Schilders, G., van Dijk, E., and Pruijn, G.J.M. (2007). C1D and hMtr4p associate with the human exosome subunit PM/Scl-100 and are involved in pre-rRNA processing. Nucleic Acids Res. *35*, 2564–2572.

Schneider, C., Leung, E., Brown, J., and Tollervey, D. (2008). The N-terminal PIN domain of the exosome subunit Rrp44 harbors endonuclease activity and tethers Rrp44 to the yeast core exosome. Nucleic Acids Res. *37*, 1127–1140.

Schuwirth, B.S., Borovinskaya, M.A., Hau, C.W., Zhang, W., Vila-Sanjurjo, A., Holton, J.M., and Cate, J.H.D. (2005). Structures of the bacterial ribosome at 3.5 A resolution. Science *310*, 827–834.

Sekiguchi, T., Hayano, T., Yanagida, M., Takahashi, N., and Nishimoto, T. (2006). NOP132 is required for proper nucleolus localization of DEAD-box RNA helicase DDX47. Nucleic Acids Res. *34*, 4593–4608.

Sekiguchi, T., Todaka, Y., Wang, Y., Hirose, E., Nakashima, N., and Nishimoto, T. (2004). A novel human nucleolar protein, Nop132, binds to the G proteins, RRAG A/C/D. J. Biol. Chem. *279*, 8343–8350.

Speckmann, W.A., Li, Z.-H., Lowe, T.M., Eddy, S.R., Terns, R.M., and Terns, M.P. (2002). Archaeal guide RNAs function in rRNA modification in the eukaryotic nucleus. Curr. Biol. *12*, 199–203.

Strezoska, Z., Pestov, D.G., and Lau, L.F. (2000). Bop1 Is a Mouse WD40 Repeat Nucleolar Protein Involved in 28S and 5.8S rRNA Processing and 60S Ribosome Biogenesis. Molecular and Cellular Biology *20*, 5516.

Sun, X.-X., Dai, M.-S., and Lu, H. (2007). 5-fluorouracil activation of p53 involves an MDM2-ribosomal protein interaction. J. Biol. Chem. *282*, 8052–8059.

Sun, X.-X., Dai, M.-S., and Lu, H. (2008). Mycophenolic acid activation of p53 requires ribosomal proteins L5 and L11. J. Biol. Chem. *283*, 12387–12392.

Sun, X.-X., Wang, Y.-G., Xirodimas, D.P., and Dai, M.-S. (2010). Perturbation of 60 S ribosomal biogenesis results in ribosomal protein L5- and L11-dependent p53 activation. J. Biol. Chem. *285*, 25812–25821.

Takahashi, N., Yanagida, M., Fujiyama, S., Hayano, T., and Isobe, T. (2003). Proteomic snapshot analyses of preribosomal ribonucleoprotein complexes formed at various stages of ribosome biogenesis in yeast and mammalian cells. Mass Spectrom. Rev. *22*, 287–317.

Tollervey, D., Lehtonen, H., Jansen, R., Kern, H., and Hurt, E.C. (1993). Temperature-sensitive mutations demonstrate roles for yeast fibrillarin in pre-rRNA processing, pre-rRNA methylation, and ribosome assembly. Cell *72*, 443–457.

Turner, A.J., Knox, A.A., Prieto, J.-L., McStay, B., and Watkins, N.J. (2009). A novel small-subunit processome assembly intermediate that contains the U3 snoRNP, nucleolin, RRP5, and DBP4. Molecular and Cellular Biology *29*, 3007–3017.

Tuteja, R., and Tuteja, N. (1998). Nucleolin: a multifunctional major nucleolar phosphoprotein. Crit. Rev. Biochem. Mol. Biol. *33*, 407–436.

Tycowski, K.T., Smith, C.M., Shu, M.D., and Steitz, J.A. (1996). A small nucleolar RNA requirement for site-specific ribose methylation of rRNA in Xenopus. Proc. Natl. Acad. Sci. U.S.a. *93*, 14480–14485.

Valdez, B.C., Henning, D., So, R.B., Dixon, J., and Dixon, M.J. (2004). The Treacher Collins syndrome (TCOF1) gene product is involved in ribosomal DNA gene transcription by interacting with upstream binding factor. Proc. Natl. Acad. Sci. U.S.a. *101*, 10709–10714.

Vanrobays, E., Gélugne, J.-P., Caizergues-Ferrer, M., and Lafontaine, D.L.J. (2004). Dim2p, a KH-domain protein required for small ribosomal subunit synthesis. Rna *10*, 645–656.

Vanrobays, E., Gélugne, J.-P., Gleizes, P.-E., and Caizergues-Ferrer, M. (2003). Late cytoplasmic maturation of the small ribosomal subunit requires RIO proteins in Saccharomyces cerevisiae. Molecular and Cellular Biology *23*, 2083–2095.

Vanrobays, E., Gleizes, P.E., Bousquet-Antonelli, C., Noaillac-Depeyre, J., Caizergues-Ferrer, M., and Gelugne, J.P. (2001). Processing of 20S pre-rRNA to 18S ribosomal RNA in yeast requires Rrp10p, an essential non-ribosomal cytoplasmic protein. The EMBO Journal *20*, 4204–4213.

Venema, J., Bousquet-Antonelli, C., Gelugne, J.P., Caizergues-Ferrer, M., and Tollervey, D. (1997). Rok1p is a putative RNA helicase required for rRNA processing. Molecular and Cellular Biology *17*, 3398–3407.

Vlachos, A., Ball, S., Dahl, N., Alter, B.P., Sheth, S., Ramenghi, U., Meerpohl, J., Karlsson, S., Liu, J.M., Leblanc, T., et al. (2008). Diagnosing and treating Diamond Blackfan anaemia: results of an international clinical consensus conference. In British Journal of Haematology, pp. 859–876.

Walne, A.J., and Dokal, I. (2009). Advances in the understanding of dyskeratosis congenita. Br J Haematol *145*, 164–172.

Wang, M., and Pestov, D.G. (2011). 5'-end surveillance by Xrn2 acts as a shared

mechanism for mammalian pre-rRNA maturation and decay. Nucleic Acids Res. *39*, 1811–1822.

Warner, J.R. (1999). The economics of ribosome biosynthesis in yeast. Trends in Biochemical Sciences *24*, 437–440.

Watanabe, Y., and Gray, M.W. (2000). Evolutionary appearance of genes encoding proteins associated with box H/ACA snoRNAs: cbf5p in Euglena gracilis, an early diverging eukaryote, and candidate Gar1p and Nop10p homologs in archaebacteria. Nucleic Acids Res. *28*, 2342–2352.

Welting, T.J.M., van Venrooij, W.J., and Pruijn, G.J.M. (2004). Mutual interactions between subunits of the human RNase MRP ribonucleoprotein complex. Nucleic Acids Res. *32*, 2138–2146.

Westendorf, J.M., Konstantinov, K.N., Wormsley, S., Shu, M.D., Matsumoto-Taniura, N., Pirollet, F., Klier, F.G., Gerace, L., and Baserga, S.J. (1998). M phase phosphoprotein 10 is a human U3 small nucleolar ribonucleoprotein component. Mol. Biol. Cell *9*, 437–449.

Wild, T., Horvath, P., Wyler, E., Widmann, B., Badertscher, L., Zemp, I., Kozak, K., Csucs, G., Lund, E., and Kutay, U. (2010). A Protein Inventory of Human Ribosome Biogenesis Reveals an Essential Function of Exportin 5 in 60S Subunit Export. PLoS Biol *8*, e1000522.

Williamson, J.R. (2003). After the ribosome structures: how are the subunits assembled? Rna *9*, 165–167.

Woese, C.R. (2001). Translation: in retrospect and prospect. Rna *7*, 1055–1067.

Wong, C.C., Traynor, D., Basse, N., Kay, R.R., and Warren, A.J. (2011). Defective ribosome assembly in Shwachman-Diamond syndrome. Blood *118*, 4305–4312.

Wu, H., Xu, H., Miraglia, L.J., and Crooke, S.T. (2000). Human RNase III is a 160-kDa protein involved in preribosomal RNA processing. J. Biol. Chem. *275*, 36957–36965.

Yadavilli, S., Mayo, L.D., Higgins, M., Lain, S., Hegde, V., and Deutsch, W.A. (2009). Ribosomal protein S3: A multi-functional protein that interacts with both p53 and MDM2 through its KH domain. DNA Repair (Amst.) *8*, 1215–1224.

Yanagida, M., Shimamoto, A., Nishikawa, K., Furuichi, Y., Isobe, T., and Takahashi, N. (2001). Isolation and proteomic characterization of the major proteins of the nucleolin-binding ribonucleoprotein complexes. Proteomics *1*, 1390–1404.

Yoon, A., Peng, G., Brandenburger, Y., Brandenburg, Y., Zollo, O., Xu, W.,

Rego, E., and Ruggero, D. (2006). Impaired control of IRES-mediated translation in X-linked dyskeratosis congenita. Science *312*, 902–906.

Yu, Y., Maggi, L.B., Brady, S.N., Apicelli, A.J., Dai, M.-S., Lu, H., and Weber, J.D. (2006). Nucleophosmin is essential for ribosomal protein L5 nuclear export. Molecular and Cellular Biology *26*, 3798–3809.

Yuan, X., Zhou, Y., Casanova, E., Chai, M., Kiss, E., Gröne, H.-J., Schütz, G., and Grummt, I. (2005). Genetic inactivation of the transcription factor TIF-IA leads to nucleolar disruption, cell cycle arrest, and p53-mediated apoptosis. Molecular Cell *19*, 77–87.

Yusupov, M.M., Yusupova, G.Z., Baucom, A., Lieberman, K., Earnest, T.N., Cate, J.H., and Noller, H.F. (2001). Crystal structure of the ribosome at 5.5 A resolution. Science *292*, 883–896.

Zanchin, N.I., and Goldfarb, D.S. (1999a). Nip7p interacts with Nop8p, an essential nucleolar protein required for 60S ribosome biogenesis, and the exosome subunit Rrp43p. Molecular and Cellular Biology *19*, 1518–1525.

Zanchin, N.I., and Goldfarb, D.S. (1999b). The exosome subunit Rrp43p is required for the efficient maturation of 5.8S, 18S and 25S rRNA. Nucleic Acids Res. *27*, 1283–1288.

Zanchin, N.I., Roberts, P., DeSilva, A., Sherman, F., and Goldfarb, D.S. (1997). Saccharomyces cerevisiae Nip7p is required for efficient 60S ribosome subunit biogenesis. Molecular and Cellular Biology *17*, 5001–5015.

Zemp, I., Wild, T., O'Donohue, M.F., Wandrey, F., Widmann, B., Gleizes, P.E., and Kutay, U. (2009). Distinct cytoplasmic maturation steps of 40S ribosomal subunit precursors require hRio2. The Journal of Cell Biology *185*, 1167–1180.

Zhang, Y., Wolf, G.W., Bhat, K., Jin, A., Allio, T., Burkhart, W.A., and Xiong, Y. (2003). Ribosomal protein L11 negatively regulates oncoprotein MDM2 and mediates a p53-dependent ribosomal-stress checkpoint pathway. Molecular and Cellular Biology *23*, 8902–8912.

Zhu, Y., Poyurovsky, M.V., Li, Y., Biderman, L., Stahl, J., Jacq, X., and Prives, C. (2009). Ribosomal protein S7 is both a regulator and a substrate of MDM2. Molecular Cell *35*, 316–326.

7. ANEXOS

7.1. Artigo publicado em co-autoria

Evidence for the association of the human regulatory protein Ki-1/57 with the translational machinery

Kaliandra de Almeida Gonçalves, Gustavo Costa Bressan, Ângela Saito, Luis Gustavo Morello, Nilson Ivo T. Zanchin, Jörg Kobarg

FEBS Letters, **585**, 2556–2560 (2011)

FEBS Letters 585 (2011) 2556–2560

FEBS Letters

journal homepage: www.FEBSLetters.org

Evidence for the association of the human regulatory protein Ki-1/57 with the translational machinery

Kaliandra de Almeida Gonçalves [a,b], Gustavo Costa Bressan [c], Ângela Saito [a,b], Luis Gustavo Morello [a,d], Nilson Ivo T. Zanchin [d,e,1], Jörg Kobarg [a,b,d,*]

[a] Laboratório Nacional de Biociências (LNBio), Centro Nacional de Pesquisa em Energia e Materiais (CNPEM), Campinas, São Paulo, Brazil
[b] Departamento de Bioquímica-Programa de Pós-graduação em Biologia Funcional e Molecular, Instituto de Biologia, Universidade Estadual de Campinas, 13083-970 Campinas, SP, Brazil
[c] Departamento de Bioquímica e Biologia Molecular, Universidade Federal de Viçosa (UFV), Viçosa, Minas Gerais, Brazil
[d] Departamento de Genética, Evolução e Bioagentes, Programa de Pós-graduação em Genética e Biologia Molecular, Instituto de Biologia, Universidade Estadual de Campinas, 13083-970 Campinas, SP, Brazil
[e] Centro de Biologia Molecular e Engenharia Genética e Faculdade de Ciências Aplicadas, Universidade Estadual de Campinas, SP, Brazil

ARTICLE INFO

Article history:
Received 9 April 2011
Revised 4 July 2011
Accepted 4 July 2011
Available online 19 July 2011

Edited by Gianni Cesareni

Keywords:
Regulatory protein
Protein–protein interaction
Translation

ABSTRACT

Ki-1/57 is a cytoplasmic and nuclear protein of 57 kDa first identified in malignant cells from Hodgkin's lymphoma. Based on yeast-two hybrid protein interaction we found out that Ki-1/57 interacts with adaptor protein RACK1 (receptor of activated kinase 1), CIRP (cold-inducible RNA-binding protein), RPL38 (ribosomal protein L38) and FXR1 (fragile X mental retardation-related protein 1). Since these proteins are involved in the regulation of translation we suspected that Ki-1/57 may have a role in it. We show by immunoprecipitation the association of Ki-1/57 with FMRP. Confocal microscopy revealed that Ki-1/57 colocalizes with FMRP/FXR1/2 to stress granules. Furthermore Ki-1/57 cosediments with free ribosomal particles and enhances translation, when tethered to a reporter mRNA, suggesting that Ki-1/57 may be involved in translational regulation.

Structured summary of protein interactions:
Ki-1/57 and **TIA-1** colocalize by fluorescence microscopy (View interaction)
Ki-1/57 physically interacts with **CIRP** by two hybrid (View interaction)
FMRP physically interacts with **Ki-1/57** by anti bait coimmunoprecipitation (View interaction)
Ki-1/57 physically interacts with **FXR1** by two hybrid (View interaction)
Ki-1/57 physically interacts with **RPL38** by two hybrid (View interaction)

1. Introduction

The protein Ki-1/57 was discovered as a cross-reactant of the monoclonal antibody Ki-1, which detects the 120 kDa surface molecule CD30 in malignant Hodgkin cells [1]. This 57 kDa protein is located in the cytoplasm, nuclear pores and nucleus [1]. Further studies revealed that several of the identified Ki-1/57-interacting proteins were found to be involved in transcriptional control, such as CHD3, p53 and MEF2C [2,3].

Ki-1/57 contains multiple RGG/RXR box clusters commonly found as methylation targets for the methyl-arginine transferase PRMT1 [4]. These motifs have been implicated in protein–RNA interaction in several RNA-binding proteins, suggesting that Ki-1/57 is involved in RNA metabolism [5]. Indeed, recent studies showed that Ki-1/57 binds to U-rich RNA probes, associates with splicing proteins such as hnRNPQ and SFRS9, modulates processing of an E1A pre-mRNA gene construct and localizes to nuclear bodies implicated in splicing regulation [5,6].

Previous yeast two-hybrid analyses also demonstrated that Ki-1/57 interacts with proteins involved in translational regulation. Among these proteins was the FXR1P protein (fragile X-related protein 1), a member of fragile X protein family, which also includes: FXR2P and FMRP (fragile X mental retardation protein) [7]. Limiting amounts of functional FMRP lead to the fragile X syndrome, which is characterized mainly by mental retardation [8]. All three FXR proteins contain RNA-binding domains and RGG boxes and are found predominantly in the cytoplasm, where they can associate with ribosomes [7]. This suggests that FXR family proteins are functionally involved in translation or mRNA stability.

* Corresponding author. Address: Laboratório Nacional de Biociências, Centro Nacional de Pesquisa em Energia e Materiais, Rua Giuseppe Máximo Scolfaro 10.000, C.P. 6192, 13084-971 Campinas, SP, Brazil. Fax: +55 19 3512 1006.
E-mail address: jorg.kobarg@lnbio.org.br (J. Kobarg).
[1] Present address: Instituto Carlos Chagas/FIOCRUZ, Curitiba, Pr, Brazil.

0014-5793/$36.00 © 2011 Federation of European Biochemical Societies. Published by Elsevier B.V. All rights reserved.
doi:10.1016/j.febslet.2011.07.010

Here, we performed immunoprecipitation and colocalization analyses that revealed an association of Ki-1/57 with FXR1P, FXR2P and FMRP in cultured human cells. Together with our sucrose gradient fractionation experiments and in vivo translation tethering assays, our data suggest that Ki-1/57 might be involved in translation regulatory events.

2. Materials and methods

2.1. Plasmid constructions

Cloning of the complete cDNA encoding Ki-1/57 into pEGFPC has been described previously [5]. To obtain an N-terminal FLAG-tagged Ki-1/57, we subcloned the Ki-1/57 cDNA into the pCDNA6 Myc/His (Invitrogen). FXR1, FXR2 and FMRP were subcloned into pEGFPC (Life Technologies). MS2-CP plasmid (pCMS2) and the bidirectional Renilla/Firefly luciferase constructs containing none or eight MS2-CP-binding sites were kindly provided by C. Gueydan (Bruxelles) [9]. Ki-1/57-MS2-CP, was obtained by sub-cloning the Ki-1/57 cDNA into pCMS2.

2.2. Co-immunoprecipitation, cell culture and microscopy

Immunoprecipitation was performed as described [5]. Briefly, cells were lysed and supernatants were incubated with rabbit anti-FMRP (Abcam) or mouse anti-Nek11 or rabbit anti-Nek6 isotype matched control antibodies on G-Sepharose 4 fast flow beads (GE Healthcare). The beads were recovered, washed and bound protein complexes were analyzed by Western blot using a hybridoma supernatant anti-Ki-1/57 (A26) or polyclonal anti-FMRP (Abcam) antiserum.

COS-7 cells were grown on glass cover slips and treated with arsenite (Sigma) (0.5 mM) for 30 min, followed by 30 min recovery. Cells were washed with PBS, fixed in 2% paraformaldehyde and then permeabilized in PBS, Triton 0.3%. After three washes cells were incubated with PBS + 100 mM of glycine, washed and blocked (BSA 2% in PBS). After five washes, primary antibody was added: polyclonal anti-FXR1, -FXR2 or -FMRP (Abcam), polyclonal anti-TIA1 (Santa Cruz Biotechnology) or monoclonal anti-FLAG (Sigma). Secondary antibodies were conjugated to the fluorophores Alexa-594, (Molecular Probes), FITC (Santa Cruz Biotechnology) or Rhodamine (Santa Cruz Biotechnology). For control, COS-7 cells were incubated with secondary antibodies only. DAPI was used to stain nuclei. Cells were analyzed on a Nikon fluorescence (Fig. 2A) or on a confocal Axioplan Carl Zeiss LSM 510 META microscope (Fig. 2B).

2.3. Sucrose gradient and cell fractionation

Polysome profiles were analyzed on sucrose gradients as previously described [10]. Cell extracts were clarified by centrifugation at 20,000*g* for 10 min at 4 °C and polysomes were fractionated by centrifugation at 40,000 rpm for 4 h at 4 °C using a Beckman SW41 rotor. Protein fractions were analyzed by Western blot using the following primary antibodies: Rabbit polyclonal anti-RPS6, anti-GAPDH (Bethyl Laboratories, 1:5000), anti-Ki-1/57 (A26, hybridoma supernatant, 1:2), and anti-RACK-1 monoclonal antibody (Transduction Laboratories, 1:2000). Secondary antibodies were: horseradish peroxidase-conjugated goat anti-mouse IgG (Calbiochem) and donkey anti-rabbit IgG (GE Healthcare), both at 1:5000.

2.4. Luciferase assay and RT-qPCR

Cell lysis and luciferase assays were performed by using the Promega Dual-Luciferase System Kit and an AB2200 luminometer (ATTO, Tokyo), essentially as recommended by the suppliers. Each

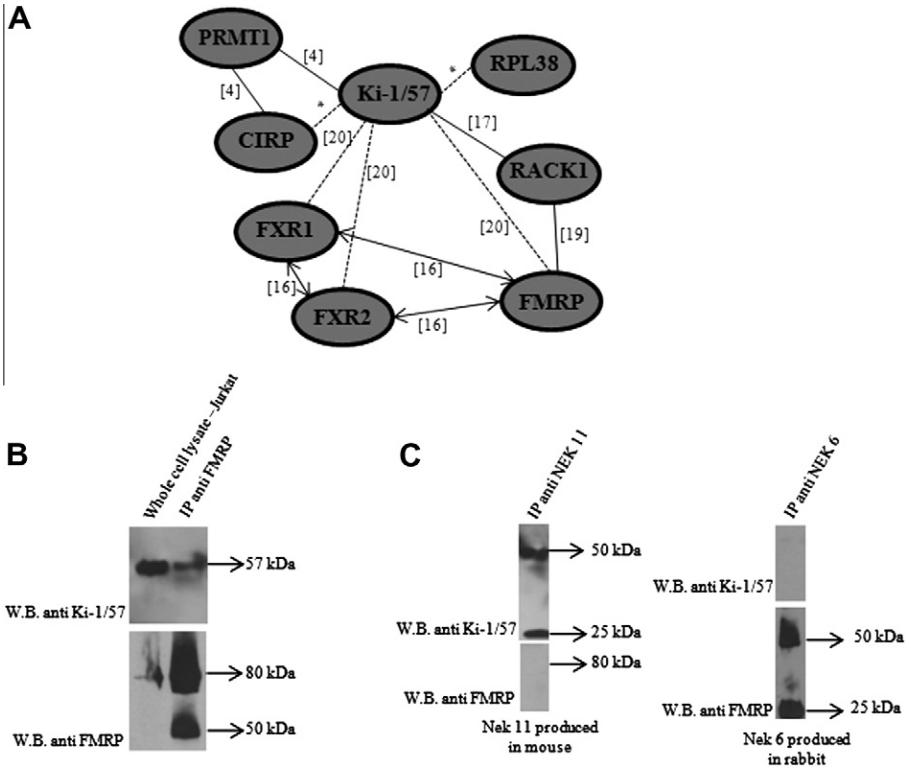

Fig. 1. Functional interconnections of Ki-1/57 with translation proteins through direct physical interactions or participation in common protein complexes. See text for details. (A) Dotted lines: experiments described here. Solid lines: previously published findings. Interrupted lines with arrows at the tips: high protein similarity among FXR family members [16]; Interactions marked by asterics (*) represent unpublished data from our group. (B) Immunoprecipitation assays (IP) of endogenous proteins in Jurkat cells and identification of the proteins by Western blot (WB). (C) Immunoprecipitation with the indicated isotype matched control antibodies anti-NEK 11 and anti-NEK 6.

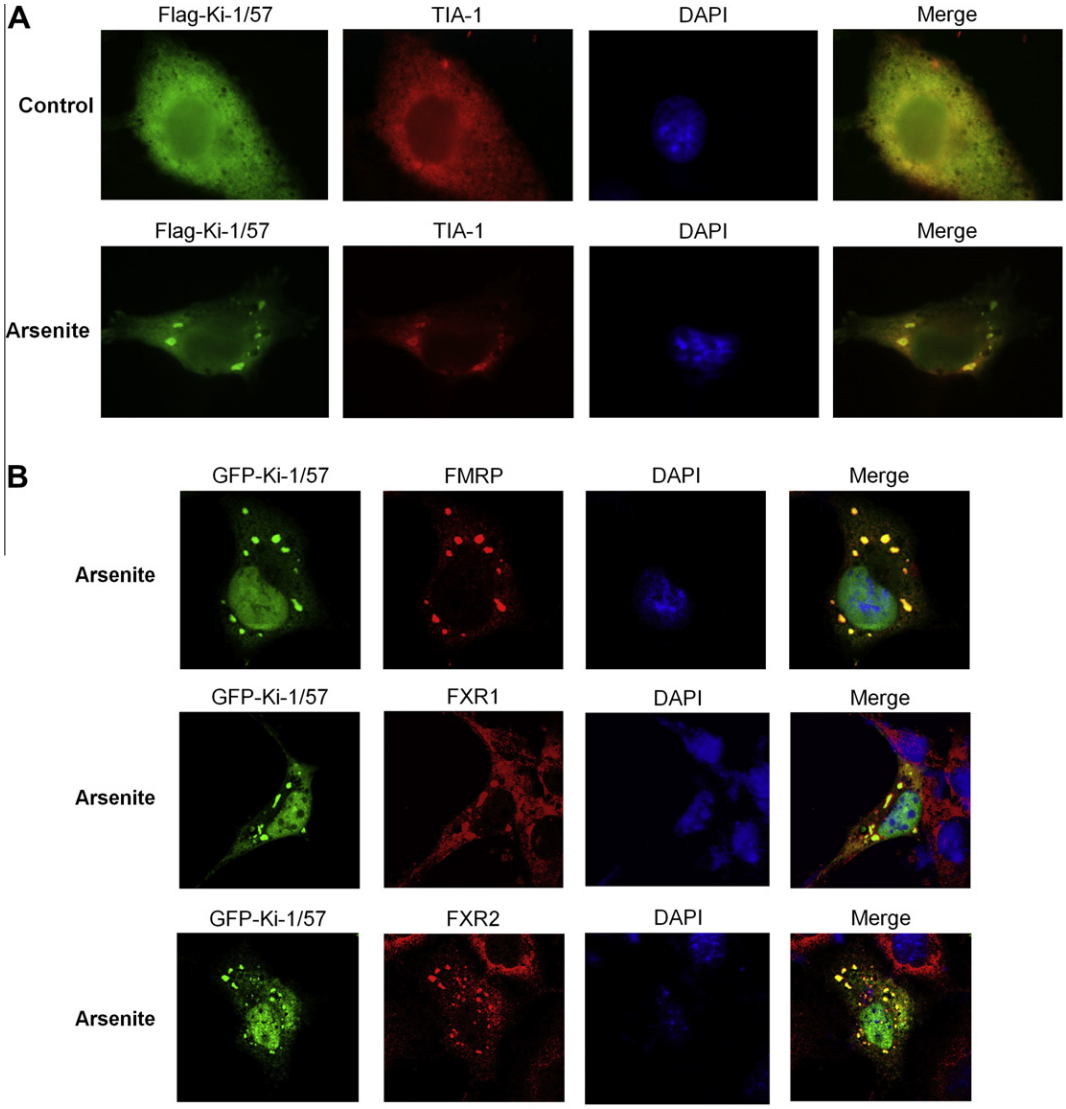

Fig. 2. Microscopy analysis of the colocalization of FLAG-Ki-1/57 with endogenous TIA-1 proteins (A) and confocal microscopy analysis of EGFPC-Ki-1/57 co-localization with FMRP/FXR1/2 in COS-7 cells after arsenite stress (B). See text for details.

assay was performed in triplicates. Statistical analyses (one way of variance ANOVA) were performed with the Oringin 6.0 software (Microcal Software, Inc.). For reverse transcription quantitative real-time PCR (RT-qPCR), total RNA was extracted using TRIzol (Invitrogen). Total RNA (1 μg) was treated with DNase (GE Healthcare) and then transcribed into first strand cDNA (GE Healthcare). RT-qPCR reactions were performed in triplicates using the Applied Biosystems 7500 Systems in a final volume of 25 μL, containing 1× SYBR Green PCR Master Mix (Applied Biosystems). Data were analyzed by relative quantification using beta-actin as endogenous reference.

3. Results and discussion

3.1. Protein–protein association analysis

In previous yeast two-hybrid analyses using Ki-1/57(1-122) as bait, we found as preys proteins involved in the regulation of translation (Fig. 1A): CIRP (cold-inducible RNA-binding protein), RPL38 (ribosomal protein L38) and FXR1 (unpublished observation). Previous studies had revealed that CIRP can down-regulate mRNA translation [11], that RPL38 confers regulatory activity to ribosomes [12] and members of the fragile X related (FXR) protein family associate with polysomes [13]. The protein FMRP has been shown to be both a negative [14] and positive [15] regulator of translation, depending on the specific target mRNA studied. FXR1 and FXR2 are very similar in overall structure to FMRP (ca. 60% amino acid identity) [16].

Moreover, now using Ki-1/57(122-413) as bait, we found that 54% of the identified clones represented RACK1, a receptor for activated PKC (protein kinase C) [17]. Literature data show that RACK1 may affect gene expression through translational regulation and activation of ribosome assembly [18]. Finally, interaction of RACK1 and FMRP [19] as well as between the possible Ki-1/57 orthologue VIG and the dFXR in *Drosophila* have been previously reported [20].

In order to test if Ki-1/57 may be also associated to translation regulatory events we first explored the potential physical association between endogenous Ki-1/57 and FMRP in vivo. Endogenous FMRP was immunoprecipitated from Jurkat cell lysates, and the coprecipitated proteins were validated by Western blot (Fig. 1B). Ki-1/57 was co-precipitated in a specific fashion, thereby providing support for the hypothesis of a functional association between Ki-1/57 and FMRP. For FXR1 we did not observe coprecipitation with endogenous proteins due to the low expression levels of FXR1.

However, when we performed the experiment with tagged, over-expressed proteins FLAG-Ki-1/57 and EGFPC-FXR1/2 in HEK-293 cells we detected coprecipitation (not shown).

3.2. Protein colocalization analysis in cells under arsenite stress

To further study a possible co-localization of Ki-1/57 with FMRP and FXR1/2 proteins in human cells we performed microscopic studies. Although all of these proteins display a diffuse distribution in the cytoplasm, previous studies reported on the localization of several translation related proteins [16], including the putative Ki-1/57 paralogue CGI-55 [21], to specific cytoplasmic foci, called stress granules, under cellular stress conditions.

We therefore performed immune colocalization analyses between Ki-1/57 and the stress granule marker protein TIA1 [22] in cells treated with arsenite (Fig. 2A) and found a clear superposition of these two proteins.

We tested next whether Ki-1/57 co-localizes also with FMRP and FXR1/2 in COS-7 cells after arsenite treatment. A clear-cut superposition of the observed foci was found, suggesting that the proteins co-localize in stress granules (Fig. 2B). Indeed members of the FXR family have previously been described as constitutive components of stress granules [16].

Besides the interaction with translational regulatory proteins, colocalization of Ki-1/57 with stress granules suggests a possible association to translational control mechanisms, since the granules transiently form in the cytoplasm of cells subjected to different stresses are enriched in RNA binding proteins involved in translational control or mRNA stability. Stress granules can lead to a general repression of translation of most mRNAs [22].

3.3. Ribosomal particle sedimentation analysis

To test the possible association of Ki-1/57 to ribosomes we performed Western blot analysis of fractions obtained with a standard sucrose density gradient sedimentation assay [10]. Ki-1/57 is enriched in the fractions near the 40–60S subunit sedimentation range, while a small but significant amount was seen in the high molecular weight polysomes (Fig. 3). RACK1 shows a sedimentation profile similar to the ribosomal protein RPS6, which overlaps with Ki-1/57 in the range of the 40–60S ribosome subunits.

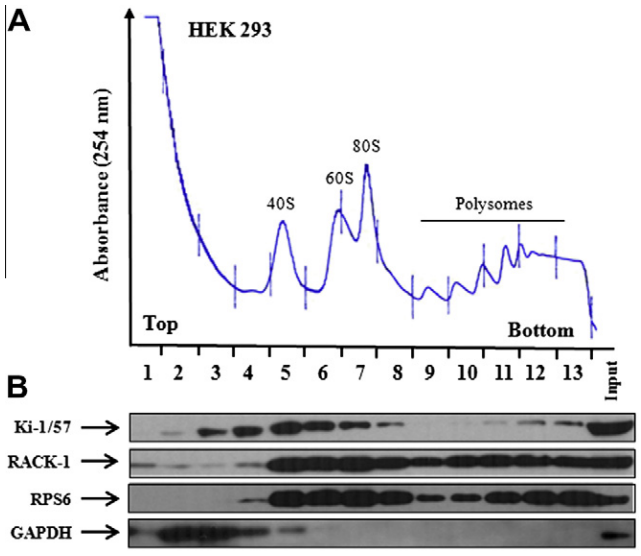

Fig. 3. Analysis of Ki-1/57 sedimentation on a sucrose density gradient. (A) Polysome profile of HEK-293T whole-cell polysomal extracts prepared according to Morello et al. (2011). (B) Western blot analysis of Ki-1/57, RACK1 and RPS6 sedimentation on a sucrose density gradient of whole-cell polysomal extracts. GAPDH was used as reference for soluble proteins.

3.4. Tethering translation assay

RNA-binding proteins are key components in the post-transcriptional regulation of gene expression. These proteins often contain conserved RNA-binding domains mediating RNA contact, subcellular targeting and protein–protein interactions [23]. Most of these proteins are nucleus/cytoplasm shuttling proteins and are involved in various aspects of RNA metabolism in both compartments. Both Ki-1/57 and CIRP share various of these features. CIRP has been described to inhibit translation [11] and therefore we decided to test the effect of Ki-1/57 using the same tethering assay. In this approach, when a protein is expressed in fusion with the bacteriophage MS2-CP protein, it is addressed onto any RNA harboring its target MS2 stem-loop (Fig. 4A), allowing the function of this protein to be analyzed in the context of mRNA stability/translation activity [24].

DNA constructs encoding MS2-CP alone and Ki-1/57-MS2-CP fusion were cotransfected in HEK-293T cells with a reporter plasmid carrying the *Firefly luciferase* (Fluc) and *Renilla luciferase* (Rluc) genes under the control of the bidirectional CMV promoter, with the *Renilla luciferase* 3′UTR containing zero (control) or 8 repeats

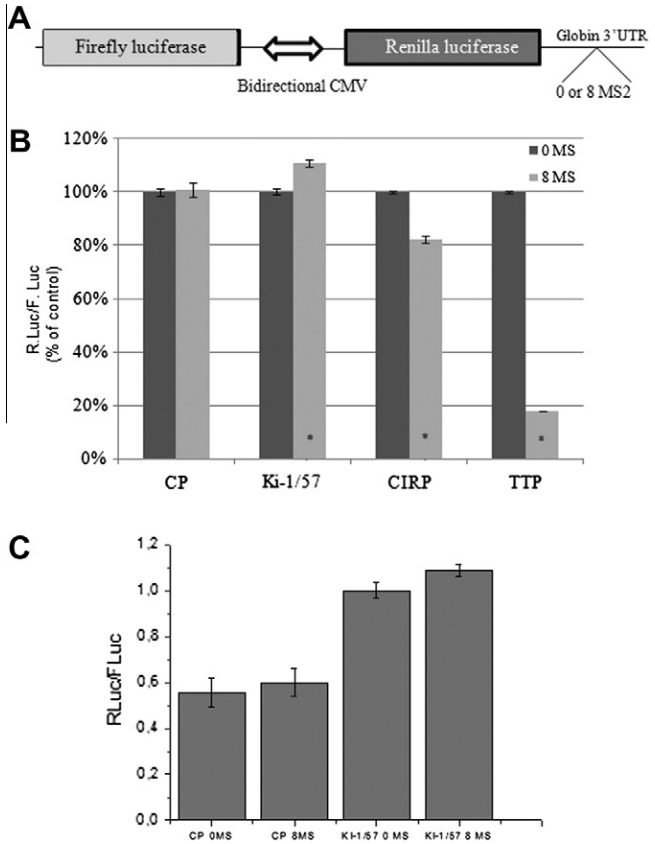

Fig. 4. Ki-1/57 induces translational activation when tethered to the 3′UTR of a reporter mRNA. (A) Diagram of the constructs used in plasmid transfection experiments. A CMV bidirectional promoter controls the transcription of both Firefly and Renilla luciferases. In the Renilla mRNA, the coding sequence is followed by human b-globin 3′UTR without any supplementary sequence element (0), or a synthetic class II ARE $(AUUU)_8$. (B) The luciferase activities measured in the cell extracts are reported as the ratio of the Rluc to Fluc activities (mean ± SD of three independent transfections). Dark grey bars: 0 MS2; Light grey bars: 8 MS2. Significant differences are marked with asterisks ($P < 0.05$). (C) RT-qPCR analysis of Rluc/Fluc mRNAs in HEK293T cells, over-expressing Ki-1/57 fused with MS2-CP. Differences between 0 and 8 MS are not significant.

of the MS2 stem-loop sequence (Fig. 4A). The effect of Ki-1/57 MS2-CP tethering towards the reporter mRNA was evaluated by comparing Rluc activities obtained with constructs with or without MS2 repeats. The Rluc values were normalized to the Fluc activity.

We observed that expression of Ki-1/57-MS2-CP leads to a ~10% increase in the Rluc/Fluc ratio for the 8 MS2-containing reporter gene compared to the control. This effect is specific to Ki-1/57-MS2-CP, since a parallel control experiment using a MS2TTP fusion (kindly provided by Dr. Cyril Gueydan) resulted in a decrease of the Rluc/Fluc ratio.

To address at which level the increase in translation was exerted, we analyzed the effect of Ki-1/57-MS2-CP expression on Rluc mRNA accumulation. To normalize the transfection and recovery efficiencies, the accumulation of Fluc mRNA was measured in the same RNA samples. As shown in Fig. 3C, the steady-state levels of Rluc mRNAs containing the 8 MS2 binding sites seemed to be slightly higher but the differences are not statistically significant. This may suggest that Ki-1/57 increases the translation of the Rluc mRNA not by stabilizing its mRNA but on another level, possibly at the initiation of translation.

4. Conclusions

Translational control plays a key role in regulation of gene expression. Previous studies in our group using the *yeast two-hybrid system* identified several proteins that interact with Ki-1/57 [2] (and unpublished data). Several of these proteins participate directly or indirectly in events related to translation (RACK1, CIRP, FXR1 and RPL38). We also have shown that Ki-1/57 co-sediments with large molecular weight complexes of 43–48S translation pre-initiation complexes and that Ki-1/57 can increase the expression level of a reporter gene luciferase. Taken together, these results suggest that Ki-1/57 might function in the context of translational regulation, thereby opening new avenues of investigation for this regulatory protein.

Acknowledgements

This study was financially supported by FAPESP, CNPq and LNBio/CNPEM. We like to thank Dr. Cyril Gueydan for providing the pCMS2 plasmids, Dr. Sara Saad and Janine S. Schincariol (UNICAMP) for support with confocal microscopy, Dr. Vadim Viviani (UFSCAR, Sorocaba) for help with the Luciferase assays, Maria Eugenia R. Camargo for technical assistance, and Dra. Beatriz Amaral de Castilho and Martin Roffe (UNIFESP) for initial help with the polyribosome profile assay.

References

[1] Rohde, D., Hansen, H., Hafner, M., Lange, H., Mielke, V., Hansmann, M.L. and Lemke, H. (1992) Cellular localization and processing of the two molecular forms of the Hodgkin-associated Ki-1 (CD30) antigen. Am. J. Pathol. 140, 473–482.

[2] Nery, F.C., Rui, E., Kuniyoshi, T.M. and Kobarg, J. (2006) Evidence for the interaction of the regulatory protein Ki-1/57 with p53 and its interacting proteins. Biochem. Biophys. Res. Commun. 341, 847–855.

[3] Kobarg, C.B., Kobarg, J., Crosara-Alberto, D.P., Theizen, T.H. and Franchini, K.G. (2005) MEF2C DNA-binding activity is inhibited through its interaction with the regulatory protein Ki-1/57. FEBS Lett. 579, 2615–2622.

[4] Passos, D.O., Bressan, G.C., Nery, F.C. and Kobarg, J. (2006) Ki-1/57 interacts with PRMT1 and is a substrate for arginine methylation. FEBS J. 273, 3946–3961.

[5] Bressan, G.C., Quaresma, A.J.C., Moraes, E.C., Manfiolli, A.O., Passos, D.O., Gomes, M.D. and Kobarg, J. (2009) Functional association of human Ki-1/57 with pre-mRNA splicing events. FEBS J. 276, 3770–3783.

[6] Bressan, G.C., Moraes, E.C., Manfiolli, A.O., Kuniyoshi, T.M., Passos, D.O., Gomes, M.D. and Kobarg, J. (2009) Arginine methylation analysis of the splicing-associated SR protein SFRS9/SRP30C. Cell. Mol. Biol. Lett. 14, 657–669.

[7] Darnell, J.C., Fraser, C.E., Mostovetsky, O. and Darnell, R.B. (2009) Discrimination of common and unique RNA-binding activities among fragile X mental retardation protein paralogs. Hum. Mol. Genet. 18, 3164–3177.

[8] Pieretti, M., Zhang, F.P., Fu, Y.H., Warren, S.T., Oostra, B.A., Caskey, C.T. and Nelson, D.L. (1991) Absence of expression of the FMR-1 gene in fragile X syndrome. Cell 66, 817–822.

[9] Barreau, C., Watrin, T., Beverley, O.H. and Paillard, L. (2006) Protein expression is increased by a class III AU-rich element and tethered CUG-BP1. Biochem. Biophys. Res. Commun. 347, 723–730.

[10] Morello, L.G., Hesling, C., Coltri, P.P., Castilho, B.A., Rimokh, R. and Zanchin, N.I.T. (2011) The NIP7 protein is required for accurate pre-rRNA processing in human cells. Nucleic Acids Res. 39, 648–665.

[11] De Leeuw, F., Zhang, T., Wauquier, C., Huez, G., Kruys, V. and Gueydan, C. (2007) The cold-inducible RNA-binding protein migrates from the nucleus to cytoplasmic stress granules by a methylation-dependent mechanism and acts as a translational repressor. Exp. Cell Res. 20, 4130–4144.

[12] Kenmochi, N., Kawaguchi, T., Rozen, S., Davis, E., Goodman, N., Hudson, T.J., Tanaka, T. and Page, D.C.A. (1998) A map of 75 human ribosomal protein genes. Genome Res. 8, 509–523.

[13] Vasudevan, S. and Steitz, J.A. (2007) AU-rich-element-mediated upregulation of translation by FXR1 and Argonaute 2. Cell 128, 1105–1118.

[14] Laggerbauer, B., Ostareck, D., Keidel, E.M., Ostareck-Lederer, A. and Fischer, U. (2001) Evidence that fragile X mental retardation protein is a negative regulator of translation. Hum. Mol. Genet. 10, 329–338.

[15] Bechara, E.G., Didiot, M.C., Melko, M., Davidovic, L., Bensaid, M., Martin, P., Castets, M., Pognonec, P., Khandjian, E.W., Moine, H. and Bardoni, B. (2009) A novel function for fragile X mental retardation protein in translational activation. PLoS Biol. 20, e16.

[16] Dolzhanskaya, N., Merz, G., Aletta, J.M. and Denman, R.B. (2006) Methylation regulates the intracellular protein–protein and protein–RNA interactions of FMRP. J. Cell Sci. 119, 1933–1946.

[17] Nery, F.C., Passos, D.O., Garcia, V.S. and Kobarg, J. (2004) Ki-1/57 interacts with RACK1 and is a substrate for the phosphorylation by phorbol 12-myristate 13-acetate activated protein kinase C. J. Biol. Chem. 279, 11444–11455.

[18] Angenstein, F., Evans, A.M., Settlage, R.E., Moran, S.T., Ling, S.C., Klintsova, A.Y., Shabanowitz, J., Hunt, D.F. and Greenough, W.T. (2002) A receptor for activated C kinase is part of messenger ribonucleoprotein complexes associated with polyA-mRNAs in neurons. J. Neurosci. 15, 8827–8837.

[19] Angenstein, F., Evans, A.M., Ling, S.C., Settlage, R.E., Ficarro, S., Carrero-Martinez, F.A., Shabanowitz, J., Hunt, D.F. and Greenough, W.T. (2005) Proteomic characterization of messenger ribonucleoprotein complexes bound to nontranslated or translated poly(A) mRNAs in the rat cerebral cortex. J. Biol. Chem. 280, 6496–6503.

[20] Caudy, A.A., Myers, M., Hannon, G.J. and Hammond, S.M. (2002) Fragile X-related protein and VIG associate with the RNA interference machinery. Genes Dev. 16, 2491–2496.

[21] Goodier, J.L., Zhang, L., Vetter, M.R. and Kazazian Jr., H.H. (2007) LINE-1 ORF1 protein localizes in stress granules with other RNA-binding proteins, including components of RNA interference RNA-induced silencing complex. Mol. Cell. Biol. 27, 6469–6483.

[22] Kedersha, N.L., Gupta, M., Li, W., Miller, I. and Anderson, P. (1999) RNA-binding proteins TIA-1 and TIAR link the phosphorylation of eIF-2 alpha to the assembly of mammalian stress granules. J. Cell Biol. 147, 1431–1442.

[23] Lunde, B.M., Moore, C. and Varani, G. (2007) RNA-binding proteins: modular design for efficient function. Nat. Rev. Mol. Cell Biol. 8, 479–490.

[24] Coller, J. and Wickens, M. (2002) Tethered function assays using 3′ untranslated regions. Methods Enzymol. 26, 142–150.

Uso exclusivo da CIBio:

Número de projeto / processo: NITZ 04.02

Formulário de encaminhamento de projetos de pesquisa para análise pela CIBio - Comissão Interna de Biossegurança da ABTLuS – Associação Brasileira de Tecnologia de Luz Síncrotron

Título do projeto: Determinação do papel das proteínas FtsJ3 e CXorf34 na síntese de ribossomos em células humanas.

Pesquisador responsável: Nilson Ivo Tonin Zanchin

Experimentador: Luis Gustavo Morello

Nível do treinamento do experimentador: [ ]-Iniciação científica, [ ]-mestrado, [X]-doutorado, [ ]-doutorado direto, [ ]-pós-doutorado, [ ]-nível técnico, [ ]-outro, especifique:_____

Resumo do projeto:

Em eucariotos, os transcritos primários produzidos a partir dos genes rRNA são processados extensivamente para gerar as formas funcionais maduras desses RNAs. Três dos quatro rRNAs são formados a partir de um precursor único, o pré-rRNA 47S, que durante o processamento, sofre extensivas reações coordenadas de clivagens endo- e exonucleolíticas, além de modificações covalentes, principalmente por metilação do grupamento hidroxila 2' de riboses específicas e conversão de resíduos específicos de uridina em pseudo-uridina. Embora os estudos sobre biogênese de ribossomos estejam bastante avançados em levedura, que foi o organismo modelo mais utilizado para isso, pouco se sabe sobre a maquinaria envolvida na biogênese de ribossomos em mamíferos. O recente descobrimento de que o rRNA é uma ribozima chave envolvida na reação peptidil transferase revitalizou o interesse por estudos relacionados à estrutura e modificações químicas que ocorrem no rRNA, principalmente em regiões funcionais do ribossomo. Trabalhos desenvolvidos em nosso laboratório sobre a síntese e função de ribossomos eucariotos nos levaram às proteínas FtsJ3 e CXorf34. FtsJ3 foi identificada como uma proteína que interage com a Nip7 humana num rastreamento pelo sistema duplo-híbrido de levedura. A Nip7 está envolvida no processamento do pré-rRNA 27S em levedura e os dados funcionais indicam que interage preferencialmente poli-uridina *in vitro*, embora ainda não se saiba se interage com algum RNA específico *in vivo*. FtsJ é um domínio conservado de RNA-metil-transferase sendo que a proteína humana FtsJ3, ainda não caracterizada, apresenta uma ortóloga em *S. cerevisiae*, Sbp1, a qual é responsável pela metilação da guanina$_{2922}$ (Gm$_{2922}$), localizada no sítio catalítico do ribossomo onde ocorre a reação de peptidil-transferase. Em estudo paralelo identificamos a interação da Nip7 com a proteína SBDS (*Shwachman-Bodian-Diamond syndrome associated protein*). Além disso, descobrimos que a proteína CXorf34 apresenta expressão aumentada em células com inibição da expressão da proteína SBDS através da técnica de RNAi. Coincidentemente, CXorf34 apresenta similaridade de seqüência à RNA metil-transferase *rum*A, envolvida na metilação do rRNA 23S em *E. coli*. Neste projeto pretendemos determinar o papel das proteínas FtsJ3 e CXorf34, na síntese de rRNA. Além disso, pretendemos estudar a importância dos sítios de metilação destas proteínas para a função dos ribossomos em células humanas.

A CIBio analisou este projeto em reunião realizada no dia: 28/11/2008 .

Parecer final: [X]-projeto aprovado, [ ]-projeto recusado, [ ]-projeto com deficiências, favor comentários abaixo:

_____

_____

_____

_____

Presidente de CIBio - ABTLuS
Prof. Dr. Jörg Kobarg

Membro da CIBio - ABTLuS
Prof. Dr. Celso Eduardo Benedetti

Membro da CIBio - ABTLuS
Prof. Dr. Nilson Ivo Tonin Zanchin

DECLARAÇÃO

Declaro para os devidos fins que o conteúdo de minha tese de doutorado intitulada "*Caracterização Funcional das Proteínas NIP7 e FTSJ3 no Processamento do RNA Ribossomal em Células Humanas*":

( ) não se enquadra no Artigo 1°, § 3° da Informação CCPG 002/06, referente a bioética e biossegurança.

(X) está inserido no Projeto CIBio (Protocolo n° NITZ 04.02), intitulado "*Determinação do papel das proteínas FTSJ3 e CXorf34 na síntese de ribossomos em céliulas humanas*".

( ) tem autorização da Comissão de Ética em Experimentação Animal (Protocolo n°_____).

( ) tem autorização do Comitê de Ética para Pesquisa com Seres Humanos (?) (Protocolo n°_____).

Aluno: Luis Gustavo Morello

Orientador: Prof. Dr. Nilson Ivo Tonin Zanchin

Para uso da Comissão ou Comitê pertinente:

(X) Deferido ( ) Indeferido

Nome:
Função:

Prof. Dr. MARCELO LANCELLOTTI
Presidente da Comissão Interna de Biossegurança
Instituto de Biologia - UNICAMP